MEMBRANE FORMATION BY IMMERSION PRECIPITATION: THE ROLE OF A POLYMERIC ADDITIVE

Remko Boom

MEMBRANE FORMATION BY IMMERSION PRECIPITATION: THE ROLE OF A POLYMERIC ADDITIVE

Proefschrift

ter verkrijging van
de graad van doctor aan de Universiteit Twente,
op gezag van de rector magnificus
prof. dr. ir. J.H.A. de Smit
volgens besluit van het College van Dekanen
in het openbaar te verdedigen
op donderdag 25 juni 1992 te 14.00 uur

door

Remko Marcel Boom

geboren op 11 mei 1965

te Utrecht

Dit proefschrift is goedgekeurd door de promotor prof. dr. C.A. Smolders en de assistent-promotor dr. ir. Th. van den Boomgaard.

Voorwoord

Het gedurende de afgelopen jaar verrichte werk is tot stand gekomen dank zij de hulp en bijstand van vele mensen, waarvan ik er hier een paar wil noemen.
De ideeën in dit proefschrift zijn in de veel gevallen tot stand gekomen met hulp van intensieve discussies met Ingrid Wienk. De eerste appendix getuigt van deze samenwerking.
Verder ben ik veel dank verschuldigd aan Sacha Schoeman en Sander Rekveld die de PICS/NANG hebben gemaakt tot wat hij nu is, Thea Heerdink voor het meten van al die diffusiecoefficienten, Rick Reinders voor het werk aan de osmometer en Ursel Cordilia die zo veel werk heeft verzet aan de PICS, en natuurlijk ook aan Erik Rolevink, die met zijn (soms letterlijk) spreekwoordelijke inzet experimenten uitvoerde.
I want to extend my special thanks to Stana Zanic: not only is the huge amount of work you did the basis of this dissertation; the cooperation with you was really also the basis of many new ideas. Thanks!
Martina Berkel wil ik bedanken voor het vele correctie werk wat betreft Engelse taal in dit proefschrift.
Thonie van den Boomgaard, als begeleider heb je een grote bijdrage aan de afgelopen vier jaar geleverd: mijn dank voor al je moeite en geduld. Als promotor heeft ook Kees Smolders een moeilijk te overschatten aandeel gehad.

Verder wil ik ook de vele andere mensen danken die allen een aandeel hebben geleverd in dit werk, bedanken, in het bijzonder de mensen in de onderzoekgroep Membraantechnologie, die door de fijne sfeer het verrichten van het onderzoek tot een plezier gemaakt hebben.

SON/NWO (the Dutch Organization for Scientific Research) is gratefully acknowledged for their financial support of this work.

CIP-GEGEVENS KONINKLIJKE BIBLIOTHEEK DEN HAAG

Boom, Remko Marcel

Membrane formation by immersion precipitation: the role of a polymeric additive / Remko Marcel Boom. - [S.l. : s.n.]. - Ill.
Proefschrift Enschede. - Met lit. opg. - Met samenvatting in het Nederlands.
ISBN 90-9005223-2
Trefw.: polymeerchemie

Druk: Copyprint 2000, Enschede.

Contents

Chapter 1

Introduction

R.M. Boom, Th. van den Boomgaard, C.A. Smolders

Membranes for separation purposes

Biological membranes are the most essential part of living creatures. They form a wall between different parts within the living cell or between the cell's contents and its exterior. Although one of their functions is protection of their contents, the most important property is their selective permeability of some of the components in the environment to the cell, and vice versa. By these exchange processes, the organism can be supplied with nutrients and oxygen, and can excrete waste products. Moreover, these exchange processes enable communications between different cells, by exchange of hormones and other molecules, which made the development possible of complex life forms.
Scientists and workers in industry quite often encounter the problem of separating a mixture in its components, or in different new mixtures. Most of the processes necessary in the chemical industry are merely separation procedures (e.g., distillation, extraction, adsorption). The majority of the separations that are necessary can in principle also be carried out by using artificial membranes.

Table 1: Some membrane separation processes arranged according to the mechanism of separation. After Mulder[1].

separation mechanism	*membrane separation process*
particle size	*filtration, microfiltration, ultrafiltration, dialysis*
solubility/diffusivity	*reverse osmosis, gas separation, pervaporation*
vapor pressure	*membrane distillation, pervaporation*
affinity, (reversible) reaction	*liquid membranes, affinity filtration*
charge	*electrodialysis, piezodialysis*
temperature	*thermal osmosis*

The principle of separation via artificial, synthetic membranes has since long been recognized. The practical application was limited to classical filtration (filtration of water, cake filtration).
Nowadays, membrane filtration is applied to almost every separation problem, based on a wide variety of separation mechanisms. A short summary is given in table 1.
As appears from table 1, the possibilities to achieve separation with membranes are diverse. The synthetic membranes necessary for these separation processes can be roughly divided into *dense* membranes and *porous* membranes.

Dense membranes
To achieve separation on a molecular scale a dense membrane is required. At the feed side, the components dissolve in the membrane matrix; an activity gradient inside the membrane causes diffusive transport towards the other side of the membrane, where the components leave the membrane and enter the permeate compartment. Separation results from differences in the solubility of the components into the membrane matrix, and differences in velocities of diffusion through the membrane. The separation properties are properties of the membrane *material*, and not of the *structure* of the membrane.
This mechanism is conveniently called the 'solution-diffusion' mechanism. Membranes falling into this category are suitable for gas separation (separation of e.g. acid gases from natural gas) and pervaporation (dehydration of ethanol, acetic acid; removal of ethanol from a fermentation product). The desalination of sea water (reverse osmosis) is performed with membranes that are in principle dense as well.

Porous membranes
For the retention of larger particles, porous membranes can be used. As an example, a feed containing macromolecules (e.g. proteins) is contacted with a membrane that contains small pores. The particles to be separated (the macromolecules) are withheld from flowing through the pores; the solution itself can flow through the pores. The reason that the particles cannot freely enter the pores is their geometric size, although interaction with the pore walls may also be of importance.
In this case the properties of the membrane are also dependent on the structure of the membrane, together with the intrinsic properties of the membrane material.
Separation of larger particles (e.g. micro-organisms) usually proceeds accor-

ding to the same mechanism.
Depending on the typical size of the pores in the selective layer, the filtration process is called 'nanofiltration' (pores between 1-10 nm), 'ultrafiltration' (5 - 50 nm) or 'microfiltration' (> 50 nm).

Other membranes
The distinction between dense and porous membranes is not very discrete. Membranes for dialysis purposes or for reverse osmosis usually consist of a material that swells considerably in the feed (e.g. water). The membrane structure during the separation process then consists for a considerable part of volume that is filled with the feed. Membranes for dialysis purposes can easily consist for 50 % of its volume of water. This volume may be called pore volume, although the membrane matrix does not contain any distinct pores.
A special class of dense membranes are the liquid membranes. In this case a layer of liquid now separates the feed and the permeate side; the transport is by dissolution and diffusion in the liquid. This liquid may for instance be immobilized in a porous support.

Membranes with a non-uniform structure
Since the properties of dense membranes are determined by the intrinsic properties of the material, it is desirable that the membranes are as thin as possible. In this this way the selectivity is preserved while the flux through the membrane is optimized. A disadvantage of a very thin membrane is that it has little mechanical strength, and therefore its applicability is limited. A common way to deal with this problem is fixing a very thin dense membrane on top of a porous support. Since this support is porous, its resistance for transport of the permeants is negligible compared to the resistance in the thin membrane on top (the 'toplayer'), while it lends sufficient mechanical stability to the membrane. This type of membrane is called a composite membrane.

Not only dense membranes can benefit from a non-uniform structure (an *asymmetric* structure, i.e. a thin selective layer and a porous support). A membrane consisting of a thin toplayer with small pores, and a sublayer containing much larger pores can have the selectivity belonging to the toplayer, combined with a high permeate flux.
Since asymmetric membrane structures are desirable over symmetric membrane structures, almost all practically applied membranes used show an asymmetric structure. This may go further than was explained above. For

the preparation of composite membranes (a support with on top a different membrane material), e.g. for gas separation or pervaporation, usually porous, asymmetric supporting membranes are used. Small pores in the surface of the support enable the toplayer to be ultra-thin; the sublayer with the larger pores gives strength to the toplayer while not contributing to the permeation resistance.

Membrane Preparation

The preparation of membranes can be divided into two parts: preparation of a sublayer, and preparation of the selective toplayer. With some techniques it is possible to prepare both toplayer and support in one single preparation procedure.
The types of membranes that were discussed can be made by different preparation techniques[1-3]. :

- sintering of particles
- stretching of a polymeric film
- track-etching
- template leaching
- coating of membranes
- interfacial polymerization
- phase inversion

Sintering of particles
Sintering of particles can be applied to ceramics and polymers. Ceramic membranes can be prepared with properties ranging from microfiltration to gas separation; sintered polymeric membranes usually are macroporous membranes (pores > 50 nm).

Stretching of a polymeric film
Film stretching yields microfiltration membranes. One usually needs crystallizable polymers for this process.

Track-etching
Track-etching, exposure of a polymer film to a beam of highly energetic particles, and etching of the created particle tracks, is a technique to obtain membranes with a uniform pore size. Only membranes for laboratory use are prepared in this way.

Template leaching
Template leaching is a technique in which first a certain heterogeneous structure is induced in a certain medium (e.g. by demixing), after which one of the components is removed by leaching. This process is applied in the preparation of porous glass membranes.

Coating of membranes
The coating of existing (porous) membranes is the usual way to prepare composite membranes. A usually asymmetric, porous membrane is taken. On top of this membrane a thin layer of a solution of a polymer is deposited. A composite membrane results, with separation characteristics belonging to the thin toplayer.
A second possibility is coating by a *non*selective polymer, instead of by a highly selective material. An asymmetric membrane, with a toplayer that contains very few small pores will not show any selectivity for gas separation, since the convective flow through the few pores dominates the diffusive transport through the rest of the toplayer. Plugging these pores by coating the membrane with a nonselective, highly permeable material results in a selectivity which is practically the intrinsic selectivity of the sublayer material.

Interfacial Polymerization
An alternative method to coat a porous membrane is by filling the pores of the membrane with a liquid that contains a reactant which can react with a second reactant in a bath, in which the membrane is immersed. At the interface between the two phases (the liquid in the pores and the bath) the reactants can form a polymer (e.g., a polyamide). A layer of this polymer (inside the pores, or on top of the membrane, depending on the reaction mechanism) can act as a selective layer.

Phase Inversion
In several of the previously discussed preparation techniques a porous membrane is used as a starting material (coating, interfacial polymerization), mostly of asymmetric structure. Phase inversion is the common technique to prepare the asymmetric precursors for other preparation techniques.
The process of phase inversion, however, is so flexible, that with this technique also integrally skinned membranes can be formed that have highly selective toplayers (either absolutely nonporous, or with a well controlled pore size) , and an open, porous sublayer, in one single operation.
The phase inversion processes[4] (a term introduced by Kesting[5]) can yield a

large variety of membrane structures. Mulder[1] reviews the following subclasses of phase inversion:

- precipitation by solvent evaporation
- precipitation from the vapor phase
- precipitation by controlled evaporation
- thermal precipitation
- immersion precipitation

Precipitation by solvent evaporation is the most simple process: the solvent in a polymer solution is allowed to evaporate, and a homogeneous polymer film results. This is the same process that is used for the preparation of a toplayer for a composite membrane.
Precipitation from the vapor phase is employed by indiffusion of nonsolvent from a vapor above a film of the polymer solution, resulting in demixing into a porous structure.
Related to this process is the controlled evaporation process. The polymer is dissolved in a mixture of a volatile solvent and a less volatile nonsolvent. The solvent is preferentially evaporated. The remaining nonsolvent causes the solution to demix.
Thermal precipitation is effectuated by quenching a polymer solution to a temperature at which the solution is not stable anymore, resulting in demixing into a porous membrane structure.
Immersion precipitation consists of contacting a polymer solution with a liquid bath that contains nonsolvent. Exchange of solvent and nonsolvent results in instability of the polymer solution which demixes into a structure that is usually asymmetric.

Immersion precipitation

Demixing of a polymer solution, resulting in an asymmetric membrane structure, is determined by the thermodynamic properties of a polymer in combination with a solvent and a nonsolvent. The demixing phenomena are induced by kinetic (mostly diffusion) processes.
Therefore two aspects of immersion precipitation are of utmost importance:

- equilibrium thermodynamics
- diffusional behavior of the components

In order to understand the immersion precipitation process, a thorough understanding of both aspects is necessary.

1. Equilibrium thermodynamics

The preparation of membranes by phase inversion is always connected with the presence of a range of compositions in which a solution is not stable but has a driving force to demix. Figure 1 shows a typical, schematic phase diagram of a ternary system consisting of polymer, solvent and nonsolvent for the polymer. This is the basic system to perform immersion precipitation.

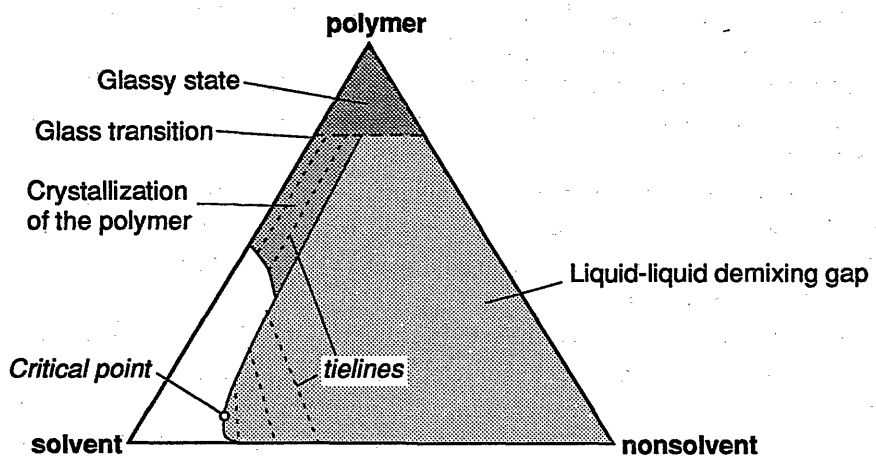

Figure 1: A schematic phase diagram typical of a ternary membrane forming system, consisting of polymer, solvent and nonsolvent for the polymer. The liquid-liquid demixing gap is always present; the region in which crystallization of the polymer can occur is not always present. During immersion precipitation, compositions in a polymer solution become richer in nonsolvent, and enter the liquid-liquid demixing gap. The resulting demixing causes an asymmetric porous membrane structure to be formed. The polymer rich phase (the membrane matrix) solidifies when it crosses the glass transition, or gels, which may be connected with a crystallization region.

Since the development of the Flory-Huggins theory[6,7], the description of equilibrium thermodynamics in polymer solutions has developed in many directions. The Flory-Huggins theory still is mainly used for the description

of the thermodynamics of a membrane forming system, since it offers a relatively simple, easily understood approach.
Hsu and Prausnitz[8] gave a comprehensive study on the thermodynamics of ternary systems, based on the Flory-Huggins approach. They used composition dependent interaction parameters (which is usually called the 'modified' Flory-Huggins approach) and were able in this way to describe the demixing gap in a more or less accurate manner. Their approach was to compute the differences in chemical potential between the two phases for all components, and minimize the square of the sum of the differences. To avoid trivial solutions (in which both phases have the same composition) they had to assume a penalty function, more or less of arbitrary form, and had to scale the volume fractions to achieve convergence.
They found that the polydispersity of the polymer could be neglected for compositions not too close to the critical point.
The interaction parameter between solvent and nonsolvent appeared to be an important parameter. The results were less sensitive to the other interaction parameters.
Altena and Smolders[9] were able to avoid the computational complications by a somewhat better numerical procedure. They gave a thorough overview of the dependence of the demixing gap on the interaction parameters and the molecular weights.
Altena and Smolders also investigated demixing by polymer crystallization[10]. It appears that most characteristics of the membrane morphologies are caused by liquid-liquid demixing. Although crystallization may have a large effect on certain properties (e.g. gas permeability), liquid-liquid demixing is the most important membrane forming process. In this work we will only consider liquid-liquid phase separation, by using only non-crystallizable polymers.

2. *Kinetics*

In recent years, many authors have investigated the diffusional mass transfer during the immersion precipitation process[11-17].
Cohen, Tanny and Prager[11] were the first to treat the diffusion of solvent and nonsolvent in a comprehensive way, on the basis of irreversible thermodynamics; they treated several systems, e.g. cellulose acetate dissolved in various solvents, coagulated with water, and polystyrene in toluene, coagulated in ethanol. Wijmans[12] showed that the derivation of their

model was not entirely correct. This was later confirmed by other authors[22]. Reuvers and Smolders *et al.*[13,14] modified the equations by Cohen *et al.*[11] to a truly ternary case; they were able to construct a more advanced model, based on the Maxwell-Stefan approach[15]. With their mass transfer model applied to cellulose acetate, various solvents and water, the two types of experimentally observed immersion precipitation processes (instantaneous vs. delayed demixing) could be explained in terms of mass transfer processes. The transition from instantaneous to delay of demixing could be accurately predicted from these calculations.

Radovanovic *et al.*[16-17] used the model by Reuvers for the system polysulfone - DMAc - i-propanol. The dependencies of the transition from instantaneous to delay of demixing on the system parameters (e.g. polymer concentration) were evaluated. The system could be divided into composition regions where demixing is proceeding either according to an instantaneous demixing regime or according to a delayed demixing regime.

Kimmerle[18] developed a model that also incorporated the demixing itself, thus attempting to describe the complete demixing process.

Reuvers' model, which has generally become more or less a standard, was based on the assumption that during some time, the composition at the interface between the polymer solution and the coagulation bath is constant. Disagreement exists on the gravity of this assumption.

Dissatisfied by the assumption, Yilmaz, Tsay and McHugh[19-23] developed a more complete model for the mass transfer, which is essentially a less further simplified version of the model by Reuvers and Smolders. Although Reuvers and Smolders were able to predict the *transition* from instantaneous to delay of demixing accurately, their simplification in the model made accurate prediction of the *length* of the delay time not possible. With the model by McHugh and coworkers, it became possible to obtain accurate prediction on the delay time. Some irregularities in their results, however, (large sensitivity on input parameters, unexpected behavior of the polymer concentration at the interface) show that their model is still not completely reliable. In combination with coming and available experimental data, this model may give significant contributions to our knowledge of immersion precipitation for ternary membrane forming systems.

Their model is already quite complicated (and computationally intensive) for a ternary membrane forming system. In our opinion, the extension to a quaternary system would not be realistic, and for a qualitative analysis it would not be necessary.

To our knowledge, it has not yet been tried to model mass transfer in a quaternary membrane forming system. We shall therefore focus on the

approach by Reuvers and Smolders, and modify this approach to a quaternary case, since this approach combines in our opinion adequate modelling possibilities with a minimum amount of computational effort.

Membrane Formation; Characteristic Structure Elements

Membranes formed by immersion precipitation have as general features:

- an asymmetric structure (toplayer and sublayer with different porosities and pore sizes)
- two demixing regimes occur: *delayed demixing*, in which only after a significant time after immersion the solution starts to demix, and *instantaneous demixing*, during which the polymer solution immediately starts to demix after immersion
- large, conical voids, called macrovoids, often across the complete thickness of the membrane. Reuvers observed that their appearance is connected to the mechanism of instantaneous demixing
- occurrence of nodular structures in the toplayer of the membranes (mostly with instantaneous demixing)

The asymmetric structures result from the ratio between solvent outdiffusion and nonsolvent indiffusion into the polymer solution. This was readily shown by the mass transfer model by Cohen *et al.* [11]
The two demixing regimes (delayed or instantaneous) followed from the mass transfer model by Reuvers and Smolders[13,14]. They found that which process takes place is determined mainly by the interaction between the solvent and the nonsolvent, and by the nonsolvent concentration in the bath. They were able to explain the different membrane properties obtained with both regimes.
With the same model, Radovanovic *et al.*[16,17] could further characterize the membrane forming properties, obtaining excellent agreement with experiments.
The appearance of macrovoids has been the subject of extensive research. Matz[24], Stevens[25], Frommer[26], Ray[27] and other investigators suggested that surface tension or concentration gradients could induce convective motion near the interface. These convective cells *under* the toplayer could then induce the formation of macrovoids, or give rise to local activity

gradients that might induce the formation of voids.
Other authors[22,23,28,29] proposed that mechanical stresses induce the formation of macrovoids. These irregularities or small ruptures at the interface could induce a local rapid inflow of nonsolvent, which is followed by the rapid growth of nonsolvent fingers in the low viscosity polymer solution beneath the toplayer. In our opinion, a high concentration of nonsolvent beneath the toplayer should result in a rapid demixing and fixation of the polymer phase, resulting in a cessation of any outgrowth of a pore. It is not clear what would then induce the rapid growth of the voids.
Gröbe[30] and Broens *et al.*[31] suggested that macrovoids are formed by anomalous growth of nuclei, because the influx of nonsolvent is so small, that the growth of the macrovoid can keep pace with the phase separation induced by the nonsolvent.
Reuvers[32] and Smolders *et al.*[33] were able to relate the mechanism suggested by Gröbe to the mass transfer model by Reuvers. They reasoned that under the toplayer, locally nuclei could be created that contain quite a high solvent concentration. This could induce local delay of demixing, which keeps the solution around the nucleus stable while the nucleus is growing. Since the solution remains stable, no new nuclei deeper in the membrane are formed and the nucleus can grow until another process stops the growth process. In our opinion, the experimental data available appear to point clearly to the mechanism by Gröbe, Reuvers and Smolders.

The nodular structures often obtained in toplayers of ultrafiltration membranes are still under extensive investigation; we will not focus on these structures in this thesis.

Quaternary systems with two polymers

Immersion precipitation in its basic form is carried out with a polymer, a solvent and a nonsolvent for the polymer. By adding a second polymer to the casting solution, completely other membrane structures can be achieved. The best-known example of these systems is the use of poly(vinyl pyrrolidone), a water-soluble polymer, in solutions of polysulfone, polyethersulfone or poly(ether imide). Several authors have contributed to this concept.[35-42]

Characteristics of these membranes, compared to membranes from ternary systems are:

- higher porosity, and a resulting higher permeability
- well interconnected pores
- suppression of macrovoid formation
- surface properties that are different from the properties of the pure membrane forming polymer
- nodular structures are often more prominent
- gas separation membranes can not be made from such systems under normal circumstances

Figure 1 shows the difference between membranes from a ternary system, and a membrane from the same system with poly(vinyl pyrrolidone) added to the polymer solution.
The differences can not be understood from the theories existing for ternary membrane forming systems, since the nature of these quaternary systems is fundamentally different. This fundamental difference is the presence of two polymers within the same solution. Polymer blends usually show a behavior that is quite different from mixtures of low molecular weight components. Especially the mutual movement of the molecules of the two polymers in a concentrated solution (e.g. 35 wt% total polymer) is not only according to a completely different mechanism (reptation) compared to mobilities with respect to low molecular weight components, but is also proceeding on a completely different time scale. These differences, together with differences in thermodynamics, cause the changes in structure, as will be shown in this thesis.

The investigation of the mechanism of membrane formation from a quaternary system with two polymers so far is limited to a few authors.
Cabasso[35,36,37] suggested that the impossibility to form dense gas separation membranes from a solution containing PVP resulted from microphase demixing between the two polymers. He did not say what the reason was for this phase separation, while the two polymers investigated by him (polysulfone and poly(vinyl pyrrolidone)) are reported to be completely miscible.
Roesink[38] has studied the system poly(ether imide) - poly(vinyl pyrrolidone) - NMP - water more extensively.

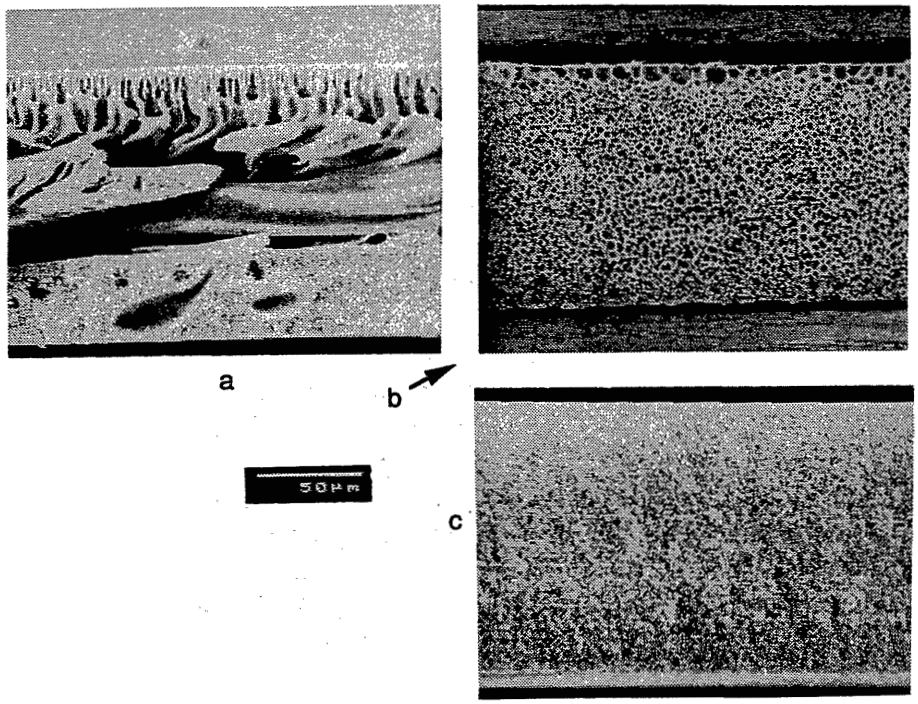

Figure 1a: Typical membrane structures: (a) 20 weight% PES in NMP, coagulated in water, (b) 20 weight% PES in NMP, coagulated in 80 wt% NMP/20 wt% water, and (c) 20 wt% PES and 10 wt% PVP in NMP, coagulated in water.

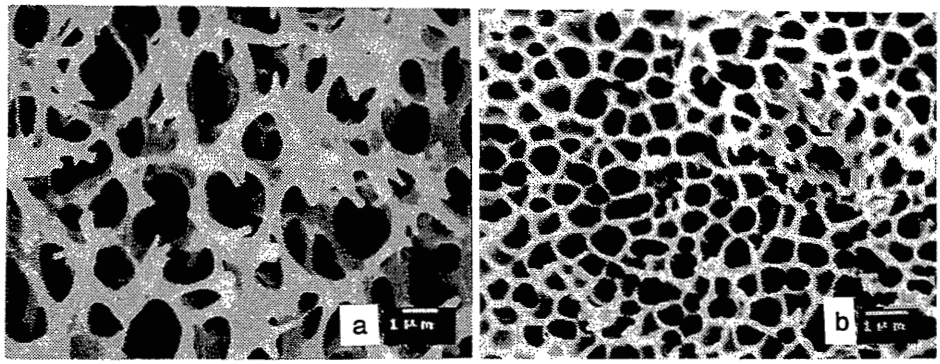

Figure 1b: Details of the pore structure of a typical membrane structure obtained without (a) and with PVP in the polymer solutions (b).

He found some unexpected results:

- a solution with PVP needs less water to become turbid than a solution without PVP (the cloudpoint is situated at lower water concentrations)
- PVP still remains for a part in the PEI rich phase, although it preferentially is transferred to the PEI lean phase. His measurements were confined to compositions near the critical point.
- From glass transition temperature measurements, a strong interaction between PEI and PVP was found, a somewhat smaller (but still very good) interaction between PES and PVP and a very strong interaction between polyimide and PVP.
- PVP slows down the demixing process during immersion precipitation, as was observed by measuring turbidity of the forming membrane as a function of time during immersion.
- A considerable fraction of PVP still remained in the final membrane, even after extensive rinsing procedures.

Roesink concluded from the first and second point that PVP should be considered to be a nonsolvent for PEI. This is in contradiction with the finding of a strong interaction between the polymers.
From the kinetic results it was concluded that the PVP causes the diffusion rates in the solution to decrease, and PVP only very slowly leaches out of the membrane, although there is a definite driving force (see also chapter 2 of this thesis).
The very open structure of the membranes was explained by a mechanism by which during the immersion step closed cells are created. The walls in between the closed cells are destroyed by drying or by another after-treatment. He showed that membranes still swollen with water had a much lower interconnectivity of the pores. The mechanism that caused the PVP to form these fragile walls, however, was not completely clear.

Scope of this thesis

The immersion process from a ternary system consisting of polymer, solvent and nonsolvent has already been adequately studied, and the understanding of this process is considerable nowadays.

From the earlier paragraphs it is clear that a systematic study of the effects of the addition of a fourth, polymeric, component to the membrane forming system is necessary in order to obtain insight in the membrane forming processes that play a role, both concerning the equilibrium thermodynamic behavior and the kinetic (diffusional) aspects.
In this thesis the fundamental properties and phenomena that are typical of quaternary membrane forming systems are studied. Due to the complexity of quaternary systems, the thermodynamic and kinetic findings are related to results obtained with only two model systems, one consisting of PES, PVP, NMP and water, and the other PES, PS, NMP and water. Figure 2 gives the structure formulae of the chemicals used.

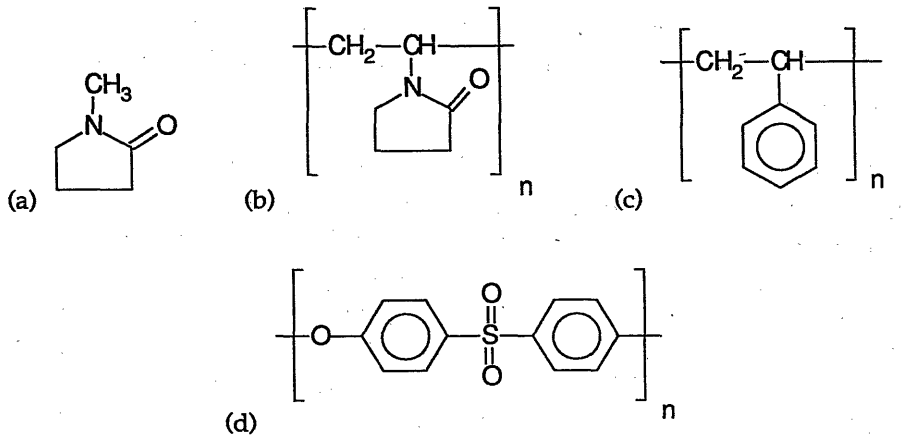

Figure 2: Structure formulae of the materials used in this thesis: (a) n-methyl pyrrolidone or NMP, (b) poly(vinyl pyrrolidone) or PVP, (c) poly(styrene), (d) poly(ether sulfone) or PES.

In *Chapter 2* the equilibrium thermodynamics, which form the basis of the membrane formation itself, are discussed. Using the Flory-Huggins theory, the properties of the quaternary solutions are investigated. Some of the properties found by Roesink[38] follow directly from the calculations. The influence of the various system variables (interaction parameters, molecular weights) is studied.

In *Chapter 3* the mass transfer during the first moments of immersion is discussed. On the basis of the model by Reuvers *et al.* a quaternary model is derived; for short times this model is independent of the assumption made by Reuvers that the compositions at the interface should remain constant.

From the very nature of the solutions, and the mobility between the two polymers, the thermodynamics appear to be quite different for the first moments of immersion, compared to the ternary system. These changes are investigated, and the results are coupled to the mass transfer model.

In *Chapter 4,* a thorough phenomenological study of the system PES-PVP-NMP-water is presented. The role of PVP in membrane formation is closely studied, from which it appears that its role is far more complex than only the effects mentioned before. The relation of the findings with chapters 2 and 3 is discussed. A hypothesis describing the demixing mechanism is presented, based on the model calculations from chapter 3. The suppression of macrovoids is connected with the mutual immobility of the polymers. Reappearance of macrovoids in membranes that are more slowly coagulated confirm this model; structures formed at extreme conditions are another confirmation of the model.

In *Chapter 5,* the effects of a polymeric additive are studied by using a completely different polymeric additive: polystyrene (PS). This additive is not soluble in the nonsolvent, water. By using this difference in solubility, the formation mechanism can be further analysed. From this system it can be seen that the mutual immobility of the polymers is indeed a limiting factor. At slow coagulation conditions the polymer-polymer movement has more opportunity, and distinctly different structures are obtained in which the polymers have separated completely. These structures can be directly related to the structures obtained from the PES-PVP-NMP-water system.
From the results it follows that the formation of the structures typically found with PVP (see figure 1) is probably based on spinodal decomposition. A general subdivision of membrane formation mechanisms for quaternary systems is formulated.

In *Chapter 6,* the kinetics of nucleation and nucleus growth is investigated by means of light scattering experiments. From an Avrami-type approach, the possible mechanisms of nucleation can be found.
A relation is derived that describes the dependence of the demixing behavior (nucleation and nucleus growth) as a function of the supercooling. The number of nuclei (of the newly formed phase) appears to be constant, regardless of demixing time or supercooling. This points to two possible, different nucleation mechanisms. Both mechanisms imply that the nuclei themselves are already present in the polymer solution.

In the *First Appendix of this Thesis,* a first experimental approach based on chapter 3 is shown. The appearance of macrovoids in the system PES-PVP-NMP-water is related to the mass transfer model from chapter 3. Some ideas are presented on the formation of nodules in the toplayer of membranes.

In the *Second Appendix of this Thesis,* a relation is presented that describes cloudpoint lines in ternary membrane forming systems as a function of only two parameters. An interpretation by means of the Flory-Huggins theory is given. The relation appears to be a powerful tool for quickly interpreting cloudpoint data, and in distinguishing between liquid-liquid demixing and solid-liquid demixing (polymer crystallization).

References

1 M.H.V. Mulder, Basic Principles of Membrane Technology, Elsevier Science Publ., Amsterdam, The Netherlands, 1991

2 H. Strathmann, J. Membrane Sci., **9** (1981) 121

3 H.K. Lonsdale, J. Membrane Sci., **10** (1982) 81

4 S. Loeb, S. Sourirajan, Advan. Chem. Ser. **38** (1962) 117

5 R.E. Kesting, Synthetic Polymer Membranes, McGraw Hill, New York, 1972

6 P.J. Flory, Principles of Polymer Chemistry, Cornell Univ. Press, New York, 1953

7 H. Tompa, Polymer Solutions, Butterworths, London, 1956

8 C.C. Hsu, J.M. Prausnitz, Macromolecules, **7** (1974) 320

9 F.W. Altena, C.A. Smolders, Macromolecules, **15** (1982) 1491

10 F.W. Altena, C.A. Smolders, J. Polym. Sci, Polym. Symp., **69**, (1981) 1

11 C. Cohen, G.B. Tanny, S. Prager, J. Polym. Sci., Polym. Phys. Ed. **17** (1979) 477

12 J.G, Wijmans, F.W. Altena, C.A. Smolders, J. Polym. Sci., Polym. Phys. **22**, (1984) 519

13 A.J. Reuvers, J.W.A. van den Berg, C.A. Smolders, J. Membrane Sci., **34** (1987) 45

14 A.J. Reuvers, C.A. Smolders, J. Membrane Sci., **34** (1987) 67

15 J.A. Wesselingh, R. Krishna, Mass Transfer, Ellis Horwood, New York, 1990

16 Ph. Radovanovic, S.W. Thiel, S.-T. Hwang, J. Membrane Sci., **65** (1992) 213

17 Ph. Radovanovic, S.W. Thiel, S.-T. Hwang, J. Membrane Sci., **65** (1992) 231

18 K. Kimmerle, Quantitative Betrachtung des Phaseninversionsprozesses bei der Herstellung van Membranen, thesis, University of Stuttgart, Stuttgart, 1988

19 L. Yilmaz, A.J. McHugh, J. Membrane Sci., **28** (1986) 287

20 A.J. McHugh, L.Yilmaz, J. Polym. Sci., Polym. Phys. Ed., **23** (1985) 1271

21 A.J. McHugh, L.Yilmaz, J. Membrane Sci., **43** (1989) 319

22 C.S. Tsay, A.J. McHugh, J. Polym. Sci., Polym. Phys. Ed., **28** (1990) 1327

23 C.S. Tsay, A.J. McHugh, J. Polym. Sci., Polym. Phys. Ed., **29** (1991)

24 R. Matz, Desalination, **10** (1972) 1

25 W.E. Stevens, C.S. Dunn, C. Petty, paper presented at the 73rd AIChE Annual Meeting, Chicago, Ill, 1980

26 M.A. Frommer, R.M. Messalem, Ind. Eng. Chem. Prod. Res. Dev., **12** (1973) 328

27 R.J. Ray, J. Membrane Sci., **23** (1985) 155

28 H. Strathmann, K. Kock, P. Amar, R.W. Baker, Desalination, **16** (1975) 179

29 J.P. Graig, J.P. Knudsen, V.F. Holland, Textile Res. J. **32** (1962) 435

30 V. Gröbe, G. Mann, G. Duwe, Fasenforsch. Textiltechn., **19** (1968) 49

31 L. Broens, F.W. Altena, C.A. Smolders, Desalination, **32** (1980) 33

32 A.J. Reuvers, Membrane Formation, diffusion induced demixing processes in ternary polymeric systems, thesis, University of Twente, Enschede, 1987

33 C.A. Smolders, A.J. Reuvers, Microstructures in Membranes Part I: formation of macrovoids, submitted for publication in J. Membrane Sci.

34 R.M. Boom, I.M. Wienk, Th. van den Boomgaard, C.A. Smolders, Microstructures in Membranes Part II: the role of a polymeric additive, accepted for publication in J. Membrane Sci.; first appendix of this thesis

35 I. Cabasso, E. Klein, J.K Smith, J. Appl. Polym. Sci., **20** (1976) 2377

36 I. Cabasso, E.Klein, J.K. Smith, J. Appl. Polym. Sci., **21** (1977) 165

37 I. Cabasso, K.Q. Robert, E. Klein, J.K. Smith, J. Appl. Polym. Sci., **21** (1977) 1883

38 H.D.W. Roesink, Microfiltration, membrane development and module design, thesis, University of Twente, The Netherlands, 1989

39 P. Aptel, N. Abidine, F. Ivaldi, J.P. LaFaille, J. Membr. Sci. **22** (1985) 199

40 T.A. Tweddle, O. Kutowy, W.L. Thayer, S. Sourirajan, Ind. Eng. Chem. Prod. Res. Dev. **22** (1983) 320

41 L.Y. Lafrenière, F.D.F. Talbot, T. Matsuura, S. Sourirajan, Ind. Eng. Chem. Res. **26** (1987) 2385

42 Q.T. Nguyen, L.L. Blanc, J. Neel, J. Membrane Sci., **22** (1985) 245

Chapter 2

Equilibrium Thermodynamics of a Quaternary Membrane Forming System with Two Polymers

R.M. Boom, Th. van den Boomgaard, C.A. Smolders

Summary

Liquid-liquid phase separation phenomena are investigated for a quaternary system containing two polymers, a solvent for both polymers, and a nonsolvent for one of the polymers (the membrane forming polymer), which is a solvent for the second polymer. The phase separation behavior studied in this chapter is related to the membrane forming properties of a system containing a macromolecular additive as second polymer.

To visualize parts of the three-dimensional quaternary phase diagrams, semi-ternary cross-sections are used in which two components are regarded as a 'lumped' component. Cloudpoint and shadow curves are given. The critical point valid for a ternary system is extended into a *critical line.*

It is found that the critical line at larger molecular weights of the second polymer, is situated at higher concentrations of the membrane forming polymer. A high molecular weight of this second polymer causes the phase diagram to become insensitive to the various interaction parameters. At constant molecular weight of the second polymer, the critical line shifts to higher polymer concentrations upon increasing the concentration of the second polymer.

Interaction effects appear to have a marginal influence, as long as the component pairs that were assumed to be miscible, remain miscible.

Introduction

The formation of symmetric or asymmetric membranes by the immersion precipitation process[1-4] is based on the phenomenon of liquid-liquid phase separation.

The basic system for the immersion precipitation process is a ternary system consisting of a polymer, a solvent and a nonsolvent for the

polymer. The solvent and the nonsolvent must be miscible.
A concentrated solution (e.g. 10 - 30 weight%) of the polymer in the solvent is immersed in a bath containing nonsolvent. The nonsolvent diffuses into the polymer solution while the solvent diffuses out. By the changes in composition, the polymer solution becomes unstable, and liquid-liquid demixing starts. If the concentration of polymer is high enough, nuclei of a polymer lean phase are created. These nuclei grow out into pores; the surrounding polymer solution gradually gets more concentrated in polymer, until a solidification process inhibits any further changes in morphology. Solidification processes that may occur are gelation by crystallization of the polymer, vitrification by crossing the glass transition region or a somewhat undefined process called aggregate formation[4-6].
A porous matrix is formed which may have a thin toplayer containing very narrow pores or even no pores at all. The pores in the sublayer can be well interconnected or may turn out to consist of closed cells. The actual morphology of the resulting membrane is strongly dependent on the thermodynamic and kinetic properties of the system studied. The membrane formation process in a ternary system has already been extensively studied. Equilibrium thermodynamics were evaluated by e.g. Hsu and Prausnitz[7], and Altena *et al.*[8], while kinetic aspects were studied by e.g. Cohen *et al.*[5], Reuvers *et al.*[6,9] and McHugh and coworkers[10-12].
In a (quasi-)ternary system, membrane structures can be obtained that have permeation properties ranging from microfiltration to gas separation. The performance of some of these membranes can be dramatically improved by using a fourth component in the system: a second polymer is added to the polymer solution, that is miscible with the nonsolvent used in the coagulation bath. For micofiltration and ultrafiltration, membrane morphologies can result that are far more regular and show superior permeabilities while retaining the required retention properties[13-16].
In this chapter, we will focus on the phase diagram, i.e. on the equilibrium liquid-liquid phase separation properties of solutions typically of interest for membrane preparation by immersion precipitation in four-component systems, containing a polymeric additive in the polymer solution which is miscible with the nonsolvent.
By using the modified Flory-Huggins theory[17,18] (i.e. the Flory-Huggins approach with concentration dependent interaction parameters) for the description of the concentration dependencies of the free enthalpy of mixing, theoretical phase diagrams are calculated. We will represent these quaternary phase diagrams by means of planar cross-sections.

As an example of a quaternary membrane forming system, the following system is used:

1 - nonsolvent: water
2 - solvent: 1-methyl-2-pyrrolidone (NMP)
3 - membrane forming polymer: poly(ether sulfone) (PES)
4 - macromolecular additive: poly(vinyl pyrrolidone) (PVP)

The interaction parameters belonging to this system are used as starting point for parameter variation. The effects of the molecular weight of the additive, and of the polymer-polymer (3-4) and additive-nonsolvent (1-4) interaction parameters are studied. The position of the *critical line* in the system, and its effect on the membrane forming properties are discussed.

Phase Diagrams

The composition of a homogeneous four-component system has three degrees of freedom. Therefore, the isothermal phase diagram of such a system should be represented in three dimensions. The most logical way to represent a quaternary phase diagram is in the form of a tetrahedron. This is shown in figure 1.

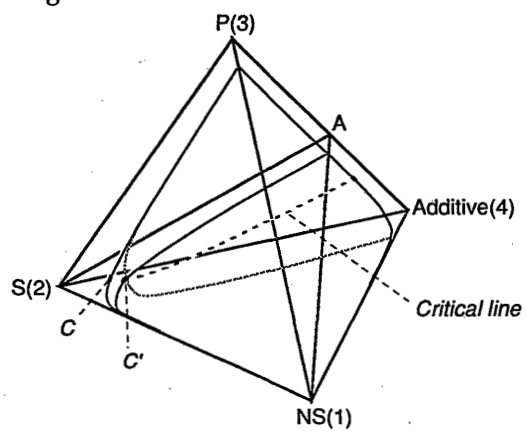

Figure 1. Schematic representation of a quaternary phase diagram; 1 and 3 are not miscible, all other pairs are miscible over the complete binary concentration range. Two ternary phase diagrams 1-2-3 and 1-3-4 show a demixing gap (outer planes of the tetraeder). One cross-sectional plane is also given (1-2-A).

Each corner represents a pure component. A point on the edge between two corners gives a binary composition, while a point on one of the outer planes represents a ternary subsystem. All points inside the tetraeder are quaternary compositions. The original ternary membrane forming system consisting of nonsolvent (1), solvent (2) and membrane forming polymer (3) is shown as the triangle at the front. It shows the usual demixing gap. The subsystem nonsolvent-polymer-polymer (1-3-4) is the other subsystem that contains a demixing gap. Other ternary subsystems do not contain a demixing gap, since the additive (4) is supposed to be miscible with all other components in the system.

The critical point in the original ternary membrane forming system (1-2-3) (point C in figure 1) is extended into a critical line (C is the starting point of this line). The position of this critical line is dependent on the molecular weights of the components present. The intersection of the critical line and the planar cross-section (1-2-A in figure 1) is the critical point for that cross-section (point C').

Since the representation of a three-dimensional phase diagram on a two-dimensional sheet is not always without complications we will make use of planar cross-sections through the quaternary phase diagram. Such a cross-section is drawn through two corners and one point on the opposite edge. The two components belonging to that edge are lumped together and represented as one (mixed) component in the corner of a *semi-ternary* phase diagram. In this phase diagram the lumped components are present at a fixed ratio between them; their total concentration changes as if they were one, third, component. By taking two such plots in which two different pairs of components are lumped together, an impression of the phase separation properties can be obtained.

In many membrane forming systems the two polymers are regarded as one polymer, so it is convenient to take the two polymers (3 and 4) together in the phase diagram. The corners of the semi-ternary phase diagram then are: component 1, component 2, and components 3 and 4 together. From such a plot the separation between polymer (3+4 together) rich and polymer lean phases can be seen; see figure 2a.

In this chapter we are focussing on the effects of the addition of a fourth, macromolecular component. The separation between the two polymers in such a system is an important factor. It is therefore useful to use also a semi-ternary phase diagram in which the solvent and the nonsolvent are taken as one component. The corners of the phase diagrams are then components 1 and 2 together, component 3 and component 4. From such a plot the polymer-polymer separation in the system is obtained. This is

shown in figure 2b.
In figure 2, the intersections of the binodal surface and the planes through the phase diagram as described are indicated as uninterrupted lines. This line is a so-called *cloudpoint curve;* it represents compositions that are just at the border of the demixing gap. The concentrations that are at equilibrium with these compositions on the cloudpoint line are situated elsewhere in the quaternary phase diagram. They are in fact incipient phase compositions. Although the incipient phases are represented in figure 2 by a dashed line, it is important to realize that generally these compositions are *not* situated in the cross-sections themselves. They are only projected onto the cross-sections.

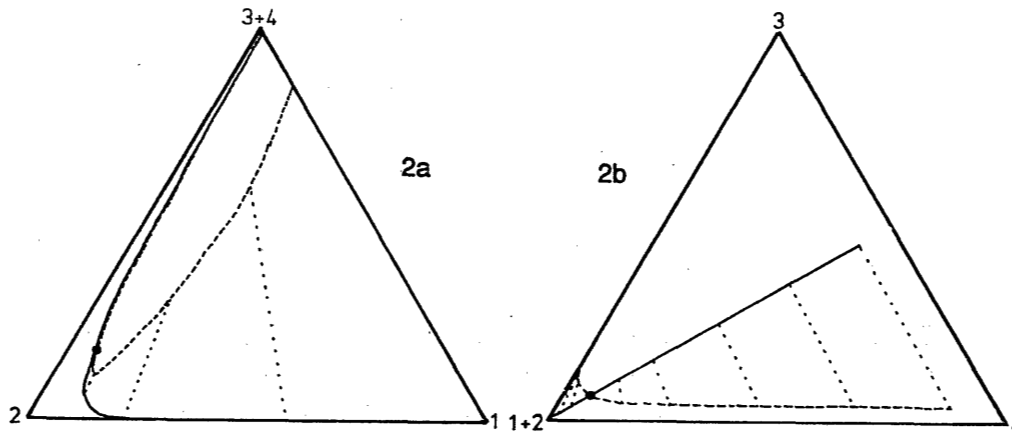

Figure 2: Cross-sections through the quaternary phase diagram, in which the ratio of components 3 and 4 is kept constant at unity. The cloudpoint lines for the cross-sections a and b are shown (uninterrupted lines). In the figures (a) and (b), the compositions that are at equilibrium with the cloudpoint curve, are shown as dashed curves (which are not *located in the plane of the cross-sections) are projected onto the cross-sections.*

It is assumed that the volume of the incipient phase is still very small; the composition of the cloudpoint phase has not yet changed. The curve (dashed curve in the figures) that represents the incipient phases may be called the *shadow curve.* This term was introduced by Koningsveld[19] for a quasi-binary system consisting of a solvent and a polydisperse polymer.

The cloudpoint curve in such a binary system is not the same as a binodal curve: the incipient phases that are at equilibrium with the cloudpoint compositions in case of a polydisperse polymer have a different molecular weight distribution than the original cloudpoint phase. The curve of compositions of the incipient phases, called the shadow curve by Koningsveld, is analogous to our shadow curve. In our situation not polydispersity of the polymer, but the presence of two polymers is the cause of the occurrence of a shadow curve.

Calculations

The procedure for calculating the phase behavior of the quaternary system is an extended version of the approach developed by Hsu and Altena *et al.*[7,8] for a ternary system.

The following index convention for the components will be used:

1 - non-solvent for the polymer (component 3)
2 - solvent
3 - membrane forming polymer
4 - polymeric additive

The phase behavior in a quaternary system is assumed to be described by the modified Flory-Huggins theory[17,18], which gives the free enthalpy of mixing as a function of concentration dependent interaction parameters.

$$\begin{aligned}\frac{\Delta G_m}{RT} = {} & n_1 \ln\varphi_1 + n_2 \ln\varphi_2 + n_3 \ln\varphi_3 + n_4 \ln\varphi_4 + \\ & + n_1 \varphi_2 g_{12}(u_2) + n_1 \varphi_3 \chi_{13} + n_1 \varphi_4 g_{14}(u_4) \\ & + n_2 \varphi_3 g_{23}(v_2) + n_2 \varphi_4 g_{24}(w_2) + n_3 \varphi_4 g_{34}(v_3)\end{aligned} \qquad 1)$$

in which ϕ_i and n_i are respectively the volume fraction and the number of moles of component i. It is assumed that the binary Flory-Huggins interaction parameters g_{ij} are truly binary, i.e. that they are only dependent on the components i and j. This implies that we assume that the interaction parameters do not change when other components are added to the system. This assumption is very probably not justified: as an example the interaction parameter g_{34} will almost certainly change upon addition of water to the system. Later in this chapter we will expore the

effects of variations in the values of the g_{ij}'s.
Formally the interaction parameters are now dependent on the following system variables:

$$\begin{aligned} &g_{12} \text{ is dependent on } u_2 = \phi_2/(\phi_2+\phi_1) \\ &g_{23} \text{ is dependent on } v_2 = \phi_2/(\phi_2+\phi_3) \\ &g_{14} \text{ is dependent on } u_4 = \phi_4/(\phi_1+\phi_4) \\ &g_{24} \text{ is dependent on } w_2 = \phi_2/(\phi_2+\phi_4) \\ &g_{34} \text{ is dependent on } v_3 = \phi_3/(\phi_3+\phi_4) \end{aligned} \qquad 2)$$

The interaction parameter χ_{13} is probably concentration dependent. It is however very difficult to obtain information concerning this concentration dependence[6]. Therefore, the interaction parameter between polymer and nonsolvent is simply assumed to be constant.
The other system variables are the ratios of the molar volumes s, r and t:

$$s = \frac{v_1 M_1}{v_2 M_2}; \qquad r = \frac{v_1 M_1}{v_3 M_3}; \qquad t = \frac{v_1 M_1}{v_4 M_4} \qquad 2a)$$

The derivatives of the free enthalpy of mixing with respect to the number of moles of each component yield the chemical potentials of mixing:

$$\left(\frac{\partial \Delta G_m}{\partial n_i}\right) = \Delta\mu_{m,i} \qquad 3)$$

Following Altena[8] and Reuvers[6], the chemical potentials of mixing are expressed per mole of segments of the nonsolvent[8,9]:

$$\begin{aligned} \frac{\Delta\mu_1}{RT} = \ln\varphi_1 - s\varphi_2 - r\varphi_3 - t\varphi_4 + (1 + g_{12}\varphi_2 + \chi_{13}\varphi_3 + g_{14}\varphi_4)(1 - \varphi_1) \\ - sg_{23}\varphi_2\varphi_3 - rg_{34}\varphi_3\varphi_4 - sg_{24}\varphi_2\varphi_4 \\ - \varphi_2 u_2 (1 - u_2)\left(\frac{\partial g_{12}}{\partial u_2}\right) - \varphi_4 u_4 (1 - u_4)\left(\frac{\partial g_{14}}{\partial u_4}\right) \end{aligned} \qquad 4)$$

$$\begin{aligned} \frac{s\Delta\mu_2}{RT} = s\ln\varphi_2 - \varphi_1 - r\varphi_3 - t\varphi_4 + (s + g_{12}\varphi_1 + sg_{23}\varphi_3 + sg_{24}\varphi_4)(1 - \varphi_2) \\ - \chi_{13}\varphi_1\varphi_3 - g_{14}\varphi_1\varphi_4 - rg_{34}\varphi_3\varphi_4 \\ + \varphi_1 u_2 (1 - u_2)\left(\frac{\partial g_{12}}{\partial u_2}\right) - s\varphi_3 v_2 (1 - v_2)\left(\frac{\partial g_{23}}{\partial v_2}\right) - s\varphi_4 w_2 (1 - w_2)\left(\frac{\partial g_{24}}{\partial w_2}\right) \end{aligned} \qquad 5)$$

$$\frac{r\Delta\mu_3}{RT} = r\ln\varphi_3 - \varphi_1 - s\varphi_2 - t\varphi_4 + (r + g_{13}\varphi_1 + sg_{23}\varphi_2 + rg_{34}\varphi_4)(1 - \varphi_3) - g_{12}\varphi_1\varphi_2 - g_{14}\varphi_1\varphi_4 - sg_{24}\varphi_2\varphi_4 - s\varphi_2 v_2(1 - v_2)\left(\frac{\partial g_{23}}{\partial v_2}\right) + r\varphi_4 v_3(1 - v_3)\left(\frac{\partial g_{34}}{\partial v_3}\right) \quad 6)$$

$$\frac{t\Delta\mu_4}{RT} = t\ln\varphi_4 - \varphi_1 - s\varphi_2 - r\varphi_3 + (t + g_{14}\varphi_1 + sg_{24}\varphi_2 + rg_{34}\varphi_3)(1 - \varphi_4) - g_{12}\varphi_1\varphi_2 - \chi_{13}\varphi_1\varphi_3 - sg_{23}\varphi_2\varphi_3 + \varphi_1 u_4(1 - u_4)\left(\frac{\partial g_{14}}{\partial u_4}\right) - s\varphi_2 w_2(1 - w_2)\left(\frac{\partial g_{24}}{\partial w_2}\right) - r\varphi_3 v_3(1 - v_3)\left(\frac{\partial g_{34}}{\partial v_3}\right) \quad 7)$$

These equations are used to calculate phase equilibria for this system. The chemical potential of mixing of each component should be equal in each phase at equilibrium in the system.
To calculate the equilibrium compositions numerically from equations 4 to 7, the following objective function is minimized:

$$F = \sum_{i=1}^{4}\left\{\frac{\Delta\mu_i^{1st\ phase}}{RT} - \frac{\Delta\mu_i^{2nd\ phase}}{RT}\right\}^2 \quad 8)$$

In our procedure, we fix the polymer concentrations ϕ_3 and ϕ_4 in one phase. The concentration of component 1 and the compositions in the other phase are varied to find the minimum of the function F. By systematically varying the ratios between 3 and 4 we can conveniently evaluate the phase diagram.
Convergence in the calculations was assumed when the objective function F had a value smaller than 10^{-32}. All calculations were done on a standard 80386/387 computer in double precision, using a multidimensional Newton-type algorithm, in which derivatives were calculated by a first order finite difference approximation. The sensitivity of the convergence on the starting guesses was still manageable, although larger than in a ternary calculation.

The system mentioned before, consisting of PES, PVP, NMP and water was taken as a model system; the following parameter values valid for this system were used in the calculations:

$g_{12} = 1.0$ $\quad g_{13} = 1.5$ $\quad g_{23} = 0.5$
$g_{14} = 0.5$ $\quad g_{24} = 0.5$ $\quad g_{34} = -1.0$

For reasons of convenience constant interaction parameters were used. The effects of changing the systems parameters (interaction parameters *and* molecular weights) are evaluated later on. The values for the PES-NMP-water system were taken from Tkacik *et al.*[20]; interactions of PVP with the other components were measured by high-pressure osmometry in our own laboratory (see appendix).
The molecular weight of PES was taken as 18 000 g/mole[20], while the molecular weight of PVP was varied.

Results

1. Molecular weight of the polymeric additive 4

The effects of the macromolecular additive, component 4, can at least be partly ascribed to the macromolecular nature of this component. Figure 3 gives cross-sections through the quaternary phase diagram for different molecular weights of component 4; the ratio of components 3 and 4 is kept at unity here.
Although the cloudpoint curve (the uninterrupted line) somewhat resembles the binodal of a ternary membrane forming system consisting of polymer, solvent and nonsolvent, this resemblance is misleading.
In all calculations it appears (see figure 4) that the two polymeric components do separate over the phases. Component 4 has always preference for the phase that is lean in component 3. Below the (semi-ternary) critical point component 4 remains in the cloudpoint phase; above the critical point component 4 accumulates in the separating, incipient phase. This is almost independent of concentrations and interaction parameters, as long as component 4 is macromolecular.
This effect is entropic in nature: two polymers in the same phase have a low entropy of mixing, and will try to maximize their entropy of mixing by separating.
At higher concentrations of polymer the cloudpoint curve and the shadow curve are both bending upward to higher polymer concentrations. In figure 3 (components 3 and 4 taken together) the cloudpoint curve and the shadow curve nearly coincide.
This does not mean that the cloudpoint composition and the incipient

phase composition are equal, as can be seen in figure 4. In this figure the cloudpoint curve itself can be seen as a straight line, since we assumed a constant ratio between components 3 and 4. At low polymer concentrations on the cloudpoint curve, (this is when the cloudpoint line in figure 4 is still near the corner of component 1 and 2) the shadow curve is above the cloudpoint curve: it represents the polymer 3 rich phase. Here the cloudpoint curve is the phase that is lean in component 3.

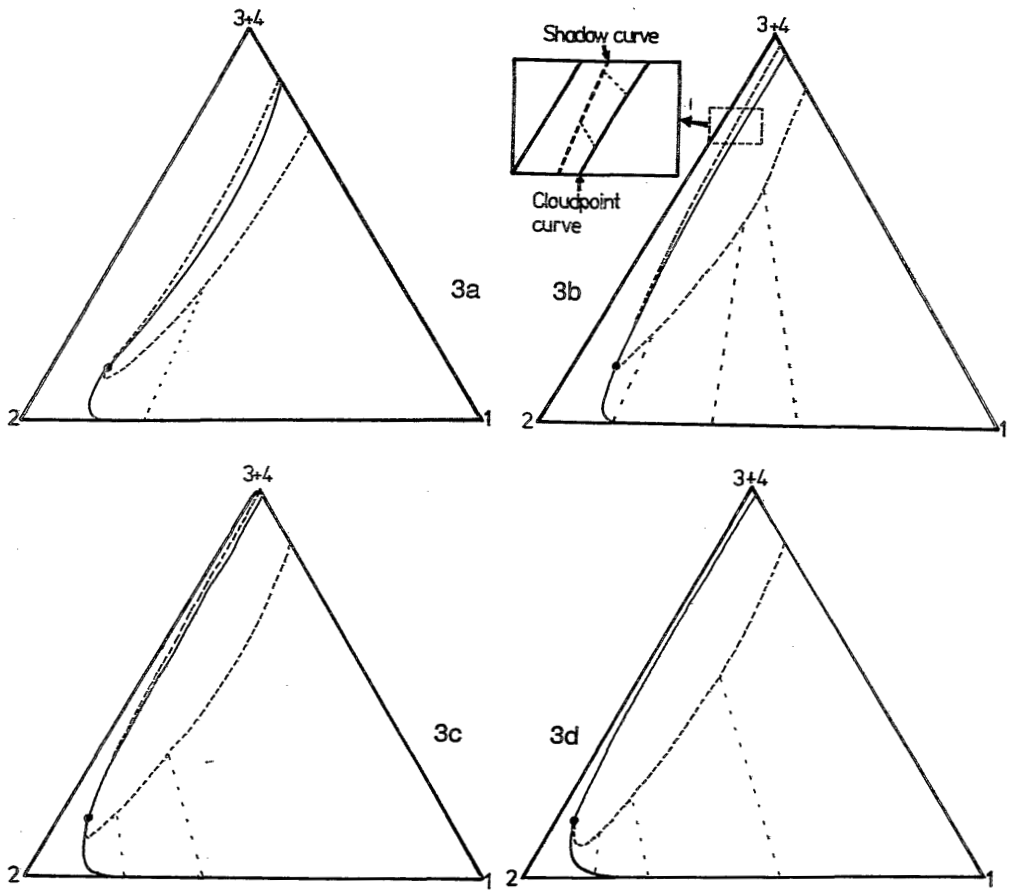

Figure 3: Cross-sections through quaternary phase diagrams at a constant ratio between the concentrations of components 3 and 4 (1:1).
Figure 3a: molecular weight of component 4 is equal to the molecular weight of component 2 (99.12 g/mole); figure 3b: mol. weight of component 4 is: 1000 g/mole; figure 3c: 3000 g/mole; figure 3d: 10 kg/mole.
Uninterrupted lines: cloudpoint curves; dashed lines: compositions at equilibrium with the cloudpoint line (shadow curves).

With increasing polymer concentration in the cloudpoint phase the cloudpoint approaches the critical line and crosses it at a certain composition. This point is given as a black dot in figures 3 and 4. It represents the critical point in our semi-ternary cross-section. At higher polymer concentrations in the cloudpoint phase, the shadow curve represents the polymer 3 lean phase, and the cloudpoint curve the component 3 rich phase.
It is interesting that at higher concentrations of the polymers, the total concentrations of polymer (component 3 and 4 together) in the two phases are almost equal.

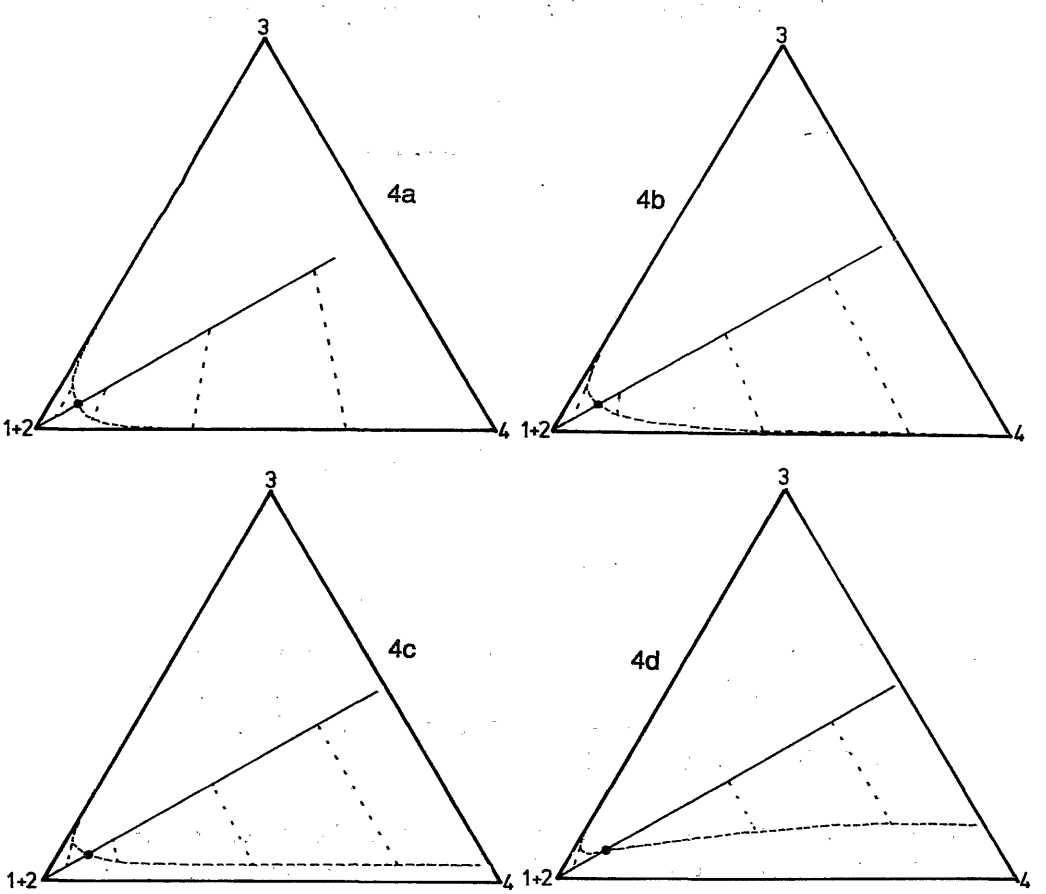

Figure 4: Ternary plots for the same cloudpoint curves as in figure 3. Here the low molecular weight components 1 and 2 are taken together. In this fashion the separation between the two higher molecular weight components can be monitored. Molecular weight of component 4 is: 99.12 g/mole in figure 4a, 1000 g/mole in figure 4b, 3000 g/mole in figure 4c and 10 kg/mole in figure 4d.

The difference between cloudpoint phase and incipient phase is mainly the ratio between the polymers 3 and 4. The total concentration of nonsolvent and solvent in both phases are practically the same. This effect is most strongly present at higher molecular weights of component 4.

It appears that with increasing molecular weight of the additive (component 4), the compatibility of the system with the nonsolvent 1 is decreasing. Figure 5 shows the amount of nonsolvent 1 in the solution at the cloudpoint, for solutions containing 10 volume% of component 3 and 10 volume % of component 4. The molecular weight of component 4 is varied.

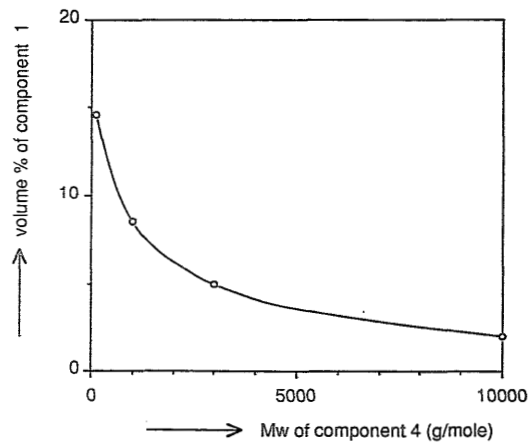

Figure 5: The amount of nonsolvent 1 that can be dissolved in a polymer solution containing 10 volume% of component 3 and 10 volume% of component 4. The molecular weight of component 4 was varied from the molecular weight of component 2 (99.12 g/mole) to 10 kg/mole.

At high concentrations of component 3 and 4 the concentration of component 3 in the phase that is lean in 3, is small when using low molecular weight component 4. The low molecular weight component 4 acts as a normal solvent for component 3. For higher molecular weights of component 4, however, the situation is different. We would expect that if the molecular weight of 4 increases, the separation between 3 and 4 should increase. In fact, in our semi-ternary cross-sections (figure 4) we see a

different behavior.
In figure 6 the calculated amount of component 3 in the incipient phase of a solution at the cloudpoint, containing 35 volume% component 3 and 35 volume% component 4 is given, as a function of the molecular weight of the additive. We see that when the molecular weight of 4 increases, the incipient phases contain more and more component 3. Therefore, it appears that the separation between 3 and 4 is decreasing. This stems from the fact that the critical line is bending upwards to higher polymer concentrations, when a high molecular weight component 4 is used. At high polymer concentrations on the cloudpoint curve, we come closer to the critical line; therefore the compositions of the two phases are nearing each other.
We will expand below on the consequences of the location of the critical line in the quaternary phase diagram.

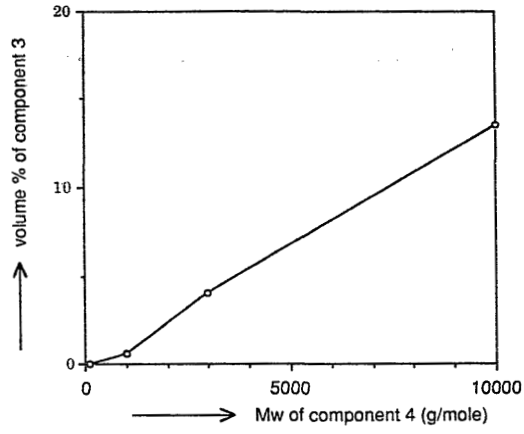

Figure 6: The amount of component 3 present in the incipient phase. The cloudpoint composition is fixed at 35 vol% of component 3, and 35 vol% of component 4. The molecular weight of component 4 is varied. It appears that with increasing molecular weight, more component 3 is present in the incipient phase.

2. Varying ratios of components 3 and 4.
In the preceding paragraph a constant ratio (1:1) of concentrations of components 3 and 4 was used. Figure 7 and 8 give cloudpoint curves of the

systems with a molecular weight of component 4 of 99.12, 1000 and 10 kg/mole. Three ratios ϕ_3/ϕ_4 are given: 2, 1 and 0.5.
It appears that with increasing concentration of component 4 the cloud-point line has not dramatically changed. A large influence however is exerted on the location of the critical point.

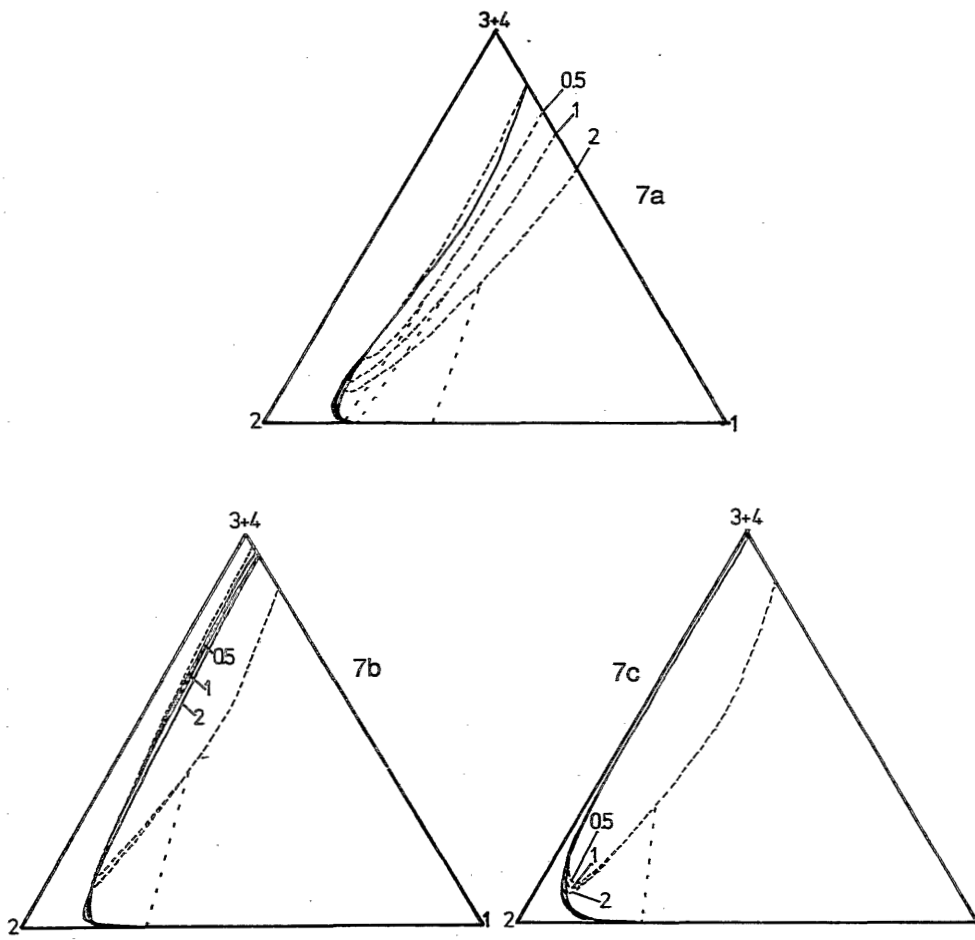

Figure 7: Semi-ternary cross-sections through phase diagrams; components 3 and 4 are plotted as one component. In each plot three ratios ϕ_3/ϕ_4 are drawn. Mol. weight of component 4 is: figure 7a: 99.12 g/mole; figure 7b: 1000 g/mole; figure 7c: 10 kg/mole. Uninterrupted lines are cloudpoint lines; dashed lines are shadow curves.

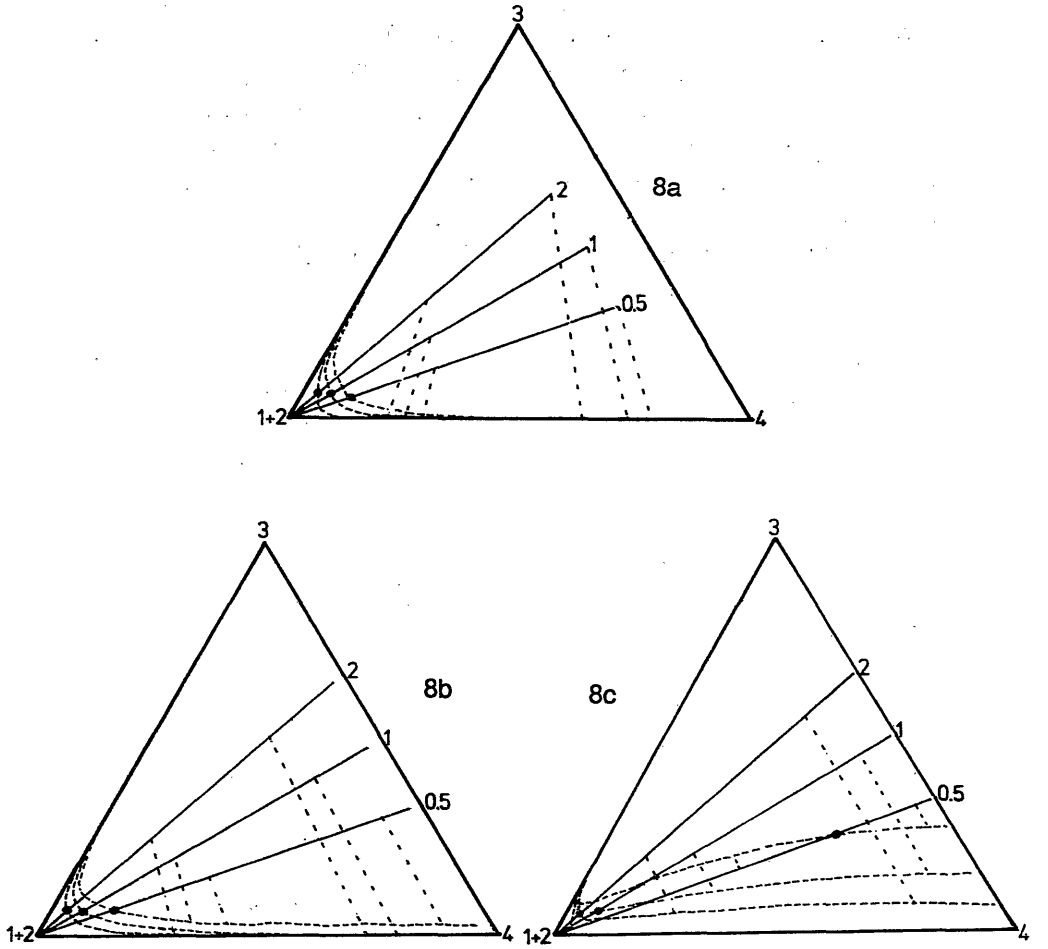

Figure 8: Plots for the cloudpoint curves shown in figure 7. The low molecular weight components 1 and 2 are plotted as one component. In each plot three ratios ϕ_3/ϕ_4 are drawn. Mol. weight of component 4 is: figure 8a: 99.12 g/mole; figure 8b: 1000 g/mole; figure 8c: 10 kg/mole.

With decreasing ratio ϕ_3/ϕ_4 (i.e. with *increasing* content of component 4), the critical point in these cross-sections is shifted to higher (total) polymer concentrations. From figure 8a it appears that the critical point is practically remaining at the same ϕ_3. This should be so, since component 4 is here equivalent to the solvent concerning molecular weights. This equivalence holds more or less up to 1000 g/mole for component 4 (figure 8b).

The situation is different for higher molecular weights of component 4. A decrease of the ratio ϕ_3/ϕ_4 then causes the critical point to shift upward. From the calculations it follows that at a ratio ϕ_3/ϕ_4 of 0.5, with a molecular weight of component 4 of 10 kg/mole, the critical point is situated at approximately 24 volume % of component 3, or 73 volume % of polymers 3 and 4 together (see figure 8c).
In figure 9 the phase diagrams of the ternary subsystems 1-3-4 corresponding to situations a, b and c in figures 7 and 8 are shown.

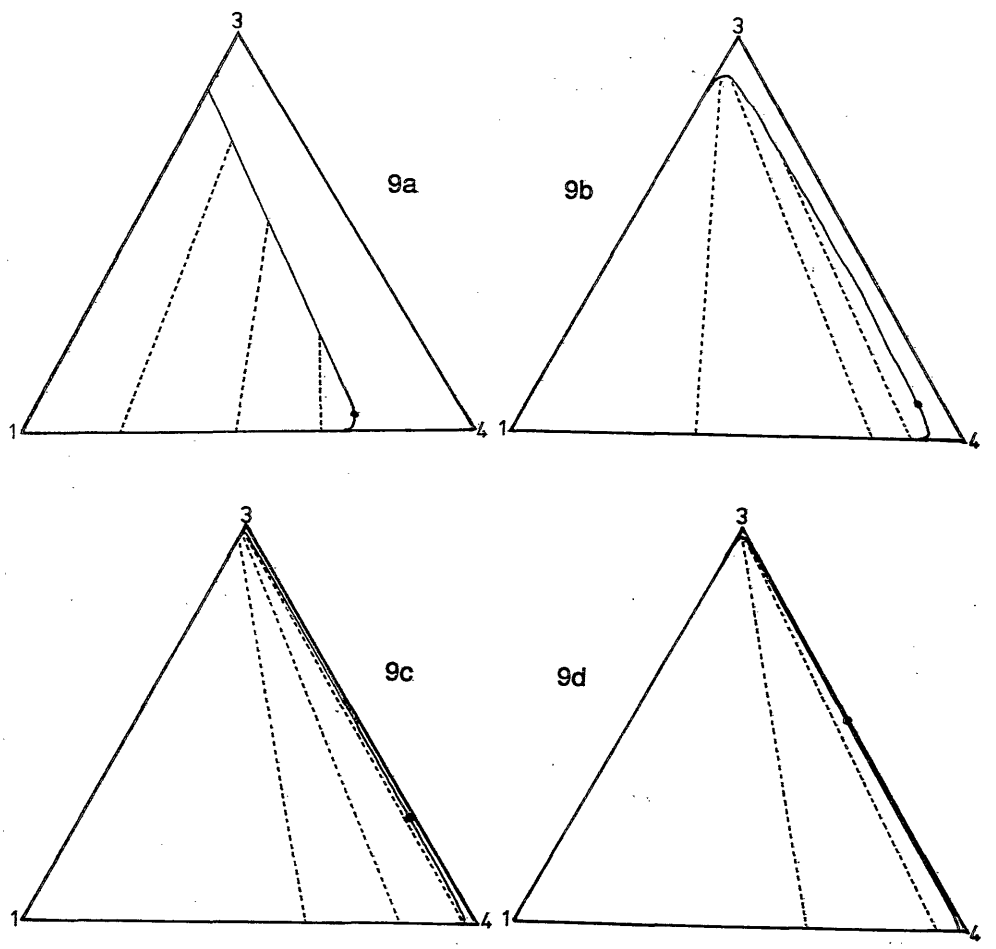

Figure 9: Ternary phase diagrams for the ternary subsystem 1-3-4. The molecular weight of component 4 is varied. Figure 9a: 99.12 g/mole, 9b: 1000 g/mole, 9c: 10 kg/mole, 9d: 100 kg/mole. The critical points are indicated by black dots.

The critical points in these ternary systems are shifting upwards with increasing molecular weight of component 4. This upward shift also occurs *inside* the quaternary phase diagram, when solvent 2 is present. This also results in the shifting upward of the critical line already at lower polymer contents, which gave the higher semi-ternary critical point.
In figure 8, we have seen that with increasing molecular weight of polymer 4, the critical point in the semi-ternary cross-section shifts upward. The critical lines themselves are shown in figure 10. These critical lines are the collection of critical points from the semi-ternary cross-sections, when the volume fraction of component 4 is systematically varied.
It follows from figure 10 that it must always be possible to have a planar cross-section that remains below the critical line. Since the critical line shifts more strongly upward with increasing molecular weight of polymer 4, the ratio ϕ_3/ϕ_4 at which the cross-section remains below the critical line is increasing for higher molecular weights of component 4.
It is therefore possible to have a semi-ternary cross-section through the quaternary phase diagram that does not contain a critical point. This implies that a solution with a ratio ϕ_3/ϕ_4 that corresponds with such a cross-section always shows nucleation of a polymer 3 rich phase, regardless of the polymer concentration; see figure 11. Membrane formation with such a solution must be impossible, since forming a porous membrane structure is closely connected with nucleation of a phase lean in polymer 3. The situation as depicted in figure 11 must lead to the formation of a dispersion of polymer 3 - rich droplets in a mixture of the other 3 components (see discussion section).

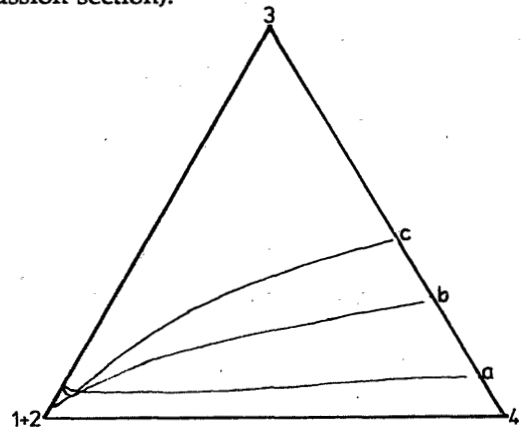

Figure 10: Semi-ternary representation of the critical lines in three systems with different molecular weights of component 4: a: 1000 g/mole, b: 10 kg/mole, c: 100 kg/mole.

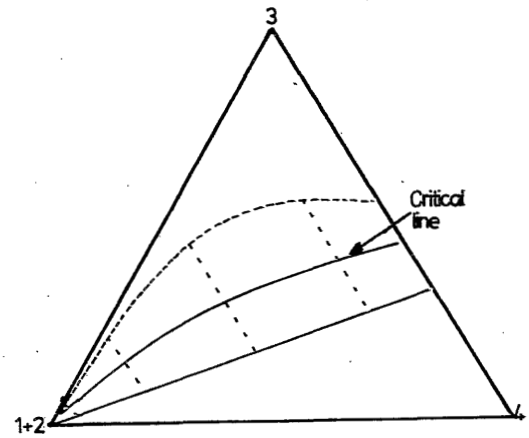

Figure 11: The situation for $\phi_3/\phi_4 = 0.5$ and molecular weight of component 4 = 100 kg/mole. The critical line always stays above this cross-section. The cloudpoint curve and the shadow curve never cross, and a critical point is not present.

3. Variation of the compatibility of the additive with nonsolvent and polymer 3.
The additive shows interactions with the three other components. The most important interactions are those with the nonsolvent and with the membrane forming polymer.
The interaction with the nonsolvent governs the tendency of the additive to be leached out of the polymer solution, into the coagulation bath. This is the most important property of an additive, which has led to the application of PVP as additive in MF and UF membranes[13-16].
The compatibility of the additive with polymer 3 is of course important since it controls the homogeneity of the resulting membrane: incompatible polymers will never form a membrane with a matrix that is homogeneous.

The influence of the interaction between the polymeric additive 4 and the nonsolvent 1 (e.g. the *hydrophilicity* of the additive PVP) is shown in figure 12, in which the interaction parameter g_{14} has been varied.
The cloudpoint line with $g_{14} = 0$ (this means a stronger mutual interaction than at $g_{14} = 0.5$) is shifted somewhat to lower nonsolvent content. At higher polymer concentrations (above 30 volume %) the cloudpoint curve remains the same.
The critical point of the cross-section appears to shift to lower polymer

concentration; the critical point shifts to only a few percent of polymer. Apparently the position of the critical point is dependent on the interaction parameters of the system.
An appreciably higher interaction parameter than 0.5 gives demixing between the additive 4 and the nonsolvent 1.

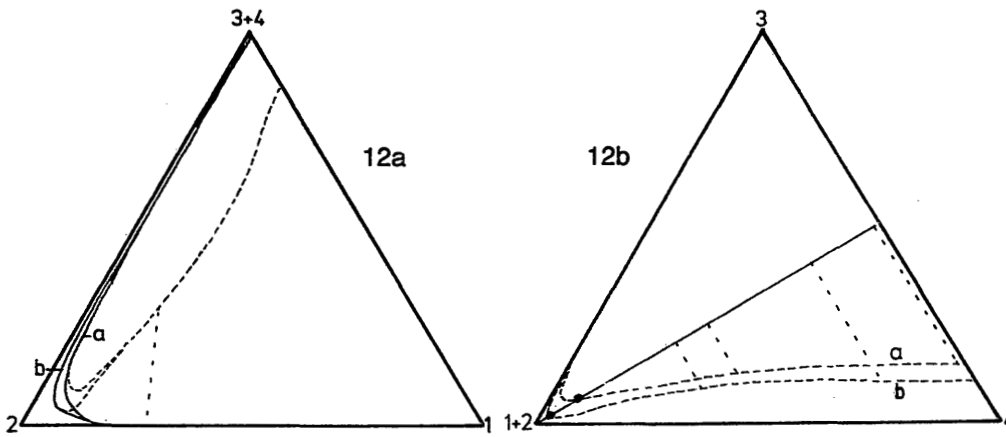

Figure 12: Variation of the interaction parameter between the polymeric additive 4 and the nonsolvent 1, g_{14}. The value was varied from 0.5 (a) to 0.0 (b).

The interaction between the two polymers is an important aspect of a system as considered here. The system we chose as an example (PES-PVP) has a strong interaction, i.e. a low interaction parameter g_{34}. In many systems PVP shows a strong interaction with the second polymer (e.g. with poly(ether imide)[16], or poly(ether amide)[24]). Figure 13 shows that actually the strength of the interaction is not very important as long as the two polymers remain miscible ($g_{34} \leq 0.5$). Only at very high polymer concentrations a difference can be seen in the shadow curve. A larger interaction parameter (i.e. weaker interaction) seems to promote separation between the two polymers over the two phases.

In the preceding discussion, it was assumed that the miscibilities between the various components remained as they were chosen. Figure 14 shows what happens when we abandon some of these assumptions.

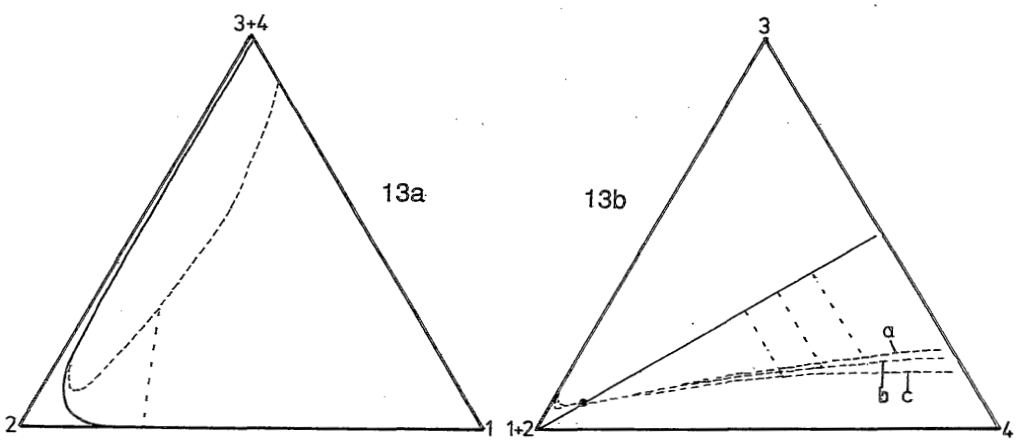

Figure 13: variation of the interaction parameter between 3 and 4, from -1.0 (a), to 0.0 (b) and to 0.5 (c). The ratio between the volume fractions of the two polymers 3 and 4 was kept at unity.

We can choose a polymeric additive that is not miscible with the membrane forming polymer (3). This is shown in figure 14a. The demixing gap now intersects the ternary subsystem 2-3-4. A solution that is concentrated in both polymers cannot be prepared anymore.

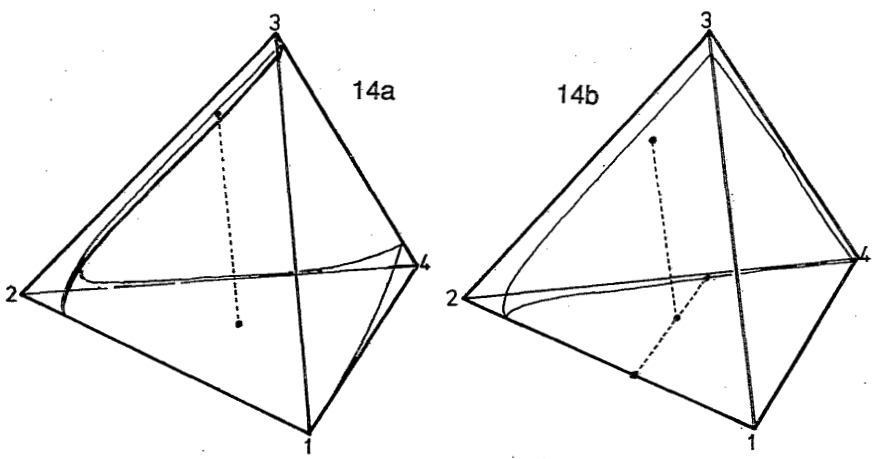

Figure 14: Situations in which the additive is incompatible with: (a): the membrane forming polymer 3, and (b): the nonsolvent 1.

We can also choose an additive that is not miscible with the nonsolvent, component 1. The phase diagram shown in figure 14b represents such a system. The tielines of the originally binodal surface now end at one side in a new ternary demixing gap, in the subsystem 1-2-4. The composition lean in polymer 3 demixes again in a phase rich in polymeric additive 4 and a phase rich in nonsolvent 1. Now we effectively have a three-phase equilibrium. A polymer solution containing a membrane forming polymer and a polymeric additive that is not compatible with the nonsolvent, which is immersed in a coagulation bath containing nonsolvent will exhibit a membrane matrix (rich in 3), a dispersed phase (rich in additive 4) and pores (rich in nonsolvent 1).
This situation is evaluated experimentally elsewhere[25].

Discussion

The molecular weight of component 4 has a profound influence on the thermodynamic properties of a quaternary membrane forming system as discussed here.
The higher this molecular weight is chosen, the higher is the concentration of the polymers at the intersection of the critical line with a certain cross-section through the quaternary phase diagrams. This effect is stronger at lower ϕ_3/ϕ_4 ratios (higher content of component 4). At a certain point the critical line does not even cross the planar cross-section at all anymore: there appears to be no critical point in the cross-section considered.
In this case a solution that is starting to demix (crossing the cloudpoint curve), will exhibit nucleation of a phase richer in component 3 than the original solution, since the shadow curve is situated at higher concentrations of component 3 than the cloudpoint curve itself. This situation can always be reached, when the concentration of component 4 in the polymer solution surpasses a certain minimum value. At higher molecular weights of component 4, this minimum amount of component 4 is smaller.
The implications of this phenomenon on membrane formation will now be discussed. A polymer solution containing components 2, 3 and 4 is contacted with a coagulation bath containing component 1. The polymer solution remains above the critical point as long as the concentration of component 4 is not very high. Any nuclei formed consist of a phase lean

in (membrane forming) polymer 3: a porous membrane will be formed.
At higher concentrations of component 4, the opposite can happen: the composition in the polymer solution that is crossing the cloudpoint curve is situated *below* the critical point: nuclei are formed that are richer in polymer 3 than the original solution. The consequence is that the continuous phase is lean in polymer 3 and richer in polymer 4. Polymer 4 dissolves in the coagulation bath, taking the nuclei rich in polymer 3 with it. The polymer solution dissolves, creating a dispersion of component 3 in the coagulation bath. In practice indeed there is a certain upper limit in the concentration of polymeric additive that can be used for membrane formation. The authors found it impossible to prepare membranes from a solution containing 15 weight % poly(ether sulfone) and 20 or more weight % poly(vinyl pyrrolidone) (of mol. weight app. 200 kg/mole) in n-methyl pyrrolidone. It leads to dissolution of the polymer solution while the coagulation bath is turning milky white. For further details see ref. 23.
In the previous lines, the situation was explained in terms of a nucleation and nucleus growth mechanism. The situation remains the same when a spinodal mechanism is taking place: the term nucleus should then be replaced by the term "phase with the smallest volume". The discussion is only performed here in terms of a nucleation and nucleus growth mechanism for matter of clarity.

At higher (total) polymer concentrations (e.g. 30 volume % of polymer) the phase separation is only taking place between the polymers 3 and 4. The incipient phase appears to have approximately the same concentration of nonsolvent 1 and solvent 2 as the cloudpoint phase from which it is formed. This is not expected, since polymer 4 is more compatible with the nonsolvent 1. One would therefore intuitively say that the phase richer in 4 should also be richer in 1. This appears not to be the case; one might say that at concentrations interesting for membrane formation (at least 20 % of polymer) phase separation only concerns phase separation between the two polymers. This result is used elsewhere for the modelling of mass transfer during immersion precipitation[21,22].
When the molecular weight of the polymeric additive increases, the amount of component 3 that is present in the phase lean in this component, is increasing, as shown in figure 6. This is only valid for the *cloudpoints;* i.e. it is only valid as long as the composition of the solution (at the cloudpoint composition) is not changed by mass transfer to the incipient phase (in other words, as long as the incipient phase is negligible in volume). Other calculations (not further evaluated here) show that

addition of somewhat more nonsolvent 1 to a cloudpoint composition (e.g. during immersion precipitation by indiffusion of nonsolvent from the coagulation bath) results in a very thorough separation between the two polymers. One phase then contains only components 1, 2 and 3 and the other contains only components 1, 2 and 4. In our calculations these concentrations of the expelled polymer can become smaller than 10^{-340}, showing that in this phase the fourth component is not present at all.
We can therefore assume that during immersion precipitation the two polymers have a driving force to separate completely. Whether they will do so depends to a large extent on the kinetics of mass transfer and on the rheology of each of the phases involved.

The interactions between the polymeric additive and the nonsolvent, and the membrane forming polymer appear not to be very important. A pair of polymers that is miscible but shows less interaction than is considered here will show approximately the same thermodynamic behavior. Polymers that do not mix will show a different behavior.
An additive that is not miscible with the nonsolvent but that is miscible with the membrane forming polymer will simply remain in the membrane matrix. It will be very hard to distinguish then between the two polymers. For membrane formation, the two polymers react as if they were one polymer.

An attempt was made to measure equilibrium compositions in the system that was chosen as model system (PES-PVP-NMP-water). This proved to be nearly impossible. The two resulting phases both contained quite some polymer (as is expected from the calculations); the resulting high viscosities of both phases prevented the two phases to become clear. Even after one year (thermostatted) sedimentation time, both phases remained turbid. To make a measurement of these compositions possible, other techniques must be developed to separate the phases in a reasonable time span.

Conclusions

It was shown that addition of a second polymer to a ternary polymer solution has a large influence on the properties of the system.
The critical point in the semi-ternary system consisting of polymer (3+4), nonsolvent and solvent, is shifting upwards with increasing concen-

tration and molecular weight of component 4. This leads to the expectation that when a certain lower limit in the concentration of component 4 is surpassed, the polymer solution does not form a membrane anymore; it dissolves while creating a dispersion of component 3. This may happen at quite high concentrations of membrane forming polymer 3. The concentration of component 4 required for this effect becomes lower when the molecular weight of polymer 4 increases. This theoretical forecast is in accordance with qualitative practical experience.
The interaction between the additive and the nonsolvent and the interaction between additive and the membrane forming polymer is not of great importance as long as miscibility is ensured.

List of Symbols

Indices indicate to the four components of the system:

1	*nonsolvent*
2	*solvent*
3	*membrane forming polymer*
4	*polymeric additive*

g_{ij}	interaction parameter between components i and j
n_i	number of moles of component i (mole)
s	$\underline{v}_1M_1/\underline{v}_2M_2$
r	$\underline{v}_1M_1/\underline{v}_3M_3$
R	gas constant (J/mol K)
t	$\underline{v}_1M_1/\underline{v}_4M_4$
T	temperature (K)
u_2	$\phi_2/(\phi_2+\phi_1)$
u_4	$\phi_4/(\phi_1+\phi_4)$
v_2	$\phi_2/(\phi_2+\phi_3)$
v_3	$\phi_3/(\phi_3+\phi_4)$
w_2	$\phi_2/(\phi_2+\phi_4)$
ΔG_m	free enthalpy of mixing (J)
$\Delta\mu_i$	chemical potential of mixing
φ_i	volume fraction of component i (-)
χ_{ij}	concentration independent version of g_{ij}

References

1. S. Loeb, S. Sourirajan, Adv. Chem. Ser. **38** (1962) 117
2. M.H.V. Mulder, Basic Principles of Membrane Technology, Elsevier, Amsterdam, 1991
3. H.Strathmann, Trennung von Molekularen Mischungen mit Hilfe synthetischer Membranen, Darmstadt, 1979
4. R.E. Kesting, Synthetic Polymer Membranes, McGraw-Hill, New York, 1972
5. C. Cohen, G.B. Tanny, S. Prager, J. Polym. Sci., Polym. Phys. Ed. **17** (1979) 477
6. A.J. Reuvers, J.W.A. van den Berg, C.A. Smolders, J. Membrane Sci., **34** (1987) 45
7. C.C. Hsu, J.M. Prausnitz, Macromolecules, **7** (1974) 320
8. F.W. Altena, C.A. Smolders, Macromolecules, **15** (1982) 1491
9. A.J. Reuvers, C.A. Smolders, J. Membrane Sci., **34** (1987) 67
10. A.J. McHugh, L.Yilmaz, J. Membrane Sci., **43** (1989) 319
11. C.S. Tsay, A.J. McHugh, J. Polym. Sci., Polym. Phys. Ed., **28** (1990) 1327
12. C.S. Tsay, A.J. McHugh, J. Polym. Sci., Polym. Phys. Ed., **29** (1991)
13. P. Aptel, N. Abidine, F. Ivaldi, J.P. LaFaille, J. Membrane Sci., **22** (1985) 199
14. L.Y. Lafrenière, F.D.F. Talbot, T. Matsuura, S. Sourirajan, Ind. Eng. Chem. Res. **26** (1987) 2385
15. T.A. Tweddle, O. Kutowy, W.L. Thayer, S.Sourirajan, Ind. Eng. Chem. Prod. Res. **22** (1983) 320
16. E. Roesink, Microfiltration, Membrame Development and Module Design, thesis, University of Twente, The Netherlands, 1989
17. J. Flory, Principles of Polymer Chemistry, Cornell University Press, New York, 1953
18. H. Tompa, Polymer Solutions, Butterworths, London, 1956
19. R. Koningsveld, A.J. Staverman, J. Polym. Sci., Part A-2, **6** (1968) 305
20. G. Tkacik, L. Zeman, J. Membrane Sci., **31** (1987) 273
21. Chapter 3 of this thesis
22. R.M. Boom, I.M. Wienk, Th. van den Boomgaard, C.A. Smolders, Microstructures in Membranes II; the Role of a Polymeric Additive, accepted for publication in J. Membrane Sci.; first appendix to this thesis
23. Chapter 4 of this thesis
24. E. Schchori, J. Jagur-Grodzinski, J. Appl.Pol. Sci. **20** (1976) 1665
25. Chapter 5 of this thesis

First Appendix to Chapter 2

Measurement of the Binary Interaction Parameters of PES and NMP, PVP and NMP, and PES and PVP by Means of High-pressure Osmometry

R.M. Boom, H.W. Reinders,
Th. van den Boomgaard, C.A. Smolders

Summary

High-pressure osmometry was used to measure the osmotic pressure of solutions of PVP and PES in NMP, relative to pure NMP. A membrane was used that did not show any permeability for the polymers, thus enabling accurate measurement of the osmotic pressure. The modified Flory-Huggins theory is used to convert the osmotic pressures into linearly concentration dependent interaction parameters.
By measuring the osmotic pressure of a ternary solution of PES and PVP together in NMP (relative to pure NMP), and applying the values found for the binary interaction parameters of PES-NMP and PVP-NMP in the Flory-Huggins theory, the interaction parameter between PES and PVP in the solution could be estimated.
The interaction parameters of PES-NMP and PVP-NMP appeared to lie around 0.5, indicating that NMP is a theta-solvent for PES and PVP. Interaction between PES and PVP appeared to be quite strong: the measured values of the interaction parameter were between -0.5 and -1.

Introduction

The thermodynamics of a polymeric system are determined by its parameters: the molecular weight of the components and the interaction parameters between the components[1]. For description of the dependency of the free enthalpy of mixing the Flory-Huggins theory[1] will be used, in which we will assume concentration dependent interaction parameters (usually called the modified Flory-Huggins approach).

The interaction parameters are a measure of the enthalpic interaction between the components; moreover they contain a non-ideality term. The determination can be performed in a number of ways. Well known are static light scattering[2] and osmometry[3]. Especially the latter method is suitable for measuring concentrated polymer solutions.
Studied here is the ternary system poly(ether sulfone) - poly(vinyl pyrrolidone) - n-methyl pyrrolidone. Solutions prepared from these components are used, together with water (a nonsolvent for PES) to prepare microfiltration and ultrafiltration membranes with outstanding properties[4-8].
The interaction between the two polymers (present in the same solution) is an important parameter. It is known that PES and PVP can blend homogeneously[4], indicating that without solvent the interaction parameter probably has a value lower than 0.5.
It is essential that at least an estimate of the interaction between the two polymers can be made. This should be done in a situation that is reasonably close to the circumstances that are valid during membrane formation. Measurement of interaction of the pure polymeric blend (e.g. by X-ray scattering experiments[9]) would not yield information that can be reliably extrapolated to a solution of 30 weight% of total polymer in a solvent.
The method we chose is as follows. First the binary systems PES-NMP and PVP-NMP are measured by osmometry. Then the ternary system PES-PVP-NMP is measured by the same method. Using the Flory-Huggins theory one is able to describe the ternary situation from binary interactions. By using of the binary interaction parameters for PES-NMP and PVP-NMP, we can obtain an estimate of the interaction between PES and PVP in a solution of NMP.

Theory

Binary systems
The Flory-Huggins theory gives the following relation for the chemical potential of mixing of the solvent in a polymeric solution:

$$\frac{\Delta\mu_2}{RT} = \ln\phi_2 + (1-\phi_2)\left(\frac{\bar{v}_3 M_3 - \bar{v}_2 M_2}{\bar{v}_3 M_3}\right) + (1-\phi_2)^2\left(\frac{\partial\phi_2 g_{23}}{\partial\phi_2}\right) \qquad 1)$$

in which the indices 2 and 3 denote respectively solvent and polymer, ϕ_i is the volume fraction of component i, $\bar{v}_i$ the specific volume and M_i the

molar mass of component i, and g_{23} the (concentration dependent) interaction parameter between component 2 and 3.
The chemical potential of mixing of the solvent given by equation 1 is related to the osmotic pressure relative to pure solvent $\Delta\pi$:

$$\frac{\Delta\mu_2}{RT} = -\Delta\pi\frac{\bar{v}_2 M_2}{RT} \qquad 2)$$

The osmotic pressure is measured; all other parameters in equations 1 and 2, except the interaction parameter, g_{23}, are known. Hence the value of g_{23} can be found from relations 1 and 2.
In this way the interaction parameters were obtained for the binary systems PES-NMP and PVP-NMP.

Ternary systems
Analogous to the binary situation, the chemical potential of mixing of the solvent can be derived for the situation in which *two* polymers (3 and 4) are dissolved (relation analogous to Reuvers[10]):

$$\frac{s\,\Delta\mu_2}{RT} = \ln\phi_2 - \phi_4 - r\,\phi_3 + (s + g_{24}\,\phi_4 + s\,g_{23}\,\phi_3)(1-\phi_2) - g_{34}\,\phi_3\,\phi_4 + \phi_4\,w_2(1-w_2)\frac{\partial g_{24}}{\partial w_2} + s\,\phi_3\,v_2(1-v_2)\frac{\partial g_{23}}{\partial v_2} \qquad 3)$$

The symbols are analogous to previous work[10,11]:

$$s = \frac{\bar{v}_4 M_4}{\bar{v}_2 M_2}; \qquad r = \frac{\bar{v}_4 M_4}{\bar{v}_3 M_3} \qquad 4)$$

while

$$v_2 = \frac{\phi_2}{\phi_2 + \phi_3}; \qquad w_2 = \frac{\phi_2}{\phi_2 + \phi_4} \qquad 5)$$

In relation 3 the interaction parameters g_{24} and g_{23} are known from previous measurements; the parameter g_{34} is unknown.
The value of the chemical potential difference (as given by relation 3) is obtained by measuring the osmotic pressure difference of a solution containing polymers 3 and 4, compared to the pure solvent. By using relation 2 and 3 together, the value of g_{34} can be found.

Interactions that are purely ternary in nature (a so-called ternary interaction parameter g_{234}) are neglected from relation 3. The results may be influenced by this assumption.

Experimental

The osmometer

As was shown by Staverman[12], special care should be taken to ensure that *equilibrium* is measured instead of under conditions of a constant (small) flux through the membrane. If the membrane, being used to separate the pure solvent from the polymer solution, is only slighty permeable for the (lower molecular weight fractions of the) polymer or polymers, a low flux of solvent through the membrane is always present, and real equilibrium is never obtained. The friction of the solvent with the membrane then results in an erroneous value for the osmotic pressure.

We therefore chose a membrane that only swells a few percent in the solvent used (NMP). It was found that Cuprophan™ membranes fulfill the requirements, while being resistant enough to enable long-term experiments.

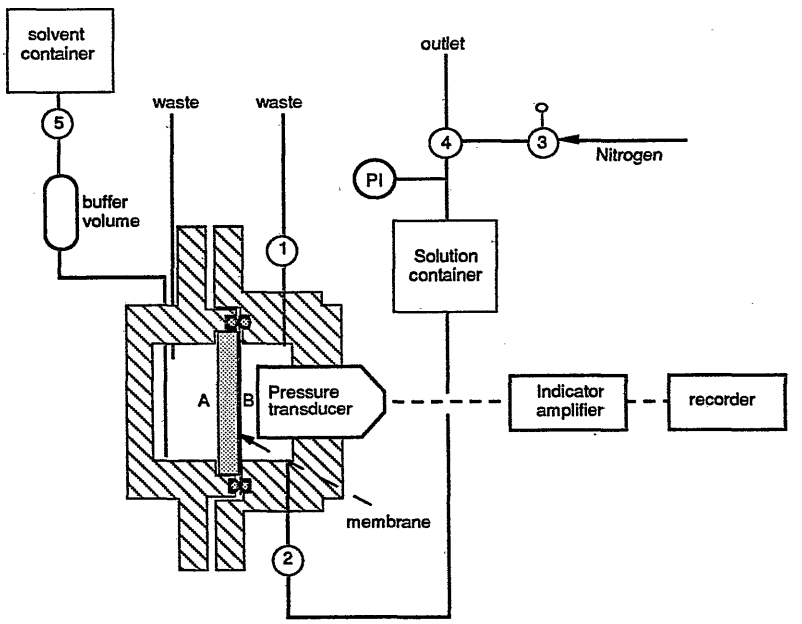

Figure 1: Experimental setup. Circles represent valves. Side A is the low (atmospheric) side, side B the high pressure side. The pressure was preset with valve 3 before each measurement. The complete setup was immersed in a thermostat bath kept at 298 K.

The experimental set-up is represented in figure 1.
Before the measurement valves 1, 2 and 3 are opened (4 is set into the position allowing transport to the solution container). A pressure is applied on the polymer solution in the solution container (up to 8 bar). The solution is slowly pushed into the cell. Valve 1 is closed, and with valve 3 the pressure is brought on the osmotic pressure as found from previous measurements. Then valve 2 is closed.
Side A of the cell, and the buffer container is filled with solvent.
The pressure is followed (resolution of 1 mbar) as a function of time. The pressure will converge to the osmotic pressure. The solvent at the solvent side (A) of the cell is refreshed several times to check for any polymer permeating through the membrane. Any permeability at all for the polymer should result in a slightly higher osmotic pressure after the refreshment. This was never observed.
The procedure is repeated several times in order to check for reproducibility, which was typically around a few tens of millibars.

Materials used
A Cuprophan™ membrane with a dry thickness of 8 μm was applied. The membrane was allowed to equilibrate in pure solvent (NMP), before application in the cell.
Poly(ether sulfone), Victrex 5200 P (ICI ltd.), with M_w = 43 800 g/mole, and M_n = 22 300 g/mole, was dried at least for 12 hours at 80 °C before usage. No further purification was applied. Poly(vinyl pyrrolidone), grade K30 from Jansen Chimica, M_w = 18 100 g/mole, and M_n = 8700 g/mole, was used without further purification. Special care was taken to avoid water sorption. N-methyl-2-pyrrolidone, or NMP, from Merck, synthesis grade, was used as received.
The solutions were not filtered before use, since the presence of any particles which are much larger than the typical size of the blobs in the solution is not important: their *mole* fraction will be negligible.

Results

The low swelling of the membrane results in a negligible permeability for the polymer through the membrane. The permeability for the solvent was also quite low: about 6 hours were needed to attain equilibrium.
The osmotic pressure did not show any decrease with time: even after two weeks the pressure was still within 10 mbar of the initial equilibrium value, during a single measurement (of course this was only checked a few

times).
Refreshing the solvent after some time should result in an increase of the pressure difference whenever polymer molecules would have diffused into the solvent compartment. We never saw any effect of refreshment at the solvent side.
Thus we could be reasonably sure that the measured pressure difference is indeed the actual osmotic pressure difference.

Since in literature[2,13,14] often linear dependencies of the interaction parameters on the composition are found, we assumed a linear dependence of the interaction parameters on the concentration.
Figure 2 gives the values found for PVP in water and NMP. The PVP-water measurements are used as a check for the validity of the experiments. Literature[15,16] gives a value of 0.48 for g_{14} at $\phi_4 = 0$. Our measurement of 0.475 is in excellent agreement. Figure 3 gives the values found for the binary systems PES-NMP and PVP-NMP (included for comparison). Reproducibility of the measurements was within a few percent.

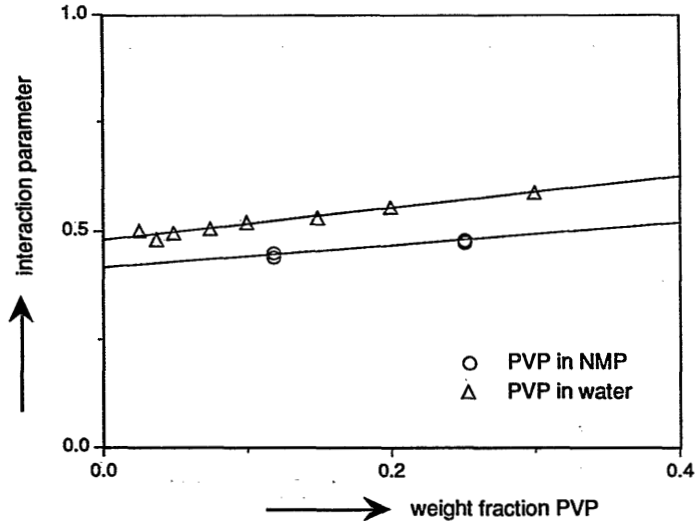

Figure 2: Interaction parameter of PVP in water and NMP. The results for PVP in water are in excellent agreement with literature values.[15,16] All measurements were performed at least in triplo; especially at higher polymer concentrations the value for g_{ij} was quite accurate; only one point could be drawn.

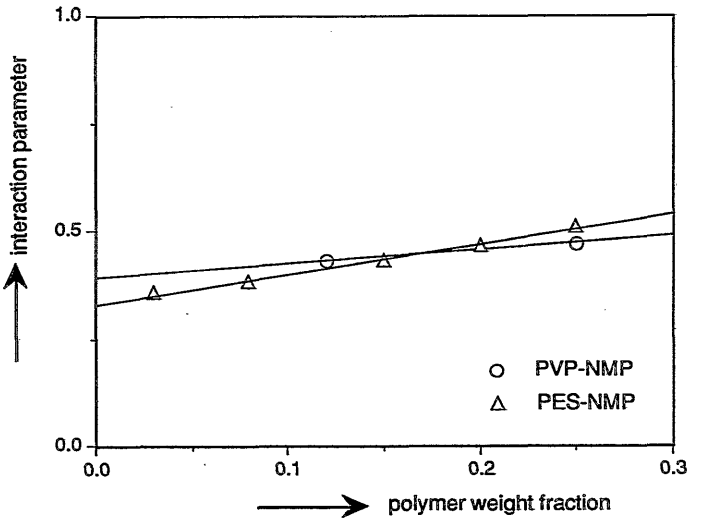

Figure 3: The concentration dependent interaction parameters for the systems PES-NMP; the system PVP-NMP is included for comparison. Reproducibility was again quite good.

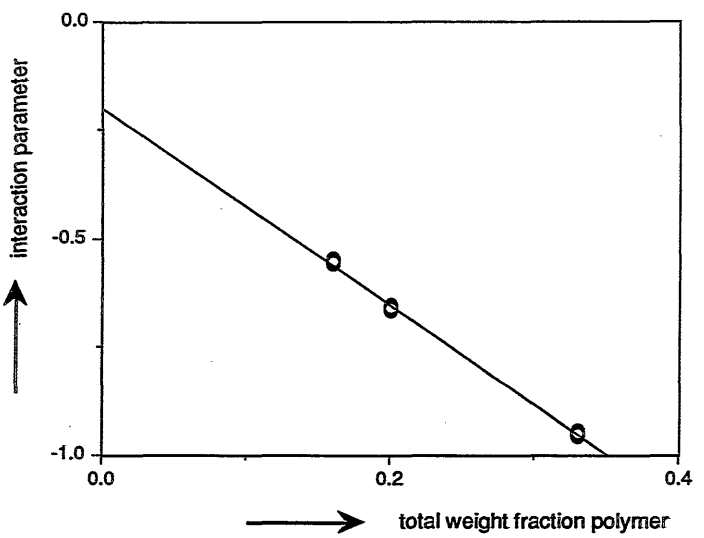

Figure 4: The interaction parameter between PES and PVP, as determined with high-pressure osmometry, measured with a ratio between PES and PVP of 2:1. Reproducibility was now slightly worse, although still within a few percent.

It appears that the interaction of PES with NMP is not very strong: the value of somewhat lower than 0.5 suggests almost theta-conditions. This is in agreement with the results by Tkacik and Zeman from static light scattering. The interaction of PVP and NMP is comparable with the interaction of PES and NMP.
The ternary experiments were done with a fixed ratio between PES and PVP of 2.03 : 1. From the measurements, the interaction between PES and PVP turns out to be quite strong: measurements give a value of -0.5 to -1.0. This indicates that the two polymers have a strong enthalpic interaction.

Discussion

The results from PVP in water indicate that our experimental set-up is quite reliable.
PVP seems to have only a weak enthalpic interaction with either water or NMP (the interaction with NMP is somewhat stronger). It is to be expected that PVP should not have high (enthalpic) interaction with NMP, since the structure of a molecule of NMP strongly resembles a segment of the PVP molecule. In the case of a polymer dissolved in its monomers, the enthalpic interactions should be zero (theta-conditions). Therefore these measurements are in agreement with the expectations.
PES has approximately the same interaction with NMP as PVP has. The results are in agreement with light scattering experiments[17]. The authors were not able to carry out accurate static light scattering experiments, since the solutions of PES in NMP always appeared to be slightly turbid. Wijmans and Smolders[18] found that this type of turbidity (in their case of polysulfone) was due to crystallization of oligomeric fractions of the polymer. GPC measurements indeed indicate that we also have a significant amount of oligomers in our polymer.

The measurement of ternary solutions is only carried out for one fixed ratio between the two polymers. For a complete picture of the interaction between the polymers we need to evaluate more mixing ratios. With the available results we can conclude that the interaction between the two polymers is strong. Roesink[4] found that a blend of PES and PVP gave only one glass transition temperature, indicating that homogenous blends were prepared. From the dependency of the glass transition on the composition he could conclude that the interaction between the two polymers is strong. He found that many (membrane forming) polymers show a strong interaction with PVP. What exactly causes of the ease of blending of a

variety of polymers with PVP is not known.

It should be noted that in our equation 3 we neglected any ternary parameters, resulting from ternary interactions[3]. Any of these effects are lumped together in the PES - PVP interaction parameter. Therefore, although the repreducibility was always within a few percent, the values measured for PES - PVP should not be seen as highly exact.

Conclusions

High-pressure osmometry appears to be a powerful tool to determine interaction parameters in binary solutions of polymers, and a good method to obtain information on the interaction parameter between two polymers in a (ternary) solution.
The results show that NMP is more or less a theta solvent for PES and PVP.
The interaction between PVP and PES appears to be very strong. The measured values of the interaction parameter lie between -0.5 and -1.0. Since only one fixed ratio between the concentrations of the polymers was measured so far, more measurements need to be carried out to obtain a complete impression.
It appears that the value suggested by Tkacik and Zeman for PES-NMP (g_{23} = 0.5) is reasonable; for qualitative evaluation, the interaction parameter for PVP-NMP can also be assumed to be 0.5. For the PES-PVP couple a low value has to be assumed: between -0.5 and -1.0.

Literature

1 P.J. Flory, Principles of Polymer Chemistry, Cornell Univ. Press, New York, 1953
2 Th.G. Scholte, Eur. Polym. J., 6 (1970) 1063;
3 F.W. Altena, Phase Separation Phenomena in Cellulose Acetate Solutions in Relation to Asymmeric Membrane Formation, thesis, University Twente, 1982
4 H.D.W. Roesink, Microfiltration, membrane development and module design, thesis, University of Twente, The Netherlands, 1989
5 P. Aptel, N. Abidine, F. Ivaldi, J.P. LaFaille, J. Membr. Sci. 22 (1985) 199
6 T.A. Tweddle, O. Kutowy, W.L. Thayer, S. Sourirajan, Ind. Eng. Chem. Prod. Res. Dev. 22 (1983) 320
7 L.Y. Lafrenière, F.D.F. Talbot, T. Matsuura, S. Sourirajan, Ind. Eng. Chem.

Res. **26** (1987) 2385

8 Q.T. Nguyen, L.L. Blanc, J. Neel, J. Membrane Sci., **22** (1985) 245

9 T. Koch, G.R. Strobl, J. Polym. Sci, Pol. Phys., **28** (1990) 343

10 A.J. Reuvers, J.W.A. van den Berg, C.A. Smolders, J. Membrane Sci., **34** (1987) 45

11 chapter 2 of this thesis

12 A.J. Staverman, Rec. Trav. Chim. Pays-Bas **70** (1951) 344

13 A.J. Reuvers, C.A. Smolders, J. Membrane Sci., **34** (1987) 67

14 Ph. Radovanovic, S.W. Thiel, S.-T. Hwang, J. Membrane Sci., **65** (1992) 213

15 F. Franks, Water Solubility and Sensitivity-Hydratation Effects, in: C.A. French (Ed.), Chemistry and Technology of Water-Soluble Polymers, Plenum Press, New York, 1983, 157

16 L.C. Cerny, T.E Helminiak, J.F. Meier, J. Polym. Sci, **44** (1960) 539

17 G. Tkacik, L. Zeman, J. Membrane Sci., **31** (1987) 273

18 J.G. Wijmans, C.A. Smolders, Eur. Polym. J., **13** (1983) 1143

Second Appendix to Chapter 2

The Influence of a Second Polymer on the Cloudpoint Curve in Quaternary Polymer Solutions

R.M. Boom, E.Rolevink, U. Cordilia,
Th.van den Boomgaard, C.A. Smolders

Summary

Experimental cloudpoint data are compared with calculations of the cloudpoint curve according to the Flory-Huggins theory, which were given earlier[1]. The effects found in the system water-NMP-PES-PVP were in accordance with results from literature for the comparable system water-NMP-PEI-PVP.

The qualitative conclusions are in agreement with the calculations: addition of a polymeric additive (that is miscible with all components including the nonsolvent) reduces the concentration of nonsolvent at the cloudpoint curve considerably. The higher the ratio of concentrations of PVP/PES, the stronger is the effect. The effects in practice are however smaller than those in the calculations. This is at least partially due to the polydispersities of the polymers, which were neglected in the calculations.

Introduction

We consider the cloudpoint compositions of a quaternary membrane forming system with two polymers:

1 - nonsolvent (water), miscible with components 2 and 4, immiscible with component 3
2 - solvent miscible with all components
3 - membrane forming polymer, immiscible with component 1
4 - polymeric additive, miscible with all components

Although it appeared that it was practically not possible to measure equilibrium compositions in such a quaternary system[1], the measurement of

cloudpoint compositions is relatively straightforward.
These cloudpoint compositions can then be compared with earlier[1] theoretical predictions.

Experimental

Poly(ether sulfone), Victrex 5200 P, supplied by ICI ltd. (M_w = 43 800 g/mole, M_n = 22 300 g/mole), was dried for at least 12 hours at 80 °C before usage; no further purification was applied. Poly(vinyl pyrrolidone), grade K90 (M_w = 228 200 g/mole, M_n = 99 800 g/mole) from Jansen Chimica, was used as received. N-methyl-2-pyrrolidone (NMP) was obtained from Merck, synthesis grade, and used as received. Water was demineralized and ultrafiltrated. All solutions were prepared with special care to prevent sorption of water from the air.
The cloudpoints were determined by a simple titration measurement. Thermostatted flasks were filled with an amount of the polymer solution. With a syringe water was added very slowly. The cloudpoint was defined as the composition at which the solution did not become clear again after 12 hours of homogenation. All cloudpoint measurements were performed at 298 K. Although some authors use temporary heating of the solution to enhance the homogenation process[2], this was not done, since this can lead to loss of water from the solution (due to the large difference in boiling points of water and NMP).
For details on the calculation procedure we refer to other work[1].

Results

Figure 1 shows the experimentally determined cloudpoints for the system water-NMP-PES-PVP, for different ratios between the two polymers. The use of PVP clearly reduces the water content at the cloudpoint curve.
Figure 2 shows results by Roesink[3] obtained in our laboratory, for the system water-NMP-PEI-PVP (PEI stands for poly(ether imide)). Also in this system we see a large influence of the addition of PVP. We clearly see that the addition of PVP to the solution results in a large decrease of the water content at the cloudpoint compositions.
In figure 3 the experimental data are compared with some calculated cloudpoint curves. Details on the calculation procedures are given

elsewhere[1]. It appears that, to obtain a reasonable fit of the experimental data, one has to assume a molecular weight of the additive that is a hundred-fold lower than the real number-average molecular weight of the additive (1000 g/mole instead of 99 800 g/mole).

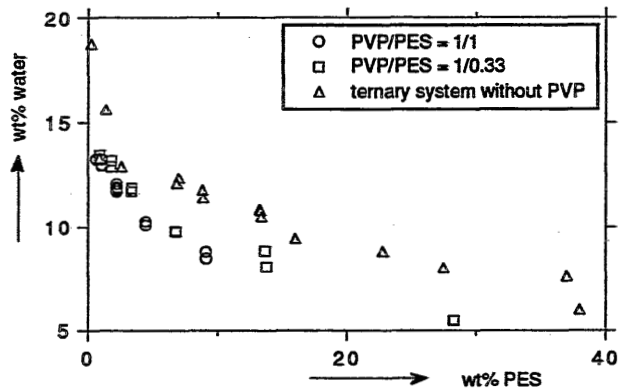

Figure 1: Experimental cloudpoints at 298 K, for three different weight ratios of PVP to PES (mol. weights are mentioned in the experimental section). One can see that the addition of PVP results in a lower water concentration at the cloudpoint composition.

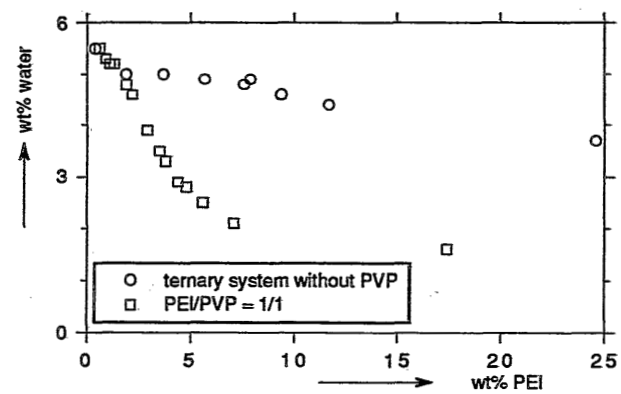

Figure 2: The effect of PVP on the cloudpoint compositions in the system water-NMP-PEI-PVP (the same type of PVP as used with PES). Measurements were performed at 20.1 to 21.5 °C. After Roesink[3].

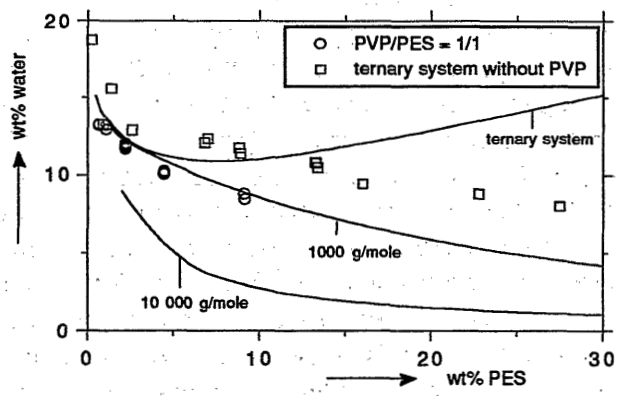

Figure 3: Comparison of experimental cloudpoints with calculations[1] for the ternary systems water-NMP-PES (a) and the quaternary system water-NMP-PES-PVP (b) in which the ratio of PVP over PES is kept at 1/1 (wt%/wt%).

Discussion

It is clear that the addition of PVP K90 reduces the amount of water that can be added to both PES-NMP and PEI-NMP solutions. A larger ratio of concentrations of PVP/PES results in a lower water content at the cloudpoint.
These conclusions followed also from calculations[1]. Figure 3 shows however, that the agreement is not more than qualitative.
It appears that for this range of concentrations, the predicted binodal for the basic *ternary* system is not very accurate. This is probably caused by the polydispersity of the polymer. Around the critical point (situated at about 8 wt% of PES, for the ternary system[4]) the influence of the polydispersity cannot be neglected[5], as was done in the calculations.
In the quaternary systems, the effect of PVP is exaggerated by the calculations, compared to the experiments, concerning the molecular weight of the PVP. This may at least partly be caused by the polydispersity of the polymers. Especially when two polymers are present, effects of polydispersity can not be neglected.
A polydisperse polymer holds only a limited fraction of high molecular weight molecules. The concentration of this fraction in the (polydisperse)

solution is lower and therefore their effect is smaller (it follows from figure 2 that the effect is smaller at smaller PVP concentrations, as expected). The lower molecular weight components of the polymer do not have such a pronounced effect on the cloudpoint composition[1]. The net result is that the cloudpoint composition of a system with polydisperse polymers may be situated at higher nonsolvent concentrations than the cloudpoint composition of a system with monodisperse polymers.
It was shown from calculations before[1] that for quaternary systems considered (PES/PVP = 1/1) both phases (the cloudpoint phase and the incipient phase) do contain polymeric substance. Moreover, the separation of the polymers over the two phases, at the cloudpoint, is not complete: both phases still contain both polymers. Unlike ternary systems with one polymer, this remains so even at quite high polymer concentrations. This incomplete separation of the polymers leads to strong effects of polydispersity[5], which influences the composition of the cloudpoints considerably.

Conclusions

The qualitative thermodynamic behavior of the solutions containing two polymeric species can be easily understood with the help of calculations based on the Flory-Huggins approach in which the polydispersities are neglected.
Addition of PVP reduces the concentration of water at the cloudpoint curve. A larger amount of PVP (relative to the amount of the other polymer) results in a larger effect on the cloudpoint composition.
For adequate *quantitative* description of the cloudpoint curve of a quaternary system, polydispersity of both polymers should be taken into account.

Literature

1. Chapter 2 of this thesis
2. W.W.Y. Lau, M.D. Guiver, T. Matsuura, J. Membrane Sci., 59 (1991) 219
3. E. Roesink, Microfiltration, Membrane Development and Module Design, thesis, University of Twente, The Netherlands, 1989
4. Chapter 6 of this thesis
5. R. Koningsveld, A.J. Staverman, J. Polym. Sci., Part A-2, 6 (1968) 305

Chapter 3

Mass Transfer and Thermodynamics During Immersion Precipitation for a Four-Component System with Two Polymers

R.M. Boom, Th. van den Boomgaard, C.A. Smolders

Summary

An extended version of the mass transfer model by Reuvers *et al.* for a four-component system has been developed, which is shown to be generally valid for short times. If the fourth component is of polymeric nature and if the binary friction coefficient between the two polymers is assumed to be orders of magnitude larger than the other friction coefficients (which is correct for short times) this leads to a simplification of the system into a semi-ternary situation. The molecular weight of the additive should be higher than a certain minimum value to justify this assumption. The thermodynamics valid under this assumption are evaluated. A shift of the binodal to higher nonsolvent concentrations seems to indicate that the polymer solution is more compatible with the nonsolvent.

Initial composition paths (concentration profiles) are calculated. It appears that delay of demixing is not possible when a polymeric additive is used, which is soluble in the nonsolvent. The thermodynamic properties under these conditions are mainly determined by the interaction of both polymers and the solvent with the nonsolvent. Mutual interaction between the two polymers has no influence, as long as they are still miscible.

Introduction

The immersion precipitation technique[1] is very suitable for preparation of asymmetric membranes with properties varying from microfiltration to gas separation. The most simple system to perform immersion precipitation is a (quasi-) ternary system consisting of a polymer, a solvent and a nonsolvent.

The immersion precipitation process is governed by the thermodynamic

and diffusional properties of the components present in the system. The understanding of the membrane structures resulting from immersion precipitation will have to come from the study of those properties, and from the study of how these properties exert their influence on the membrane formation process.

The thermodynamics underlying membrane formation in such a ternary system have already been studied intensively by e.g. Tompa[2], Hsu *et al.*[3], and Altena *et al.*[4] They showed that from the Flory-Huggins theory[5] for a system consisting of a monodisperse polymer, a solvent and a nonsolvent, the phase behavior of the membrane forming system can be quite reasonably predicted. In such a system, the influence of the polydispersity of the polymer is less pronounced than the effects of the interaction parameters[4].
It became clear that by assuming concentration dependent interaction parameters between polymer and solvent, and solvent and nonsolvent, the use of ternary interaction parameters could be avoided[4].
Altena also showed that crystallization of the polymer is usually a very slow process compared to normal liquid-liquid demixing. It appeared thus sufficient for most systems to focus on liquid-liquid demixing as the essential membrane forming mechanism. Only rapidly crystallizing polymers (e.g. some aliphatic polyamides) form an exception.

On the basis of the thermodynamics, a thorough study of the kinetic basis of the immersion precipitation process was started by Cohen *et al.*[6] Reuvers *et al.*[7,8] further developed this model; they showed that the assumptions on cross-diffusional coefficients that Cohen made could not be justified.
Reuvers' model assumes that the compositions at the interface between coagulation bath and polymer solution remain constant as long as the diffusion front has not reached the bottom of the polymer solution film. If this is the case, it implies that every position in the polymer solution film undergoes the same compositional changes (with different velocities). This point will later be elucidated further on. The compositions of all positions together are therefore called a *composition path,* which is a curve representing all compositions existing in the polymer solution at one moment, or all compositions at all times at one position in the polymer solution.
Reuvers *et al.*[7,8] showed that the use of binary data on thermodynamics

and on the diffusional behavior of the components could lead to a prediction of the observed characteristics of membrane formation.
More specifically the two types of demixing (and therefore of membrane formation), that can be distinguished for a ternary membrane forming system, can be adequately predicted. The first type, called *delayed demixing*, is characterized by a measurable time between the moment of immersion of the polymer solution in the coagulation bath, and the moment that the polymer solution becomes turbid due to demixing into a polymer lean phase (which ultimately forms the pores) and a polymer rich phase (which finally results in the membrane matrix). In practice, this delay time is several tens of seconds to several minutes; in some cases it may even be measured in hours. With the help of the mass transfer model, Reuvers was able to predict this delay time reasonably well. It became also possible to understand that this type of demixing usually results in gas tight membranes, which have a thick (several μm), dense toplayer, and a sublayer with isolated pores.
The second type of demixing, called *instantaneous demixing*, is characterized by the fact that demixing starts immediately after immersion of the polymer solution in the precipitation bath. There is no noticeable delay between immersion and the start of demixing. In terms of the composition path: the composition path immediately crosses the binodal, introducing instable compositions in the polymer solution. In contrast, in the case of delay of demixing, the composition path is completely situated outside the binodal in the beginning. The membrane that results from the instantaneous demixing process possesses an ultrafiltration-type toplayer, with a sublayer that is more porous than a delay of demixing sublayer. The most specific property of the instantaneously formed sublayer is the occurrence of large conical voids, usually called macrovoids, which may extend through the entire sublayer of the membrane.
Smolders and Reuvers[9] noticed that macrovoids are connected with the instantaneous demixing mechanism. They proposed a mechanism for the formation of macrovoids which can be summarized as follows: during the instantaneous demixing process, it is possible that at a certain distance from the interface nuclei are created that have a high solvent concentration. This high solvent concentration then induces *local* delay of demixing between the nucleus and the surrounding polymer solution. Delay of demixing usually is characterized by a shrinkage of the polymer solution and an increase in volume of the coagulation bath. In this case this corresponds with the undisturbed growth of the nucleus. As long as delay of demixing continues the nucleus will grow: a macrovoid results.

The model by Reuvers *et al.*[7,8] is only meant as an approximation for the time span that the polymer solution film can still be regarded as being infinitely thick. In recent years, McHugh *et al.*[10-12] have further developed the mass transfer models to describe the solvent/nonsolvent exchange process not only in the first moments, but until the demixing takes place.
In our case, we restrict ourselves to the initial composition path (vide infra). Therefore the extra computational effort for the McHugh approach is not useful for us. We will only apply the Reuvers model[7,8].

Understanding of the processes taking place in a ternary system is absolutely essential as a basis for comprehending the membrane formation mechanism. However, in practice membranes are never made from only the three components mentioned earlier. Usually, extra components (additives) are used, which can result in membrane structures in a far greater variety than can be explained with a ternary model.
As an example, a weak nonsolvent may be added to the polymer solution. This causes the polymer solution to become less compatible with the coagulation bath. Demixing is faster and e.g. macrovoid formation may be suppressed[13].
In the past decades, several authors[14-16] reported on the use of a nonsolvent (water) soluble polymeric additive to the polymer solution, which suppressed macrovoid formation, and increased pore interconnectivity. Higher porosities and a modification of the surface properties of the membrane pores could be obtained. The hydrophobic membrane-forming polymer appeared to be "coated" with a layer of the water-soluble polymer. This increased the hydrophilicity of the membranes, and significantly improved the fouling properties of the membranes. Recently, Roesink[17] developed a very well defined microfiltration membrane on the basis of poly(ether imide) and poly(vinyl pyrrolidone), PVP.
A real understanding of the effects of such an additive is not yet available. Cabasso[18] suggested that the PVP not really mixes with the polymer used and therefore created "islands" of PVP in a membrane forming polymer matrix. These islands were then later removed during rinsing of the membranes after the precipitation step. This could explain the fact that with PVP added to the polymer solution, gas separation membranes could never be prepared. If this were the correct explanation however, one would expect the PVP to be rinsed out completely from the membrane, which is not the case.
Roesink[17] suggested that during immersion in the coagulation bath, the

PVP molecules started to diffuse out of the polymer solution, into the nuclei formed, and became trapped on their way out, due to the extremely low diffusivities in a concentrated polymer solution. Although this approach explained the fact that PVP can never be completely removed from the membrane by rinsing, it could not explain other effects, like the effect of PVP addition on macrovoid formation.
In our opinion, a quaternary membrane forming system consisting of a nonsolvent, a solvent, a membrane forming polymer and a polymeric additive, is too complicated to be approached without a fundamental basis. As an illustration of the complexity of the system, one should realize the following facts: to describe thermodynamic properties of such a system completely, one would need six binary, three ternary and one quaternary interaction parameters, and four molecular weights. To describe the kinetics comprehensively, one would need six diffusivities, instead of three in the ternary case. All these (concentration dependent) parameters can have influence on the membrane forming process. In our opinion it is not possible to estimate all the effects that can occur in such a system without systematic modelling.

In this chapter we will therefore develop a mass transfer model for a four component system, from the three-component mass transfer model by Reuvers *et al.* The thermodynamics are described by the modified Flory-Huggins theory, in which we have assumed that all ternary and quaternary interaction parameters can be neglected.
The model will then be specified for our system, which contains two polymers in the same solution. Most likely the diffusivity between the two polymers is low, due to their high molecular weights. This has a large influence on the thermodynamics and especially on the initial kinetic behavior. The significance of the results for the basic phenomena of membrane formation will be discussed.

Modelling mass transfer

1. The polymer solution

We will use the mass transfer model developed by Reuvers *et al.*[7,8] on the basis of the work of Cohen *et al.*[6], derived for a four-component system. The following indices will be used to indicate the four components:

1 - nonsolvent
2 - solvent
3 - membrane forming polymer
4 - polymeric additive

Component 4 is soluble in or miscible with all other components; the only pair in the system that is not miscible is pair 1 - 3.
A volume balance in terms of the volume fraction of component i, ϕ_i, is written for a Cartesian system:

$$\frac{\partial \varphi_i}{\partial t} = -\frac{\partial \tilde{J}_i}{\partial x} \qquad i = 1, 2, 3, 4 \qquad 1)$$

in which t is the time. The fluxes $\tilde{J}_i$ are relative to the laboratory frame. The spatial coordinate x is transformed to m (after Crank[19]):

$$m = \int_0^x \varphi_3 \, dx \qquad 2)$$

to account for the moving interface between the coagulation bath and the polymer film. This transformation is based on the fact that the polymer stays behind in the polymer solution, and can therefore act as a reference component. Figure 1 shows the meaning of m with respect to x.

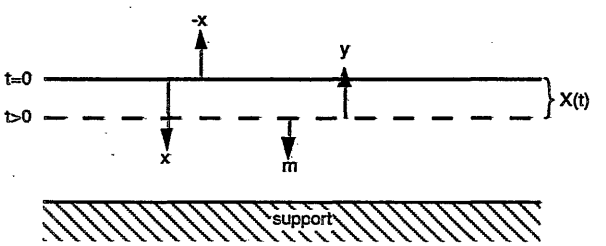

Figure 1: The coordinates in the polymer solution and in the coagulation bath. After Reuvers.[6]

The system is described relative to the motion of a reference component, the polymer (3), and a new mass balance results (a complete derivation is shown by Reuvers[6]):

$$\frac{\partial\left(\frac{\varphi_i}{\varphi_3}\right)}{\partial t} = -\frac{\partial J_i}{\partial m} \qquad i = 1,2,4 \qquad 3)$$

in which the fluxes are taken relative to the motion of the polymer, component 3. The fluxes are here defined as

$$J_i = \varphi_i (v_i - v_3) \qquad i = 1,2,4 \qquad 4)$$

in which v_i is the velocity (ms^{-1}) of component i in laboratory coordinates. The fluxes are linearly related to the chemical potential gradients, according to the theory of irreversible thermodynamics[20]:

$$J_i = - \sum_{j=1,2,4} \left\{ \underline{v}_i L_{ij} \frac{\partial \mu_j}{\partial m} \right\} \qquad 5)$$

Here, μ_i is the chemical potential, and $\underline{v}_i$ the specific volume of component i (appearing from the conversion from mass fluxes to volume fluxes, which are used here). The L_{ij}'s are called phenomenological coefficients and are diffusivities stripped of their thermodynamic part.
The complete set of diffusion equations for a quaternary solution is obtained by combining these flux equations 5 with the mass balance 3 (again the complete derivation is given by Reuvers[7]):

$$\frac{\partial\left(\frac{\varphi_i}{\varphi_3}\right)}{\partial t} = \underline{v}_i \frac{\partial}{\partial t} \left\{ \sum_{j=1,2,4} \varphi_3 L_{ij} \frac{\partial \mu_j}{\partial m} \right\} \qquad 6)$$

To find expressions for the phenomenological coefficients L_{ij}, the Maxwell-Stefan approach[7,8,21] can be used. The Maxwell-Stefan equations for this system are:

$$\frac{\partial \mu_i}{\partial x} = \sum_{j=1}^{4} c_j R_{ij} (v_j - v_i) \qquad i = 1,...,4 \qquad 7)$$

R_{ij} is the friction coefficient between components i and j; c_i is the concentration of component i (defined as $\phi_i / \underline{v}_i$), and v_i is the velocity in laboratory coordinates again.
From this, it can be derived that the driving forces X are related to the friction coefficients by:

$$\overline{X} = \overline{R} \begin{bmatrix} v_1 - v_3 \\ v_2 - v_3 \\ v_4 - v_3 \end{bmatrix} \qquad 8)$$

in which

$$X_i = \frac{\partial \mu_i}{\partial x}$$

and the 3x3-matrix R has the elements $\mathbb{R}_{ij}$:

$$\mathbb{R}_{ii} = \sum_{j \neq i} R_{ij} c_j \qquad i=1,2,4 \qquad 9)$$

$$\mathbb{R}_{ij} = R_{ij} c_j \qquad i,j=1,2,4;\ i \neq j$$

In this terminology, the 3x3-matrix of phenomenological coefficients $\overline{L}$ is determined by:

$$\overline{L} = \overline{R}^{-1} \qquad 10)$$

by which the phenomenological coefficients are now related to the friction coefficients.

The diffusion behavior in the polymer solution is described by equations 6, while the coefficients in these equations are determined with relation 10.

2. Coagulation bath

Again we are using the approach used by Reuvers *et al.*[7] Irreversible thermodynamics gives for the description of mass transfer in the coagulation bath:

$$\frac{\partial \varphi_i}{\partial t} = v_i \frac{\partial}{\partial x} \left\{ L_{1i} \frac{\partial \mu_1}{\partial x} + L_{2i} \frac{\partial \mu_2}{\partial x} \right\} \qquad i = 1,2,4 \qquad 11)$$

To take into account the movement of the boundary between polymer solution and coagulation bath, the spatial coordinate x is converted to reflect the motion with respect to the interfacial boundary:

$$y = -x + X(t) \qquad 12)$$

which then results in the diffusion equations valid for the coagulation bath:

$$\frac{\partial \varphi_i}{\partial t} = \underline{v}_i \frac{\partial}{\partial y}\left\{ L_{1i} \frac{\partial \mu_1}{\partial y} + L_{2i} \frac{\partial \mu_2}{\partial y} \right\} - \frac{\partial \varphi_i}{\partial y} \sum_{k=1,2,4} J_k^{y=0} \qquad i = 1,2,4 \qquad 13)$$

The relation between the phenomenological coefficients and the friction coefficients follow from relation 10.

3. Initial and boundary conditions

As in the model of Reuvers[7], we will assume:

- local equilibrium at the interface, and
- the fluxes of components 1,2 and 4 to be equal at both sides of the interface

Our system is now defined. The chemical potentials are determined by the Flory-Huggins theory. Knowledge of the friction coefficients enables us to calculate all diffusion profiles.

A solution for short times

Immediately after the polymer solution has been brought into contact with the coagulation bath, the concentration profiles are step wise functions. This causes, mathematically, the fluxes to be infinitely large at t=0. In other words: the diffusion behavior features a singular point at t = 0 and m = 0. To overcome this, the Boltzmann-conversion[6,7,22,23] may be used:

$$\begin{aligned} \text{spatial/time coordinate } \zeta &= \frac{m}{2\sqrt{t}}; \\ \text{time coordinate } \tau &= \sqrt{t} \end{aligned} \qquad 14)$$

the spatial coordinate m is converted to $m/(2\sqrt{t})$ while time is converted to $\sqrt{t}$. The diffusion equations 6 then become:

$$\tau \frac{\partial\left(\frac{\varphi_i}{\varphi_3}\right)}{\partial \tau} = \zeta \frac{\partial\left(\frac{\varphi_i}{\varphi_3}\right)}{\partial \zeta} + \frac{1}{2} \frac{\partial}{\partial \zeta} \sum_{j=1,2,4} \left\{ \underline{v}_i \, \varphi_3 \, L_{ij} \frac{\partial \mu_j}{\partial \zeta} \right\} \qquad 15)$$

Normally, fluxes in such a problem are dependent on the square root of time. It can be proven[22] that while the time-derivatives of the concentra-

tions at t = 0 and m = 0 are singular, the τ-derivatives are not (they are actually constant). For small times therefore:

$$\left\{ \tau \frac{\partial \left(\frac{\varphi_i}{\varphi_3} \right)}{\partial \tau} \right\} \rightarrow 0 \text{ when } \tau \rightarrow 0 \qquad 15a)$$

One now sees that it is not necessary for the time-derivative of the compositions to be zero at the interface, as Reuvers *et al.* assumed. They may even be infinitely large, as long as the τ-derivative is finite.
It appears that we obtain the same approximation as found by Reuvers, but without the assumption of constant interfacial compositions. We have an approximation now, valid only for short times:

$$\zeta \frac{\partial \left(\frac{\varphi_i}{\varphi_3} \right)}{\partial \zeta} + \frac{1}{2} \frac{\partial}{\partial \zeta} \sum_{j=1,2,4} \left\{ v_i \varphi_3 L_{ij} \frac{\partial \mu_j}{\partial \zeta} \right\} = 0 \qquad i = 1,2,4 \qquad 16)$$

A similar relation can be found for the coagulation bath.
It is thus shown that for the first moments of immersion the composition path is indeed only dependent on ζ.

Calculation procedure

We will approximate relation 15 by calculating the true diffusion equations 7 for a very short time (e.g. 0.1 s) with the help of the E03PGF-routine from the National Algorithms Group library[24].
The procedure is as follows:

1. An interfacial composition on the binodal is assumed
2. The diffusion profiles in the polymer solution are calculated
3. The fluxes to and from the polymer solution are calculated
4. The fluxes are used to calculate the diffusion profiles in the coagulation bath
5. the fluxes to and from the coagulation bath are calculated
6. These fluxes are compared with the fluxes from step 3.
7. The whole procedure is repeated with different interfacial compositions, until the fluxes from step 3 and step 5 are equal.

The friction coefficients

In our model we will use the same assumptions as Reuvers used. That is: quaternary friction coefficients R_{ij} are only dependent on the two components i and j. Therefore the binary friction coefficients may be used in the form of:

$$R_{ij}^{quaternary} = R_{ij}^{binary} \left(\frac{\varphi_i}{\varphi_i + \varphi_j} \right) \qquad 18)$$

This enables us to use data measured in the limiting binary systems[7].
As a model system, we will use the system consisting of:

1 - nonsolvent: water
2 - solvent: 1-methyl-2-pyrrolidone (NMP)
3 - membrane forming polymer: poly(ether sulfone) (PES)
4 - polymeric additive: poly(vinyl pyrrolidone) (PVP)

Since on the diffusivity of poly(ether sulfone) in NMP not so many data are available, the relation from Radovanovic *et al.*[23] for the diffusivity of polysulfone in DMAc is used.

$$\frac{v_3 RT}{M_2 R_{23}} = 18.0 \cdot 10^{-9 - 4.386 \varphi_3} \qquad m^2/s \qquad 19)$$

This relation approximately agrees with the experimental data from Tkacik *et al.*[25,26] on the system PES-NMP-water, and with values measured in our laboratory.

Diffusion coefficients of NMP in water are taken from ref 26. The friction coefficient obtained from these data is estimated to be constant:

$$\frac{v_1 RT}{M_2 R_{12}} = 6.0 \cdot 10^{-10} \qquad m^2/s \qquad 20)$$

The thermodynamic data from the system PES-NMP-water is based on the work by Tkacik *et al.*[25], and work from our lab. The data on the interaction of PVP with other components are given in reference 27.

A system with two polymers in one phase

In *diluted* solutions (i.e. *under* the overlap concentration), binary diffusion coefficients for low molecular weight substances and polymers are usually inversely related to the square of the molecular weight of the polymer.
Polymer solutions meant for membrane formation are always quite concentrated: a typical concentration in a system considered here is: 25 weight% membrane forming polymer and 15 weight% polymeric additive. A total polymer weight content of 40 weight% indicates that the polymer solution can be regarded as an intertwined network of polymer molecules 'swollen' with solvent and nonsolvent molecules. Since the two polymers that are used mix well, they will be well entangled.
De Gennes[29] has developed theoretical ideas on such concentrated solutions. According to his ideas, such a solution can be regarded as consisting of 'blobs', parts of a polymer chain that mainly interact with themselves, and that do not interact with other chains. The number of blobs is related to the concentration of the polymers. In rather concentrated solutions, the properties of the solution are determined by the properties of the blobs, and not by the properties of the complete chains. This situation is schematically shown in figure 2a. The molecular weight of the polymers has no effect on diffusion of *solvent* (or nonsolvent) molecules through such a network of blobs, since the molecular weight of a blob is much smaller than that of the complete polymer chain. Therefore, *above* the overlap concentration, the diffusion coefficient between a solvent and a polymer is *independent of the molecular weight of the polymer.*
Diffusion of one of the polymer molecules through the solution, however, is very difficult. A polymer chain can only move along its long axis. One may visualize this as movement of the polymer coil in a tube, shown in figure 2b; while the polymer coil is moving, new parts of the tube are created at one end, while at the other end parts of the tube are destroyed (see De Gennes[29]). De Gennes showed that in this situation the diffusion coefficient is inversely proportional to the square of the molecular weight of the polymer(s).
Summarizing, for *more concentrated* solutions (i.e. clearly above the overlap concentration), the diffusion rate between solvent and polymer is *independent* of the molecular weight of the polymer; the polymer-polymer diffusion rate is quite dependent on the molecular weight. This is schematically shown in figure 2c.

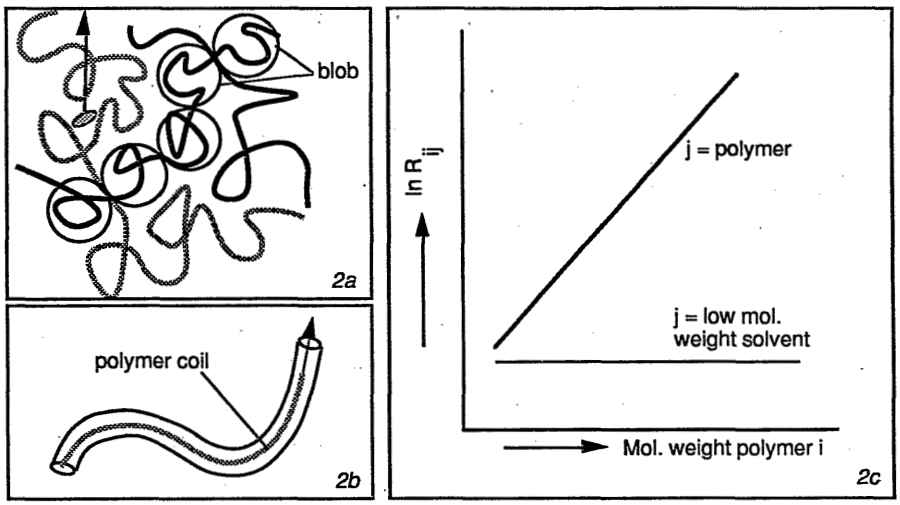

Figure 2a: A schematic picture of diffusion processes in a concentrated solution. Nonsolvent and solvent can diffuse through the network of blobs (figure 2a), while movement of polymeric molecules with respect to other polymer molecules is restricted to movement through a 'tube' (reptation; figure 2b). The consequence is shown in figure 2c: the friction coefficient between two polymers (i and j) increases with the square of the molecular weight; the friction coefficient between a low molecular weight component (j) and a polymer (i) is independent on the molecular weight of the polymer.

The implication of this is, that accordingly the mass exchange of solvent and nonsolvent is much faster than the diffusional processes between the polymers. During the very first moments of immersion, the polymeric additive does not have the possibility to move at all relative to the membrane forming polymer. The two polymers behave as one polymeric network.
In our mass transfer model, which is only meant for the first moments of immersion, one can conclude that the friction coefficient between the two polymers is very large when compared to the other friction coefficients in the system. We can therefore assume that the velocity difference between the two polymeric components is negligible compared to the other velocity differences in the diffusion system.

The condition of no movement between the two polymers imposes two alterations on the system.

The first one concerns the mass transfer model. Since the polymers behave as one single polymer, the system reduces into a semi-ternary system. The phenomenological coefficients can be calculated from:

$$\bar{L} = \begin{bmatrix} c_3 R_{13} + c_4 R_{14} & c_2 R_{12} \\ c_1 R_{12} & c_3 R_{23} + c_4 R_{24} \end{bmatrix}^{-1} \qquad 21)$$

Comparison with the analogous expressions by Reuvers shows that the polymer network behaves as a weighted average over the two polymeric components.

The second adaptation to be made is thermodynamic in nature. During the first moments of immersion, the assumption of local equilibrium at the interfacial boundary cannot be maintained.
During phase separation, the two polymers present always tend to separate, regardless of their mutual miscibility, as long as one polymer is mainly soluble in only one phase (the membrane forming polymer) and the other polymer is soluble in both phases (the polymeric additive). This has entropic reasons: two polymers have very low entropy of mixing. This effect has been clearly shown earlier[30].
For the initial stage we can only assume local equilibrium for the low molecular weight components, solvent and nonsolvent, since they can move freely through the polymeric network and the coagulation bath. We pose on the system the restriction that all polymer remains present in the polymer phase, and that in the other phase no polymer is present at all. In the next paragraph this restriction will be worked out in detail.

Thermodynamics for the first moments of immersion

As was discussed before, the phase behavior at the interface for short times is different from the equilibrium phase behavior for the quaternary system. Due to the kinetic restrictions of the system, we have to assume that the polymers act as one single polymeric network.
The phase diagram for the first moments is calculated by assuming equilibrium for the solvent and nonsolvent, while forcing the polymer concentrations in the diluted phase to be zero. The polymer concentrations in the concentrated phase are chosen as independent variables.
For the concentrated phase, the following relations are used to describe the chemical potentials of solvent and nonsolvent[30]:

$$\frac{\Delta\mu_1}{RT} = \ln\varphi_1 - s\varphi_2 - r\varphi_3 - t\varphi_4 + (1 + g_{12}\varphi_2 + \chi_{13}\varphi_3 + g_{14}\varphi_4)(1 - \varphi_1) - sg_{23}\varphi_2\varphi_3 - rg_{34}\varphi_3\varphi_4 - sg_{24}\varphi_2\varphi_4 - \varphi_2 u_2 (1 - u_2)\left(\frac{\partial g_{12}}{\partial u_2}\right) - \varphi_4 u_4 (1 - u_4)\left(\frac{\partial g_{14}}{\partial u_4}\right) \quad 22)$$

$$\frac{s\Delta\mu_2}{RT} = s\ln\varphi_2 - \varphi_1 - r\varphi_3 - t\varphi_4 + (s + g_{12}\varphi_1 + sg_{23}\varphi_3 + sg_{24}\varphi_4)(1 - \varphi_2) - \chi_{13}\varphi_1\varphi_3 - g_{14}\varphi_1\varphi_4 - rg_{34}\varphi_3\varphi_4 + \varphi_1 u_2 (1 - u_2)\left(\frac{\partial g_{12}}{\partial u_2}\right) - s\varphi_3 v_2 (1 - v_2)\left(\frac{\partial g_{23}}{\partial v_2}\right) - s\varphi_4 w_2 (1 - w_2)\left(\frac{\partial g_{24}}{\partial w_2}\right) \quad 23)$$

while for the diluted phase, binary equations are used (no polymer is present here).

$$\frac{\Delta\mu_1}{RT} = \ln\varphi_1 - s\varphi_2 + (1 + g_{12}\varphi_2)\varphi_2 - \varphi_2^2\varphi_1\left(\frac{\partial g_{12}}{\partial \varphi_2}\right) \quad 24)$$

$$\frac{s\Delta\mu_2}{RT} = s\ln\varphi_2 - \varphi_1 + (s + g_{12}\varphi_1)\varphi_1 + \varphi_1^2\varphi_2\left(\frac{\partial g_{12}}{\partial \varphi_2}\right) \quad 25)$$

In these relations, the binary interaction parameters are assumed to be only dependent on the two components indicated by the interaction parameter itself. The following parameters have been introduced[30]:

g_{12} is dependent on $u_2 = \phi_2/(\phi_2+\phi_1)$
g_{23} is dependent on $v_2 = \phi_2/(\phi_2+\phi_3)$
g_{14} is dependent on $u_4 = \phi_4/(\phi_4+\phi_1)$
g_{24} is dependent on $w_2 = \phi_2/(\phi_2+\phi_4)$
g_{34} is dependent on $v_3 = \phi_3/(\phi_3+\phi_4)$

Any concentration dependence of χ_{13} cannnot be measured (since components 1 and 3 are not miscible); the absence of concentration dependence is therefore assumed[4]. The entropic parameters are the ratios of the molar volumes of the different species:

$$s = \frac{\underline{v}_1 M_1}{\underline{v}_2 M_2}; \qquad r = \frac{\underline{v}_1 M_1}{\underline{v}_3 M_3}; \qquad t = \frac{\underline{v}_1 M_1}{\underline{v}_4 M_4} \quad 26)$$

in which $\underline{v}_i$ is the specific volume and M_i is the molecular weight of component i.

For the calculation, the usual numerical procedure is used (see Hsu[3], Altena[4]). The chemical potentials as defined by equations 22 to 25 are set equal for each component, by varying the nonsolvent concentrations in both phases. The concentrations of components 3 and 4 are fixed in one phase; component 2 is determined by the mass balance.

Phase diagrams calculated in this way are shown in figure 3 a to h. In these figures the thermodynamic parameters are varied. Since these binodals are only valid for very short times, and are completely different from the real binodal, one might call these curves *virtual binodals.*

It appears from figure 3a that the addition of component 4 decreases the size of the demixing gap: the solution becomes more compatible with the nonsolvent. It should be remembered that the real cloudpoint curves of these systems (i.e. when kinetics are not hampered) are around one volume percent of nonsolvent or less[30]: the solutions are in reality very *in*compatible with the nonsolvent. Nevertheless, for short times, figure 3a shows that the solution can contain up to 50 volume% of nonsolvent (this is as long as no movement between the two polymers is possible). This is not very dependent on the molecular weight of the additive, as long as the additive is still macromolecular in nature. This is shown in figure 3b. When the molecular weight of the additive becomes too low (i.e. < 5000 g/mole), the binodal shifts even further to the right. Since we already need a high molecular weight for the additive to hinder the diffusion between the two polymers (e.g., several tens of thousands g/mole), we can assume that the actual molecular weight has no influence on these virtual binodals.
Figures 3c and 3d give the effects of the parameters that are alreay present in a ternary system without component 4; we see the same behavior as in a ternary system[4].
It is observed that polymer-solvent interactions, g_{23} and g_{24}, are not important, of course as long as miscibilities are ensured (see figures 3e and 3f). The interaction between the polymeric addditive and the nonsolvent, g_{14} (figure 3g) is analogous to the g_{13}.
The interaction between the two polymers, g_{34}, seems not to have any influence (again as long the polymers are still miscible), as shown in figure 3h.
Generally, from figure 3 it may be concluded that for the short-term thermodynamic behavior of the polymer solution only the interactions with the nonsolvent are important, i.e. the parameters g_{12}, g_{13} and g_{14}

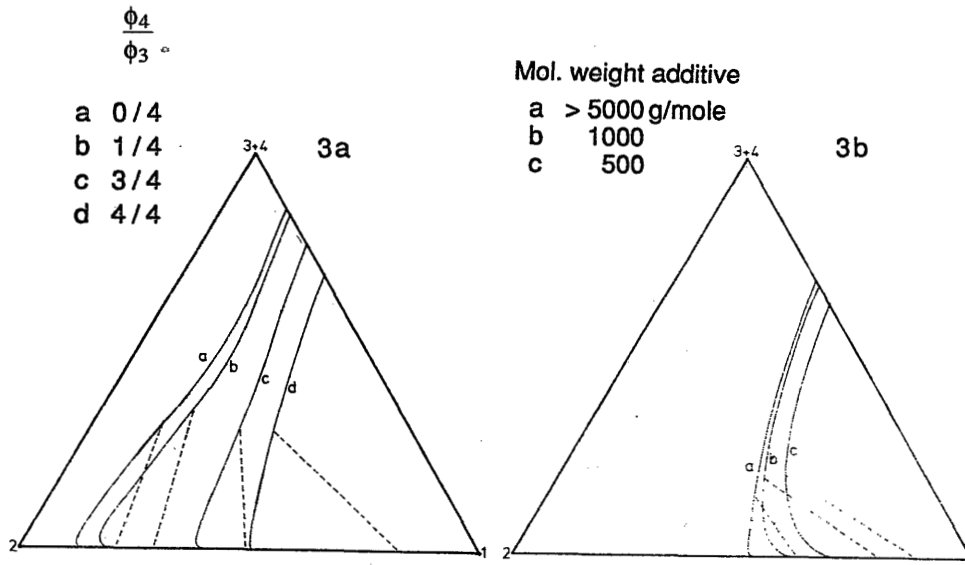

Figure 3a: Variation of the ratio of additive to polymer between 0 and 1; other parameters see below. Figure 3b: Variation of the molecular weight of the additive between 500 and 500 000 g/mole.

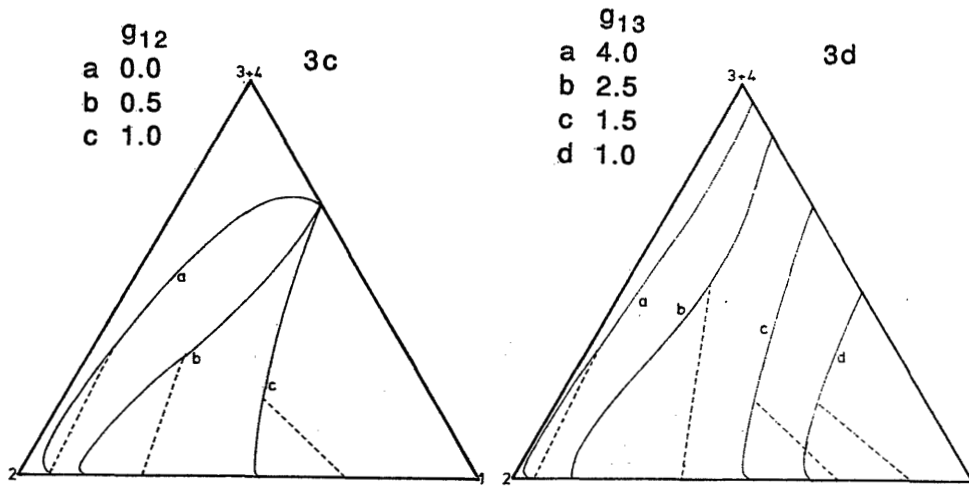

Figure 3c: Solvent-nonsolvent interaction: variation of g_{12} between 0.0 and 1.0. Figure 3d: Nonsolvent-polymer interaction: variation of g_{13} between 4.0 and 1.0.

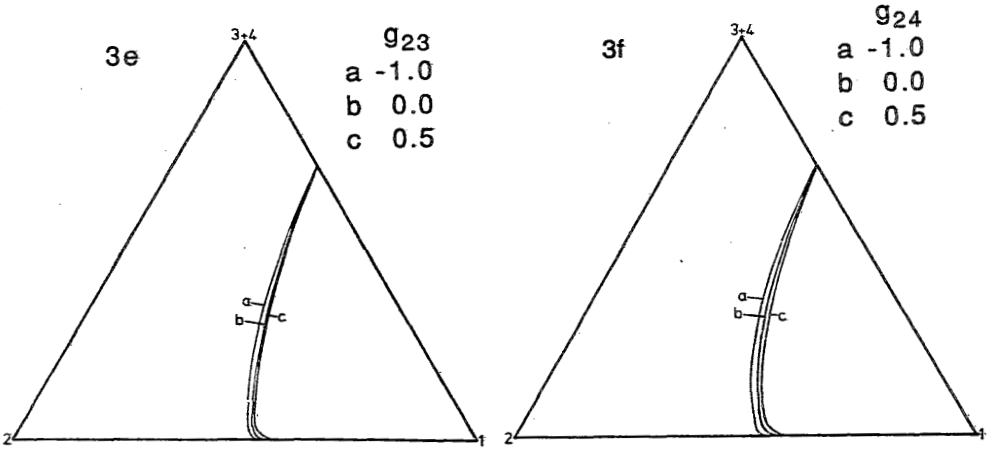

Figure 3e: Solvent-polymer interaction: variation of g_{23} between -1.0 and 0.5.
Figure 3f: Solvent-additive interaction: variation of g_{24} between -1 and 0.5.

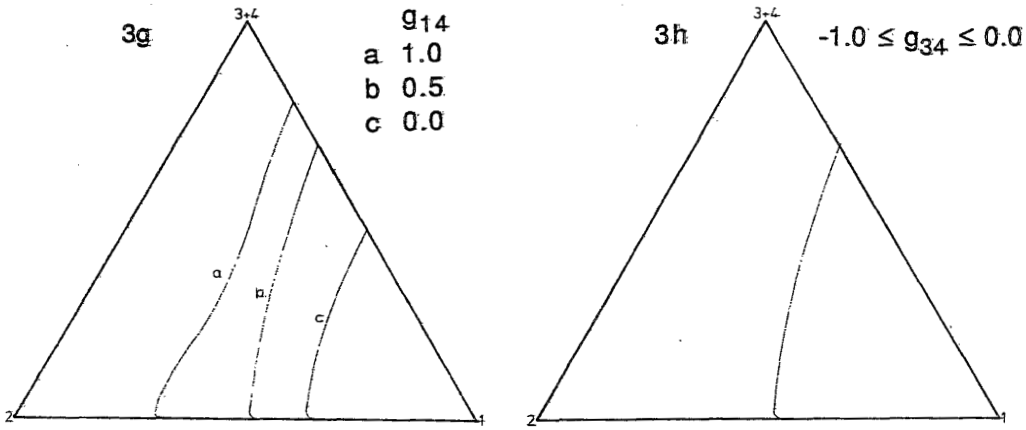

Figure 3g: Nonsolvent-additive interaction: variation of g_{14} between 1.0 and 0.0.
Figure 3h: Polymer-additive interaction: variation of g_{34} between -1 and 0.

Figure 3: Phase diagrams for the first moments of immersion. The following parameters were used unless indicated differently: $g_{12} = 1.0$, $g_{13} = 1.5$, $g_{14} = 0.5$, $g_{24} = 0.5$, $g_{23} = 0.5$, $g_{34} = -1$; $s = 0.182$, $r = 0.001$; $t = 0.001$. Except in 3a, the ratio between polymer and additive in the concentrated phase was kept at unity. In each diagram one variable is varied.
Dotted lines are tielines. Uninterrupted lines are virtual binodals.

(see figures 3c, 3d and 3g). The influence of the solvent-nonsolvent interaction parameter has been well investigated by Smolders and coworkers[4,8]. We may say that in our quaternary system, this influence looks analogous. The same can be said of the polymer-nonsolvent interaction parameter. The influence of the additive seems to be mainly governed by the interaction between the additive and the nonsolvent, g_{14}. This can be easily understood. If the value of this parameter were the same as the value of g_{13}, there should be no shift of the binodal whatsoever, the additive should behave exactly the same as the membrane forming polymer. The parameter g_{14} therefore is a measure of the difference between the two polymers.
To summarize the effects shown in figure 3, it appears that the thermodynamics during the first moments of immersion are mainly governed by one parameter, the nonsolvent-additive parameter, which expresses the "hydrophilicity" (when the nonsolvent is water) of the additive. Apart from effects from the basic ternary membrane forming system without polymeric additive (effects of g_{13}, g_{23}, and g_{13}), the system is relatively insensitive to the other parameters in the system.

Mass Transfer

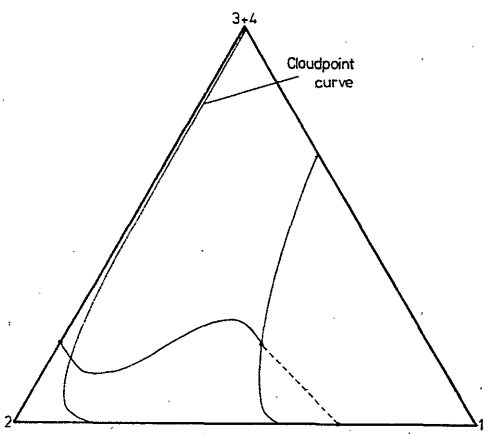

Figure 4: An initial composition path for a system with an equal amount of additive 4 and polymer 3. The friction coefficients R_{i4} are chosen as equal to the friction coefficients R_{i3}. Other parameters are as in figure 3, and as indicated in the text. Initial composition of the polymer solution: 20 vol% polymer (3+4) in solvent. Initial composition of the coagulation bath: pure nonsolvent.

The "short-term" thermodynamics (valid for the first seconds of immersion) as shown on the preceding pages is used as the basis for the calculation of composition paths for the system.

Figure 4 shows a typical initial composition path. The nonsolvent flux through the interface is much higher than in the ternary system, and that it is comparable to the solvent flux.
Preliminary measurements performed in our lab indicated that the diffusivity of PVP is of the same magnitude as the diffusivity of PES. We therefore assumed that they were the same and possessed the same concentration dependency.

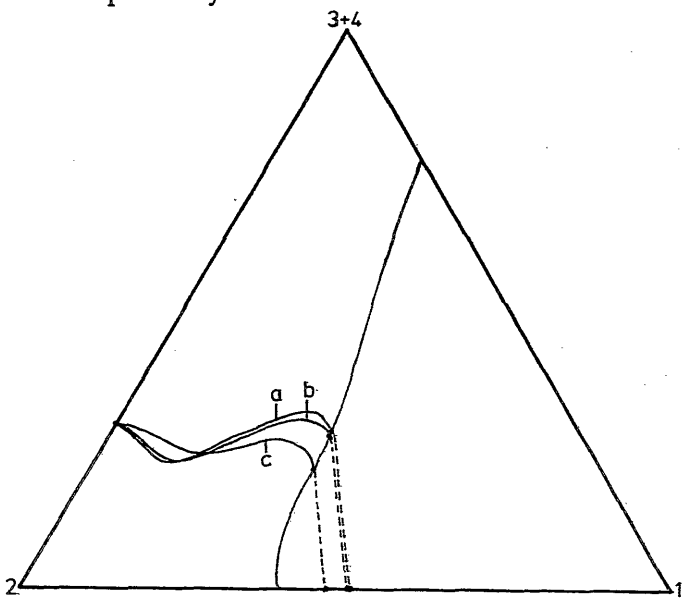

Figure 5: Initial composition paths that show the influence of the choice of values for R_{i4}: (a) $R_{i4} = 0.1\ R_{i3}$; (b) $R_{i4} = R_{i3}$ and (c) $R_{i4} = 10\ R_{i3}$. Other parameters and concentrations are as in figure 4.

Figure 5 shows the influence of a deviation from this assumption. It appears that although there are deviations, the composition path remains largely the same when the diffusivities are changed over two orders of magnitude. Apparently, the composition paths are not very sensitive to exact values of the friction coefficients. Since we have only few exact data on the system, this is an important conclusion.
On the basis of the preceding figures, we now may look into the behavior

of the systems more closely. In figure 6 the ratio of additive to polymer in the system is varied from zero to unity. A characteristic feature appears with increasing ϕ_4/ϕ_3 viz. a lowering in polymer concentration in the toplayer. When the ratio ϕ_4/ϕ_3 is enlarged further, the interfacial polymer concentration stays approximately constant. From the calculations it appears that nonsolvent fluxes through the interface increase approximately three-fold when increasing the ratio from zero to 0.25; after this they remain approximately the same.

We can see that the initial composition path without any addition, which is typically of an instantaneous demixing type, shifts to a delay of demixing type when additive is present. No demixing takes place as long as the two polymers cannot move relative to each other. Of course we should remember that this assumption holds only for the first few moments. After this initial stage the two polymers start to move relative to each other. The demixing itself is determined by the demixing between the two polymers[30].

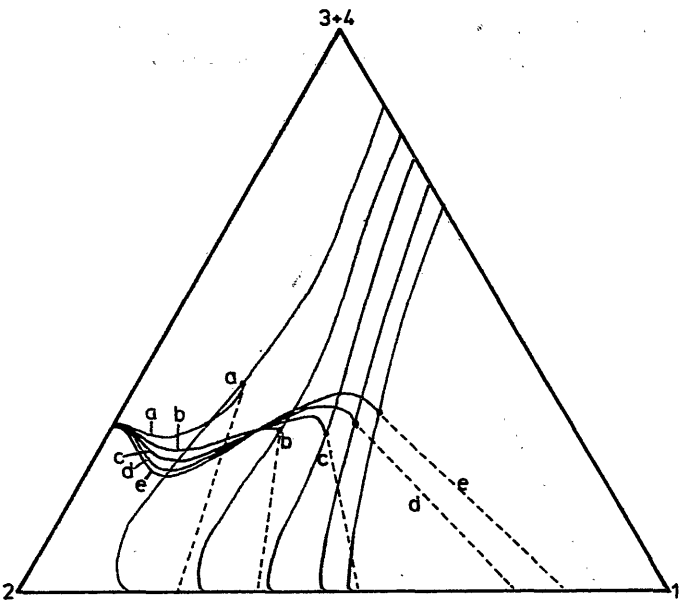

Figure 6: Initial composition paths with a varying amount of additive in the polymer solution. Ratios of additive (4) to polymer (3) are a: 0, b: 0.25, c: 0.5, d: 0.75, e: 1.0. Other parameters and concentrations are as in figure 4. Dashed lines represent the (local) equilibrium at the interface.

Regarding the mechanism of formation of macrovoids the behavior of the solution immersed in a coagulation bats that contains increasing amounts

of solvent is of importance.
In the basic ternary membrane forming system, an increase of the solvent concentration in the coagulation bath results in a slowing down of the nonsolvent indiffusion. Above a certain solvent concentration, the instantaneous type of demixing is replaced by a delayed type of demixing.
The composition of the coagulation bath for a quaternary system, from zero to 80 volume% of solvent; see figure 7. As we can see, the polymer concentration at the interface decreases to zero: at around 50 vol% of solvent in the coagulation bath, there is no discrete interface to prevent membrane forming polymer to diffuse into the coagulation bath. Since our model is based on the stagnancy of components 3 and 4, and is developed only for short times, these initial composition paths should not be taken too literally, although they might still be used qualitatively. What one expects on the basis of figure 7 is the following. When the solvent concentration in the coagulation bath increases, the polymer concentration in the toplayer drops to zero. Initially this means that the membrane forming polymer (together with the additive) dissolves in the coagulation bath.

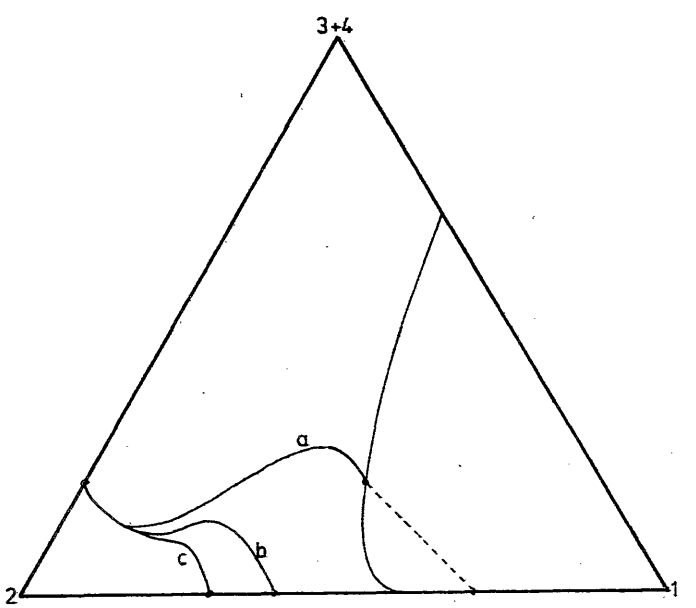

Figure 7: Initial composition paths with a varying coagulation bath; a: pure nonsolvent, b: 40 vol% solvent; c: 60 vol% solvent. All concentrations and parameters are as in figure 4.

In the polymer solution near the interface, the polymer concentration becomes very low, allowing relatively fast polymer-polymer interdiffusion. When this interdiffusion has become possible, the compositions in the toplayer are very instable; they are actually situated inside the spinodal area of the normal phase diagram. This solution will therefore relatively quickly demix according to a spinodal decomposition mechanism. It is important to notice that under conditions that would normally cause delay of demixing (i.e. high solvent concentration in the coagulation bath), the use of a polymeric additive which is soluble in the nonsolvent makes delay of demixing impossible as a membrane forming mechanism.

General conclusions

A mass transfer model for a quaternary membrane forming system is developed for the first moments of immersion.
It is shown that a particular system, incorporating two polymers in the same solution, has some specific characteristics. By using an additive with a certain minimum molecular weight, the movement between the two polymers is negligible initially, compared to the movements of non-solvent and solvent. It is therefore possible to distinguish two different time scales during membrane formation with such a system.

- During the shorter time scale, movement of one polymer compared to the other can be assumed zero. Only solvent and nonsolvent are exchanged. A high nonsolvent concentration in the polymer solution results.
- In the longer time scale, the movement between the two polymers is possible again. The polymeric additive forms a second (pore) phase; the original polymer (4) forms the membrane.

It is essential that the molecular weight of the polymeric additive is high enough to decrease the polymer-polymer diffusion dramatically. A precise estimate of such a minimum molecular weight cannot be given; on the basis of a reptation mechanism one might expect quite a large molecular weight to be necessary.
During the shorter time scale, both the kinetic and the thermodynamic properties of the system are changed. The polymer solution appears to be more compatible with the nonsolvent. The thermodynamics during the shorter time scale are mainly determined by the enthalpic interaction of

the polymeric additive with the nonsolvent. Other interactions do not deviate from the effects in the ternary situation without the fourth component. Significant is that the interaction between the two polymers does not seem to have any effect, as long as the two polymers remain miscible.
Calculation of the *initial* composition paths indicates that when a polymeric additive is used, the polymer concentration in the skinlayer remains low. The initial nonsolvent flux though the interface increases very much upon addition of the nonsolvent-soluble polymer.
It appears that the initial composition paths are not very sensitive to the values of the kinetic parameters.
An increase of the amount of solvent in the coagulation bath resulted in a reduction of the amount of polymer in the toplayer until it becomes zero. This facilitates the transition to the behavior belonging to the longer time scale (i.e. demixing into two phases), since all diffusion processes are faster in more diluted solutions. Effectively, the addition of solvent to the coagulation bath will cause the polymer solution to demix quickly. This implies that even for very high solvent concentrations, delay of demixing is not possible. This is in accordance with practical experience[28].
The cloudpoint curves valid for the longer time scale are always situated close to the polymer-solvent axis. During the shorter time scale, very instable compositions in the skinlayer are created, according to the phase behavior of the longer time scale. One could say that the short time scale is equivalent to a very deep quench of the polymer solution. It may initiate spinodal decomposition processes.

Summarizing, we can say that the introduction of a nonsolvent-soluble polymeric additive inhibits any delay of demixing, as long as the diffusion between the two polymers is significantly slower than the other diffusion processes taking place.

List of Symbols

c_i concentration of component i (kgm^{-3})
g_{ij} interaction parameter between components i and j (-)
J_i volume flux of component i relative to component 3 ($m^3m^{-2}s^{-1}$)
$\tilde{J}_i$ volume flux relative to the glass plate ($m^3m^{-2}s^{-1}$)

$\bar{L}$ matrix of phenomenological coefficients
L_{ij} phenomenological coefficient between components i and j
m spatial coordinate corrected for movement of the interface (m)
M_i molecular weight of component i (g/mole)
s $\underline{v}_1M_1/\underline{v}_2M_2$
r $\underline{v}_1M_1/\underline{v}_3M_3$
$\bar{R}$ inverse matrix of $\bar{L}$
R_{ij} friction coefficient between components i and j
$\mathbb{R}_{ij}$ matrix element of $\bar{R}$
t $\underline{v}_1M_1/\underline{v}_4M_4$, or time (s)
u_2 $\phi_2/(\phi_2+\phi_1)$ (-)
u_4 $\phi_4/(\phi_4+\phi_1)$ (-)
v_i velocity of component i (ms^{-1})
v_2 $\phi_2/(\phi_2+\phi_3)$ (-)
u_3 $\phi_3/(\phi_3+\phi_4)$ (-)
$\underline{v}_i$ specific volume of component i (m^3g^{-1})
w_2 $\phi_2/(\phi_2+\phi_4)$ (-)
$\bar{X}$ vector of driving forces (chemical potential gradients)
x spatial coordinate in the polymer solution (m)
X(t) distance between the interface on t and the interface on t=0 (m)
y spatial coordinate in the coagulation bath (m)
μ_i chemical potential of component i ($Jmole^{-1}$)
ϕ_i volume fraction of component i (-)

References

1. S. Loeb, S. Sourirajan, Adv. Chem. Ser. **38**, 1962, 117
2. H. Tompa, Polymer solutions, Butterworths, London 1956
3. C.C. Hsu, J.M. Prauznitz, Macromolecules, **7**, 1974, 320
4. F.W. Altena, C.A. Smolders, Macromolecules, **15**, 1982, 1491
5. P.J. Flory, Principles of Polymer Chemistry, Cornell University Press, New York, 1953
6. C. Cohen, G.B. Tanny, S. Prager, J. Polym. Sci., Polym. Phys. Ed. **17**, 1979, 477
7. A.J. Reuvers, J.W.A. van den Berg, C.A. Smolders, J. Membrane Sci., **34**, 1987, 45
8. A.J. Reuvers, C.A. Smolders, J. Membrane Sci., **34**, 1987, 67
9. C.A. Smolders, A.J. Reuvers, Microstructures in Membranes, part I: macrovoid formation, to be published.

10. L. Yilmaz, A.J. McHugh, J. Membrane Sci., **28**, 1986, 287
11. C.S. Tsay, A.J. McHugh, J. Polym. Sci., Polym Phys. Ed., **28**, 1990, 1327
12. C.S. Tsay, A.J. McHugh, paper presented at the international congress on Progress in Membrane Science and Technology (PMST), June 1991, University of Twente, The Netherlands
13. J. A. van 't Hof, Wet Spinning of Asymmetric Hollow Fibres for Gas Separation, University of Twente, The Netherlands, 1988
14. P. Aptel, N. Abidine, F. Ivaldi, J.P. LaFaille, J. Membrane Sci., **22**, 1985, 199
15. L.Y. Lafrenière, F.D.F. Talbot, T. Matsuura, S. Sourirajan, Ind. Eng. Chem. Res. **26**, 1987, 2385
16. T.A. Tweddle, O. Kutowy, W.L. Thayer, S. Sourirajan, Ind. Eng. Chem. Prod. Res. Dev. **22**, 1983, 320
17. E. Roesink, Microfiltration; membrane development and module design, thesis, University of Twente, The Netherlands, 1989
18. I.Cabasso, E. Klein, J.K. Smith, J. Appl. Polym. Sci. **21**, 1977, 165
19. J. Crank, The Mathematics of Diffusion, 2nd ed., Clarendon Press, Oxford, 1975
20. S.R. de Groot and P. Mazur, Non-equilibrium Thermodynamics, Amsterdam, North-Holland Publishing Co., 1962
21. J.A. Wesselingh, R. Krishna, Mass Transfer, Ellis Horwood ltd, New York, 1990
22. F. van Beckum, private communications
23. Ph. Radovanovic, S.W. Thiel, S.-T. Hwang, J. Membrane Sci., **65** (1992) 213
24. P.M. Dew, J.E. Walsh, ACM Trans. Math. Software **7**, 1981, 295
25. G. Tkacik, L. Zeman, J. Membrane Sci., **31**, 1987, 273
26. L. Zeman, G. Tkacik, J. Membrane Sci.,**36**, 1988, 119
27. First appendix to chapter 2 of this thesis
28. Chapter 4 of this thesis
29. P-G. De Gennes, Scaling Concepts in Polymer Physics, Ithaca, Cornell University Press, 1979
30. Chapter 2 of this thesis

Chapter 4

Membranes Prepared From a Polymeric Blend Part I:

Membranes from Poly(Ether Sulfone) and Poly(Vinyl Pyrrolidone)

R.M. Boom, S. Zanic, Th. van den Boomgaard, C.A. Smolders

Summary

Membranes were prepared from poly(ether sulfone), with poly(vinyl pyrrolidone) as polymeric additive, 1-methyl-2-pyrrolidone as solvent and water as nonsolvent. In the polymer solution, the membrane forming polymer concentration, the polymeric additive concentration and its molecular weight were varied, as well as the solvent concentration in the coagulation bath.

A series of empirical rules is found to describe the resulting membrane morphologies. It appears that PVP is a macrovoid suppressor at fast demixing conditions only (low solvent content in the coagulation bath); at slow demixing conditions (high solvent content in the coagulation bath), PVP *promotes* macrovoid formation. Delay of demixing as known for ternary systems is suppressed by PVP.

A mechanism for the effects of PVP is proposed, based on the assumption that under fast demixing circumstances, the polymer-polymer diffusion is much slower than other diffusion processes in the system. Structures formed under extreme circumstances (very high solvent concentration in the coagulation bath, very thick membranes) can be comprehended from the proposed mechanism for the effects of PVP addition.

Introduction

It is known that ultrafiltration or microfiltration membranes prepared by the immersion precipitation technique[1], with a water-soluble polymeric additive such as poly(vinyl pyrrolidone), have superior properties when compared to membranes prepared in the same way but without the additive[2-6].

The fouling properties of the membranes are improved since the origi-

nally hydrophobic surface of the membrane acquires *hydrophilic properties* from the additive molecules which for a part remain in the membrane after preparation[6]. The effects of the additive on the morphology of the membranes[2,3] are of equal importance.

Much work has already been done in the past on the preparation of membranes using poly(vinyl pyrrolidone),[2-6] PVP, as an additive. In general, *macrovoid formation* is found to be *suppressed* by the addition of PVP. One needs a certain minimum concentration of PVP, with at least a certain minimum molecular weight. This turns out to be dependent on other process conditions, such as the concentration of the membrane forming polymer. Further, on a smaller scale, the pore structure obtains a *better interconnectivity* by the addition of PVP. This results in higher fluxes through the membrane, while maintaining high particle retentions. The overall porosity of the membrane is larger when compared with the same membrane prepared without the use of such an additive.

In summary, the most important effects of PVP on the membranes are:

- increased hydrophilicity of the membrane (pore) surface
- suppression of formation of macrovoids
- enhanced interconnectivity of the pores

Despite all investigations, a systematic study of the effects of PVP on the membrane morphology has never been carried out.

In this chapter some of the most important process parameters of the immersion precipitation process are varied: the membrane forming polymer concentration, the concentration of the polymeric additive (PVP), and the solvent (NMP) concentration in the coagulation bath.

The morphological changes resulting from the concentration variations are compiled into a number of empirical rules that describe the different effects of PVP on membrane structure. Light transmittance through the membranes as a function of time has been recorded during the preparation of all membranes. It is shown that the effects of PVP on membrane morphology are closely connected to changes in the light transmittance profiles.

It has been shown earlier that the most important effect of the presence of PVP in the polymer solution is that the mutual diffusion between the two polymers is significantly slower compared to the other diffusion processes in the system. This has a profound influence on the immersion precipitation process[7]. The effects of this low interpolymer mobility are used to explain the effects of PVP addition on membrane structure shown in this chapter.

Experimental

Poly(ether sulfone), Victrex 5200 P, supplied by ICI Ltd., was dried at least for 12 hours at 80 °C before usage. No further purification was applied. Poly(vinyl pyrrolidone), grade K30 and K90 from Jansen Chimica, was used as received. In table 1 the molecular weights of the various polymers are given.

Table 1: Molecular weights of the polymers used, measured by gel permeation chromatography

Polymer	M_n (g/mole)	M_w (g/mole)
PES Victrex 5200 P	22 300	43 800
PVP K30	8 700	18 100
PVP K90	99 800	228 200

N-methyl-2-pyrrolidone, or NMP, was obtained from Merck, synthesis grade, and was used without further purification. Water was demineralized and ultrafiltrated.

The polymer solutions were cast with a thickness of 0.2 mm on a glass plate. It was found that the temperature of the coagulation bath has a significant effect on the membrane morphology. Therefore the coagulation bath temperature was fixed at 298 K. The membranes were left in their coagulation bath until they got completely detached from the glass plate. Then they were transferred to a rinsing bath of pure water. After several hours they were transferred to a solution of 4 g/l of sodium hypochlorite in water, in which they stayed for three days, to crosslink PVP[6]. Finally, membranes were kept under water until further investigation.

Samples for the scanning electron microscope were broken in the wet state under liquid nitrogen, and dried *in vacuo* for at least 6 hours. A thin layer of gold was deposited on top of the sample with the Balzers Union SCD 040 sputtering apparatus. Samples were studied with a Jeol JSM T220 A scanning electron microscope.

The setup used for the transmission experiments[9] is shown in figure 1.

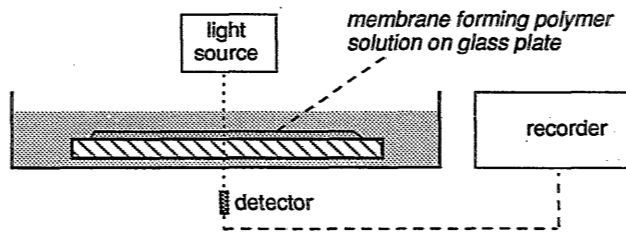

Figure 1: Experimental setup to measure light transmission through the polymeric solution during the immersion precipitation step[9].

Tables 2 and 3 show all polymer solutions and coagulation baths used. All membranes were prepared in triplo; whenever the corresponding membranes did not match qua structure, more membranes were prepared (from the same polymer solutions) under the same circumstances.

Table 2: Polymer solutions

No.	wt% PES	wt% PVP	PVP type
1	15	5	K30
2	15	10	K30
3	15	15	K30
4	15	20	K30
5	15	5	K90
6	15	10	K90
7	15	15	K90
9	20	5	K30
10	20	10	K30
11	20	15	K30
12	20	5	K90
13	20	10	K90
14	15	0	-
15	20	0	-

Table 3: Coagulation baths

Bath No.	wt% NMP
1	0
2	10
3	20
4	30
5	40
6	50
7	60
8	70
9	75
10	80

Results

Membranes prepared without addition of PVP to the polymer solution, with varying NMP concentrations in the coagulation bath are shown in figure 2. Structures obtained are in agreement with findings by Reuvers *et al*[8-10]. One can see from the structures and from transmission experiments (figure 9) that a transition in the mechanism of membrane formation from instantaneous demixing to delay of demixing occurs at approximately 70 weight% of NMP in the coagulation bath. This is accompanied by a vanishing of the macrovoids which are typical for instantaneously demixed membranes[10]. One can observe that enlarging the polymer concentration deminishes the tendency to form macrovoids. The situation of the transition from instantaneous to delay type of demixing is not significantly influenced.
The membranes prepared by delay of demixing exhibit a layer of larger pores close to the interface with the coagulation bath.

In figure 3 the effect of the addition of PVP to the polymer solution, coagulated in a bath with a low (40 wt%) concentration of NMP in water is shown. The structures are the same as the structures prepared with a still lower concentration of NMP (or even pure water) in the coagulation bath (not shown).
For 15 wt% PES, use of low molecular weight PVP gives a slight tendency to reduce macrovoid formation. This effect is much stronger when high molecular weight PVP is used as addition to the polymer solution. Here, it appears that all macrovoids have disappeared upon adding 10 weight% of PVP K90.
The use of 20 wt% PES shows different results. It appears here that addition of low molecular weight PVP promotes macrovoid formation. At 15 wt% PVP K30, the toplayer has a regular porous structure; the macrovoids start somewhat deeper in the membrane. A high concentration of PVP K90 reduces macrovoid formation; a regular, more or less co-continuous structure is formed.

Figure 4 shows membranes coagulated in a bath of 50 wt% of NMP in water. Addition of PVP, whether low molecular weight or high molecular weight, now first *promotes* the formation of macrovoids. When the concentration of the high molecular weight additive is further enlarged, the initial increase in macrovoid formation is overtaken by a decrease.

This is also, but far less clearly visible in figure 3. With a low concentration of solvent in the coagulation bath, in combination with low molecular weight PVP as additive, the suppressing effect of PVP on macrovoid formation is not very large. It is, therefore, not surprising that the suppression of macrovoids with low molecular weight PVP cannot be found at all with 50 weight% of NMP in the coagulation bath. One only sees the increase in macrovoid formation.
A more or less co-continuous structure appears around the macrovoids (e.g. visible at 10 wt% PVP K30 and 5 wt% PVP K90, with 15 wt% PES). The walls of the macrovoids obtain a much more open structure by the addition of PVP.

Figure 5 shows membranes prepared with a coagulation bath of 60 wt% NMP in water. Again one can see that PVP K30 promotes macrovoid formation. The co-continuous structure mentioned for figure 4, seen around macrovoids, is more pronounced here.
At a higher concentration of PVP K90, a regular open porous structure is obtained that has been described by Roesink[6]. The structure shows completely interconnected pores: a typical co-continuous structure.
Comparison of the membranes prepared with 10 wt% PVP K90 (and 15 wt% PES) with 40, 50 and 60 wt% NMP in the coagulation bath (figures 3, 4 and 5) shows that an *increase* of the NMP concentration in the coagulation bath *enlarges* the typical pore size in the open porous structures.

The transition from instantaneous to delay of demixing without PVP lies just below 70 wt% of NMP in the coagulation bath. Membranes prepared just beyond this transition, with 70 wt% NMP in the coagulation bath, are presented in figure 6.
Results with 15 wt% PES are discussed first. Low molecular weight PVP up to a concentration of 10 weight% seems to maintain the cellular (delay of demixing) structure. The closed pores have become much larger here. The larger cells appear near the interface with the coagulation bath. The more PVP is added, the larger the effect is.
Unlike a typical membrane from a ternary system, formed by delay of demixing, small pores appear in-between the large cells. We will see later that this is a general phenomenon of systems with PVP coagulated under these circumstances.
A concentration of 15 weight% PVP K30 in the polymer solution causes macrovoids to be formed. A low concentration (5 wt%) of high molecular weight PVP (K90) leads to a structure with macrovoids, and a very open,

completely interconnected pore structure in-between. The pores in this structure are much larger than the pores in the membranes with less (0 wt%) or more (10-15 wt%) PVP K90. This might be compared with the creation of larger cellular pores by using up to 10 wt% PVP K30. Addition of more PVP K90 again gives the typical open porous structure reported earlier by Roesink[6] without any macrovoids.
The use of 20 wt% PES in the polymer solution does not show the observed increase in size of the closed cells, at low PVP concentrations. One sees again that addition of PVP induces macrovoid formation. At 15 wt% PVP K30, a structure is obtained that is similar to the structure of 15 wt% PVP K30 or 5 wt% PVP K90 with 15 wt% PES, in the same coagulation bath. It features oval voids, with an interconnected pore structure and a typically large pore size.

Further increase of the NMP concentration in the coagulation bath to 75 wt%, as shown in figure 7, shows the same trends, although more pronounced.
Again membranes from 15 wt% PES are considered first.
A small addition of PVP K30 does not enlarge the typical size of the closed cells, although the cellular structure itself is maintained. At 20 wt% PVP K30, a different structure is obtained. It seems that the walls of the pores contain some small pores themselves. The structure can be characterized as bicontinuous, in which both the (large) pores and the polymer matrix are continuous.
PVP K90 approximately shows the same trends. The co-continuous structure now appears already at 5 wt% PVP K90. The thickness of the bicontinuous membranes is smaller than membranes with a cellular structure. One can see more clearly here that the pore walls themselves are porous. A larger PVP K90 concentration results in smaller pores, and an increase of the overall thickness of the membranes. At 15 wt%, a more or less normal open porous structure[6] is obtained.
Membranes prepared with 20 wt% PES also show the transition from a closed cell structure to a co-continuous structure, accompanied by a decrease in membrane thickness. Addition of 15 wt% PVP K30 causes the formation of irregular voids. The same addition with 15 wt% PES gave a structure with smaller and more regular pores. PVP K90 does not give the structure with large voids. The structure directly changes from a cellular structure (5 wt% PVP K90) to a relatively fine, co-continuous structure (10 wt% PVP K90).

The largest concentration of NMP in the coagulation bath studied is 80 wt%, which is more than 10 wt% above the transition from delayed to instantaneous demixing for a ternary system without PVP. Structures are given in figure 8.
Membranes from 15 wt% PES are first discussed. With low PVP K30 concentration, again a cellular structure is obtained. An addition of 10 wt% PVP K30 shows an irregular, cellular structure similar to the structures obtained with lower NMP content in the coagulation bath.
The occurrence of a co-continuous structure is much more pronounced here. Large voids are obtained in a matrix which is porous by itself, featuring a closed cell structure. The *surface* of the walls of the voids is not very open. Note that generally, the use of PVP causes the surface of the walls of *macro*voids to be quite open (see e.g. figure 4). Apparently there is a difference between *macro*voids and the voids occurring here. We will later expand on this.
Further increase of the PVP K30 concentration reduces the size of the voids. At 15 wt% PVP K30, a more or less co-continuous structure with large pores is obtained, while inside the walls of these pores, a closed cell structure is still clearly present.
At 5 wt% PVP K90, we can see both closed pores, and the typical irregular voids discussed earlier. An increase in PVP K90 content lowers the pore size. Comparison of the structure obtained with 10 wt% PVP K90 with the structure from 15 wt% PVP K30, shows a more regular structure in the case of PVP K90. The interface between the large pores and the closed cells inside the pore walls is nonporous again. Further increase of the PVP K90 content results in a smaller pore size and thicker membranes again.
The use of 20 wt% PES maintains the cellular structure up to higher PVP content. At 15 wt% PVP K30, the voids are so large, that not much can be said about the rest of the structure.

Transmittance profiles
In figure 9, the transmittance profiles at the start of membrane formation are given as recorded for the membranes shown in figure 2 (no PVP added). One can see that there is a clear transition from instantaneous demixing to delay of demixing.
This is different when PVP is added to the polymer solution. In figure 10 the transmittance profiles are given for different polymer solutions, under variable coagulation conditions.

From 0 to 60 wt% NMP in the coagulation bath, roughly the same transmittance profiles are obtained, although the absolute velocity of decrease of the transmittance is higher with less solvent in the coagulation bath. The differences between the different polymer solutions remain the same. Therefore, only the profiles for 60 wt% NMP and higher in the coagulation bath are shown.
Up to 60 wt% NMP in the coagulation bath, all profiles indicate instantaneous demixing. It appears that addition of PVP *slows down* the demixing processes.

At 70 wt% NMP in the coagulation bath, membranes without PVP show delay of demixing. Addition of a moderate amount of PVP (> 5 wt%) to the polymer solution induces instantaneous demixing. A large amount of PVP K30 added (≥ 15 wt%) results in a minimum in the transmittance, after which the transmittance temporarily increases again. The more PVP is added, the stronger this effect. The minimum can not be observed at 70 wt% NMP with PVP K90, although irregularities in the profiles could indicate that the effect is present.
Although the initial delay of demixing is suppressed (the transmittance starts to decrease earlier), later-on the transmittance is decreasing more slowly than without the use of PVP. Summarizing: demixing starts *earlier*, but proceeds *more slowly* by addition of PVP.
A coagulation bath of 75 wt% NMP in water also shows the minimum in transmittance. The slowing down of the decrease in transmittance by PVP is more pronounced here. The initial rate of decrease in transmittance is quite large when PVP is used: the demixing process is clearly instantaneous.

At 80 wt% of NMP in the coagulation bath, one can also see the minimum in transmittance with the solutions of 15 wt% PES and PVP K90.
Addition of more solvent to the coagulation bath lowers the *velocity* of demixing, as is expected.
Delay of demixing can only be somewhat preserved when small concentrations of low molecular weight PVP are used. This is reflected in the closed cell structures obtained with low PVP K30 content (see e.g. figure 6). Still, even the conditions which gave these cellular structures show a (small) initial decrease of transmittance.

Thickness of the membranes
In figure 11 the thickness of the membranes are represented as a function

of the PVP concentration.
For membranes without PVP, the membrane thickness somewhat decreases upon enlargement of the solvent concentration in the coagulation bath. At higher PVP concentration the decrease of the membrane thickness with increasing solvent content in the bath becomes stronger.

Increase of the concentration of PVP results generally in thicker membranes. Some membranes are even thicker than the original casting thickness. This is in (qualitative) agreement with results found from mass transport calculations performed earlier[7], which showed that PVP in the polymer solution enlarged the inflow of nonsolvent considerably; it appears that while in a ternary system mostly nonsolvent influx is smaller than solvent outflux, PVP causes the indiffusion process to be usually larger than the outdiffusion. This appears in figure 11 as an increase in thickness of the membranes when increasing PVP concentration.

Summary of the effects of PVP

The previously discussed effects of PVP on the membrane structure can be summarized in a set of empirical rules.

General

1. The ternary system PES-NMP-water gives structures as expected from the work of Reuvers and Smolders *et al.*[8-10]
2. Additions of PVP K30 and PVP K90 show approximately analogous trends. The effects of PVP K90 are *stronger*, but equivalent to the effects of PVP K30.
3. Addition of PVP suppresses delay of demixing, as shown by transmission experiments. Demixing starts earlier. PVP slows down the rate of decrease in transmittance whenever demixing has started. Generally, addition of PVP results in an increase in the thickness of the membranes.

Macrovoid formation

4. At conditions of fast demixing (i.e. low NMP content of the coagulation bath) PVP *suppresses* macrovoid formation partially or completely. A certain minimum concentration and molecular weight of PVP is necessary for this effect.

5. At slower demixing conditions (higher NMP content) and moderate concentrations of PVP, PVP *promotes* macrovoid formation.
6. At larger PVP concentrations, macrovoid formation is again suppressed.
7. Even at conditions that would give delay of demixing in the absence of PVP, macrovoids are formed when PVP is present. This is closely connected to point 3.
8. When macrovoids are formed in the presence of PVP, the walls of the macrovoids are more open than when no PVP would have been used (such an effect has also been observed for other types of additions, like glycerol).
9. Around these macrovoids, a co-continuous structure is observed that resembles the structure to be mentioned under 13 and 14.

Pore structure

10. Upon addition of PVP, the poorly interconnected pore structure typical for ternary instantaneous demixing is modified into an open porous, co-continuous structure, as earlier reported[6]. This structure is characterized by a fairly regular pore size. After a post-treatment to remove excess PVP, the pores are completely interconnected.
11. An increase of the solvent concentration in the coagulation bath enlarges the typical pore size, as long as macrovoid formation is suppressed.
12. An increase of the PVP content lowers the pore size.
13. At concentrations of solvent in the coagulation bath that are considerably above the transition from delay to instantaneous demixing in the ternary system without PVP, the cellular structure changes into an irregular structure, characterized by large pores or voids, surrounded by walls that are porous themselves. The occurrence of this structure is accompanied by a decrease in membrane thickness.
14. At higher PVP concentrations this structure with large pores becomes more or less co-continuous (the pore walls break up). The structure then resembles the original structure obtained (mentioned in point 10), for coagulation with a small amount of solvent in the coagulation bath and sufficient PVP present.

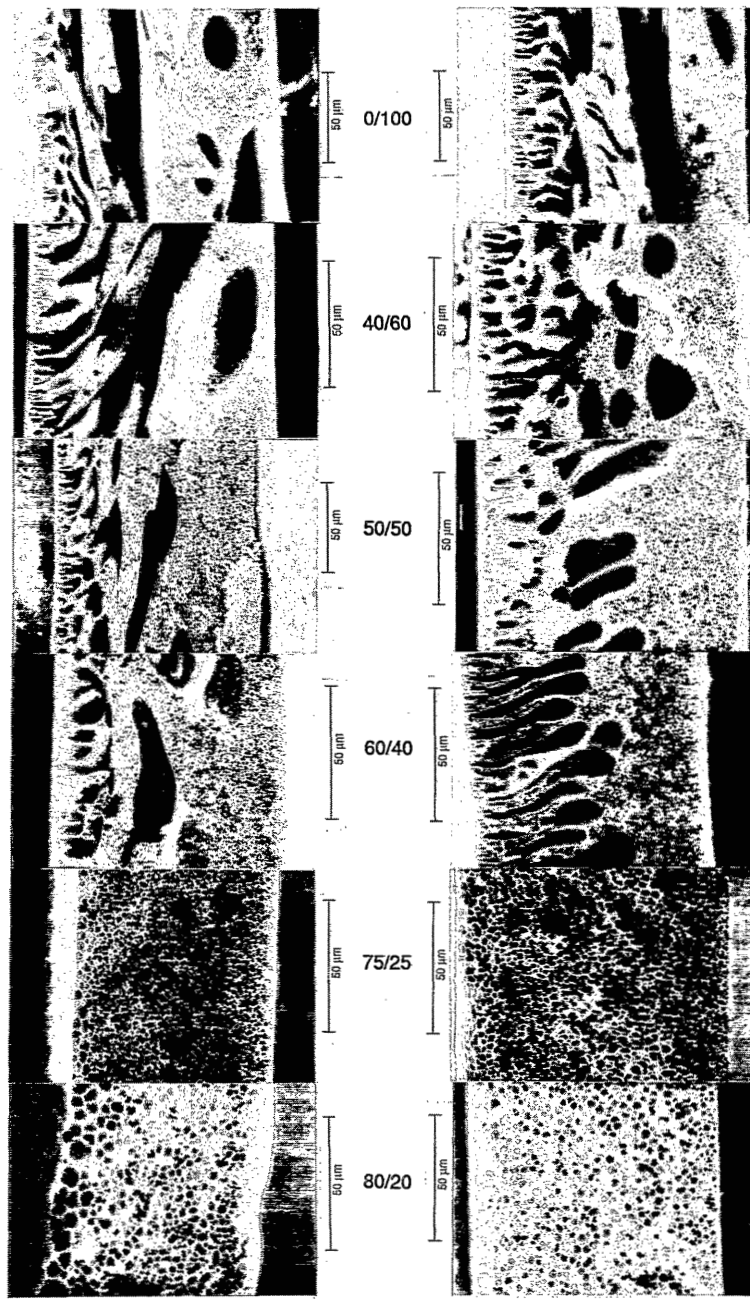

2a 2b

Figure 2: Membranes prepared without the use of PVP. Figure 2a: 15 weight% PES in NMP; figure 2b: 20 weight% PES in NMP.
The coagulation baths used are indicated on the pictures as weight ratios NMP/water.

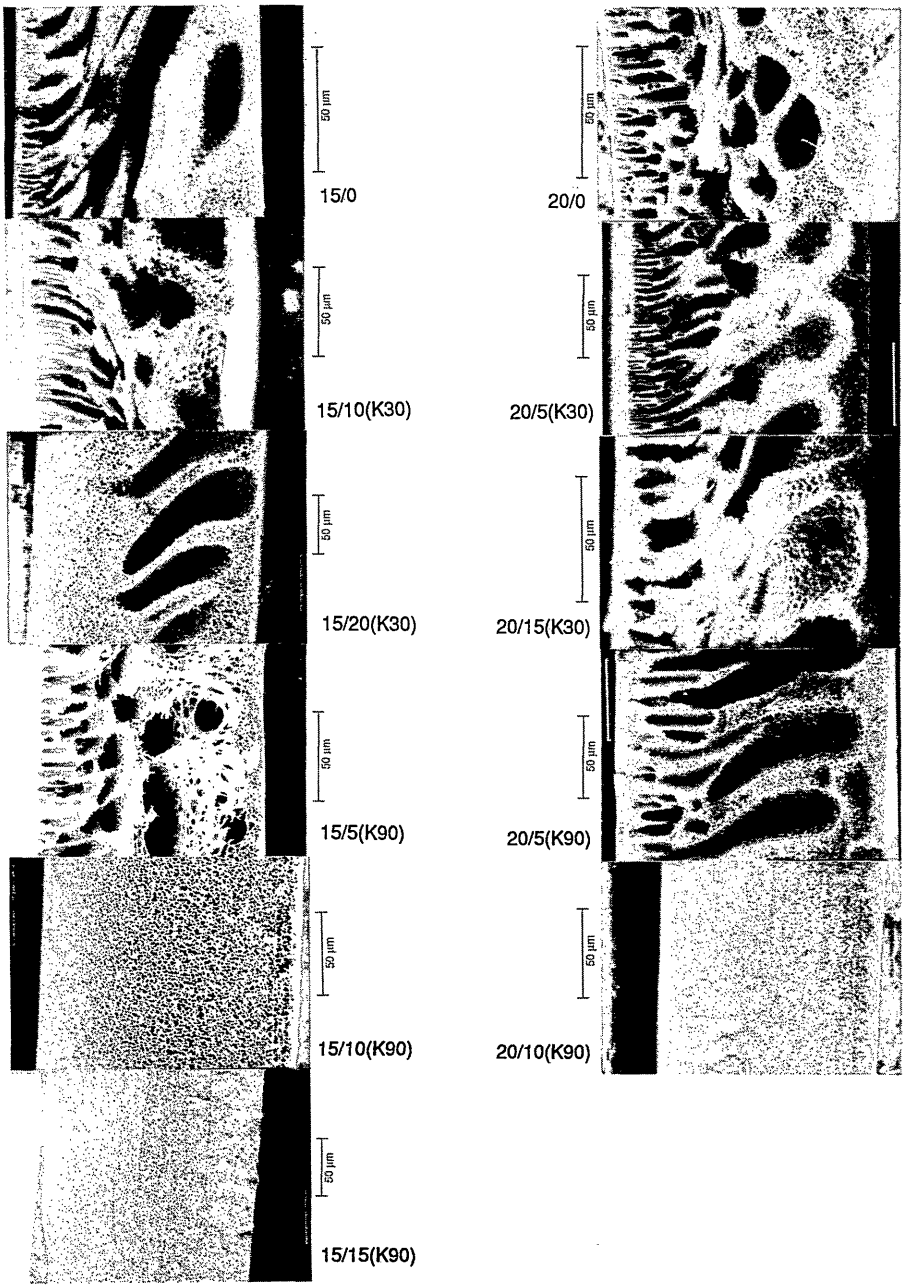

Figure 3: Membranes prepared in a coagulation bath of 40 wt% NMP in water. The polymer solutions used are indicated as: wt% PES/wt% PVP (type of PVP), in NMP.

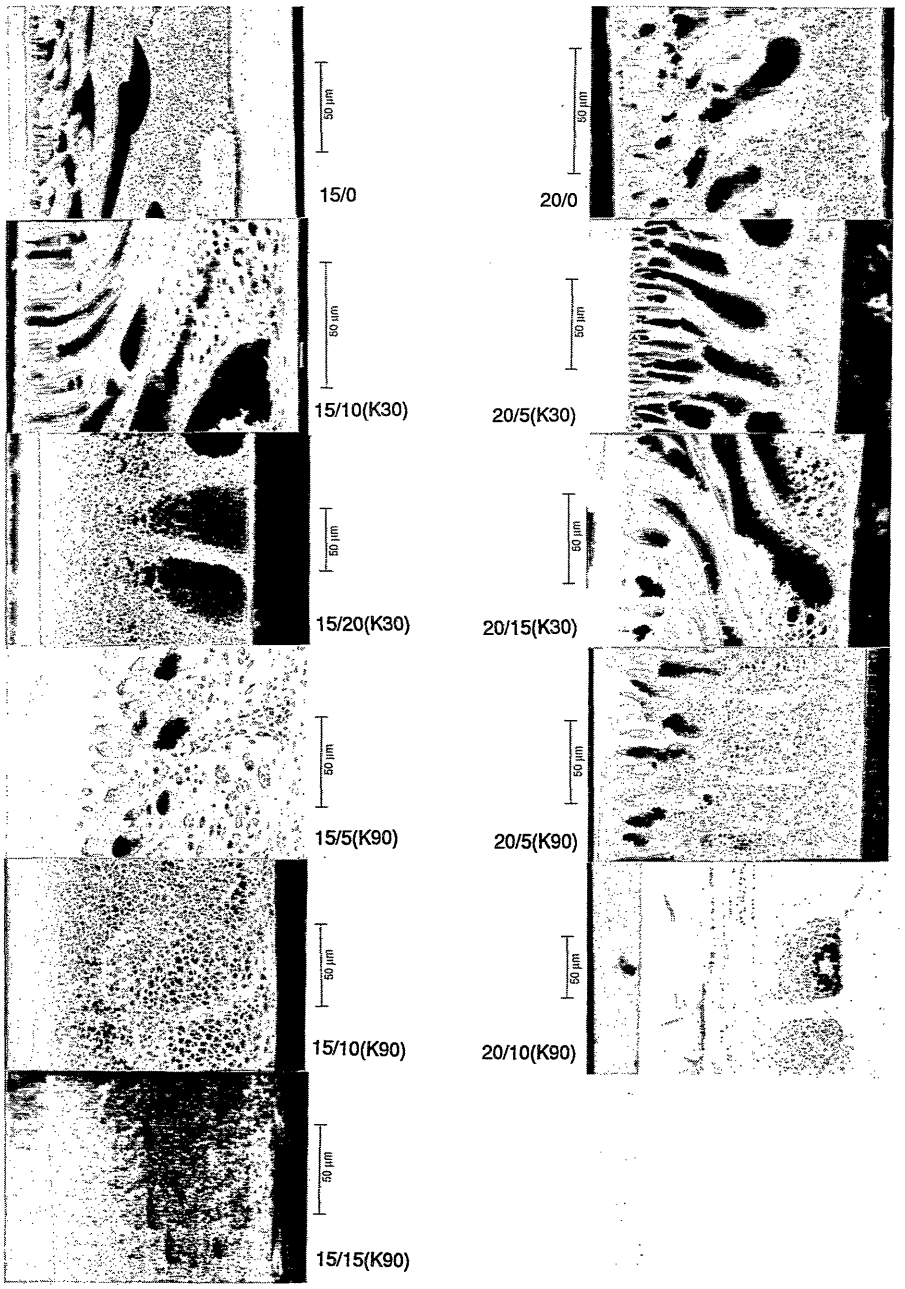

Figure 4: Membranes prepared in a coagulation bath of 50 wt% NMP in water. The polymer solutions used are indicated as: wt% PES/wt% PVP (type of PVP), in NMP.

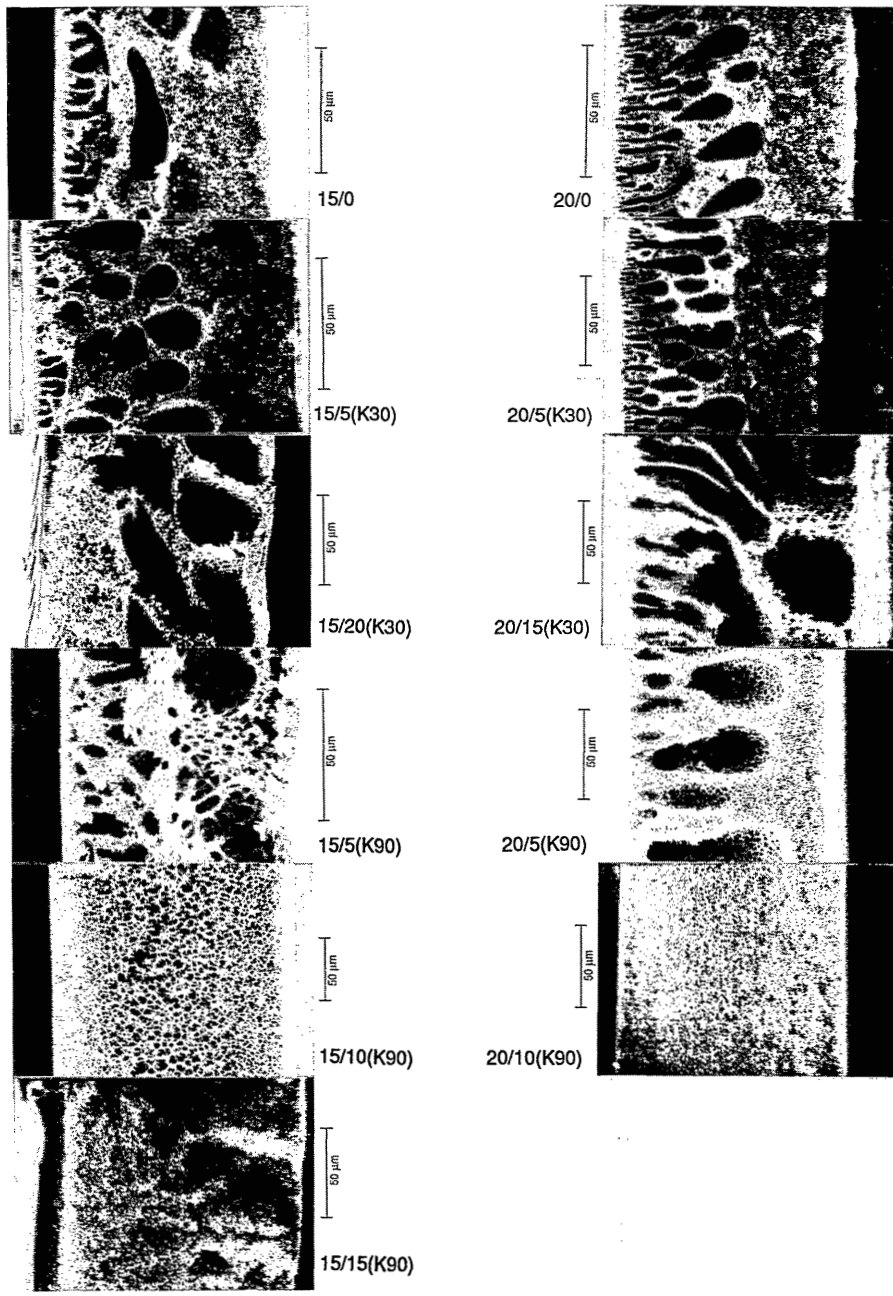

Figure 5: Membranes prepared in a coagulation bath of 60 weight% NMP in water.
The polymer solutions used are indicated as: wt% PES/wt% PVP (type of PVP), in NMP.

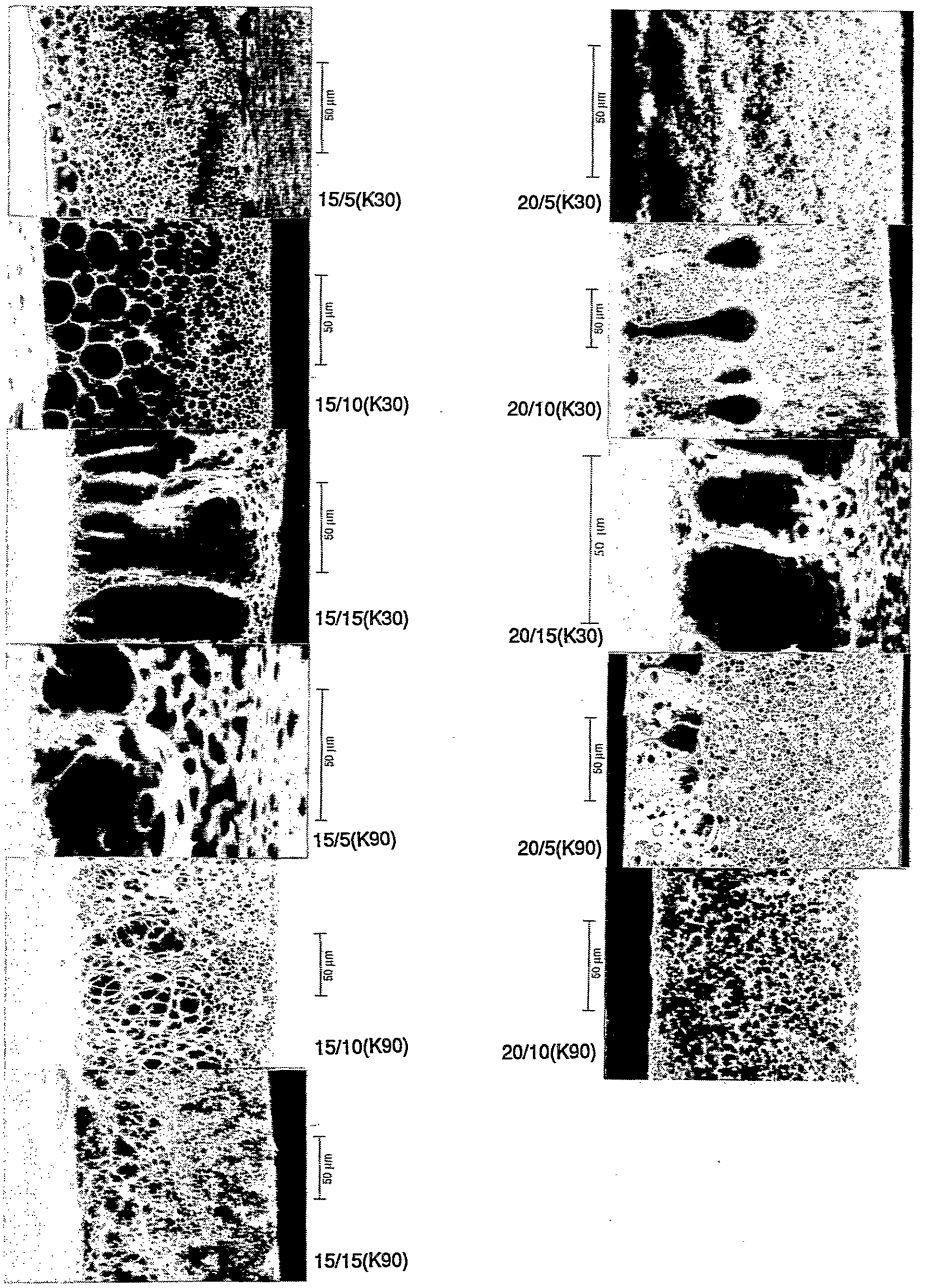

Figure 6: Membranes prepared in a coagulation bath of 70 weight% NMP in water.
The polymer solutions used are indicated as: wt% PES/wt% PVP (type of PVP), in NMP.

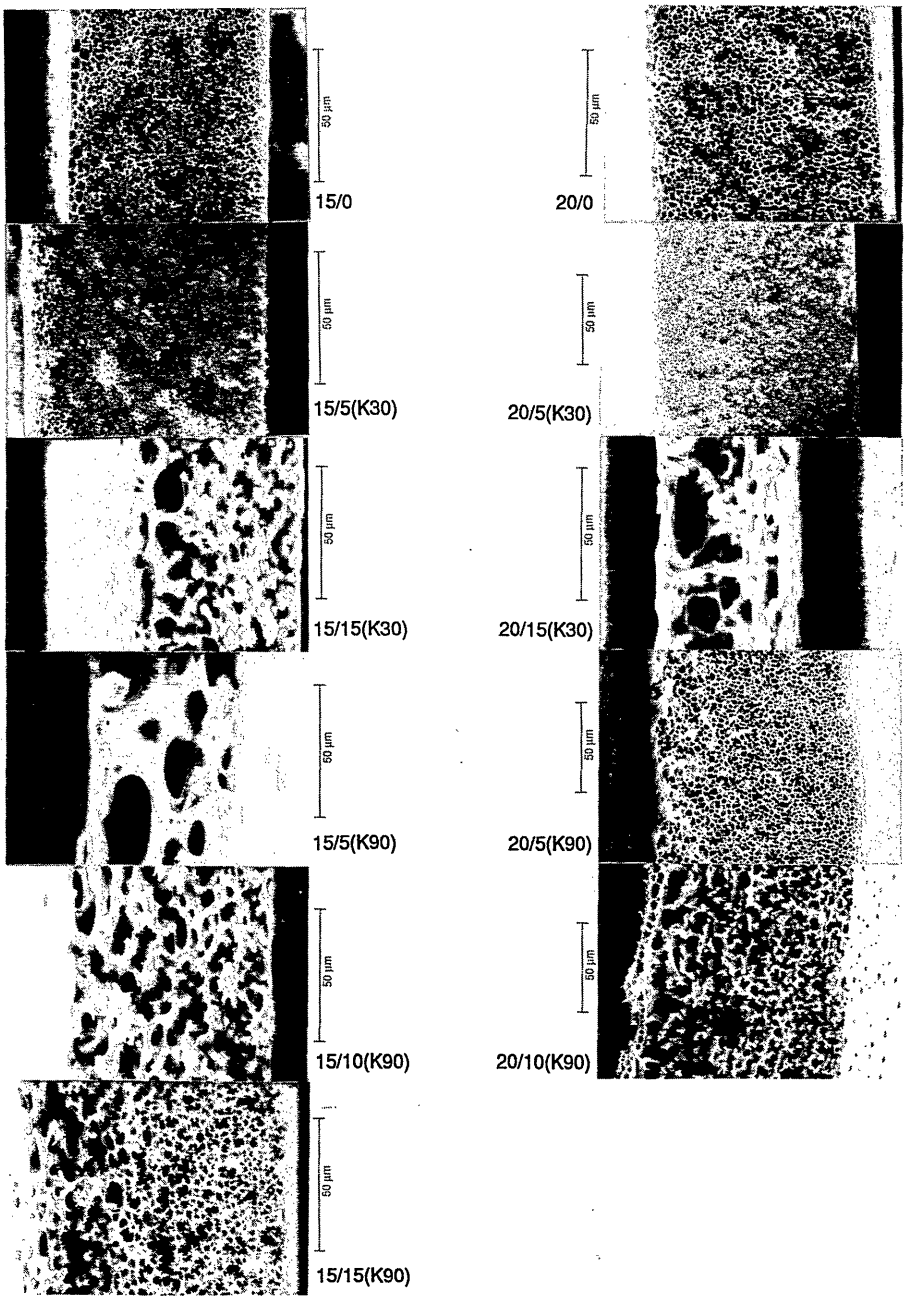

Figure 7: Membranes prepared in a coagulation bath of 75 weight% NMP in water.
The polymer solutions used are indicated as: wt% PES/wt% PVP (type of PVP), in NMP.

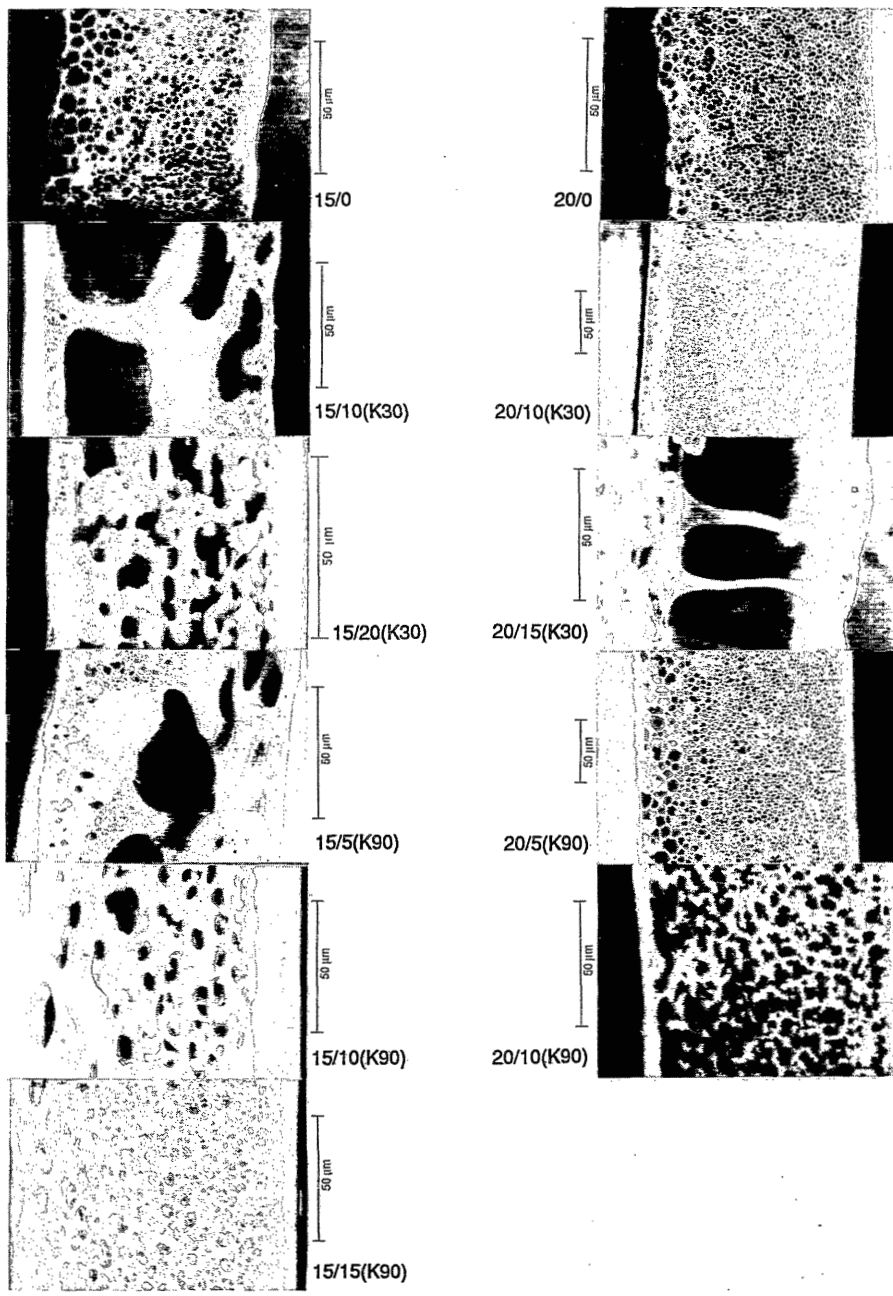

Figure 8: Membranes prepared in a coagulation bath of 80 weight% NMP in water.
The polymer solutions used are indicated as: wt% PES/wt% PVP (type of PVP), in NMP.

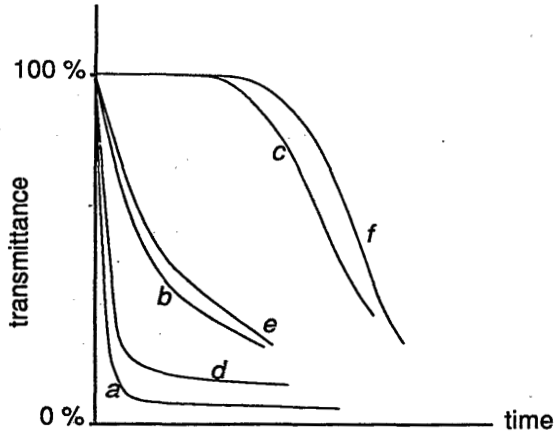

Figure 9: Transmission profiles for membranes with 15 and 20 wt% PES in NMP, and varying amounts of NMP in the coagulation bath. No PVP was used. The indices a to f indicate the different concentrations used:

index	*Polymer solution wt% PES in NMP*	*Coagulation bath wt% NMP in water*
a	*15*	*0*
b	*15*	*60*
c	*15*	*75*
d	*20*	*0*
e	*20*	*60*
f	*20*	*75*

wt% NMP in bath	15 weight% PES	
	PVP K30	PVP K90
60%		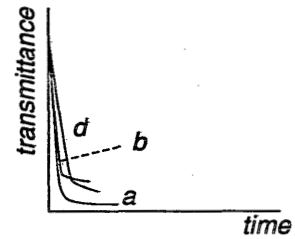
70%	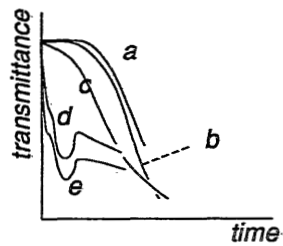	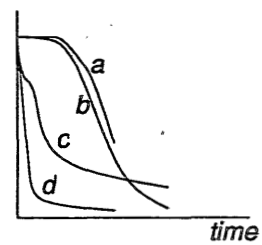
75%	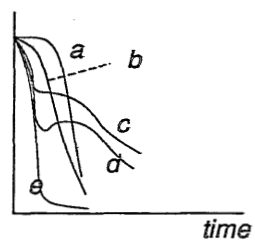	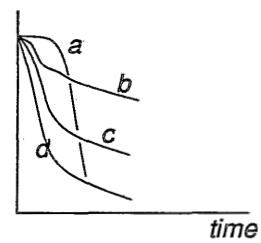
80%	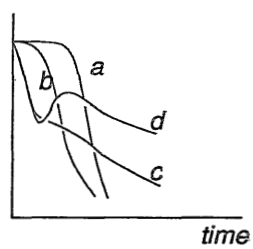	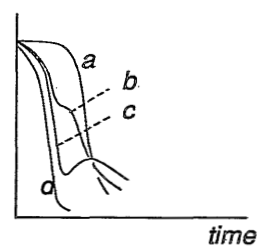

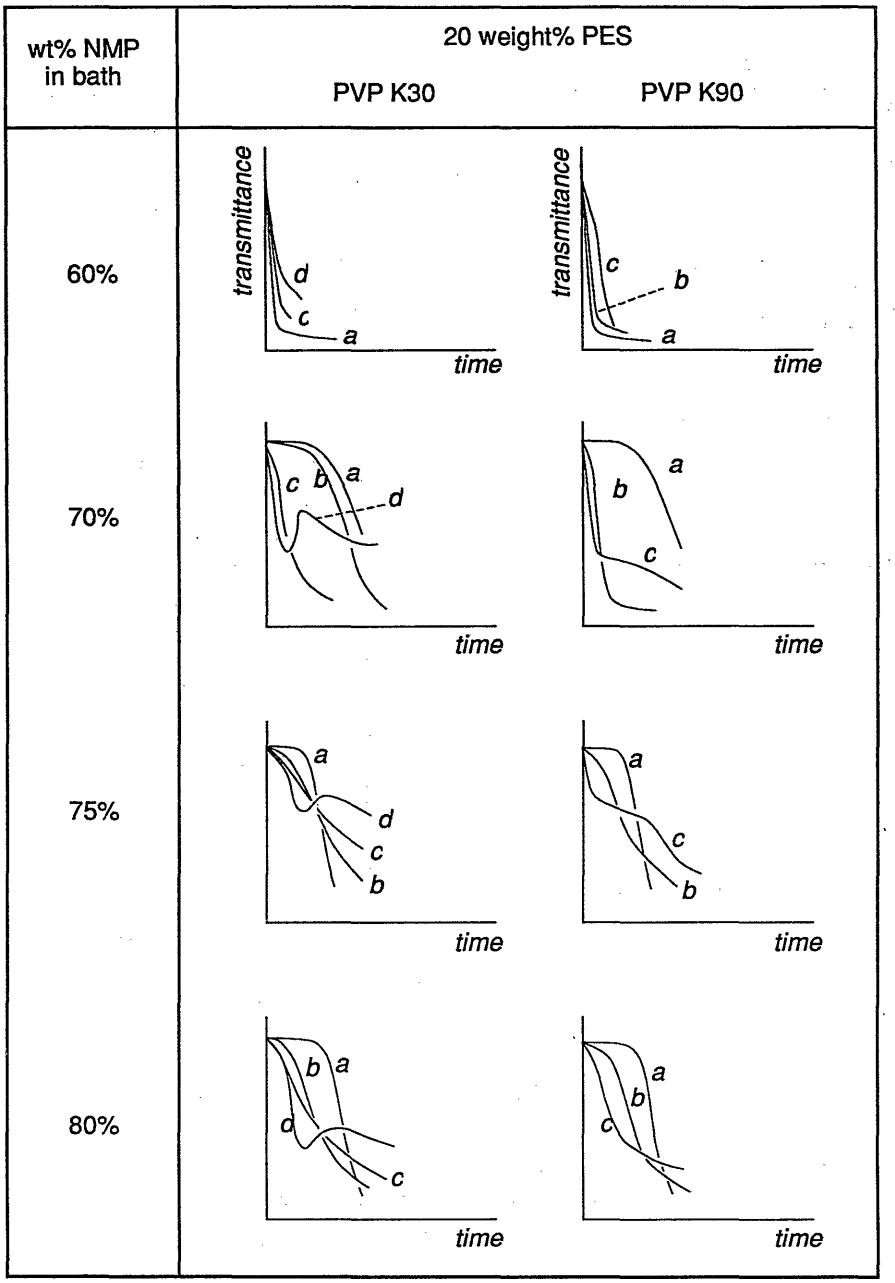

Figure 10: Recorded transmittance profiles for membranes shown in figures 2 to 8. Indices reflect the PVP concentrations of the polymer solutions: (a) 0, (b) 5, (c) 10, (d) 15, (e) 20 wt% PVP.

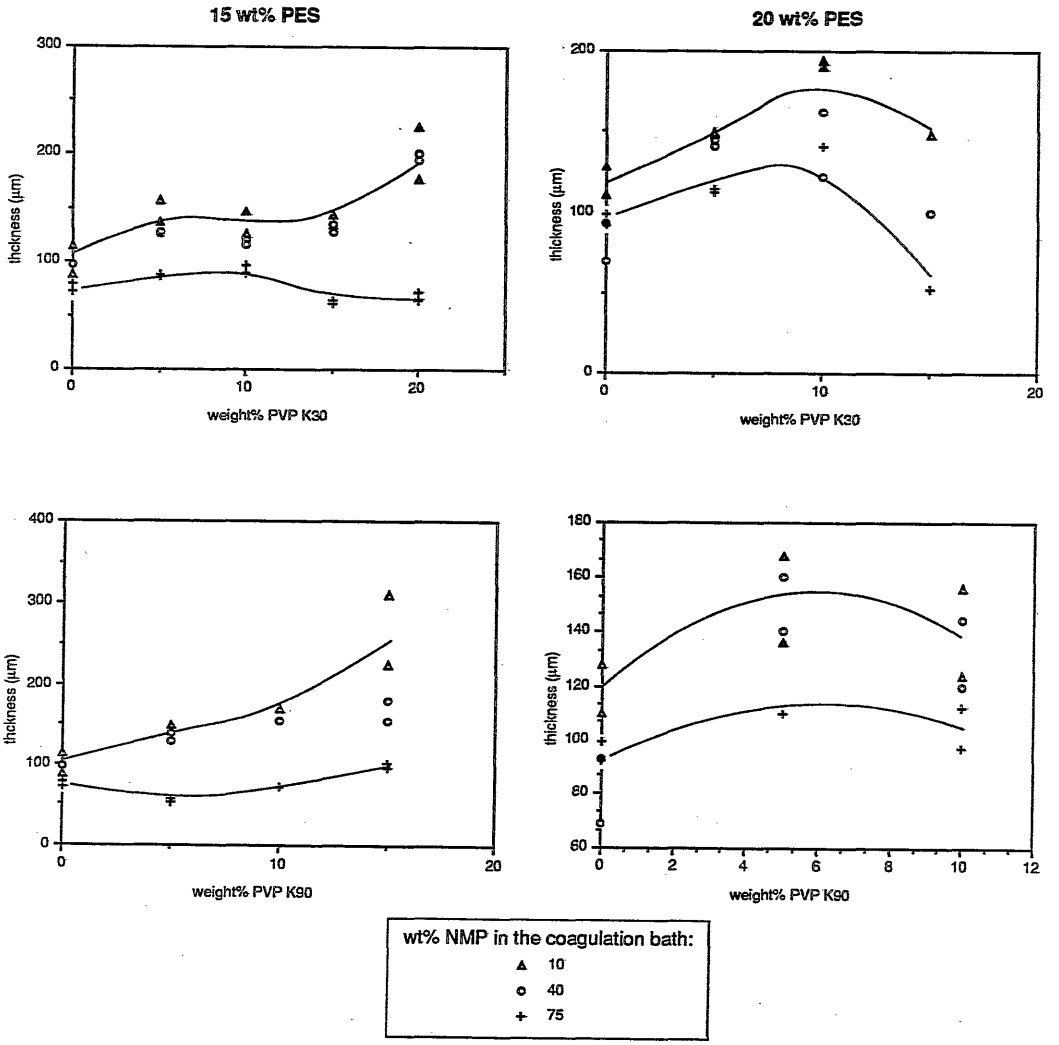

Figure 11: Thickness of membranes obtained with 15 and 20 wt% PES, for various quench conditions (compositions of the coagulation bath, and for various amounts of PVP (K30 and K90) added to the casting solution).

Discussion

We will now discuss the empirical rules found in the preceding paragraphs for the effects of addition of PVP to the polymer solution, on membrane formation.

Ad 1: Absence of PVP.
From Reuvers *et al.*[8,9] we can see that for every polymer solution, delay of demixing can be obtained by adding a certain critical amount of solvent to the coagulation bath. Figure 12 shows some calculated initial composition paths for the ternary system.

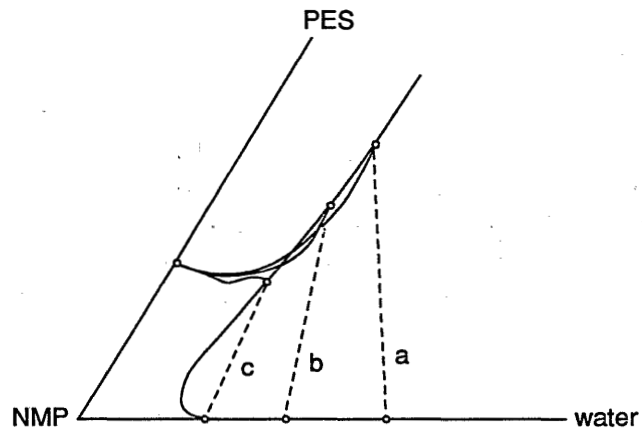

Figure 12: Composition paths calculated for the ternary system PES-NMP-water, for different amounts of solvent in the coagulation bath: a: pure water bath; b: 50 % NMP in water; c: 70 % NMP in water. Only part of the phase diagram is shown.
Parameters used are given in reference 7. One can see that at a certain amount of solvent the composition path shows delay of demixing (case c).

The transition from instantaneous to delay of demixing is more or less adequately predicted from the Reuvers model. It appears in figure 2 that the delay of demixing membranes (coagulated with 70 or more wt% NMP in the coagulation bath) are characterized by the appearance of large cells just below the (dense) toplayer. An explanation for this can be found in figure 12. At high solvent concentrations in the coagulation bath, the polymer concentration in the toplayer remains low. Nuclei being created just below the toplayer can grow larger than with less solvent in the

coagulation bath.
The reason that still a dense toplayer is created is that while nuclei *at* the toplayer can not be created (the toplayer itself is in local equilibrium with the coagulation bath), the nuclei underneath the toplayer extract solvent and nonsolvent from the polymer solution between interface and nucleus, leaving there a higher concentration of polymer, which then forms a dense toplayer.
The thicknesses of the membranes follow the trends as expected from the model by Reuvers and Smolders[8,9,15].

Ad 2: Analogy between PVP K30 and PVP K90
It has been shown before[12,7] that thermodynamically, not much difference exists between the addition of PVP with a low (18 kg/mole) or a high (230 kg/mole) molecular weight. In both cases the solution becomes less compatible with water.
It was also argued before that the direct influence of the molecular weight of the additive on the diffusion processes of solvent and nonsolvent is not large[7,13]. The only substantial effect is the influence of the chain length on the reptation mechanism of diffusion which is thought to determine the diffusion of polymeric additive relative to the membrane forming polymer during membrane formation[11,13]. On the basis of the difference in normal, 'cooperative' diffusion and reptation or 'tracer' diffusion, a model was proposed that describes the influence of PVP on macrovoid formation under fast demixing conditions[7,14]. The observation that PVP K30 and PVP K90 behave analogously, but on different concentration scales, is a confirmation of this mechanism. For the sake of clarity, the model will be summarized shortly. It will be further used in the discussion for point 4.
The essence of this mechanism is that the movement of the two polymers is assumed to be slow compared to the movement of solvent and nonsolvent through the polymeric network. This is only valid as long as the additive (PVP) has a high enough molecular weight[7].
The relative immobility between the two polymers leads to a simplification in the system at the initial stage: the two polymers together act as one polymer, in a mixture of solvent and nonsolvent. From thermodynamic calculations[7] it appeared that, depending on the concentration of additive, this one (hypothetical) polymer is relatively compatible (but not yet miscible) with the nonsolvent, water. The inflow of nonsolvent into the polymer solution is high, as a result of which the polymer concentration in the toplayer remains relatively low. Compositions are created that are

unstable at the moment that the two polymers can move relative to each other. The situation remains the same even for quite high concentrations of solvent in the coagulation bath. Figure 13 shows a typical system, based on the thermodynamic and kinetic parameters available for the system PES-PVP-NMP-water, with a fixed ratio between PES and PVP, and varying coagulation bath compositions.

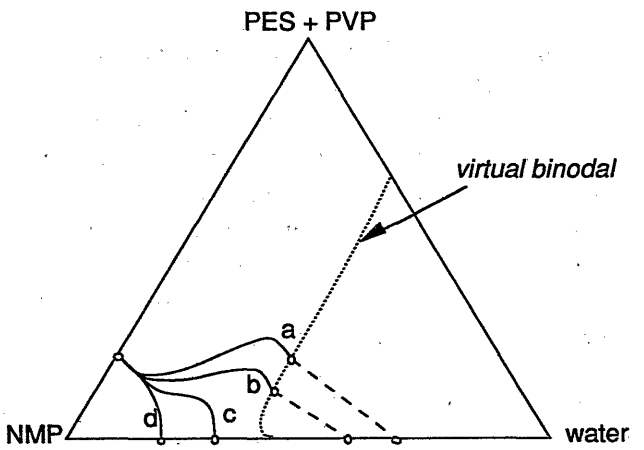

Figure 13: Initial composition paths for the system PES-PVP-NMP-water. Ratio PES/PVP is 5/3, as is often used in practice. Coagulation bath composition was varied from 100 % water (a), to 40 (b), 60 (c) and 75 % NMP in water (d). The dashed curve is the calculated 'virtual' binodal, valid only for the first moments of immersion.[7]

This one-polymer situation is valid as long as the reptation (tracer) diffusion velocity is small compared to the normal cooperative diffusion processes[7]. Unlike cooperative diffusion, the reptation velocity is strongly dependent on the molecular weights of the diffusing components. The difference in reptation diffusivity between the two types of PVP can be estimated with a scaling relation by De Gennes[13]:

$$\frac{D_{K30}}{D_{K90}} = \left(\frac{M_{K90}}{M_{K30}} \right)^{2 \text{ to } 2.5}$$

From this relation it is estimated that for PVP K90, the reptation diffusitity is 160 to 560 (two to three orders of magnitude) lower than for PVP K30.
It is therefore logical that PVP K90 has a stronger effect on the membrane structure.

Ad 3: Suppression of delay of demixing.

From the proposed mechanism, it can be seen that experimentally *no* delay of demixing can be observed when a significant amount of PVP is used. In figure 13 some initial composition paths are shown[7]. The cloudpoint curve for the systems considered is situated at a few percent of nonsolvent (water)[11]. When the water concentration in the polymer solution becomes higher, the two polymers in the system will phase separate.

During the first moments of immersion, compositions are created that contain much more water than a few percent[7], as is shown in figure 13. This is even true when e.g. 70 or 80 vol% of solvent in the coagulation bath is used. Although delay of demixing is obtained according to the thermodynamic regime valid for the *first moments* of immersion, the compositions created in the polymer solution are so rich in water that the polymers phase separate. Even for very high concentrations of solvent in the coagulation bath, demixing takes place relatively quickly. Delay of demixing therefore is suppressed by phase separation between the two polymers. This is confirmed by the transmission profiles already shown in figure 10. Addition of PVP inhibits the occurrence of delay of demixing up to very high concentrations of solvent in the coagulation bath.

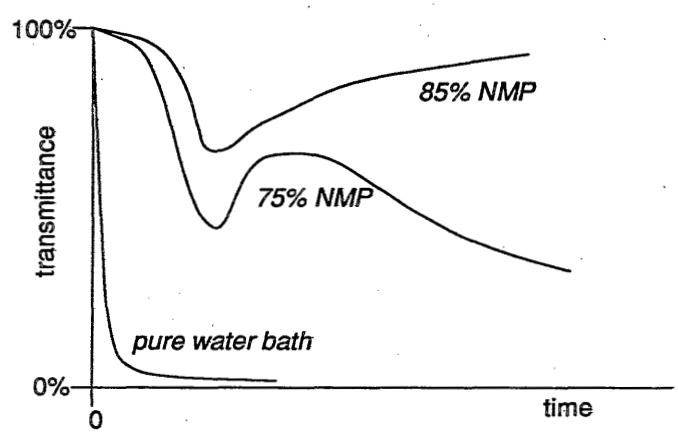

Figure 14: Transmittance profiles for a solution of 15 wt% PES and 20 wt% PVP, with 0, 75 and 85 wt% NMP in the coagulation bath. Other polymer solutions showed similar behavior. The coagulation bath with 85 wt% NMP did not yield a membrane: after an initial decrease in transmission, all material dissolved in the coagulation bath.

Only at very high solvent concentrations (e.g. 85 wt%) no instantaneous demixing is obtained. The term 'delay of demixing' is not appropriate here, since the polymer solution simply dissolves in the coagulation bath. Still, instead of giving no demixing at all, the films first become slightly turbid (indicating some phase separation between the two polymers), before they dissolve into the coagulation bath. Even now, delay of demixing is apparently not taking place. Figure 14 shows this behavior and how it compares with the behavior at lower solvent concentration in the coagulation bath.

The increase of the thickness of the membranes when PVP is added to the polymer solution is a result of the higher influx of nonsolvent from the coagulation bath[7].

Ad 4: Suppression of macrovoid formation.
To understand the effects of the addition of PVP on the formation of macrovoids, we must first discuss the mechanism of formation of macrovoids, as proposed by Reuvers *et al.*[10,15].
The instantaneous demixing process is characterized by a composition path that lies partly within the demixing gap, even directly after immersion in the coagulation bath. Just beyond the demixing front (i.e. in a thin layer past the point at which demixing has begun), the solution generally is instable, due to the fast penetration of nonsolvent. In that region one expects continuous formation of new nuclei i.e. the coagulation front will generally proceed rapidly.
The further the demixing front has advanced from the interface with the coagulation bath, the slower the diffusion processes at the diffusion front take place. At a certain moment it is possible that locally, the solution beyond the demixing front is *not* instable anymore. Since this stability of the polymer solution is characteristic of delay of demixing, we might call this phenomenon *local* delay of demixing. It is accompanied by a high concentration of solvent in the nucleus. The nucleus now grows further until another process stops the growth. A very large pore (a macrovoid) results.
It has been shown earlier that PVP has a large effect on the demixing behavior[7]. As long as the two polymers present cannot move relative to each other, the total system exhibits delay of demixing: no demixing takes place for some time. In other words, the separation of the two polymers is *essential* in the demixing process. We have seen that the movement between the polymers is much slower than other diffusion processes.

From earlier mass transfer calculations[7] it appeared that after immersion of the polymer solution an initial composition path results that includes deeply instable compositions concerning polymer-polymer separation.
During the immersion step the formation of a phase that is lean in membrane forming polymer (PES) and rich in additive (PVP), is so slow that along the diffusion profile instability of the solution exists even at large penetrating distances in the membrane. Local delay of demixing cannot occur, and thus the formation of macrovoids is suppressed.
Since the difference in diffusivity between the two polymers relative to that of other components is essential in this effect, we can see that reduction of the velocity of indiffusion of nonsolvent (by reducing the nonsolvent concentration in the coagulation bath) must lead to less suppression of the formation of macrovoids. We can also see that enlarging the thickness of the membrane should always result in the formation of macrovoids at great distances from the interface. We will exploit this later on.

Ad 5 and 6: Macrovoid formation under various conditions.
The difference in polymer-polymer diffusivity and other diffusivities is essential in the suppression of macrovoids. Reduction of the amount of nonsolvent in the coagulation bath results in a slower indiffusion of the nonsolvent (lower water flux from coagulation bath to polymer solution), and the difference with the polymer-polymer diffusivity becomes less. Then more time is available for the formation of a phase that is lean in PES, and macrovoids can be formed more easily.
Introduction of a larger amount of PVP in the polymer solution induces a larger quench of the polymer solution[7]; the instability in the polymer solution is larger and macrovoids are more effectively suppressed.
The use of high molecular weight PVP (K90) gives suppression of macrovoids at lower concentrations of additive, since the (reptation-) diffusion of longer polymer coils is far slower than the diffusion of lower molecular weight additive (PVP K30).
The difference in the diffusion effects for PVP K30 and PVP K90 can be seen in figure 10. At high NMP concentrations in the coagulation bath, the diffusion of PVP K30 is still so fast that the separation between PES and PVP can be completed (i.e. low transmittance) before other demixing processes can start. Later on, the transmittance increases again due to coalescence of the PVP phase. A distinct minimum in the transmittance curves results. PVP K90 separates so slowly from PES, that although the

effect can be vaguely identified, separation between PES and PVP is still going on when other demixing processes start.

Ad 7: Macrovoids above the ternary transition to delay of demixing.
The transition from instantaneous demixing to delay of demixing as encountered in the ternary system without PVP[8,9] does not occur in the quaternary system studied when at least a moderate amount of PVP has been added (see point 3). Solvent concentrations in the coagulation bath higher than the one at which this transition would be situated in the ternary system still give normal instantaneous demixing, and macrovoids are formed (given the right circumstances).
However, at sufficiently *low* concentrations of PVP K30, the delay of demixing character is maintained. Cellular structures are formed. In this case an increase in the size of the isolated pores can be seen. This can be explained in the following way: In the beginning of the immersion step, PVP induces a higher influx of water in the toplayer (it has been shown[7] that even a small addition of PVP enhances the inflow of nonsolvent considerably). The polymer concentration in the toplayer is somewhat lower than without PVP. PVP fairly quickly phase separates from PES, but because the concentration of PVP is low, this is not noticed in the transmission profiles (only a slight decrease in turbidity results). The demixing between the PES phase then follows a normal delay of demixing process.
For higher concentrations of PVP, the delay of demixing is replaced by instantaneous demixing. At moderate PVP concentrations, macrovoids are formed, and at still higher PVP concentrations formation of macrovoids is suppressed (see also the discussions around points 4 - 6).

Ad 8 and 9: Structures surrounding macrovoids.
These points will be discussed together with points 13 and 14.

Ad 10: Formation of a co-continuous pore structure.
The formation of an open porous structure, induced by the addition of PVP has been discussed earlier by Roesink[6]. For the sake of clarity, his ideas on this subject will be summarized shortly.
In his thesis, Roesink suggests that, after nucleation of the phase lean in membrane forming polymer (poly(ether imide), PEI in his case) has taken place, PVP is partly transferred into the nucleus while the membrane forming polymer moves away from the nucleus. The interpolymer movement that is the basic phenomenon underneath this transfer should create a boundary layer between the membrane matrix and the nucleus, which is

lean in PEI and rich in PVP. According to Roesink, part of the PVP becomes trapped in the PEI matrix during the diffusion process, and cannot diffuse into the nucleus.
Transfer of PVP into the nucleus indeed takes place, since the ultimate membrane only contains a few percent of PVP; nevertheless some remarks should be made on this movement. The interface between polymer solution and nucleus is characterized by a stepwise change in the concentration of the components over the interface. On the nucleus side of this interface, the PES (PEI) concentration is practically zero. PVP in the nucleus is surrounded only by solvent and nonsolvent. The composition in the nucleus is homogeneous (no concentration gradients). It is therefore not expected, as Roesink assumes, that a boundary layer on the nucleus side of the interface is created that is rich in PVP and lean in PEI or PES. Just outside the nucleus, the concentration profiles that give rise to outdiffusion of PVP must give a *higher* PEI (PES) concentration and a *lower* PVP concentration than in the polymer solution bulk. After rinsing and aftertreating the membrane to remove the PVP out of the pores, a structure should result which has a low PVP concentration at the surface. Figure 15a shows the essentials of this process. In practice we find a hydrophilic pore surface[6], which suggests that the aforementioned mechanism is at least not complete.
Another problem is that the growing nuclei of the PES lean phase 'push' PES forward: PES molecules accumulate in the solution between the growing pores. One would therefore expect that a little later, in-between the pores solid walls would be present, that cannot be opened up by a post-treatment. Since in reality the walls between the pores *do* break, the PES concentration in the walls between the pores must remain relatively low. This process is shown in figure 15b.

We have shown that the mechanism presented by Roesink is probably not complete. It is an experimental fact that part of the PVP is transferred to the nuclei, and that also the walls between the pores break up. There must be a process that keeps the concentration of membrane forming polymer in between the growing nuclei at a relatively low level.
This process may stem from the mechanism of spinodal decomposition. In every solution, concentration fluctuations are present[16-19]. They are caused by Brownian motions. The size of the concentration fluctuations depends on the stability of the solution. In a very stable solution, the force (phenomenologically, the concentration-derivatives of the osmotic pressure) to restore the original composition is large and concentration

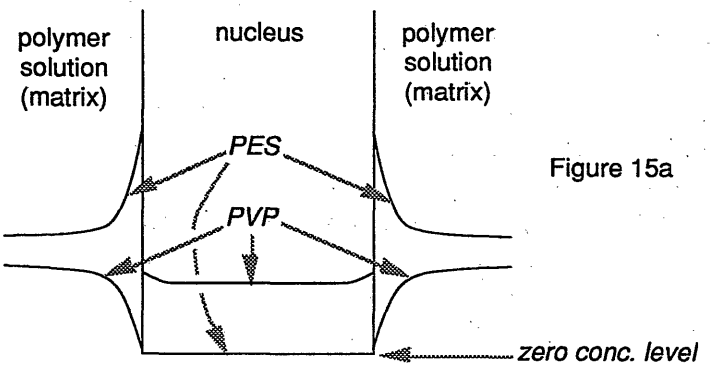

Figure 15a

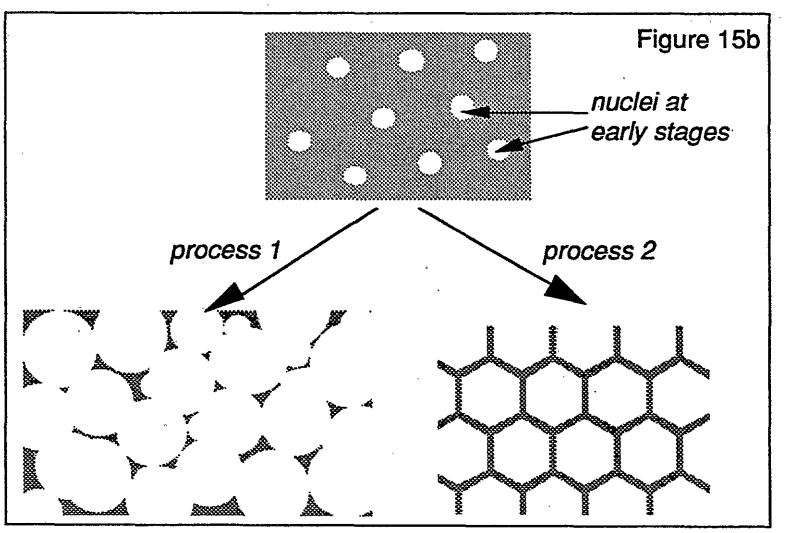

Figure 15b

Figure 15a: Concentration profiles during nucleus growth, according to the authors. The PVP concentration at the matrix side of the interface always remains low, due to thermodynamic and kinetic restrictions.

Figure 15b: Nucleus growth according to the assumed process can not lead to the very open porous structures obtained with PVP. The polymer solution in between two nuclei becomes more and more concentrated in PEI or PES. Coalescence between pores (as shown in process 1) on a regular basis is improbable; more likely is that a honeycomb structure (structure 2; the regularity of the structure is exaggerated) would result. A honeycomb structure is usual in membranes prepared without the use of PVP.

fluctuations remain small. In a solution that is less stable the driving force to eliminate fluctuations[16] is smaller. A solution on the border of *in*stability, the spinodal, has no driving force at all against fluctuations. The fluctuations are permanent. Inside the spinodal, the solution will demix according to created concentration fluctuations. This is called spinodal decomposition[18].

The situation during the first moments of immersion, with two polymers present, is complicated. We assume that the polymers are immobile relative to each other. We showed before[7] that under this assumption the binodal shifts to the nonsolvent corner of the phase diagram. Since this is not the real binodal (the real binodal is connected with the separation of the polymers), it may be called a 'virtual binodal'. The virtual binodal is related to phase separation between the polymer solution and a phase without polymer. Figure 16 shows examples of the position of the virtual binodal as a function of the amount of the polymeric additive. The compositions created during the first moments of immersion are only stable during these first moments.

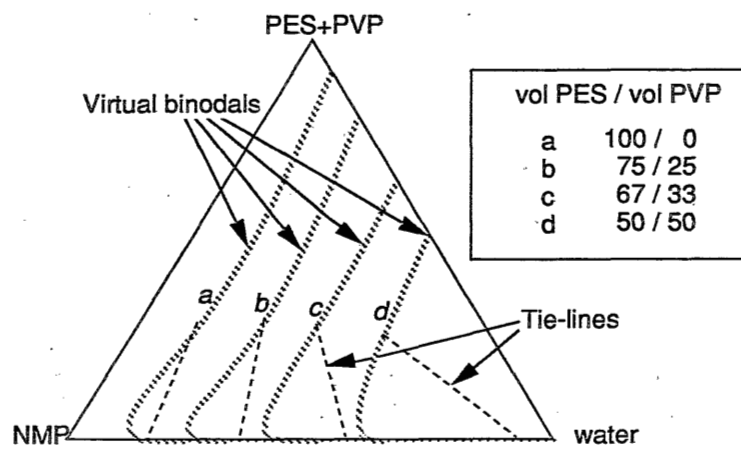

Figure 16: Calculated virtual binodals for the system PES-PVP-NMP-water, valid as long as no movement between the two polymers is possible[7].

The real cloudpoint curve (binodal) of the system lies at a few vol% of nonsolvent[11]. Compositions with more nonsolvent have a tendency to phase separate. The phase separation consists mainly of a separation between the two polymers, as followed from the study of the equilibrium thermodynamics[7]. From the phase diagrams, it appears that the compositions created during the first moments are situated far into the demixing

gap. A large driving force for polymer - polymer separation is present.

In our system *two* different kinds of concentration fluctuations can occur. The first kind consists of fluctuations of the total polymer concentration. These correspond with the concentration fluctuations possible in a ternary membrane forming system without additive. The polymer reacts as a network. It can locally be densified or diluted; much interpolymer movement is not necessary. Most of the transport is between the polymer and low molecular weight components (*cooperative* diffusion[13]).
The second kind is a fluctuation of concentrations of the two polymers relative to each other. A somewhat equivalent phenomenon in ternary systems with one polymer is the self-diffusion of a polymer coil. The fluctuations are created by a *reptation* (tracer) diffusion mechanism[13]. This diffusion process was earlier reported as being much slower than other diffusion processes occurring in the system[7]. The driving force for these fluctuations is related to the driving force for the polymer-polymer phase separation, which is the driving force present in our system.
We have seen earlier[7,11] that a large driving force for the creation of polymer-polymer concentration fluctuations is present during the first moments of the immersion step. After immersion, concentration fluctuations start to be formed between PES and PVP. Areas are formed that have higher PES (PEI) concentration and lower PVP concentration, and vice versa. In between two areas with higher PES concentration an area is located with a lower concentration of PES. Areas with the lowest PES concentration are identical to areas with the highest PVP concentration. For reasons of convenience, an area with a maximum concentration of PES (and a minimum concentration of PVP) will be called a maximum. A minimum has a low concentration of PES, and a high concentration of PVP. In between two maxima *and* two minima is a saddle point. Such a saddle point is characterized by approximately the average concentration of all components present.
The difference in concentration between a minimum and a maximum (the amplitude) increases in time. The minima form a PES lean phase (the pores), and the maxima form the solid structure around the pores. In between two pores, not a maximum, but a saddle point is situated. In between two pores therefore the polymer concentration remains relatively low. When the growing minima (pores) approach each other, the polymer concentration in the 'wall' between the pores (the saddle point) remains low, and the wall will easily break up. A structure results in which the pores are well interconnected. Thus the most probable demixing type for

the case of two polymers, the spinodal mechanism, gives a natural explanation for the formation of well interconnected pores.
The concentration gradients during the spinodal decomposition regime are continuous: near a minimum, the PVP concentration gradually gets higher when approaching a minimum, while the PVP concentration in a saddle point (the wall between two pores) has not changed considerably. The amount of PVP in the ultimate membrane structure will therefore be significant.

Ad 11: Dependence of the pore size on the amount of solvent in the bath.
From the mechanism discussed ad point 10, one can see that more solvent in the coagulation bath will enlarge the characteristic pore size: the concentration of nonsolvent in the polymer film will then increase more slowly, thus causing a less deep quench into the demixing gap. Theories of concentration fluctuations[19] show that the typical wavelength (geometric diameter) of the concentration fluctuations decreases when enlarging the quench depth. Therefore, with increasing NMP content in the coagulation bath, and consequently less deep penetration in the instability region, the typical pore size should increase.

Ad 12: Dependence of the pore size on the PVP concentration.
In the same way the decrease of the pore size with increasing amount of PVP can be explained. Figure 16 shows that with a higher concentration of PVP in the polymer solution, the binodal valid for the first moments of immersion shifts further to the nonsolvent corner of the phase diagram.
This implies that when a larger amount of PVP is used in the polymer solution, the quench depth by nonsolvent will be stronger. As said before, a larger quench into the instability zone reduces the fluctuation wavelength: pores become smaller.

Ad 13 and 14; 8 and 9: Co-continuous structures.
At very high concentrations of solvent in the coagulation bath, the nonsolvent concentration in the polymer solution is increasing so slowly that the two polymers have time enough to phase separate. After the immersion, a phase rich in PVP and a phase rich in PES are created. Figure 17 illustrates this process.
At these high concentrations of solvent in the coagulation bath, a ternary system consisting of PES, NMP and water would exhibit delay of demixing. The created phase that is rich in PES shows renewed delay of demixing. After removal of PVP from this phase, no further demixing occurs for

some time. The other phase, the phase rich in PVP and lean in PES, is stable with all coagulation bath compositions and cannot possibly demix further. In summary, after the first step in phase separation between the two polymers, further demixing stops for some time. The concentrations of the polymers remain relatively low, and the viscosities of the two phases remain low. Coalescence of the PVP rich phase occurs. Large, somewhat irregular voids are formed which contain PVP, solvent and nonsolvent. In between these voids, a solution is present that contains PES, NMP and water. After a certain time (the delay time of demixing), this solution starts to demix again. In the PES phase, a new porous structure results, with much smaller pores than the pores that contain PVP. The pore structure inside the walls can be compared with the morphologies found at delay of demixing conditions when no, or very little PVP is used (structures with 70 wt% NMP or more in the coagulation bath shown in figure 2).

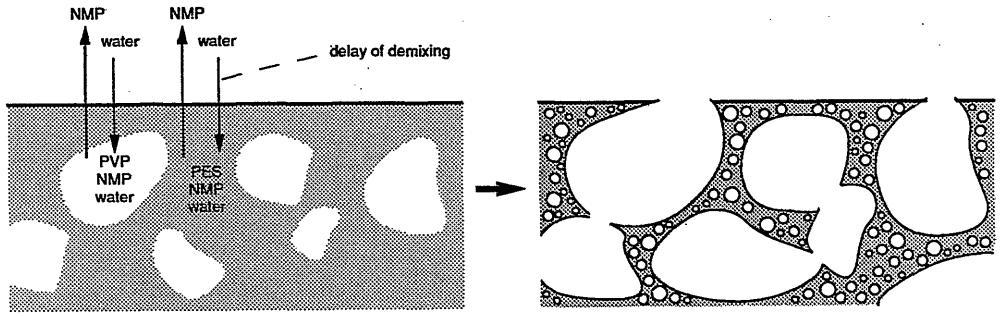

Figure 17: Schematic representation of the processes that lead to the formation of the irregular voids and the cellular pores around them. PVP is transferred to a new phase, which forms the voids. The remaining PES solution exhibits delay of demixing, and gives a closed cell structure around the voids.

At lower PVP concentrations, the volume fraction of the PVP phase is so low, that the voids remain more or less isolated. The higher the concentration of PVP, the larger the volume fraction of the PVP phase will be, and the more this phase can establish interconnectivity. A co-continuous structure can result again, when the volume fractions of both phases are comparable in size. Indeed we found that for high PVP content the structure obtained a much better interconnectivity.

This process can actually also be found in membranes formed with less

extreme coagulation bath compositions (see points 8 and 9).
During ternary membrane formation, macrovoids are formed by a local high concentration of solvent in a nucleus of the polymer lean phase, which induces local delay of demixing.
It was shown, that in our quaternary system delay of demixing is not occurring anymore. A slightly different mechanism must therefore be responsible for the growth of macrovoids.
We have seen that at very high solvent concentrations in the coagulation bath, indiffusion of nonsolvent is so slow that the two polymers separate first. After this, the two phases are stable with respect to the coagulation bath again. This is also what happens when macrovoid formation occurs in systems with PVP. Near the interface with the coagulation bath, the solvent and nonsolvent diffusion processes are fast relative to the polymer - polymer movement. The demixing process may well follow spinodal decomposition. No macrovoids are formed. Deeper in the polymer solution, diffusion of solvent and nonsolvent is slower. The polymer-polymer diffusion becomes of the same order of magnitude. A PVP phase and a PES phase are created. The situation then corresponds to the membrane formation with very high solvent concentrations in the coagulation bath.

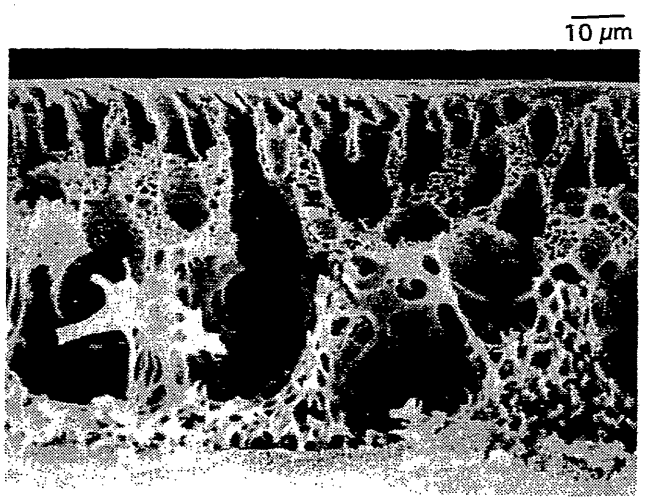

Figure 18: A membrane in which macrovoids end in a very open, co-continuous structure. Composition of the polymer solution: 15 wt% PES, 5 wt% PVP K90 in NMP; coagulation bath 60 wt% NMP in water.

Due to the high solvent content, the two phases have not too high viscosities. Other droplets of the PVP phase can coalesce with the growing macrovoid. Since the PES phase shrinks, the polymer concentration inside this phase increases, and the coalescence will not be complete. A macrovoid results, with walls that contain large openings. It is the expectation that the membrane matrix around the macrovoid is somewhat porous itself, with a closed cell structure. The reason for this was given earlier.
In practice, circumstances can be found under which the transition from the macrovoid to the underlying co-continuous structure is gradual: here, the coalescence of the macrovoid with the underlying PVP phase has progressed further than usual. Figure 18 shows such a structure. Detailed study of the macrovoid walls shows indeed some porosity in these walls. Figures 2 to 7 give other examples of the typical open macrovoids.

Very thick membranes
It was argued before that if the polymer-polymer movement is the limiting process that causes the supression of macrovoids, macrovoids

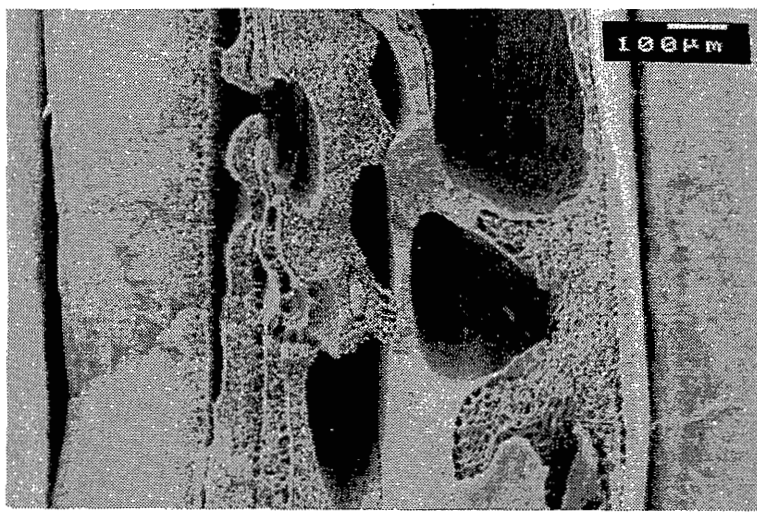

Figure 19: A very thick membrane (casting thickness 2 mm) prepared by coagulating 15 wt% PVP K90 and 15 wt% PES in NMP, in a pure water bath. Coagulation time was taken longer than two weeks. The voids probably are macrovoids, although they have a somewhat irregular shape, due to the extreme circumstances.

will be formed anyhow, but further away from the interface between polymer solution and coagulation bath. It should therefore always be possible to obtain macrovoids with any polymer solution, when the membrane is made thick enough.
From experiments it appears that it is indeed possible to obtain macrovoids in a system with 15 wt% PVP K90 and 15 wt% PES in the solution, coagulated in pure water (see figure 19). In normal membranes this polymer solution does not give macrovoids, but a co-continuous structure (see e.g. figure 2).
Only at a depth of approximately 240 μm the first macrovoids are formed, thus indicating that in a normal membrane (thickness up to 200 μm) these macrovoids would not have been formed.

Conclusions

It turns out that the additive PVP introduces a wide variety of effects on membrane formation. At low solvent content in the coagulation bath, PVP suppresses macrovoid formation. At higher solvent concentrations in the coagulation bath, it promotes formation of macrovoids, although a high enough concentration of a high molecular weight PVP still reduces macrovoid formation.
A transition from a not very well interconnected pore structure in a ternary system to a completely interconnected, co-continuous pore structure is obtained by the addition of PVP, in which pore sizes are influenced by the amount of PVP added and the concentration of solvent in the coagulation bath.
Delay of demixing such as occurring in the ternary system is effectively suppressed by addition of PVP. At very high solvent concentrations in the coagulation bath a more or less bimodal structure (two distinct sizes of pores) is created. This structure is related to structures found around macrovoids, occurring in membranes coagulated with moderate amounts of solvent in the coagulation bath (e.g. 50 wt% NMP in water). see also figure 18.
A hypothesis was given for the mechanism of membrane formation in these quaternary systems, based on the properties found earlier with equilibrium[11] and mass transfer calculations[7]. The formation of the completely interconnected, co-continuous pore structure may well be

spinodal of nature.
A prediction from this hypothesis concerning very thick membranes (e.g., 10 times as thick as normally used) appears to be correct.

References

1. S. Loeb, S. Sourirajan, Adv. Chem. Ser. **38**, 1962, 117
2. I.Cabasso, E. Klein, J.K. Smith, J. Appl. Polym. Sci. **21**, 1977, 165
3. T.A. Tweddle, O. Kutowy, W.L. Thayer, S. Sourirajan, Ind. Eng. Chem. Prod. Res. Dev. **22**, 1983, 320
4. P. Aptel, N. Abidine, F. Ivaldi, J.P. LaFaille, J. Membrane Sci., **22**, 1985, 199
5. L.Y. Lafrenière, F.D.F. Talbot, T. Matsuura, S. Sourirajan, Ind. Eng. Chem. Res. **26**, 1987, 2385
6. E. Roesink, Microfiltration; membrane development and module design, thesis, University of Twente, The Netherlands, 1989
7. Chapter 3 of this thesis
8. A.J. Reuvers, J.W.A. van den Berg, C.A. Smolders, J. Membrane Sci., **34**, 1987, 45
9. A.J. Reuvers, C.A. Smolders, J. Membrane Sci., **34**, 1987, 67
10. C.A. Smolders, A.J. Reuvers, Microstructures in Membranes, part I: Macrovoid Formation, to be published.
11. Chapter 2 of this thesis
12. P.J. Flory, Principles of Polymer Chemistry, Cornell University Press, Ithaca, NY, 1953
13. P.-G. De Gennes, Scaling Concepts in Polymer Physics, Cornell Univesity Press, 1979, NY
14. R.M. Boom, I.M. Wienk, Th. van den Boomgaard, C.A. Smolders, Microstructures in Membranes Part II: the Role of a Polymeric Additive, to be published in J. Membrane Sci.; first appendix of this thesis
15. A.J. Reuvers, Diffusion Induced Demixing Processes in Ternary Polymeric Systems, thesis, University Twente, The Netherlands, 1989
16. A. Einstein, A. Phys, **33**,1910, 1275; H. van Schmoluchowsky, Ann. Phys. **25**, 1908, 205
17. M.B. Huglin (ed.), Light Scattering From Polymer Solutions, Academic Press, London, 1972
18. J.W. Cahn, J. Chem. Phys. **42**, 1965, 93
19. C.A. Smolders, J.J. van Aartsen, A. Steenbergen, Kolloïd-Z. u. Z. Polymere **243**, 1974, 14

Chapter 5

Membranes from a Polymeric Blend Part II;

Membranes Prepared from PES and PS; Comparison with the PES-PVP System

R.M. Boom, E. Rolevink, Th. van den Boomgaard, C.A. Smolders

Summary

Membranes were prepared from solutions of poly(ether sulfone) and poly(styrene) in 1-methyl-2-pyrrolidone. Mixtures of the solvent and water were used as the coagulation medium.

At fast quenching conditions (pure nonsolvent baths) the two polymers appeared not to have separated on a macroscopic scale, although DSC measurements indicate that the polymers are phase separated. At lower quenching rates (higher amount of solvent in the bath) the poly(styrene) could separate into a clearly distinguishable phase. At very high solvent content in the coagulation bath the separation between the two polymers was complete.

These results support an earlier developed model that describes the formation of membranes from systems like poly(ether sulfone) and poly(vinyl pyrrolidone); it is based on the difference in rates of diffusion of polymer coils and of solvent molecules through a semi-dilute polymer solution.

On the basis of the results obtained with PES and PS, membrane preparation from the PES-PVP system could be arranged into four distinctly different demixing regimes, giving characteristic structures.

Introduction

Since the development of the phase inversion process[1], membranes prepared by phase inversion have become of great importance both in research and in industrial applications. Most if not all polymeric membranes contain asymmetric structures emerging from a phase separation

step.
The immersion precipitation process is one of the simplest versions of phase inversion. A polymer solution is immersed in a bath that contains a nonsolvent for the polymer and which is miscible with the solvent present in the polymer solution. Exchange of solvent and nonsolvent between the coagulation bath and the polymer solution causes the polymer solution to demix into a porous film which may or may not posses a dense toplayer. This process has already been the subject of extensive research. On the basis of the mass transfer model by Cohen *et al.*[2], Reuvers *et al.*[3,4] were able to compose a complete mass transfer model that could describe the essential phenomena during the immersion precipitation process. The two modes of membrane formation usually observed, i.e. via instantaneous demixing or delay of demixing, appeared from their model as intrinsically following from the mass transfer process. The model was later applied to more systems by Radovanovic *et al.*[5,6] Smolders and Reuvers[8] were able to extend the ideas from Gröbe *et al.*[7] on the formation of macrovoids (i.e. large fingerlike cavities throughout the whole membrane cross-section) to a clear formation mechanism of these voids. Tsay and McHugh[9,10] have extended the mass transfer model to a more general case.

The use of more than one polymer in the casting solution turned out to give new possibilities for the preparation of UF and MF membranes. Membranes prepared from a polymeric blend of poly(vinyl pyrrolidone) and a membrane forming polymer like poly(ether sulfone), poly(sulphone) or poly(ether imide) show greatly improved permeation properties while maintaining high particle rejection values.[11-14]
With such a blend it became possible to suppress the formation of macrovoids that usually are disadvantageous for the mechanical strength of a membrane. Furthermore, the interconnectivity between the pores could be enhanced, thereby reducing the flow resistance through the membrane. Thirdly, the surface properties of membranes prepared with poly(vinyl pyrrolidone) could be changed, affecting the fouling properties of the membranes positively[14].
The present authors have extended the Reuvers model for the case in which two polymers are present in the polymer solution, resulting in a quaternary membrane forming system[15-17]. The model clarifies the effects of PVP from a fundamental point of view. The suppression and the formation of macrovoids, the pore structures found, and the structures found at extreme (either fast or slow) quenching conditions can be

explained.
From thermodynamic considerations[18] it appears that phase separation in a solution containing two polymers, induced by the addition of a nonsolvent for one of the polymers into the polymer solution, almost exclusively consists of separation between the two polymers at equilibrium. This shows that the demixing of a solution containing two polymers must be accompanied by diffusion of one of the polymers present through the polymer solution. On the other hand, during immersion precipitation, the demixing is induced by indiffusion of nonsolvent from the coagulation bath. Thus, during the immersion in the coagulation bath, two diffusion processes must be active: diffusion of low molecular weight components (solvent, nonsolvent) through the semi-dilute polymer solution, and diffusion of the *polymers* with respect to each other.
De Gennes[19] has defined these two modes of diffusion as *cooperative motion* (in which the intertwined polymer coils do not move with respect to each other) and *tracer diffusion* or *reptation*, which is typically the diffusion of a single polymer coil in a concentrated polymer solution. He showed that in a concentrated polymer solution these two diffusion coefficients differ many orders of magnitude in size. The reptation mechanism is always much slower than the cooperative diffusion process. High molecular weights of the polymers present and higher concentrations of the polymers enlarge the difference in speed between the two diffusion processes[15-18].
In our immersion precipitation process this means that the phase separation between the two polymers is much slower than the diffusion process of exchange of nonsolvent and solvent with the coagulation bath. This is the basis of the model proposed earlier.
For the first moments of immersion, we may assume that the two polymers can hardly move with respect to each other. They act as if they were one single polymer. It was shown that this results in a large flux of nonsolvent into the polymer solution, while the demixing process (based on polymer-polymer movement) remains relatively slow.

Occurrence of local delay of demixing, according to Smolders and Reuvers[8] necessary for the formation of macrovoids, can not take place since the indiffusion of nonsolvent is much faster than nucleation or any other demixing process. Macrovoid formation is suppressed as long as the movement of the two polymers relative to each other is clearly slower than the movement of solvent and nonsolvent.
Under slower quench conditions (i.e. in a coagulation bath in which a considerable amount of solvent is present) the indiffusion of nonsolvent is

slowed down, since the driving force for nonsolvent indiffusion is much smaller. The two diffusion modes may then become comparable in velocity. The velocity of formation of a second phase (e.g. nucleation of a membrane forming lean phase) is compatible with the speed of the nonsolvent/solvent exchange. Local delay of demixing is not impossible anymore and macrovoids can be formed again.
At very slow quench conditions (very high solvent content in the coagulation bath), the demixing process between the two polymers has time enough to reach completion. Effectively, the nonsolvent indiffusion is now made slower than the polymer-polymer interdiffusion. After demixing in a phase rich in membrane forming polymer and a phase rich in polymeric additive (e.g. poly(vinyl pyrrolidone)), the membrane forming polymer phase shows delay of demixing: the mass transfer with the coagulation bath continues while this phase not yet demixes. Large irregular voids of the polymeric additive phase are formed surrounded by regions of a membrane forming polymer phase, which has a porous closed cell structure, once it demixes.
It was shown before that this is in complete accordance with experimental data on the system poly(ether sulfone) - poly(vinyl pyrrolidone) - n-methyl pyrrolidone - water[17]. Preliminary results with another polymeric additive that is soluble in water, i.e. poly(ethylene oxide), indicate that indeed the behavior is not restricted to poly(vinyl pyrrolidone) but is characteristic of a quaternary membrane forming system with a polymeric additive that is soluble in the nonsolvent.
Summarizing, the model is based on two principles:

a - the demixing in such quaternary polymer solutions, given enough time is mainly taking place between the two polymers present.
b - the exchange of nonsolvent and solvent is faster than the diffusion (reptation) process of polymer-polymer interdiffusion.

We can check the proposed membrane forming mechanisms by investigating a system in which a *different kind* of polymeric additive is chosen, namely in which the compatibility between the additive and the nonsolvent is bad. An example of such a system is:

1 - nonsolvent: water
2 - solvent: 1-methyl-2-pyrrolidone
3 - membrane forming polymer: poly(ether sulfone)
4 - polymeric additive: poly(styrene)

In this chapter we will first look into the differences between this system and the system with poly(vinyl pyrrolidone) as an additive. We will then compare experimentally obtained membrane morphologies with the structures xpected on the basis of the model that was put forward.

Theory

We will use poly(styrene) (further abbreviated as PS) as additive to check whether the movement of the polymer coils through the entangled polymer solution under fast quenching conditions is slower than the nonsolvent indiffusion from the coagulation bath. This is the second principle, mentioned earlier, of the model proposed to describe the membrane forming behavior of a polymeric solution containing a polymeric additive.

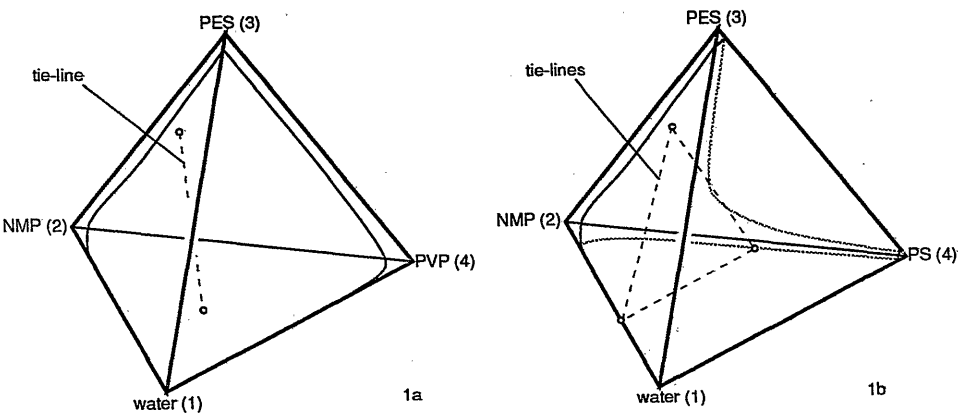

Figure 1: Schematic phase diagrams of two systems: (a) water-NMP-PES-PVP and (b) water-NMP-PES-PS. PVP is assumed to be miscible with all other components present. PS is assumed to be only miscible with NMP, and not with water or PES.

We first have to study the thermodynamic differences and similarities between the systems using PS and poly(vinyl pyrrolidone) (PVP) as additives.
Figure 1 shows schematic phase diagrams of both systems. We have strong indications that PVP is miscible with all other components present, inclu-

ding the membrane forming polymer, poly(ether sulfone) (PES).
Poly(styrene) is probably immiscible with PES. We start the formation of the membranes by preparing a *homogeneous* solution. Clear polymer solutions were obtained in all experiments, with up to 30 wt% of total polymer, at any ratio of concentrations of the polymers. We may therefore assume that the influence of this ternary demixing gap is not very large.
PS is quite immiscible with water. A demixing gap in a third ternary subsystem is introduced: in the system nonsolvent-solvent-PS (1-2-4). The other ternary demixing gaps present are the demixing gaps in the ternary systems 1-2-3 and 1-3-4, which are also present in the system with PVP.
PS does not have a driving force to move into the water phase, during immersion in a water bath. On the other hand, PS does have a driving force to phase separate from PES. In short, a three phase equilibrium is created: (i) a phase rich in PES, (ii) a phase lean in PES and rich in PS and (iii) a phase lean in both polymers. We may therefore conclude that the PS has an analogous driving force to phase separate from PES, as PVP has, although with PS the demixing process is more complex.
In both cases (the systems PES-PVP and PES-PS) the polymer-polymer demixing is of entropic nature; it results from a very low entropy of mixing between the two polymers. We can therefore compare the separation of PS from PES with the separation of PVP from PES.

The phase separation between the polymer (PES + PS) lean phase and the PS phase causes the PS to remain in the membrane. This enables us to find out where the PS has moved.
Taking relatively fast quenching conditions first, we should expect some differences between membrane structures from the PVP system and the PS system. From the model, it appears that the presence of PS should not hinder or delay the nucleation of a polymer lean phase. Therefore, if our model is correct, addition of PS should not suppress macrovoid formation. We must obtain the morphology of an instantaneously demixed membrane (see also Reuvers and Smolders[3,4,8]) in which the macrovoids are surrounded by a heterogeneous blend of the polymers. Furthermore, if indeed the polymer-polymer interdiffusion is slow relative to the nonsolvent indiffusion, the blend should only be microphase separated.
Reducing the quench speed by adding a significant amount of solvent to the coagulation bath should result in a separation between the two polymers on a larger scale.
In a situation in which the interpolymer movement is not the rate limiting step in the membrane formation anymore (i.e. for large solvent content of

the coagulation bath), we should expect phase separation of the polymers showing large regions of one polymer phase dispersed in the other polymer phase.

Experimental

Membranes were prepared from poly(ether sulfone), Victrex™ 5200P, kindly supplied by ICI PLC. Poly(vinyl pyrrolidone), from Janssen Chimica, grade K90 and poly(styrene), no. 29789 from BDH Chemicals Ltd., were used as additives. Solvent used was 1-methyl-2-pyrrolidone, synthesis grade, from Merck, and the nonsolvent was water, demineralized and ultrafiltrated before usage.
To redissolve PS from the membrane matrices, toluene, synthesis grade, from Merck was used.
Before preparation of the polymer solutions, PES and PS were dried for several hours at 80 °C.
Molecular weights are listed in table 1.

Table 1: Molecular weight of the polymers used, obtained by GPC.

Polymer	M_n (g/mole)	M_w (g/mole)
PES Victrex 5200 P	22 300	43 800
PVP K30	8 700	18 100
PVP K90	99 800	228 200
PS		± 100 000*

**as reported by the manufacturer*

The membranes were cast on a glass plate, with a thickness of 0.2 mm. The time between casting and immersion in the coagulation bath was kept as short as possible. After coagulation, the membranes were extensively rinsed with water, and dried at 80 °C.
Membrane samples were broken under liquid nitrogen, and evacuated for at least 6 hours. A thin layer of gold was sputtered on top of the sample with the Balzers Union SCD 040 sputtering apparatus, before evaluation with a Jeol JSM T220 A scanning electron microscope.
DSC scans were performed on a Perkin Elmer DSC-7 with a scan rate of 15 °C/min, from 75 to 250 °C. Each sample was scanned twice.

Results and Discussion

Figure 2 shows membranes obtained by immersion of polymer solutions of 15 weight% PES and 10 weight% PS in NMP, into coagulation baths of pure water, 60 weight% NMP and 80 weight% of NMP in water, respectively.

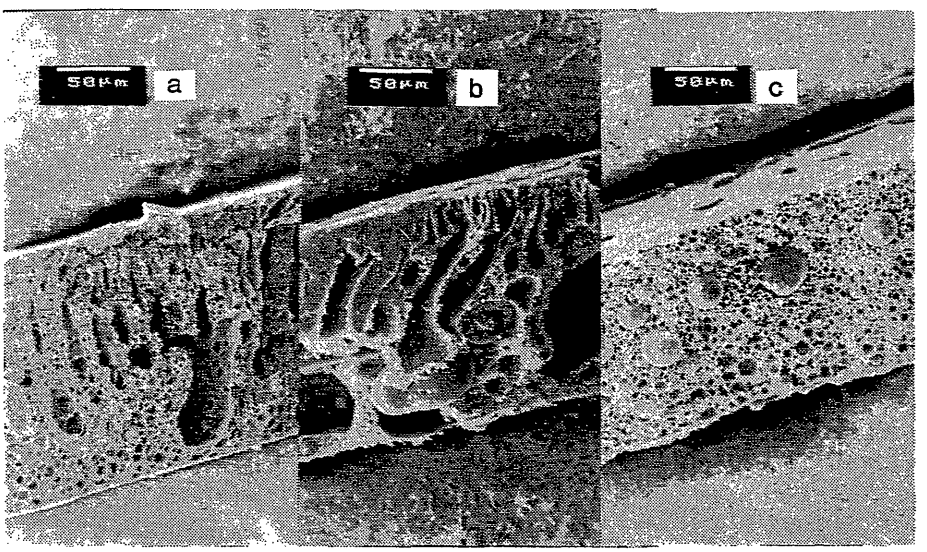

Figure 2: Cross-sections of membranes prepared with a solution of 15 wt% PES and 10 wt% PS in NMP. Coagulation baths: (a) pure water, (b) 60 wt% NMP/40 wt% water, (c) 80 wt% NMP/20 wt% water.

The membrane formed in the pure water coagulation bath contains, as expected, many macrovoids. No structures can be observed (at magnifications of up to a few thousand times) that may represent a PS phase. It appears that the indiffusion of nonsolvent here took place faster than the phase separation between the two polymers.

A coagulation bath of 60 wt% NMP in water results in approximately the same structure. Deeper in the membrane, under the macrovoids, we can see some spherical entities (probably consisting of PS) embedded in the membrane matrix. Apparently, the polymers did not have time to phase separate before the membrane structure was formed. *Below* macrovoids which are formed, local delay of demixing should be present. Local delay of demixing means that under the macrovoids, no demixing into a polymer lean phase can yet take place; only mass transfer is going on. Of course here the two polymers have time to phase separate. The PS droplets being

formed coalesce to form larger droplets, which can be seen in the region below the macrovoids.

The membrane prepared with 80 wt% of solvent in the coagulation bath shows a completely different morphology. From a later experiment we will see that the spheres consist of PS.
Apparently the two polymers here had enough opportunity to phase separate before a polymer lean phase was formed. What happened is probably as follows. The PS diffused out of the PES solution, forming drops of PS in NMP, surrounded by a polymer solution containing PES and NMP (and some water). Both phases exhibit delay of demixing with respect to the coagulation bath. No further demixing takes place for some time. Only when enough water has accumulated in the polymer solutions (the PES and the PS phases), they both phase separate again, forming pores and a membrane matrix. Indeed from photographs (at higher magnifications) it appears that the spheres themselves are also porous.

We can compare these spheres with the spheres found under the macrovoids in the structure prepared with 60 wt% solvent in the coagulation bath. We see that, although in that case the spheres were somewhat less regular, they look alike. This indicates that below the macrovoids local delay of demixing is indeed present[8]. Both the membrane matrix and the spheres are porous with a closed cell structure. The demixing between the two polymers must have preceded the demixing into the polymer rich phase(s) and a polymer lean phase (the formation of pores).
The formation of these latter structures is analogous to the formation of the irregular structures formed under the same circumstances with PVP as additive[17]. In the case with PVP, the large voids should be compared to the spheres of the PS phase. The PVP forms one phase with the nonsolvent, and we then see a *bimodally* porous structure: large voids resulting from PVP-PES phase separation and small closed cells in the PES phase formed by the formation of a PES lean phase.
Figure 3 shows the typical morphology of the pores in the membranes from figure 2. The membrane precipitated in pure (figure 3a) water shows an irregular structure in-between the pores. This may indicate that around the pores the two polymers have phase separated on a smaller scale, forming a more or less co-continuous microstructure surrounding the pores.
The membrane prepared with 60 wt% solvent in the coagulation bath (figure 3b) also shows an irregular pore wall structure, in which small pores

are present.
The membrane from 80 wt% of NMP in the coagulation bath shows a normal closed cell structure typical of membranes formed by a delayed demixing process[3,4]. Apparently the pores were formed after the transfer of the PS from the solution into the spheres, as was explained. Figure 3c therefore shows a structure formed by pure PES in which no PS is present anymore.

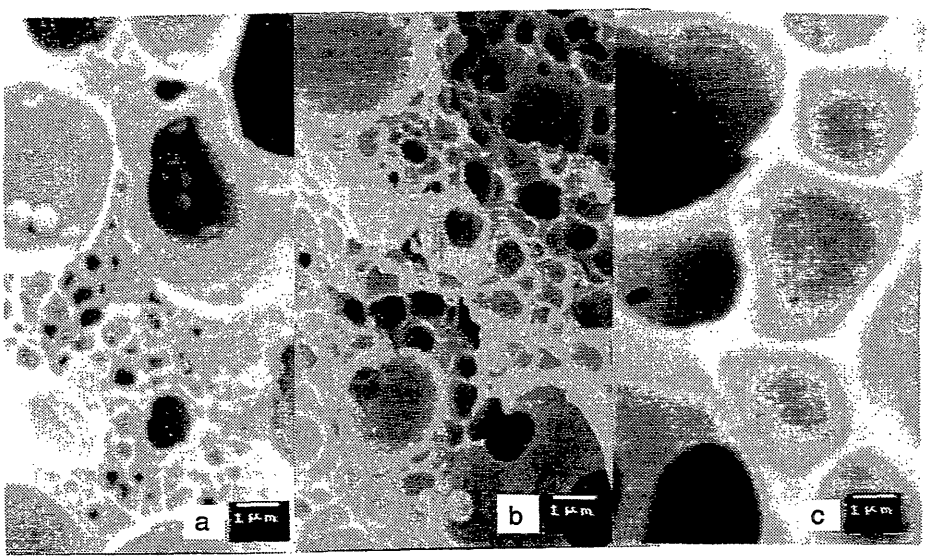

Figure 3: Details of the membranes shown in figure 2. Photograph (a) is a membrane immersed in a pure water bath, (b) is immersed is a bath of 60 wt% NMP in water and c in a bath containing 80 wt% NMP / 20 wt% water.

We can check the PS content of the spheres by immersing the membranes in a solvent for PS which is a nonsolvent for PES: toluene. Immersion of the membrane prepared with a coagulation bath of 80 wt% NMP into toluene results in a structure in which the spheres have gone (see figure 4). This shows that the spheres consist of the PS phase, and that the surrounding phase does not contain much PS anymore. Phase separation between the polymers has taken place almost completely.
Immersion of the membrane prepared with a pure water bath (fast quenching) into toluene results in the complete disruption of the membrane structure. Only some loose fibres remain after some time. The PS absorbs large amounts of toluene; the swelling of the PS phase then causes the PES phase to be torn apart, since both phases formed a co-continuous,

intertwined structure. The swelling of PS can be directly observed, by a side effect. Immediately after immersion of the dry membrane in toluene, air bubbles appear at the surface of the membrane. It looks like the PS phase also swells into the pores containing air, thereby replacing the air.

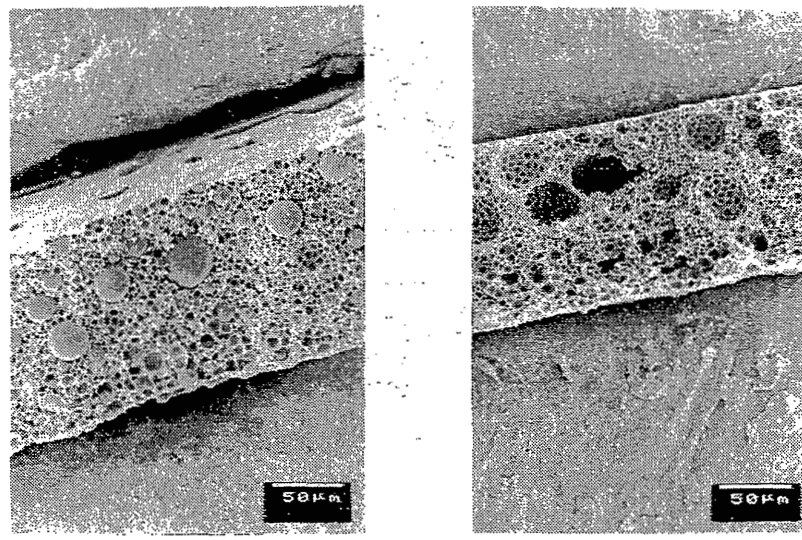

4a 4b

Figure 4: A membrane from a polymer solution consisting of 15 wt% PES, 10 wt% PS in NMP, coagulated in a bath containing 80 wt% NMP and 20 wt% water. After rinsing and drying, the membrane was immersed in toluene to remove the PS from the membrane. Figure (a) is before, and (b) is after the immersion in toluene.

From the fact that in this case the structure is destroyed we can conclude that PS was at least in close contact with PES. Either the two polymers were still homogeneously blended or the two phases were well entwined. This suggests that the demixing between the two polymers could have followed a spinodal demixing process.

DSC scans were performed on samples of the membranes to investigate whether the polymer blend is homogeneous or heterogeneous of nature: membranes from a solution of 15 wt% PES and 10 wt% PS, coagulated in a water bath, and in 80 wt% NMP in water. Table 2 shows the measured glass transition temperatures. Both membranes show the two glass transition temperatures of PS and PES, which indicates that in both samples the polymers have phase separated. In the sample coagulated in the water bath, a large relaxation peak is found just above the first (PS) glass transition,

indicating that the PS phase was not yet free of stresses. This relaxation peak was absent in the second run.

Table 2: Glass transition temperatures for the pure components, and the membranes from a solution of 15 wt% PES and 10 wt% PS in NMP.

Sample	1st T_g (°C)	2nd T_g (°C)
Pure PS	107.5	-
Pure PES	-	227.5
Membrane from pure water bath	± 107 *	± 225
second run	106.9	± 230
Membrane from 80% NMP bath	± 107	227
second run	107	± 230

**a large relaxation peak appeared app. 5 °C above this glass transition*

The glass transition temperatures are not shifted relative to the pure components. This indicates that in all membranes, PES and PS are phase separated, even in the membranes where no separate PS phase could be recognized in SEM pictures (see figure 3). Therefore, the two polymers must have phase separated on a very small scale.

In summary, the experiments showed that under fast quench conditions the polymer-polymer movement is slow compared to the indiffusion of nonsolvent from the coagulation bath. The polymers have phase separated, but only on a very small scale. Slowing down the quench rate by adding solvent to the coagulation bath results in a complete separation between the polymers.

Comparison with the system where PVP is the additive

We observed before that a polymer lean phase could be formed, when using PS as the additive, and as a consequence also macrovoids were formed. This is a direct confirmation of the earlier result from our model[16], from which it appeared that the hydrophilicity of PVP is crucial in suppressing macrovoid formation. It was shown earlier that the low mobility of the two polymers with respect to each other, in combination with the miscibility of the polymeric additive PVP with the nonsolvent,

resulted in a dramatic decrease in size of the (semi-)ternary demixing gap. This was illustrated by the occurrence of a so-called *virtual binodal*[15]. It results in a strong initial increase in the concentration of nonsolvent in the polymer solution while the polymer concentration in the toplayer had not increased at all. With respect to the real demixing gap (related to the separation of the two polymers), these compositions are very unstable. This makes the occurrence of local delay of demixing which is necessary for macrovoid formation[8,16], impossible.
With the help of our model system using PS, we come to the conclusion that polymer-polymer demixing from very instable solutions could well develop along a spinodal decomposition mechanism, almost independently from the quench rate, with the following line of thought. Let us take a large amount of PS and only a small amount of PES. A structure should be formed consisting of a PS matrix, and some PES islands (spheres?) in this matrix. On the other hand we have seen that the use of a little PS in a PES solution results in PS spheres in a PES matrix. In between these two cases there should be a region in which the volume fractions of the two phases are approximately equal. In other words, we then prepare a polymer solution that is near its critical point[18]. A co-continuous structure must result upon separation.
Thus, it should *always* be possible to obtain an intertwined, co-continuous structure of the two polymer phases (usually identified with spinodal decomposition between the polymers), by varying the ratio between the two polymers, but *irrespective* of the absolute polymer concentrations in the solutions.

The deeper the quench step is (e.g. by using a pure nonsolvent coagulation bath), the less probable it is that nucleation of one of the polymer phases can take place in time. If we slow down the quench (by adding solvent to the coagulation bath, the region in which spinodal demixing takes place becomes smaller (becomes more sensitive to the exact ratio of the two polymers). In practical terms, if we take a solution that shows spinodal decomposition (but of course has not the exact ratio of polymer concentrations connected to the critical point), we may bring it back to binodal nucleation and growth by adding enough solvent to the coagulation bath.

This line of thought is also valid for a system with PVP instead of PS as the second polymer. Earlier, the theoretical phase behavior was calculated as a function of the ratio of the two polymers in the solution[18]. It was indeed

found that by adding more high-molecular weight PVP to the polymer solution, the critical point shifted strongly upwards. It is even possible to eliminate the critical point in the system completely by imposing a ratio of PVP over PES above a certain value. The shift of the critical point as a function of the concentration of additive is given in figure 5. Here we recall that the position of the critical point is important for the question which phase (lean or rich in polymer) will nucleate. If the composition path enters the demixing gap at *higher* content of a polymer than the critical point, the nucleating phase will be *lean* in the polymer, and vice versa.

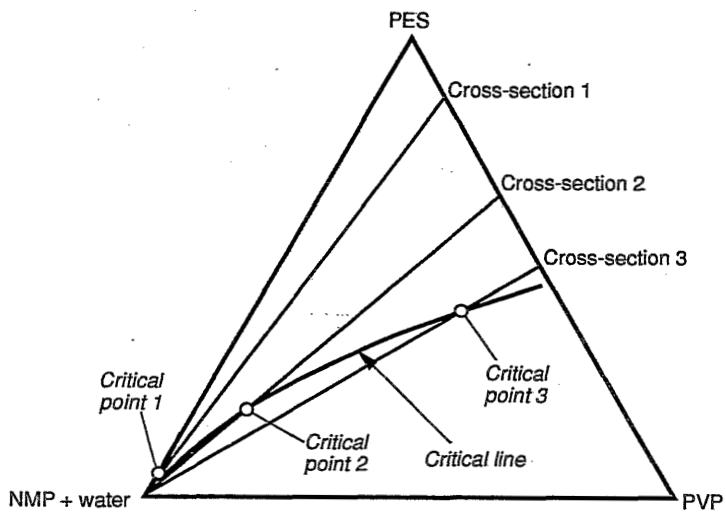

Figure 5: Semi-ternary cross-section of a theoretical quaternary phase diagram of the system water-NMP-PES-PVP. Water and NMP are plotted as one component. The critical line is shown for a system with PVP, M_w = 100 kg/mole. Several cross-sections (fixed ratios PES/PVP) are shown in which the critical point (= intersection with the critical line) is shifting to higher polymer concentrations when more PVP is present in the system[18].

We may now use the same reasoning as was given above for the PS-PES system. If we take a small amount of PVP, the effect of the PVP is not large enough to change the type of nucleation, or to eliminate macrovoid formation: we see a normal 'instantaneously demixed' structure. On the other hand, if we take a large enough amount of PVP in the solution, the solution remains below the critical point during the immersion (see figure 5). Nucleation of a PES rich phase results. The continuous phase is rich in

PVP, and the polymer solution dissolves into the coagulation bath, forming a fine dispersion of PES. In between these two regions there should be a region in which the polymer solution is near its critical point, so that spinodal decomposition between the two polymers takes place.

We should remember that usually diffusive mass transfer across the spinodal is not possible, since (the determinant of the matrix of) the diffusion coefficients become zero, as was shown by Radovanovic *et al.*[5,6] In this case however, the polymers react as one polymer during the first moments of immersion. The demixing must take place between the two polymers, which is not directly connected to the diffusive exchange of nonsolvent and solvent. Therefore in *our* specific case, spinodal demixing, following a diffusive solvent/nonsolvent mass transfer across the spinodal, is possible. In the system with PS as additive, spinodal demixing between a polymer lean phase and a polymer rich phase is not possible (hence macrovoids can be formed) but spinodal decomposition between the two polymers inside the already created polymer rich phase is possible.

Different regimes of demixing

In the preceding paragraphs we have seen that we should expect at least three different regimes of demixing when an additive like PVP is used (PVP is here used as an example), under strong quench conditions (small concentration of solvent in the coagulation bath):

1 - at low PVP concentrations: a normal membrane structure is formed, characterized by nucleation of a polymer lean phase, and formation of macrovoids
2 - at intermediate PVP concentrations, an intertwined structure can be formed, originating from spinodal decomposition
3 - At very high concentrations of PVP in the polymer solution, the PVP rich phase is the continuous phase, and the demixing solution dissolves under the formation of a PES dispersion.

In practice, we indeed see three clearly different demixing regimes:

1 - at low PVP concentrations macrovoids are still formed
2 - at intermediate PVP concentrations, the macrovoids disappear, and the pore structure clearly changes in nature (see figure 6).

3 - At quite high PVP concentrations in the polymer solution, a membrane is not formed, but the polymer solution slowly dissolves under a slight increase of turbidity of the coagulation bath.

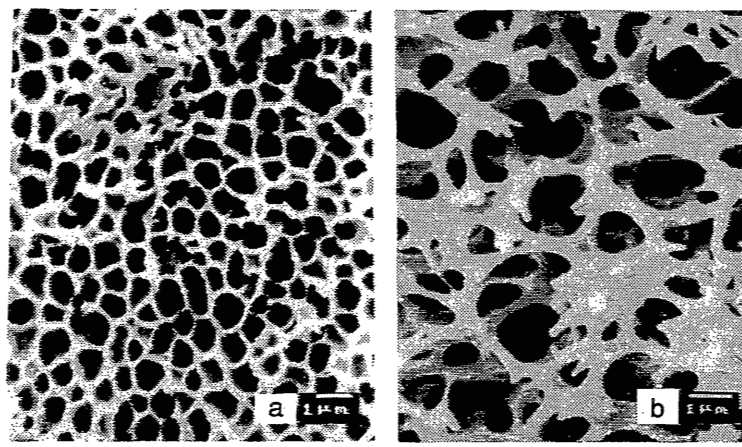

Figure 6: Typical membrane structures (sublayer); (a) without any PVP, (b) with 10 wt% PVP K90 in the solution. PES concentration in the polymer solution was 15 wt%, the solvent was NMP and the coagulation bath was pure water.

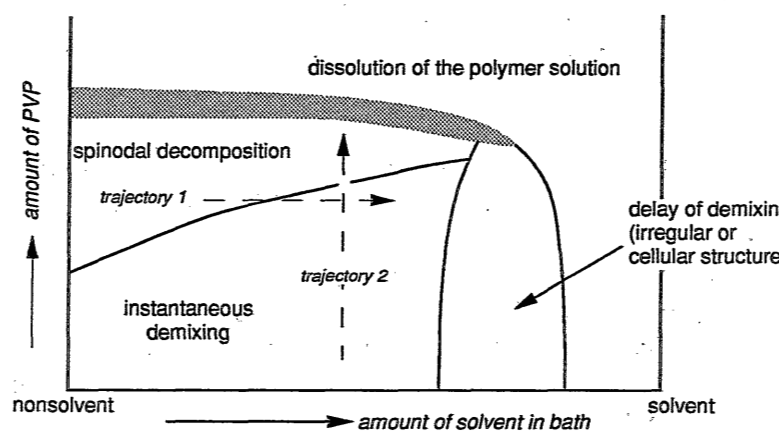

Figure 7: The three demixing regimes as expected from the hypothesis proposed. The transition from spinodal decomposition to dissolution in the coagulation bath is not clearly defined: even spinodal demixing can result in dissolution of a polymer into the coagulation bath, if the volume fraction of the PES rich phase becomes too small (by a ratio PVP/PES that is high).

We have to assume that the structure of figure 6, connected with the disappearance of macrovoids, is formed by spinodal demixing, since at higher PVP concentrations the solution dissolves (regime 3), and at lower PVP concentrations macrovoids are formed (regime 1).
Figure 7 summarizes the expected behavior from our hypothesis.
When a film of a blend solution is immersed in a pure water bath, the polymers do not have much time to diffuse relative to each other. As was explained, the indiffusion of nonsolvent is fast enough to let the solution cross the metastable region without formation of nuclei. Experiments with the PES-PS blend in this chapter show that this is indeed possible. Increase of the solvent concentration in the coagulation bath (a decrease of the quench depth) results in a slower indiffusion of nonsolvent (indicated in figure 7 as trajectory 1), which enables nucleation of a PVP rich phase, implying that macrovoids can be formed. At higher concentrations of PVP, this transition should appear at higher solvent concentration in the coagulation bath.
On the other hand, it should usually be possible to go from a structure formed by nucleation and nucleus growth to a spinodally demixed structure by adding enough PVP to the solution (shown as trajectory 2). The transition from binodally demixed structures (whether according to instantaneous or according to delayed demixing) to spinodal demixing should shift to higher required PVP content at higher solvent concentrations in the coagulation bath. Still higher concentrations of PVP should lead to dissolution of the polymer solution film (assuming that the second polymer has a high enough molecular weight).
Experimental results presented earlier[17] show indeed most of these trends, although sometimes not very clearly. In figure 8 some typical results obtained with PVP as additive (earlier presented in a more extensive fashion[17]) are shown. We can see that at low solvent concentrations in the coagulation bath, the mechanism that forms the co-continuous structure (shown in figure 6b) is more dominant than at higher solvent concentrations. For PVP K30, the molecular weight of the additive is so low (appr. 10 000 g/mole) that the polymer-polymer diffusion limitation is hardly fulfilled. Only for a few cases the typical co-continuous structure as obtained by Roesink[14] could be found here. PVP K90 on the other hand has such a high moleculer weight (approximately 200 000 g/mole) that almost everywhere the co-continuous structure was formed, as long as a certain minimum amount of PVP was present.
The structures containing macrovoids, formed with little PVP in the solution, change into delay of demixing type structures at high solvent concen-

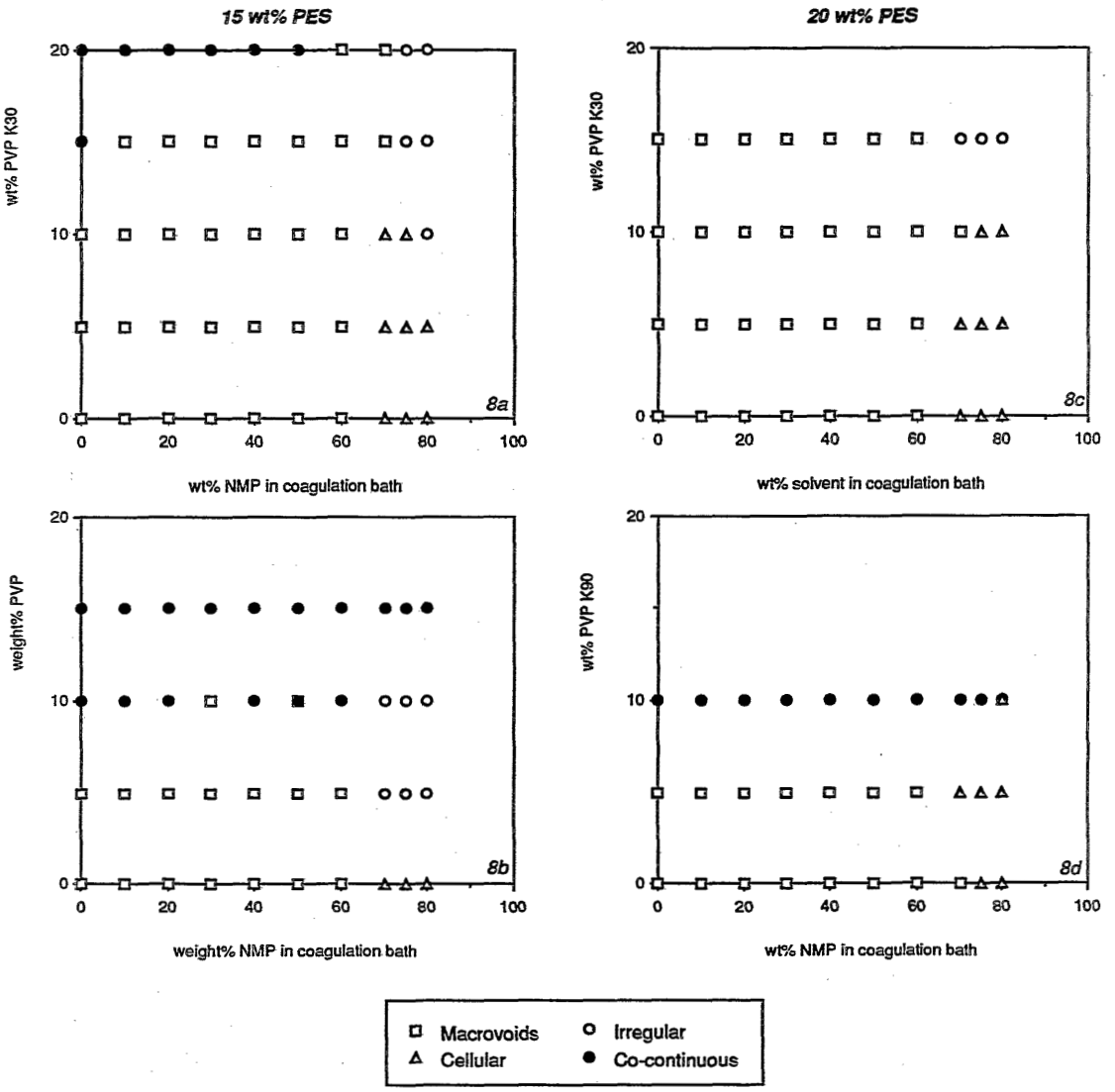

Figure 8: The structures found when using of PVP K30 and PVP K90, in solutions with 15 wt% and 20 wt% PES[17]*:*

8a: 15 wt% PES, PVP K30, 8c: 20 wt% PES, PVP K30,
8b: 15 wt% PES, PVP K90, 8d: 20 wt% PES, PVP K90.

trations in the coagulation bath, which are cellular in nature. At somewhat higher concentrations of PVP, this structure changes into irregular structures, which are formed along a mechanism of polymer-polymer separation, given in the theory[17]. The irregular strucures are formed by nucleation and growth of a PVP rich phase. The fact that the observed structures are the structures expected from theory[18,15] is a confirmation of our assumption that separation of the *polymers* is the demixing process taking place.

Unfortunately no exact experimental points are available at very high PVP contents. We performed some measurements, however, on a polymer solution containing 15 wt% PES and 25 wt% PVP K90. The solution did not yield a membrane when contacted with a water bath but just dissolved into the coagulation bath, while the coagulation bath became turbid. This is in accordance with theory, but more precise measurements should be carried out to confirm this first, qualitative, result.

Conclusions

From membranes prepared with poly(styrene) as an additive, it could be shown that under fast quenching conditions, polymer-polymer interdiffusion is considerably slower than nonsolvent indiffusion and nucleation of a polymer lean phase. This confirms one of the two principles of a model that described the membrane forming mechanism in systems containing poly(vinyl pyrrolidone) as additive. By varying the ratio between the two polymers present, at constant concentration of membrane forming polymer, the formation mechanism can be varied.
From the results, it became clear that conditions for spinodal decomposition in a solution of a polymeric blend are realized readily.
It was shown that the typical co-continuous structure of membranes prepared with PVP as an additive can be described as a result from a spinodal decomposition mechanism.
We arrived at a subdivision of membrane forming processes for a polymeric blend containing PVP into four classes:

- at low PVP contents normal instantaneous demixing occurs
- at intermediate PVP contents and lower solvent content in the coagulation bath (depending also on the molecular weight of the PVP) spinodal decomposition takes place
- at very high PVP content dissolution of the polymer solution takes place
- at high *solvent* contents an irregular structure is formed by nucleation of a PVP phase followed by delay of demixing in the membrane forming phase

These predictions are in accordance with the structures found in practice.

Acknowledgement

The authors wish to express their gratitude to ir. I.M. Wienk for the GPC analyses of the polymers, to ir. A.M.W. Bulte for performing the DSC measurements, and to both for enlightening discussions.

References

1. S. Loeb, S. Sourirajan, Adv. Chem. Ser. **38**, 1962, 117
2. C. Cohen, G.B. Tanny, S. Prager, J. Polym. Sci., Polym. Phys. Ed. **17**, 1979, 477
3. A.J. Reuvers, J.W.A. van den Berg, C.A. Smolders, J. Membrane Sci., **34**, 1987, 45
4. A.J. Reuvers, C.A. Smolders, J. Membrane Sci., **34**, 1987, 67
5. Ph. Radovanovic, S.W. Thiel, S-T. Hwang, J. Membrane Sci., **65** (1992) 213
6. Ph. Radovanovic, S.W. Thiel, S-T. Hwang, J. Membrane Sci., **65** (1992) 231
7. V. Gröbe, G. Mann, Faserforsch. Textiltechn. **19** (1968) 49
8. C.A. Smolders, A.J. Reuvers, Microstructures in Membranes, part I: macrovoid formation, to be published.
9. C.S. Tsay, A.J. McHugh, J. Polym. Sci., Polym Phys. Ed., **28**, 1990, 1327
10. C.S. Tsay, A.J. McHugh, paper presented at the international congress on Progress in Membrane Science and Technology (PMST), June 1991, University of Twente, The Netherlands, to be published in J. Appl. Pol. Sci.
11. P. Aptel, N. Abidine, F. Ivaldi, J.P. LaFaille, J. Membrane Sci., **22**, 1985, 199
12. L.Y. Lafrenière, F.D.F. Talbot, T. Matsuura, S. Sourirajan, Ind. Eng. Chem. Res. **26**, 1987, 2385

13. T.A. Tweddle, O. Kutowy, W.L. Thayer, S. Sourirajan, Ind. Eng. Chem. Prod. Res. Dev. **22**, 1983, 320
14. E. Roesink, Microfiltration; membrane development and module design, thesis, University of Twente, The Netherlands, 1989
15. R.M. Boom, Th. van den Boomgaard, C.A. Smolders, Mass Transfer and Thermodynamics during Immersion Precipitation with a Macromolecular Additive, chapter 3 of this thesis
16. R.M. Boom, I.M. Wienk, Th. van den Boomgaard, C.A. Smolders, Microstructures in Membranes Part II: the role of a macromolecular additive, accepted for publication in J. Membrane Sci., first appendix of this thesis
17. R.M. Boom, S.Zanic, Th. van den Boomgaard, C.A. Smolders, Membranes from a Polymeric Blend Part I: Membranes from PES and PVP, chapter 4 of this thesis
18. R.M. Boom, Th. van den Boomgaard, C.A. Smolders, Equilibrium Thermodynamics of a Quaternary Membrane Forming System with Two Polymers, chapter 2 of this thesis
19. P.-G. De Gennes, Scaling Concepts in Polymer Physics, Cornell Univesity Press, 1979, NY

Chapter 6

Metastable Demixing Phenomena in the Systems PES-NMP-water and PES-NMP-PVP-water

R.M. Boom, S. Rekveld, U. Cordilia,
Th. van den Boomgaard, C.A. Smolders

Summary

The kinetics of metastable or binodal demixing is investigated in the systems PES-NMP-water and PES-PVP-NMP-water, by thermally induced demixing experiments. A general Avrami-type model is developed that can distinguish different regimes of nucleation.
From the Flory-Huggins theory, a relation is derived that describes the dependence of the demixing kinetics on the supercooling quite well.
It appears that the number of nuclei in the solution are independent on the demixing time, and on the supercooling. The results indicate that either heterogeneous nucleation takes place on a substrate that exhibits extremely strong interaction with the nucleating phase, or that large concentration fluctuations in the solution may act as nuclei for demixing.
The experimental demixing velocity as a function of the polymer concentration as measured by light scattering is found to exhibit a maximum around 15 weight% of polymer. With independent measurements it could be established that this may be related to a transition to spinodal decomposition at lower polymer concentrations. Interpretation of the results is further complicated by effects of the refractive indices of the phases.
Addition of PVP to the polymer solution hardly influences the light scattering behavior. This is probably connected to the separation of the polymers during phase separation, which is typical for these quaternary systems.

Introduction

Membranes made by phase inversion[1] form the majority of the membranes available for industrial or practical use. Phase inversion consists of submitting a thin layer of a solution of the membrane forming polymer to conditions in which the solution becomes instable. The essential

characteristic of these processes is that the membrane formation proceeds according to a combined mass transfer and phase separation process taking place in the film of the polymer solution[2,3,4].

In many systems the polymer is semi-crystalline. The polymer can form ordered regions (crystallites, aggregates) during membrane formation[5,6]. In most systems however, crystallization of the polymer is not possible or is a relatively slow process, compared to liquid-liquid demixing between a phase lean and a phase rich in polymer. The structure of the membrane is then controlled by liquid-liquid phase separation and not by crystallization. In this chapter we will focus exclusively on liquid-liquid demixing by considering only polymers that are completely amorphous.

An important phase inversion process is *immersion precipitation*. The polymer solution is contacted with a liquid bath that contains nonsolvent for the polymer. The nonsolvent must be miscible with the solvent in the polymer solution[2-4]. Rapid exchange of solvent and nonsolvent causes the polymer solution to demix, finally resulting in a porous membrane structure.

Thermally-induced phase inversion can exhibit two different types of demixing processes: metastable demixing and spinodal decomposition[7,8]. In the metastable region of the phase diagram, an activation energy must be overcome before nuclei of a new phase can be formed. The process starts with the formation of small nuclei that grow out into droplets of the newly formed phase. This mechanism is the same as is assumed for the immersion precipitation process.

Immersion precipitation usually shows demixing from a metastable state: demixing by nucleation of a polymer lean phase and successive growth of these nuclei, although in specific cases spinodal decomposition may be possible, or even nucleation of a phase rich in polymer. Spinodal decomposition is beyond the scope of this chapter.

Work by Gordon and coworkers on the pulse induced critical scattering (PICS) technique[9,10] gave some phenomenological information on the process of metastable (binodal) liquid-liquid demixing, which was further developed by Ronner *et al.*[11] However, a thorough understanding of the processes during metastable liquid-liquid demixing has not yet been developed.

In this chapter we will investigate the kinetics of the process of binodal demixing. Light scattered by demixing polymer solutions is measured as a function of time after the demixing starts. The results are interpreted in terms of a model that describes the demixing behavior of the polymer solutions.

Theory

The process of binodal demixing consists of two distinct steps:

1 - nucleation of a second phase;

2 - growth of the freshly formed nucleus.

For convenience, we discuss the nucleation of a second phase in a *binary* system consisting of a polymer and a solvent. The situation of one polymer and two solvents (or a solvent and a nonsolvent) is analogous to the extent that for the nucleation process and the early nucleus growth, the mixture of solvents can be regarded as being one solvent.

In figure 1 the (approximate) dependence of the free enthalpy of mixing of such a solution as a function of the composition is shown. This follows from the Flory-Huggins relation[12,13]:

$$\frac{\Delta G_m}{RT} = n_1 \ln \varphi_1 + n_2 \ln \varphi_2 + n_1 \varphi_2 g_{12} \qquad 1)$$

in which g_{12} denotes the (possibly concentration dependent) interaction parameter between solvent (1) and polymer (2). From figure 1 it appears that a polymer solution with composition X can lower its total free enthalpy of mixing by demixing into two different compositions, A and C, which are the equilibrium compositions.

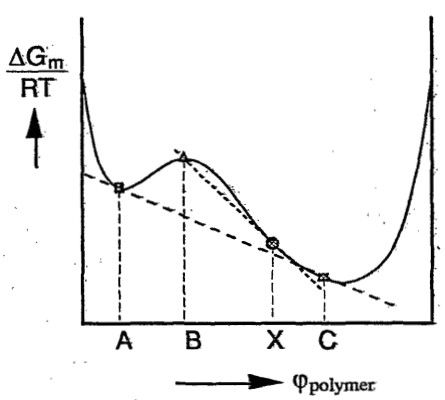

Figure 1: The free enthalpy of mixing of a binary solution of polymer and solvent. The distance BX represents the difference in composition that a nucleus should obtain before it can become stable. The points A and C are the points that give the equilibrium compositions to which the demixing process will converge. In this figure, effects of surface tension between the two phases are not yet included.

Only nuclei that possess a composition at the left of point B (the crossing of the tangent in point X and the curve of the free enthalpy of mixing) can contribute to a lowering of the free energy of mixing of the total system.
For an embryonic nucleus situated at the left hand side of point B, an activation energy must still be overcome before the nucleus can be stable. This is caused by the surface free enthalpy of the nucleus. The smaller a nucleus, the higher is the surface free enthalpy of such a nucleus per unit volume. The free enthalpy of the nucleus $\Delta G'_m$ can be expressed by introducing a surface free enthalpy term in the Flory-Huggins relation:

$$\frac{\Delta G'_m}{RT} = n_1 \ln \varphi_1 + n_2 \ln \varphi_2 + n_1 \varphi_2 g_{12} + \frac{4 \pi r^2 \gamma}{RT} \qquad 2)$$

In this relation, γ is the surface free enthalpy of the nucleus, in Jm^{-2}, or the interfacial tension, in Nm^{-1}, and r is the radius of the nucleus. Expressed per unit volume of the nucleus ($V_{nucleus}$) this equation gives:

$$\frac{\Delta G'_m}{V_{nucleus}\, RT} = \frac{n_1}{V_{nucleus}} \ln \varphi_1 + \frac{n_2}{V_{nucleus}} \ln \varphi_2 + \frac{n_1}{V_{nucleus}} \varphi_2 g_{12} + \frac{3 \gamma}{r RT} \qquad 3)$$

We see that if the nucleus has a smaller radius, the free enthalpy of mixing is higher.
Thus we have one more independent variable that describes the free enthalpy of mixing of the solution inside the nucleus: except for its composition (polymer concentration) also the nucleus size varies.

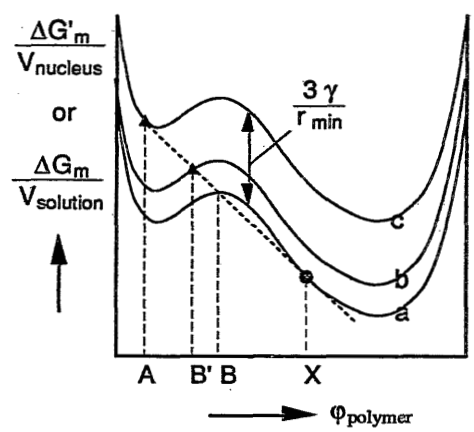

Figure 2: The free enthalpy of mixing for (a) the bulk of the polymer solution (r = ∞) and for two nuclei with different radii (b) and (c). The radius of nucleus c is smaller than the radius of nucleus b.

In the following we will assume that the interfacial enthalpy is not dependent on the composition of the nucleus.
The free enthalpy of mixing of the polymer solution in a nucleus is situated on another curve than that for the bulk of the polymer solution: the line is shifted upwards. How much the line is shifted upwards depends on the surface free enthalpy γ. The larger γ, the larger is the effect of the nucleus size.
In the hypothetical case that $\gamma = 0$ and we still have distinct nuclei, there is no surface enthalpy effect (only curve a in figure 2 is valid), and nuclei of any size may be stable, as long as their composition is positioned at the left hand side of B in figures 1 and 2. In this case, *no* activation energy exists, and metastability cannot occur, although we still need nucleation and nucleus growth to obtain phase separation.
One can see that at a radius of the nucleus which is smaller than a certain minimum value (indicated with curve c in figure 2) no stable nucleus can be formed; the tangent in point X (dashed line) then is not crossing the curve valid for the nucleus anymore. The larger the nucleus created, the smaller will be the composition difference with the bulk.
A nucleus that has the size r_{min} (and possesses a composition A in figure 2) is stable and can grow out. The radius can increase, and therefore its free enthalpy can decrease. An activity gradient from the polymer solution to the nucleus is established and the growth process is continued. When the radius has become large enough, the surface free enthalpy term in relation 2 becomes vanishingly small, and the enthalpy difference between the nucleus and the polymer solution is only determined by the compositions of both phases.
For the situation as represented in figure 2, a well-known relation for the activation energy necessary for nucleation, ΔG^*, during a liquid-liquid demixing process is applicable:

$$\Delta G^* = \frac{16\,\pi\,\gamma^3}{3\,\Delta G_v^2} \qquad 4)$$

Walton[14] found that here ΔG_v is the difference in free enthalpy of mixing between the original solution X and the weighted mean of the free enthalpy of mixing of both phases in equilibrium (A and C in figure 1). The relation is better known for crystallization phenomena; in that case the enthalpy of mixing between the crystal and the bulk should be used for ΔG_v.

There are two possible ways to overcome the activation enthalpy ΔG^* during the formation of nuclei:

1 - homogeneous nucleation
2 - heterogeneous nucleation

In the first case, the solution has to create nuclei in the bulk of the solution, from thermal (critical) fluctuations. In the second process, inhomogeneities in the solution, such as dust, small crystallites, possibly from a low molecular weight fraction of the polymer, can act as precursors for the nuclei. The solution then forms nuclei on the surface of these inhomogeneities, also by critical fluctuations.
For liquid-liquid demixing the surface free energy γ is considerably smaller than for crystallization phenomena. Although for crystallization usually heterogeneous nucleation is the nucleation mechanism (as clearly shown by Koenhen *et al.*[5]), for liquid-liquid demixing homogeneous nucleation may be of importance.
We therefore have to consider both nucleation mechanisms.

Homogeneous nucleation
Homogeneous nucleation takes place by outgrowth of (critical) concentration fluctuations that are always present in a solution.
The time dependence is conveniently described by an equation given by Kantrowitz[17] for the nucleation frequency as a function of time:

$$F(t) = F_0 \exp\left(-\frac{\tau}{t}\right) \qquad 5)$$

in which τ is a measure of the transient time necessary to reach the equilibrium nucleation frequency F_0, and F is the time dependent nucleation frequency, in $s^{-1}m^{-3}$. Wijmans *et al.*[6] simplified this relation to a step function:

$$F(t) = 0 \quad \text{for } t < \tau \qquad 6)$$
$$F(t) = F_0 \quad \text{for } t > \tau$$

which approximates relation 5 well. The value of F_0 is dependent (among others) on the value of the activation energy for nucleation, ΔG^*, mentioned in relation 4.

Heterogeneous nucleation
The difference of heterogeneous nucleation compared to homogeneous nucleation is the presence of a surface on which droplets of the incipient

phase can be formed. Figure 3 shows this situation.

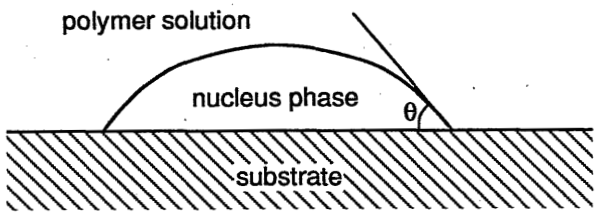

Figure 3: A surface on which heterogeneous nucleation takes place. The nucleating phase has a smaller contact angle with the substrate than the surrounding solution; the embryo of the nucleus is formed by critical concentration fluctuations in the solution, at the solution/substrate interface.

The activation energy of heterogeneous nucleation can now be written as:

$$\Delta G^*_{het} = \frac{16\,\pi\,\gamma^3}{3\,(\Delta G_v)^2}\,\frac{(2+\cos\theta)(1-\cos\theta)^2}{4} = \Delta G^*_{hom}\,A(\theta) \qquad 7)$$

The factor $A(\theta)$ is dependent on the contact angle θ of the incipient phase on the substrate, with the polymer solution as the surrounding medium. If the contact angle is smaller than 180°, ΔG^*_{het} is smaller than ΔG^*_{hom}, and the presence of such a substrate then results in heterogeneous nucleation. We can see that heterogeneous nucleation follows the same mechanism as homogeneous nucleation: concentration fluctuations at the solution/substrate interface must give rise to a local embryonic nucleus that is large enough to posses a higher free enthalpy of mixing than the activation free enthalpy (see e.g. figure 2). The difference for heterogeneous nucleation is, that the activation energy is lowered, and that therefore the nucleation rate can be considerably higher.
The time dependence of heterogeneous nucleation should follow relation 5, although the values of τ and F_0 are different.

Growth of the nuclei

The growth of nuclei has been described by Nielsen[16]. Fick's second law reads in spherical coordinates:

$$\frac{\partial\phi}{\partial t} = D\left(\frac{\partial^2\phi}{\partial r^2} + \frac{2}{r}\frac{\partial\phi}{\partial r}\right) \qquad 8)$$

in which ϕ is the volume fraction in the polymer solution around the nucleus, dependent on the distance r from the center of the nucleus and time t. Integration between the constant bulk volume fraction ϕ_∞ (the composition X in figure 1) and the constant boundary volume fraction ϕ_0 outside the nucleus (which should be the composition C in figure 1) gives the following solution of equation 8:

$$\frac{\phi(r,t) - \phi_0}{\phi_\infty - \phi_0} = 1 - \frac{r_0}{r}\left\{1 - \mathrm{erf}\left(\frac{r - r_0}{\sqrt{2Dt}}\right)\right\} \qquad 9)$$

in which r_0 is the (current) radius of the nucleus; $r > r_0$. Mathematically after $t \rightarrow \infty$ but physically after t has surpassed a finite value, the error function becomes negligible compared to unity, and 9 can be rewritten as:

$$\frac{\phi(r,t) - \phi_0}{\phi_\infty - \phi_0} = 1 - \frac{r_0}{r} \qquad 10)$$

The derivative to r is then:

$$\frac{d\phi}{dr} = \frac{r_0}{r^2}(\phi_\infty - \phi_0) \qquad 11)$$

The growth rate dr_0/dt of the nucleus is coupled to the volume fraction (concentration) gradient at the surface of the nucleus, according to Fick's first law:

$$\frac{dr_0}{dt}(\phi_n - \phi_0) = D\left(\frac{\partial\phi}{\partial r}\right)_{r=r_0} \qquad 12)$$

in which ϕ_n is the volume fraction *in* the nucleus (composition A in figures 1 or 2). Substituting relation 11 in relation 12, we find:

$$\frac{dr_0}{dt} = D\frac{(\phi_\infty - \phi_0)}{(\phi_n - \phi_0)}\frac{1}{r_0} \qquad 13)$$

We find that the growth rate dr_0/dt is linearly dependent on the supersaturation $\phi_\infty - \phi_0$, and that the nucleus shows parabolic growth. Integrating this relation gives the dependence of the radius of the nucleus on time:

$$r = \left\{r_{min}^2 + 2Dt\left(\frac{\phi_\infty - \phi_0}{\phi_n - \phi_0}\right)\right\}^{\frac{1}{2}} \qquad 14)$$

Simultaneous nucleation and growth

A demixing experiment is visualized in figure 4. A polymer solution is brought from a stable condition (e.g., high temperature) to a metastable condition (lower temperature) at t = 0. At this moment the number of nuclei is zero; only after a transient time τ, the formation of nuclei starts; it is assumed that it immediately reaches its equilibrium nucleation frequency. Between $t = \tau$ (the onset of nucleation) and $t = t_m$ (the moment of observation), a constant nucleation frequency is valid, while all nuclei are growing.

Wijmans *et al.*[4] reasoned that the nuclei should all have a volume

$$V(t) = b(t_m - \tau)^{1.5} \qquad 15)$$

in which b is a constant. This would only be true if all nuclei would have formed at time τ, which is generally not the case.

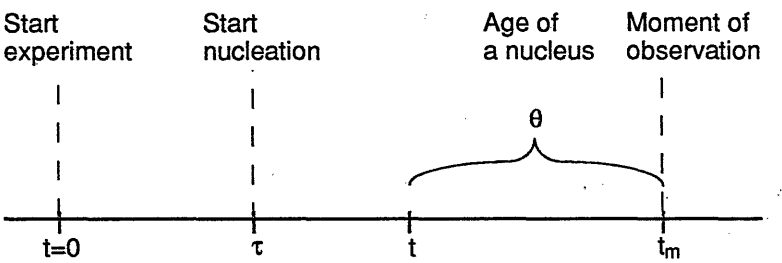

Figure 4: Time scale for a demixing experiment. At t = 0 the experiment starts, at $t = t_m$ the observation is performed. At time $t = \tau$, nucleation starts, and the nucleation frequency is fixed at F_0.

Due to the continuous formation of nuclei, a *size distribution* exists, from the critical (minimum) nucleus volume (formed at $t = t_m$) to the maximum nucleus volume (formed at $t = \tau$), equal to $b(t_m-\tau)^{1.5}$.

The size distribution of nuclei as a function of the *radius* of the nuclei is given by:

$$\left(\frac{\partial N}{\partial r}\right) = \frac{\left(\frac{\partial N}{\partial \theta}\right)}{\left(\frac{\partial r}{\partial \theta}\right)} \qquad 16)$$

θ is the age of the nucleus. The numerator on the right hand side of

equation 16 can be derived from the growth relation (equation 14), in which we neglect the critical nucleus size r_{min}:

$$r = c\,\theta^{\frac{1}{2}} \qquad 17)$$

Here θ is the age of the nucleus, equal to $(t_m - t)$; the c is a constant, consisting of:

$$c = \left\{ 2\,D \left(\frac{\phi_\infty - \phi_0}{\phi_n - \phi_0} \right) \right\}^{\frac{1}{2}} \qquad 17a)$$

The denominator in relation 16 is the derivative of relation 17 with respect to the nucleus age θ:

$$\frac{\partial r}{\partial \theta} = \tfrac{1}{2} c\,\theta^{-\frac{1}{2}} \qquad 19)$$

We assume a constant nucleation frequency for $t > \tau$ (relation 6):

$$\frac{\partial N}{\partial \theta} = F_0 \qquad 6a)$$

combining this relation with 16 and 19 yields:

$$\frac{\partial N}{\partial r} = \frac{F_0}{\tfrac{1}{2} c\,\theta^{-\frac{1}{2}}} = 2\,c^{-1}\,F_0\,\theta^{\frac{1}{2}} = 2\,c^{-2}\,F_0\,r \qquad 20)$$

It appears that the (differential) nucleus size distribution is linear with radius r of the nuclei.

Light scattering experiments

The technique used for following the demixing process is to measure the light scattered by the nuclei as a function of time, after bringing the sample to a certain supercooling. In the Rayleigh scattering regime, the scattered light at a fixed angle ϑ is dependent on the volume of the scattering particles as[17]:

$$I_\vartheta \sim I_0 \left(1 + \cos^2\vartheta\right) \left(\frac{n_n^2 - n_0^2}{n_0^2} \right) \int_0^{r_{max}} \frac{\partial N}{\partial r} V(N)^2\,dr \qquad 21)$$

where n_n and n_0 are the refractive indices of the nucleus phase and the polymer solution, respectively, and I_0 is the intensity of the incident beam of light.
Using the size distribution (relation 20), we obtain:

$$I_\vartheta \sim \int_0^{r_{max}} 2\,c^{-2}\,F_0\,r\left(\frac{4}{3}\pi r^3\right)^2 dr \qquad 22)$$

which yields after using relation 17, and integration:

$$I_\vartheta \sim \frac{4\,c^{-2}\,\pi^2\,F_0\,r_{max}^8}{9} = \frac{4\pi^2}{9}\,c^6\,F_0\,(t_m - \tau)^4 \qquad 23)$$

or:

$$I_\vartheta = K\,(t_m - \tau)^4 \qquad 24)$$

with K a growth constant, dependent on the supercooling. Here Wijmans *et al.*[6] obtained a third power relationship from the same starting point.
A third power *is* obtained when it is assumed that we do not have any further nucleation during the experiment, but that all nuclei have formed at one single moment τ. The size distribution of the nuclei is then monodisperse. Relation 24 becomes in this case:

$$I_\vartheta = K'\,(t_m - \tau)^3 \qquad 24a)$$

The fact that Wijmans *et al.*[6] found a third power experimentally, indicates that in their solutions small crystals already were present as nuclei. This situation was also found by Koenhen *et al.*[3]. The interpretation of the induction time τ then becomes somewhat ambiguous.

Summarizing, we can distinguish between mechanisms of nucleation by plotting the logarithm of the increase in scattering intensity as a function of the logarithm of time minus an arbitrary time τ. The slope of the line will give information on the mechanism of demixing. A slope of 3 indicates that the nuclei are already present in the polymer solution before the experiment starts. A slope of four indicates that nucleation is going on *during the experiment*. This approach is a specific case of the well-known Avrami approach[18].

There is a third type of demixing possible: spinodal decomposition. Especially for quenches to lower temperatures, this may play a role. In this

case nucleation is not necessary at all, since the activation energy for nucleation is zero (one might say that the critical nucleus size is negative).

Dependence on supercooling

Let us now continue with the kinetics of binodal demixing. In figure 5, the plot of the free enthalpy of mixing versus composition is given again. Points A and C indicate the equilibrium compositions. We assume that the supersaturation, $\Delta\varphi$, is quite small.

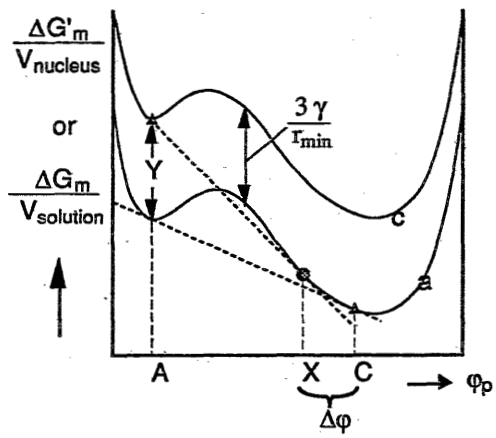

Figure 5: The thermodynamic situation during nucleation (see also ref. 14). The quantity Y is the free enthalpy that the nucleus should have in excess to the bulk of the solution (= $3\gamma/r_{min}$). Note that the chemical potential of the supersaturated solution and of the nucleus is equal.

Near point C (the cloudpoint composition), the free enthalpy of mixing in point X close to point C can be described by a second order Taylor expansion series.

$$\frac{\Delta G_m}{RT}(\phi_C+\Delta\phi) = \frac{\Delta G_m}{RT}(\phi_C) + \Delta\phi \frac{\partial}{\partial\phi}\left(\frac{\Delta G_m}{RT}(\phi_C)\right) + \frac{1}{2}\Delta\phi^2 \frac{\partial^2}{\partial\phi^2}\left(\frac{\Delta G_m}{RT}(\phi_C)\right) + O\left(\Delta\phi^3\right) \quad 26)$$

in which $\Delta\phi$ (= ϕ_X-ϕ_C) denotes the supersaturation. The slope of the tangent in point $\phi_X = \phi_C+\Delta\phi$ (the chemical potential) is then given by:

$$\frac{\partial}{\partial\phi}\left(\frac{\Delta G_m}{RT}(\phi_C+\Delta\phi)\right)=\frac{\partial}{\partial\phi}\left(\frac{\Delta G_m}{RT}(\phi_C)\right)+\Delta\phi\,\frac{\partial^2}{\partial\phi^2}\left(\frac{\Delta G_m}{RT}(\phi_C)\right)+O(\Delta\phi^2) \qquad 27)$$

The difference in free enthalpy between the nucleus and the solution bulk Y is then given by (see figure 5):

$$Y=(\phi_C-\phi_A)\frac{\partial}{\partial\phi}\left(\frac{\Delta G_m}{RT}(\phi_C+\Delta\phi)\right)-(\phi_C-\phi_A)\frac{\partial}{\partial\phi}\left(\frac{\Delta G_m}{RT}(\phi_C)\right) \qquad 28)$$

In combination with relation 27 this gives:

$$Y=(\phi_C-\phi_A)\,\Delta\phi\left\{\frac{\partial^2}{\partial\phi^2}\left(\frac{\Delta G_m}{RT}(\phi_C)\right)\right\} \qquad 29)$$

Since Y is equal to the surface free energy term in relation 3 (see also figure 5), we can find the following expression for the supersaturation $\Delta\phi$:

$$\Delta\phi=\frac{Y}{(\phi_C-\phi_A)\left\{\frac{\partial^2}{\partial\phi^2}\left(\frac{\Delta G_m}{RT}(\phi_C)\right)\right\}}=\frac{3\gamma}{r_{min}RT\,(\phi_C-\phi_A)\left\{\frac{\partial^2}{\partial\phi^2}\left(\frac{\Delta G_m}{RT}(\phi_C)\right)\right\}} \qquad 30)$$

We can observe that the critical nucleus size r_{min} is inversely proportional to the supersaturation imposed on the system. The larger the quench into the metastable region, the smaller is the critical nucleus size.

In our experiments we will induce supersaturation by cooling the solution under its cloudpoint temperature. The supercooling ΔT (cloudpoint temperature minus current temperature) can be assumed to be proportional to the supersaturation, for small supercoolings:

$$\Delta\phi\sim\Delta T \qquad 31)$$

This is visualized in figure 6.

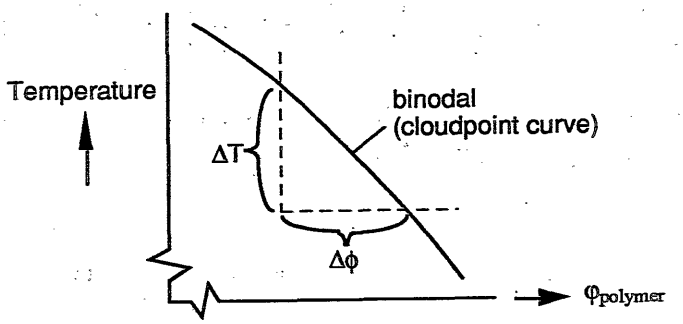

Figure 6: For small supercoolings the cloudpoint curve may be assumed to be a straight line, and the supercooling is linearly dependent on the supersaturation.

It appears from the relations 30 and 31 that

$$\Delta T \sim \frac{\gamma}{r_{min}} \qquad 32)$$

Relations 4 or 7 give the activation energy for nucleation, which can also be expressed as a function of r_{min}:

$$r_{min} = \frac{3\gamma}{\left|\frac{\Delta G^*}{V_{nucleus}}\right|} \qquad 33)$$

$$\Delta G^* = \frac{4}{3}\pi (r_{min})^2 \gamma A(\theta) \qquad 34)$$

in which ΔG^* is actually the same as Y, and $A(\theta)$ is the factor incorporating the effects of a heterogeneous substrate (homogeneous nucleation can be seen as the case where $\theta = 180°$, and $A(\theta)$ is unity).
By combining relations 32 and 34, we see that there is a relation between ΔG^* and ΔT:

$$\Delta G^* \sim \frac{\gamma^3}{(\Delta T)^2} \qquad 35)$$

We now assume that all nuclei are already present at the start of the experiment, as will be shown to be the case in the experimental section.

We can assume that in the solution a wide range of (sizes or surface energies of) nuclei is present. A Boltzmann equation gives the number of nuclei suitable for further growth:

$$N = N_0 \exp\left(- \frac{\Delta G^*}{kT} \right) \qquad 36)$$

Using the relation for ΔG^* (equation 35), we find for the number of suitable nuclei present:

$$N = N_0 \exp\left(- \frac{A}{(\Delta T)^2} \right) \qquad 37)$$

A is here a constant, dependent on γ and T.
Since we are *here* assuming the nuclei to be all of the same age, the light scattering caused by the nuclei is given by:

$$I_\vartheta \sim N V^2 \qquad 38)$$

therefore the scattering growth factor K as defined by relation 24 or 24a is dependent on ΔT, because:

$$\begin{aligned} I_\vartheta \sim N \left(\frac{4}{3} \pi r^3 \right)^2 = N \left(\frac{4}{3} \pi \left\{ 2 D t \left(\frac{\phi_\infty - \phi_0}{\phi_p - \phi_0} \right) \right\}^{\frac{3}{2}} \right)^2 \\ \sim N_0 \exp\left(\frac{-A}{(\Delta T)^2} \right) \left\{ 2 D t \left(\frac{\phi_\infty - \phi_0}{\phi_p - \phi_0} \right) \right\}^3 \end{aligned} \qquad 39)$$

from which it follows that (since $(c_\infty - c_0) \sim \Delta\phi \sim \Delta T$):

$$I_\vartheta = K_{red} (\Delta T)^3 \exp\left(\frac{-A}{(\Delta T)^2} \right) t^3 = K t^3 \qquad 40)$$

$$\text{in which } K = K_{red} (\Delta T)^3 \exp\left(\frac{-A}{(\Delta T)^2} \right)$$

in which the K_{red} is the reduced scattering growth constant (independent of the suprcooling). The scattering behavior of the solution is thus described as a function of time t, and as a function of the supercooling ΔT.

Experimental Set-up

The experimental set-up chosen is similar to the original approach of Derham and Gordon[9,10]. A sealed sample tube (app. 1 mm in diameter) was vertically placed in a quartz cuvette through which a thermostatted water flow was led. Just before the water entered the cuvette it passed through a small heating coil. To ensure proper homogenation of the polymer solution in-between the temperature quenches, the water was heated by the coil at least 10 °C. At time zero, the electric current through the heating coil was stopped, while at the same moment a valve between the thermostat bath and the cuvette (that only permits a small water flow during homogenation) was opened.

By inserting a thermocouple into the outlet of the cuvette, we measured a characteristic cooling time of 0.08 seconds. Since the sample itself is considerably nearer to the heating coil, the temperature step of the sample tube should be even better.
Through the sample, horizontally polarized light from a HeNe laser was led. The scattered light was detected in a vertical plane at a fixed angle (app. 15°).
The temperature was controlled by a Colora KT 120 cryothermostat, which in turn was controlled by a computer that was also used for data collection. An Analog Devices RTI-820 D/A, A/D and D/D converter was used to communicate with the experimental part of the setup. Data were collected using 'direct memory access' techniques to ensure high signal resolution.

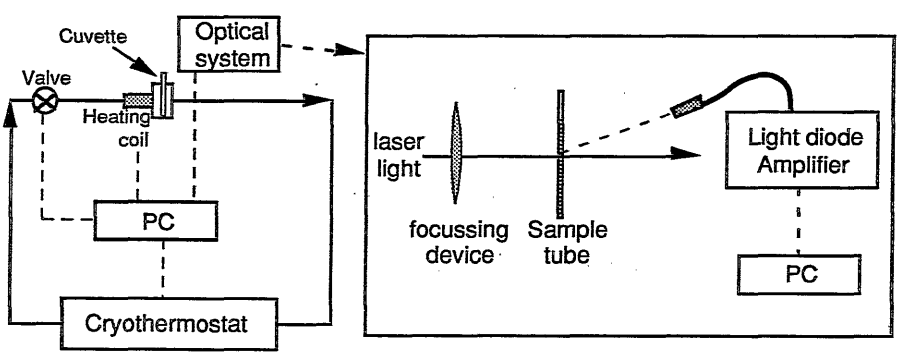

Figure 7: The experimental setup. Dashed lines represent information and control flows. In the left scheme, the uninterrupted lines are the flow of the thermostatting medium.

Sample preparation

Poly(ether sulfone), Victrex 5200 P, supplied by ICI Ltd., was dried at least for 12 hours at 80 °C before usage. No further purification was applied. Gel permeation chromatography measurements showed the PES sample used to have a M_w of 43 800 g/mole, and M_n of 22 300 g/mole.
Poly(vinyl pyrrolidone), grade K90 from Jansen Chimica, was used as received. Special care was taken to avoid water sorption. From Gel permeation chromatography the PVP turned out to have M_w 228 200 g/mole and M_n 99 800 g/mole.
N-methyl-2-pyrrolidone, or NMP, was obtained from Merck, synthesis grade, and was used without further purification. Water, used as nonsolvent, was demineralized and ultrafiltrated.

Results

The Mechanism of Nucleation
The mechanism of the nucleation process should first be determined. We fitted a number of experiments with a power law equation. In figure 8 a double logarithmic plot of intensity versus time is given for a typical measurement. The slope of the plot is approximately 3, showing that nucleation only takes place at the beginning, suggesting a heterogeneous nucleation mechanism. For smaller supercoolings actually a small decrease of the slope can be seen, which might indicate that the parabolic relation for the growth of nuclei is here not a completely valid relation.
By fitting the results with a power relation

$$I = K(t-\tau)^n \qquad 41)$$

in which K, τ and n are used as fitting parameters, we could observe that the power n was always close to 3 (mostly somewhat lower), while τ always remained zero. The absence of a transient time τ and the occurrence of a power of 3 both indicate a heterogeneous nucleation mechanism. In order to be sure that the absence of the transient time was real, the experimental data was also fitted with a fixed power 4. The fit was considerably worse now, but the transient time τ still remained zero.
For further interpretation, a power 3 was assumed (which in all cases gave

an adequate fit), and transient time of zero ($\tau = 0$).

In figure 9 the dependence of the parameter K is shown as a function of the supercooling, and of the cloudpoint temperature. The dependence is of the same form as observed by Wijmans *et al.*[6] for the crystallization of poly(phenylene oxide) in mixtures of trichloro ethylene, octanol and methanol.

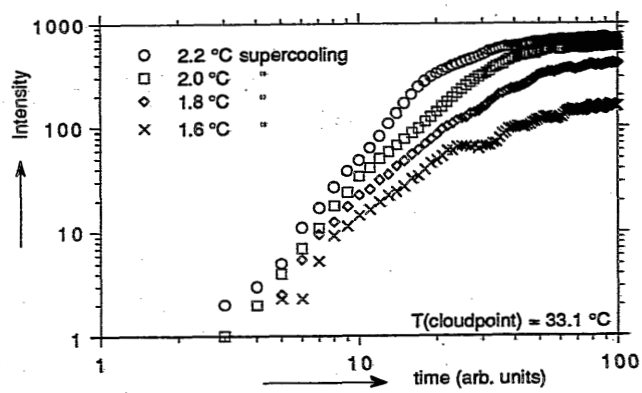

Figure 8: The typical scattering intensity as a function of time, plotted double-logarithmically. The slopes of the first parts of the lines give information on the nucleation mechanism.

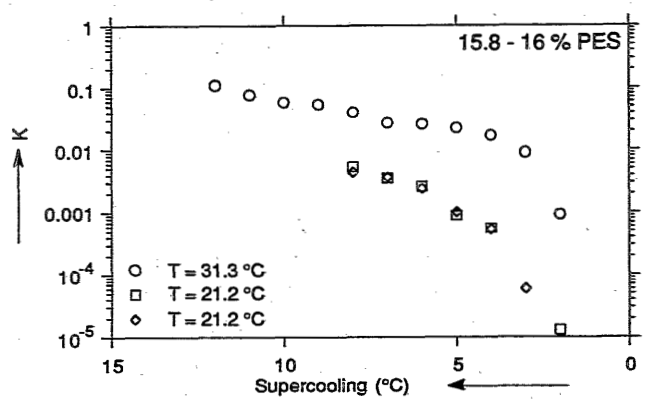

Figure 9: Dependence of the growth constant K on the cloudpoint temperature, and the supercooling.

A higher cloudpoint temperature gives a larger growth constant K, which is expected from the higher diffusion rates at higher temperature.
In figure 10, the influence of the polymer concentration on the growth constant is given. We see here a remarkable and reproducible result: with increasing polymer concentration, the growth constant first increases and then decreases again. The maximum is positioned around 16 wt% of PES in the solution.
In figure 11 the influence of PVP in the polymer solution is shown.

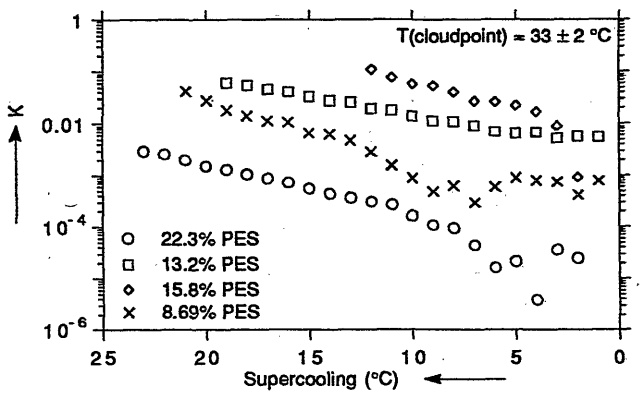

Figure 10: Dependence of the growth factor K on the polymer concentration, at constant cloudpoint temperature.

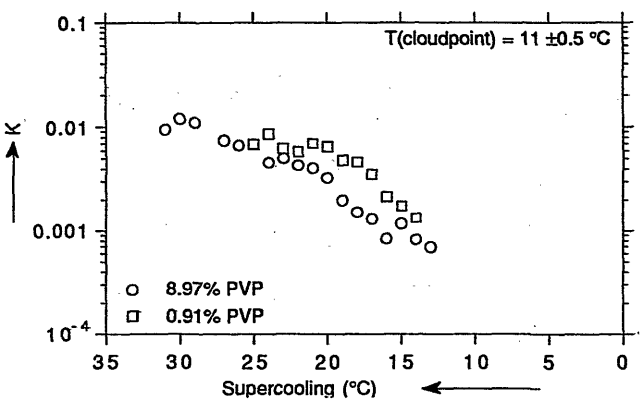

Figure 11: The influence of addition of PVP to the polymer solution on the growth constant. Concentration PES was 13.6 wt%.

It seems that the growth constant is hardly dependent on the concentration of PVP in the solution.
The model for the dependence of the growth constant K on the supercooling is used in figure 12. The dependence of K on the supercooling is well-expressed by a third-power relation, although the complete relation given by equation 40 gives a marginal improvement.

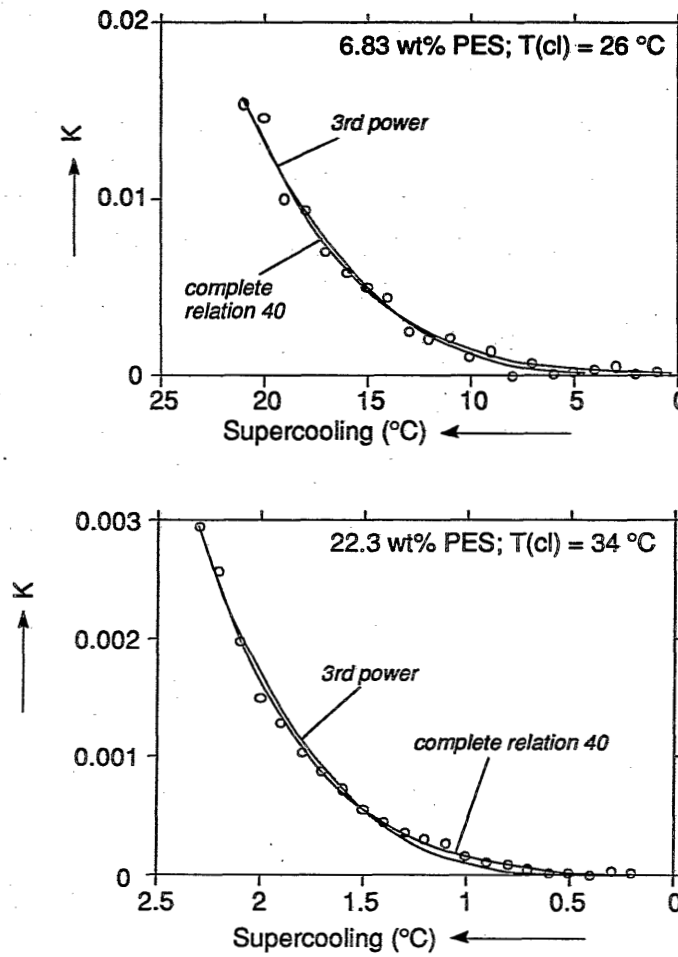

Figure 12: Typical fits obtained with a simple third-power relation, and with the complete relation 40. The improvement in the fits by incorporating the exponential term in the relation (see equation 40) is not significant. It appears that the growth constant can be readily described by a third power relation.

From the experiments it therefore appears that the number of nuclei during one run remains constant for various supercoolings.
Since both for homogeneous and heterogeneous nucleation regimes the number of nuclei should increase sharply with increasing supercooling, another nucleation process was apparently observed. The nuclei themselves appear to be already present in the solution.

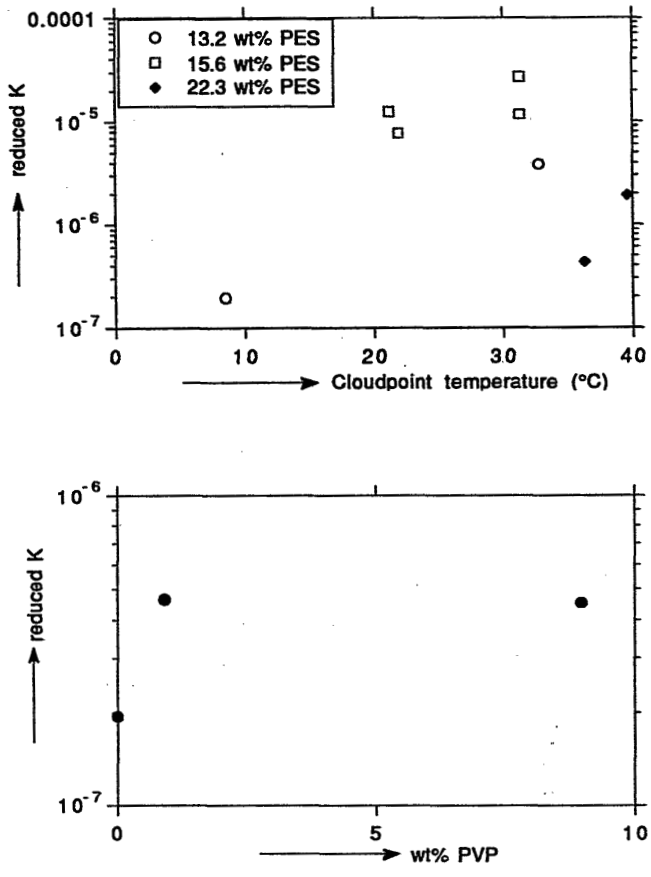

Figure 13: Reduced growth constant, as a function of the polymer solution composition and demixing circumstances: upper graph: as a function of the cloudpoint temperature at various concentrations of PES; lower graph: as a function of the PVP concentration at a fixed cloudpoint temperature (10 °C) and a fixed PES concentration (13.6 wt%).

In figure 13, the *reduced* growth constant, given by:

$$K_{red} = \frac{I_\vartheta}{t^3 (\Delta T)^3} \qquad 42)$$

is plotted as a function of the parameters of the systems. Since this reduced growth constant is independent of the demixing time and the supercooling, we might interpret this parameter as a measure of the demixing behavior of the solution.

Discussion

The experiments clearly show that nucleation is not a function of the quenching time. If nucleation during the quench had taken place, a power n that was higher than 3 (or in figure 8 a slope larger than 3) would have been observed. The fact that a power of three or slightly smaller was always observed indicates that all nuclei were already present at the beginning of the experiment. It appeared that the number of nuclei was independent on the supercooling. This implies that the number of nuclei is constant during the experiment.

For nucleus generation a few possibilities exist:
1. Homogeneous nucleation can take place at the start of the experiment. This type of nucleation is usually halted by depletion of the surrounding solution. The nuclei should be very near each other, and the simple third-power dependence on time should not be observed. A strong dependence of the number of nuclei on the supercooling is expected from this mechanism. This dependence on supercooling during the experiments was not observed.

2. Heterogeneous nucleation is in agreement with the third-power dependence of light scattering on the demixing time. Precursors of the nuclei are present from the start of the experiment.
Heterogeneous nucleation is usually associated with the presence of dust particles in the polymer solution. If nucleation took place on dust particles we would expect a poor reproducibility of the experiment: in different samples, different concentrations of dust would be present, since no extra precautions were taken to avoid dust in our solutions. However, a reasonable reproducibility of the experiments was found. Therefore, if

heterogeneous nucleation were the mechanism, the nuclei should be inherent with the polymer solutions as prepared (e.g., small crystallites of a low molecular weight fraction of the polymer).
For heterogeneous nucleation in general, one would expect that the nucleation density would increase sharply with increasing supercooling (since the activation energy for nucleation decreases with larger supercooling). Since that the number of nuclei was independent of the supercooling, heterogeneous nucleation as described appears not to be in accordance with the experimental data.

3. A third possibility is that the nuclei themselves already are present in the homogeneous solution (in *heterogeneous* nucleation, a substrate is present that facilitates nucleation; the nuclei *themselves* are not yet present). In this case one would expect both a third power dependence of the intensity of the scattered light on demixing time and on the supercooling (see equation 40).
The origin of these nuclei may now be discussed. Growth of the nuclei should not cost any additional energy (otherwise a dependence on the supercooling would be present). There are two possibilities.
- Heterogeneous particles may be present that have much better surface interaction with the nucleating phase (the polymer lean phase) than with the surrounding polymer solution. From figure 14 it can be found that if $\theta = 0$ and if:

$$\gamma_{13} > \gamma_{12} + \gamma_{23} \quad (\cos\theta = 0) \qquad 43)$$

the enlargement of the surface between nucleus and substrate is more favorable than enlargement of the surface between substrate and polymer solution. The γ_{ij}'s are the surface tensions between the three pairs of the phases, substrate (1), nucleus phase (2) and surrounding solution (3).
If the contact angle of the nucleating phase with a substrate (in a surrounding polymer solution) is zero, all embryos can grow out into nuclei, regardless of their radius r.
The condition that the interaction between nucleating phase and substrate is much better than the interaction between polymer solution and substrate is not trivial: the only difference between the two phases is that in the polymer solution, polymer coils are present. In both phases, solvent and nonsolvent are present; solutions are used that are only moderately concentrated in polymer (up to 23 wt% of PES). A substrate that has high interaction with a mixture of solvent and nonsolvent, but which has a bad

interaction with the polymer solution (while it should not dissolve in one of the phases) is not very probable.

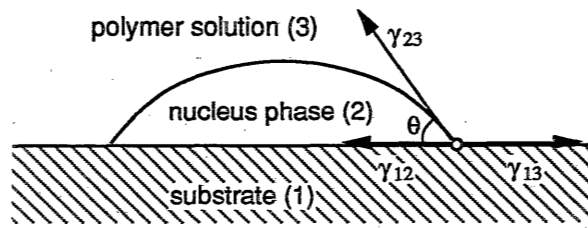

Figure 14: Contact angles for the different pairs of phases present. Certain conditions can be found under which the possibility for growth of a nucleus is independent of the radius of the nucleating phase.

- The second possibility for the presence of nuclei is: the occurrence of large critical fluctuations in the polymer concentration. These fluctuations are created by thermal (Brownian) movements in the solution. The closer a solution is to its spinodal (the border of *in*stability), the larger these concentration fluctuations are (*at* the spinodal they become infinitely large). They are responsible anyhow for the mechanism of homogeneous and heterogeneous nucleation. Moderately concentrated polymer solutions (5 - 20 wt% polymer) near their cloudpoint composition, such as investigated here, are actually quite near the spinodal curve, since they are also near the critical point. The critical concentration fluctuations therefore are considerable in size - even while the solutions are still stable. The areas that are lean in polymer may act as a nucleus. Since their content has originated from the polymer solution itself, the activation energy is low. The size and concentration of the fluctuations are determined by the properties of the solution (distance from the spinodal, dependence of the osmotic pressure on the concentration).

This is actually a special case of homogeneous nucleation, only valid for solutions that are near the critical point.

Summarizing, two different nucleation mechanisms are in accordance with the experimental data:

- heterogeneous nucleation on a substrate with extremely strong specific interaction with the nucleating phase
- homogeneous nucleation from large critical concentration fluctuations near the critical point.

To distinguish between the two possible mechanisms, solutions might be investigated that have a considerably higher polymer concentration. The cloudpoint composition is then further away from the spinodal; critical

concentration fluctuations are smaller and the formation of nuclei by the second mechanism becomes much slower. We should see then a transition to a fourth-power relationship of the scattered light intensity versus time (nucleation is then going on during the experiment).
Choosing a higher polymer concentration makes the preferential adhesion of a nucleus on a substrate only larger. If the first mechanism of nucleation is occurring, the third-power relation of the scattering intensity with time should be preserved, even at quite high polymer concentrations.

The system PES-NMP-water
In figure 10 a maximum in the growth constant K was observed at approximately 16 weight% PES. The maximum can also be seen in figure 13.
It was supposed that the maximum is connected to the critical point, where demixing is always governed by spinodal decomposition. Since no nucleation is necessary, one should expect demixing at this concentration to be the fastest. Independent measurements on the position of the critical point in the system PES-NMP-water are performed according to the measuring scheme proposed by Scholte[19-21]. Slowly and continuously samples of the polymer solution were cooled down, while a (HeNe) laser beam was passing through the sample. The light scattered at an angle of 20° was measured as a function of the temperature. On this principle the PICS technique[9-11] was developed. The reciprocal of the scattered light intensity extrapolated to zero should give the spinodal temperature. By cooling the samples very slowly, the cloudpoint temperature could be determined during the same run. In figure 15 some results are shown.
In figure 15a, the difference between cloudpoint temperature and spinodal temperature is zero, indicating that the critical point is near 9 wt% PES.
From figures 15a and 15b it can be seen that the difference between the cloudpoint temperature and the spinodal temperature (i.e. the width of the metastable, or binodal region) is very small. Therefore even with small supercooling values, spinodal decomposition can occur. Only solutions that have a higher concentration of polymer than 13.5 wt% of PES (see figures 15c and 15d) must always yield binodal (metastable) demixing. Therefore, the maximum of the demixing growth constant K_{red} at 16 wt% of PES in figure 13a might actually indicate a transition from spinodal decomposition to binodal demixing. Even when binodal demixing is occurring, there are however more complicating effects:
1. As the polymer concentration becomes higher, the demixing slows

down, due to the higher solution viscosity (diffusion rate). This is the effect that *should* be measured.

2. The light scattering is dependent on the differences in the refractive indices of the two phases (nucleus and bulk; see relation 21). The higher the polymer concentration in the bulk, the larger is the difference in refractive index between bulk and nuclei. At equally fast demixing kinetics, one might therefore expect more light scattering. The effect of the difference in the refractive indices is important especially at lower polymer concentrations. Only the real slowing down of the demixing behavior of the solution should be measured (point 1).

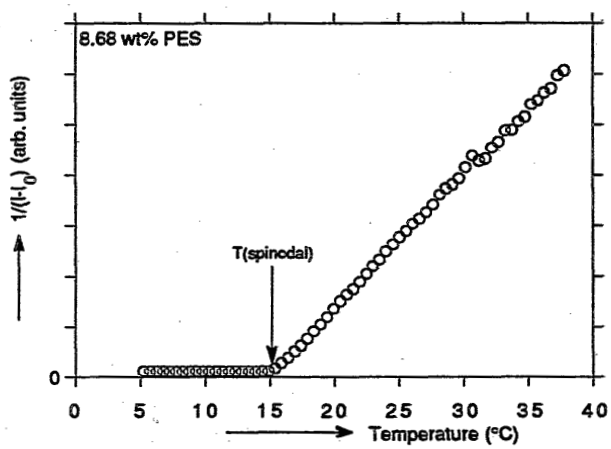

Figure 15a

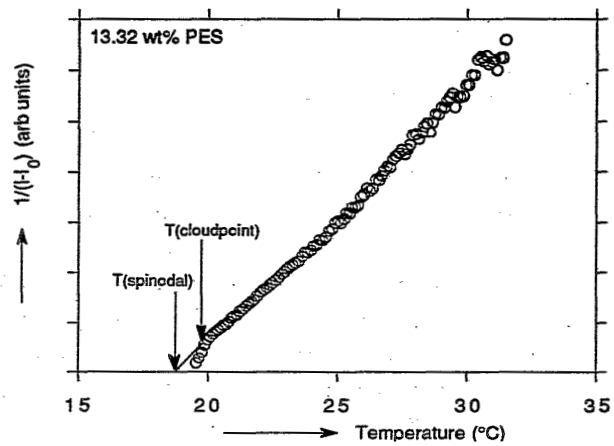

Figure 15b

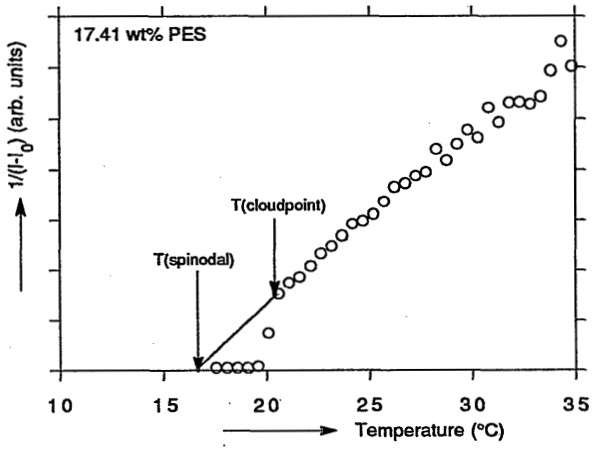

Figure 15c

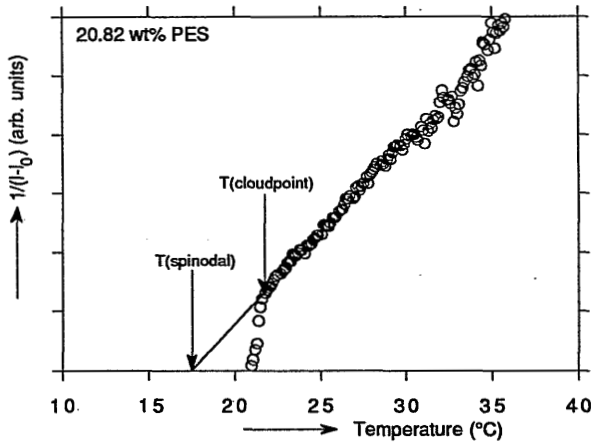

Figure 15d

Figure 15: Scholte plots for solutions with (a) 8.68, (b) 13,32, (c) 17.41 and (d) 20.82 weight% PES in a mixture of water and NMP (the exact amount of water is adapted to obtain the right cloudpoint temperature). The critical point must be around 9 weight% PES. The cloudpoint and the spinodal temperature are indicated.

The scattering behavior of the polymer solutions might therefore not reflect the real growth factor in the demixing behavior of the polymer

solutions.
It should be noted that in this case the maximum is a complication of the measurement technique (light scattering), and has nothing to do with the demixing kinetics themselves which are monotonously decreasing.

The effect of adding PVP
From figure 13, it seems that the influence of PVP on the system is not very large. A few percent of PVP enlarges the growth constant, after which it appears approximately constant.
The same effect from changes in refractive indices as discussed before might play a role here. Earlier thermodynamic calculations[22] by the authors showed that the PVP is always preferentially transferred to the phase lean in PES, i.e. the nucleus. Thus, both phases (bulk and nucleating phase) are rich in either one polymer. This lessens the difference in refractive index between the two phases considerably, and reduces the amount of light scattered by the nuclei.
A rather low PES concentration (13.6 wt%) was applied. Since it was found that addition of PVP to the solution shifts the critical point to higher polymer concentrations, spinodal decomposition circumstances may have been reached also here.

Conclusions

It was found that the demixing kinetics are controlled by a mechanism in which all nuclei are present right from the beginning of the experiment.
The number of nuclei is not dependent on the value of the supercooling.
The experiments indicate that there may be two possible nucleation mechanisms:

- Heterogeneous nucleation might take place on a substrate that shows extremely strong interaction with the nucleus phase, compared with the interaction of the substrate with the polymer solution itself.
- Large concentration fluctuations in a polymer solution relatively near the critical point may act as nuclei.

From a physical point of view the last possibility seems to be most probable. Which model occurs may be found out by repeating the measurements with samples that have a much higher polymer concen-

tration (e.g., 40 - 50 wt% of polymer); continued dependence of the light scattering on time according to a third power points to the first mechanism; if the power shifts to a higher value, the latter mechanism is more probable.

At higher polymer concentrations (22 wt% PES) a somewhat higher power could be observed than at lower polymer solutions (see figure 8). This could point to a nucleation that is slower at high polymer concentration, confirming that at low polymer concentrations the fluctuation mechanism is the nucleation mechanism.

An independent check of the demixing kinetics appears to be essential: at lower polymer concentrations spinodal decomposition can not be avoided. It is quite difficult to compare measurements of solutions that have different polymer concentrations; the refractive indices of the phases in the system are changing with the polymer concentrations in a quantitative manner. The same is true for measurements carried out with various amounts of PVP as fourth component in the solution.
Measurements by a different technique might give extra information to further interpret data from light scattering experiments.

Acknowledgements

The authors wish to express their gratitude to Dr. W.J. Briels for his stimulating ideas on the subject (especially on the nucleus size distributions).

List of Symbols

A	constant in the nucleation relation 37 (K^2)
b	volume growth rate ($m^3s^{-1.5}$)
c	radius growth constant ($ms^{-0.5}$)
D	diffusion coefficient (m^2/s)
F(t)	nucleation frequency (s^{-1})
F_0	constant nucleation frequency (s^{-1})
g_{ij}	interaction parameter (-)
I_θ	light intensity at angle θ
I_0	intensity of the incident light beam

K	scattering growth constant (defined by relations 24 and 24a) (-)
K_{red}	reduced scattering growth constant (independent of the supercooling) (-)
n_i	number of moles of component i (mole)
n_n	refractive index of a nucleus (-)
n_0	refractive index of the polymer solution around a nucleus (-)
r	radius of a nucleus (m)
r_{min}	critical (minimum) nucleus size (m)
R	gas constant (J/mole K)
t	time (s)
t_m	moment of observation (s)
T	temperature (K)
$V_{nucleus}$	volume of a nucleus (m^3)
$V(t)$	time dependent volume of a nucleus (m^3)
Y	free enthalpy difference between bulk and nucleus defined in figure 4 (J)
γ	surface free enthalpy (Jm^{-2}) or surface tension (Nm^{-1})
ΔG^*	activation free enthalpy for nucleation
ΔG_m	free enthalpy of mixing (J)
$\Delta G'_m$	free enthalpy of mixing of a nucleus with size r (J)
ΔG_v	free enthalpy of the volume inside a nucleus (without any surface terms) (J/m^3)
ΔT	supercooling (K)
$\Delta\varphi$	supersaturation (-)
θ	age of a nucleus (s); contact angle (°)
ϑ	scattering angle (°)
τ	transient time to reach the equilibrium nucleation frequency (s)
φ_i	volume fraction of component i
$\phi(r,t)$	volume fraction as a function of radius r and time t
ϕ_∞	bulk volume fraction
ϕ_n	volume fraction in the nucleus
ϕ_0	volume fraction at the interface between bulk and nucleus

References

1. M.H.V. Mulder, Basic Principles of Membrane Technology, Elsevier, 1991
2. C. Cohen, G.B. Tanny, S. Prager, J. Polym. Sci., Polym. Phys. Ed. 17, 1979, 477
3. A.J. Reuvers, J.W.A. van den Berg, C.A. Smolders, J. Membrane Sci. 34, 1987, 45

4. A.J. Reuvers, C.A. Smolders, J. Membrane Sci. **34**, 1987, 67
5. D.M. Koenhen, C.A. Smolders, M. Gordon, J. Polym. Sci., Polym. Symp. **93**, 1978,61
6. J.G. Wijmans, H.J.J. Rutten, C.A. Smolders, J. Polym. Sci. Polym. Phys. Ed.
7. J.W. Cahn, J. Chem. Phys, **42**, 1965, 93
8. J.W. Cahn, J.E. Hilliard, J. Chem. Phys. **28**, 1958, 258
9. M. Gordon, P. Irvine, J.W. Kennedy, J. Polym. Sci., Polym. Symp. **61**, 1977, 199
10. K. Derham, J. Goldsbrough, M. Gordon, Pure and Appl. Chem. **38**, 1974, 97
11. J.A. Ronner, S. Groot Wassink, C.A. Smolders, J. Membrane Sci. **32**, 1989, 27
12. J. Flory, Principles of Polymer Chemistry, Cornell University Press, New York, 1953
13. H. Tompa, Polymer Solution, Butterworths, London, 1956
14. A.G. Walton, Nucleation in Liquids and Solutions, Chapter 5, 225, in: A.C. Zettlemoyer (Ed.), Nucleation, Marcel Dekker, New York, 1969
15. A. Kantrowitz, J. Chem. Phys. **19**, 1951, 1097
16. A.E. Nielsen, Kinetics of Precipitation, Pergamonn Press, 1964
17. G. Oster, J. Colloid Sci. **B9**, 1974, 435
18. M. Avrami, J. Chem. Phys. **7**, 1939, 1103; **8**, 1941, 212; **9**, 1941, 177
19. P. Debye, J. Chem. Phys. **31**, 1959, 680
20. Th. G. Scholte, J. Polym. Sci. **A2**, 1970, 841
21. Th. G. Scholte, J. Polym. Sci. **C**, 1972, 281
22. R.M. Boom, Th. van den Boomgaard, C.A. Smolders, Chapter 2 of this thesis

First Appendix to this Thesis

Microstructures in Phase Inversion Membranes Part 2: The Role of a Polymeric Additive

R.M. Boom, I.M. Wienk,
Th. van den Boomgaard, C.A. Smolders
University of Twente, P.O. Box 217,
7500 AE Enschede, The Netherlands

Summary

Membranes were prepared from a casting solution of a water-soluble polymer, poly(vinyl pyrrolidone) (PVP), and a membrane forming polymer, poly(ether sulfone), in 1-methyl-2-pyrrolidone (NMP) as solvent, by immersing them in mixtures of water and NMP.
It was found that the addition of PVP to the ternary system suppresses the formation of macrovoids in the sublayer, while the ultrafiltration-type toplayer consists of a closely packed layer of nodules.
Using a model for mass transfer in this quaternary system, it is possible to explain the effects of the additive on macrovoid formation.
Strong indications are found that the appearance of a nodular structure in the toplayer follows a mechanism of spinodal decomposition during the very early stages of the immersion step.

Introduction

Phase inversion is the most important process to prepare symmetric or asymmetric membranes. Because of the significance of immersion precipitation (phase inversion), the mechanism of formation of these membranes has been the subject of extensive investigation[1,2].
In recent years, Reuvers et al.[1] developed a model for the description of mass transfer during the immersion step. Two types of demixing occurring during immersion precipitation followed from this model:

Accepted for publication in J. Membrane Sci.

instantaneous demixing and delayed demixing. Taking this model of mass transfer in combination with liquid-liquid phase separation, effects of variations in the composition of the casting solution and the coagulation bath could be explained.

On the basis of the distinction between delayed and instantaneous demixing, Reuvers et al. proposed a mechanism for the formation of large fingerlike cavities (macrovoids), often occurring in the sublayer of immersion precipitation membranes (see preceding part I).

Although this model is strictly valid only for ternary systems consisting of a membrane forming polymer, a solvent and a non-solvent for the polymer, some effects of the addition of a fourth component to the system can be explained with it.

In order to obtain an optimal membrane structure, an additive (a fourth component) is frequently used. Usually, the additive is a weak non-solvent for the polymer, e.g. glycerol in a system consisting of polysulfone, DMAc and water, or maleic acid in a system of cellulose acetate, dioxane and water.

Such an additive to the casting solution brings the initial composition of the casting solution nearer to the binodal. According to the mechanism proposed by Reuvers, this decreases the tendency of the solution to form macrovoids.

In other systems, polymeric additives are used. Well-known is the addition of poly (vinyl pyrrolidone) to a system consisting of polysulfone, and a solvent such as DMAc[3]. The most important effects of this type of additive are suppression of macrovoids, improved interconnectivity of the pores and higher porosities in the toplayer and the sublayer. Further, it appears that the toplayers of these membranes have a nodular structure. Reuvers' model can not account for the effects of this type of additive.

In this paper we will show some of the effects of the addition of poly(vinyl pyrrolidone) to the system consisting of poly(ether sulfone) and 1-methyl-2-pyrrolidone, coagulated with water.

In part A of this paper the mechanism underlying macrovoid formation will be discussed. We will present a model to describe mass transfer in a quaternary system consisting of two miscible polymers in a common solvent precipitated by a non-solvent for one of the polymers. On the basis of this model, we will come to a mechanism that can explain some of the effects of the polymeric additive.

In part B, the occurence of nodular structures in UF-type toplayers will be discussed. Experimental evidence will be given for a possible spinodal mechanism of formation of these nodular structures in toplayers.

A. Macrovoid formation in systems with a macromolecular additive

Theoretical considerations

The system we want to investigate consists of four components:

- a non-solvent for the polymer, initially present in the coagulation bath (component 1).
- a solvent for the polymer, initially present in the polymer solution, and in some cases in the coagulation bath (component 2)
- the membrane forming polymer (component 3), present only in the polymer solution and in the final membrane
- the macromolecular additive used (component 4)

We assume that the additive is miscible with all components present. A typical model system for this is the system used in our experiments: water (1) - 1-methyl-2-pyrrolidone (2) - poly(ether sulfone) (3) - poly(vinyl pyrrolidone) (4).

Thermodynamics

In our system we have two macromolecular components, both present at high concentrations in the same solution. Typical concentrations in casting solutions are 15 to 20 weight percent membrane forming polymer and 10 to 15 weight percent additive. The two polymers both are far above their overlap concentrations and form entangled, intertwined coils, since we know that the two polymers are well miscible. This implies that we assume that the Flory-Huggins interaction parameter between the additive and the membrane forming polymer is low. In the case of poly(ether sulfone) and poly(vinyl pyrrolidone) this interaction parameter has been determined (with high-pressure osmometry) to be lower than zero, which indicates that the two polymers form homogeneous blends at all concentrations.

Phase separation in such a system involves the demixing of the intertwined polymers. In equilibrium, the polymeric additive has moved to the membrane forming polymer lean phase. This process is considerably slower than the exchange processes of solvent and non-solvent between the casting solution and the coagulation bath occurring directly upon

immersion, because the separation of the two polymers involves the movement of one polymer with respect to the other.
It is therefore convenient to distinguish two time scales for the first moments of the immersion step.

1. The shorter time scale is valid for the process of exchange of solvent and non-solvent. On this time scale, the two polymers, effectively behave as one component. Transport of the low-molecular weight components through the polymeric network is possible; transport of the polymers with respect to each other is not possible.
2. The longer time scale is the time scale at which the two polymers can move relative to each other: the polymeric additive moves into the polymer lean phase.

These time scales have different thermodynamic regimes to which they respond. Therefore, the phase diagrams of both time scales should be evaluated.
From a thermodynamic point of view, the short time scale is characterized by the absence of any polymer in the polymer lean phase. It only contains solvent and non-solvent. This characteristic feature will be used to determine the thermodynamics on the short time scale.
During the longer time scale, the macromolecular additive is allowed to be present in the membrane forming polymer lean phase.

Equilibrium calculations
The basis of the calculations is the Flory-Huggins expression for the chemical potential of mixing in a quaternary systems:

$$\frac{\Delta G_m}{RT} = n_1 \ln\varphi_1 + n_2 \ln\varphi_2 + n_3 \ln\varphi_3 + n_4 \ln\varphi_4 + g_{12} n_1 \varphi_2 + \chi_{13} n_1 \varphi_3 + g_{14} n_1 \varphi_4 + g_{23} n_2 \varphi_3 + g_{24} n_2 \varphi_4 + g_{34} n_3 \varphi_4 \qquad 1)$$

All ternary and quaternary interaction parameters are neglected. This means that the phase diagrams calculated should only be used in a semi-quantitative way.
The derivatives of the free enthalpy of mixing with respect to the number of moles of each component are the chemical potentials of mixing. Phase equilibria are calculated by using the algorithm proposed by Altena[3]. The following objective function F is minimized:

$$F = \sum_{i=1}^{4} \left(\frac{\mu_i^a - \mu_i^b}{RT} \right)^2 \qquad 2)$$

in which the index ^{a} belongs to the concentrated phase while the index ^{b} is for the diluted phase, and φ_i and μ_i denote the volume fraction and the chemical potential of component i, respectively. T is the temperature, and R is the gas constant.

As discussed before, it is assumed that in the diluted phase no polymer is present. In all calculations concerning ternary systems, it appears that, excluding the area around the critical point, the polymer is absent in the polymer lean phase (see e.g. Altena c.s.[3]). Since in our, quaternary, case in the beginning the two polymers cannot move relative to each other, we have an anologous situation. We assume that both polymers do not significantly move into the coagulation bath.

Note, however, that component 4 *has* a driving force to diffuse out. Whenever a single component 4 molecule would diffuse out, the diffusion rate in the coagulation bath is so much higher, compared to the out-diffusion from the polymer solution, that it will diffuse quickly away, and will have no influence on the interface situation.

Therefore, we can assume that in the coagulation bath only components 1 and 2 are present. The relations for the chemical potentials collapse to those for a binary system, and the objective function F in equation 2 consists only of two terms (i = 1,2), those for the chemical potentials of the nonsolvent 1 and the solvent 2.

Modelling of mass transfer

To describe mass transfer in the polymer solution and in the coagulation bath, we expand the model developed by Reuvers[1]. We will summarize the most important points from this model.

The continuity equations are in our case the same as the ones Reuvers used:

$$\frac{\partial}{\partial t}\left(\frac{\varphi_i}{\varphi_3}\right) = \sum_{\substack{j=1 \\ j \neq i}}^{4} \left\{ \frac{\partial}{\partial m}\left(v_i \, \varphi_3 \, L_{ij} \, \frac{\partial \mu_j}{\partial m} \right) \right\} \qquad 3)$$

while the binary diffusion in the coagulation bath is described by:

$$\frac{\partial \varphi_i}{\partial t} = \frac{\partial}{\partial y}\left(D_{ij}\frac{\partial \varphi_i}{\partial y}\right) - \frac{\partial \varphi_i}{\partial y}\left(J_1^{y=0} + J_2^{y=0}\right) \qquad 4)$$

The $J_i^{y=0}$ means here the flux (ms^{-1}) of component i through the boundary layer between polymer solution and coagulation bath.
The spatial coordinate m in equation 3 is described by:

$$m = \int_{\xi=0}^{\xi=x} \varphi_3 d\xi \qquad 5)$$

in which x is the distance from the moving interface (between the polymer solution and the coagulation bath) into the polymer solution. The spatial coordinate y into the coagulation bath is taken from the (moving) interface.
It is assumed that both the coagulation bath and the polymer solution are semi-infinite.
The mobility coefficients L_{ij} can be found with the Stefan-Maxwell approach, which relates the driving forces (the chemical potentials) to the velocities $\bar{v}_i$ of the components.

$$\frac{\partial \mu_i}{\partial x} = \sum_{j=1}^{4} c_j R_{ij}(\bar{v}_j - \bar{v}_i) \qquad i = 1,2,3,4 \qquad 6)$$

Here, R_{ij} is the so-called friction coefficient between component i and j; c_i stands for the concentration of component i. For a detailed description of how the mobility coefficients are related to the Stefan-Maxwell friction coefficients R_{ij} we refer to Reuvers et al.[1], who describes this for a ternary system.
Our calculations are aimed only at the short time scale. It is assumed that the two polymers cannot move with respect to each other. In formula:

$$\bar{v}_3 - \bar{v}_4 = 0 \qquad 7)$$

The Stefan-Maxwell equations now simplify to a semi-ternary problem.

$$\frac{\partial \mu_i}{\partial x} = c_1 R_{i1}(\bar{v}_1 - \bar{v}_i) + c_2 R_{i2}(\bar{v}_2 - \bar{v}_i) + (c_3 R_{i3} + c_4 R_{i4})(\bar{v}_3 - \bar{v}_i) \qquad i = 1,2 \qquad 8)$$

Equations 8 are used in combination with the continuity equations (equations 3 and 4) to calculate the composition profiles as a function of time.
We assume that the concentrations at the interface between the casting solution and the coagulation bath are constant. This is a reasonable suggestion for the first moments of immersion. Reuvers[1] showed that in this case, the composition profile is only dependent on the variable (a partial Fourier number):

$$l = \frac{m}{\sqrt{t}} \qquad 9)$$

This indicates that the composition profile calculated not only represents the initial composition profile in the toplayer, but also the dependence on time of the compositions at each position in the polymer solution.
The composition profiles were calculated in double precision, with the D04PGF routine from the NAG-library.
Calculations were performed according to the following scheme:

1. Equilibrium conditions are assumed at the interface; the polymer concentration at the interface is estimated as a first guess.
2. Composition profiles are calculated both in the polymer solution and in the coagulation bath.
3. The fluxes at both sides of the interface, found from the calculated composition profiles, are compared.
4. The steps 1 to 3 are repeated with varying polymer concentration at the interface, until the flux through the interface of each component is equal at both sides of the interface.

Experimental set up

Materials
The membrane forming polymer poly(ether sulfone) (Victrex 5200P) was supplied by ICI. Molecular weight was 43800 g/mole as determined by GPC measurements. The additive poly-vinylpyrrolidone (PVP) was purchased from Janssen Chimica. Different types of PVP were used indicated by a K-number, K15 (Mw 10 000 g/mole), K 30 (Mol. weight 40 000 g/mole), K60 (Mol. weight 160 000 g/mole) and K90 (Mol. weight 360 000 g/mole). 1-

Methyl-2-pyrrolidone (Merck, synthetic grade) was used as solvent, while the non-solvent used was water.

The spinning process
Hollow fibers were spun by the dry-wet spinning technique or by a two bath system. The filtered and degassed polymer solution was pumped through a spinneret. In the dry-wet technique the solution leaving the spinneret passes an airgap (the first stage) after which it enters into a coagulation bath (the second stage). On the bore side an internal coagulation bath was pumped. In case of the two bath system the first and second stage were two different outer coagulation baths. The first bath and the internal coagulation bath were NMP-water mixtures at ambient temperatures. The second stage always was a water bath and its temperature could be varied. After spinning, residual solvent was removed by flushing with water for two days.

Electron Microscopy
Morphology of the membranes was studied with an electron microscope (JEOL JSM T220A). Sample preparation was done as follows. After displacement of water by ethanol and ethanol by hexane the membranes were dried in air. In a sputtering apparatus (Balzers union SCD 040) a thin gold-layer was deposited on the membranes.

Results

Experimental
The effects of a polymeric additive on the membrane morphology obtained is shown in figure 1, which gives cross-sections through membranes made with varying concentrations of polymeric additive and varying molecular weights of the additive.
It appears that the molecular weight of the polymeric additive is an important parameter. Addition of a polymeric additive of a certain minimum molecular weight results in the absence of macrovoids in the membrane structure.
It further appears that a certain minimum concentration of polymeric additive is needed to suppress macrovoid formation.

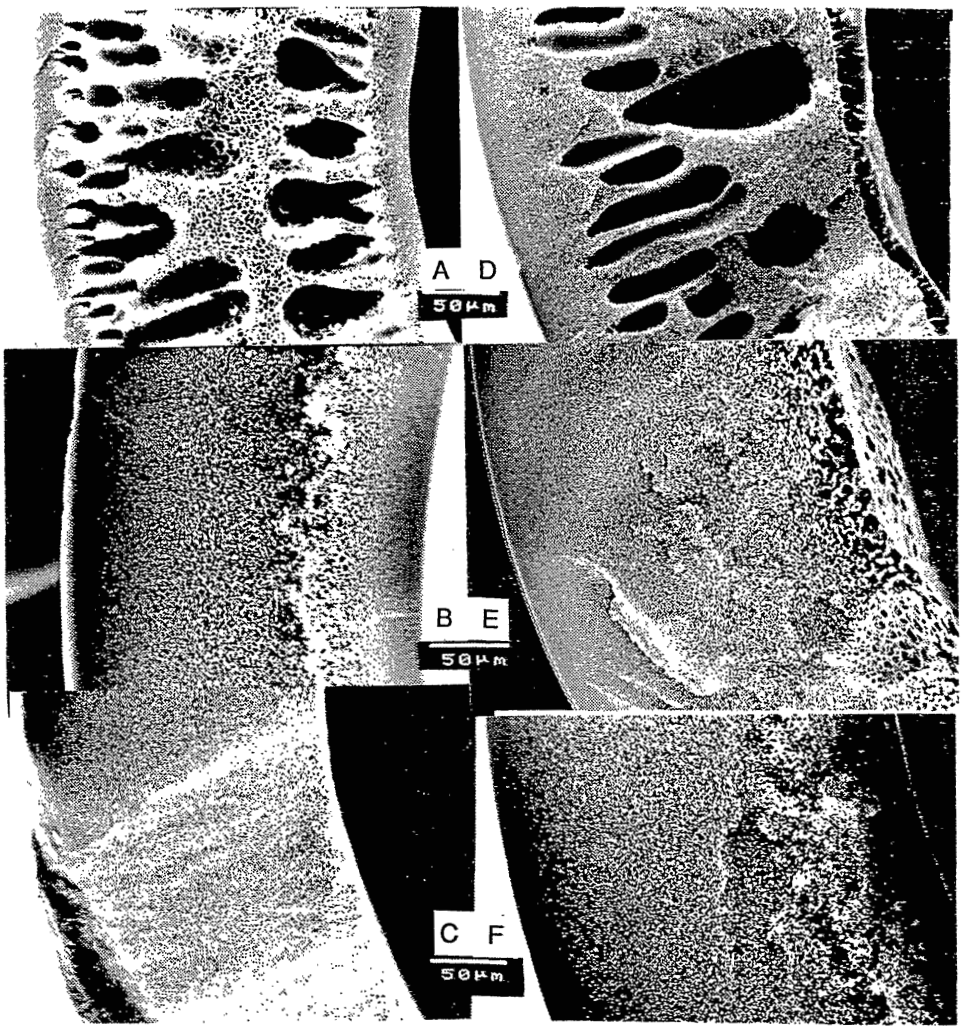

Figure 1: Scanning electron microscopic pictures of cross-sections through hollow fibers. Concentration of PES was 20 wt%; 5 wt% water was added to the casting solution. In case of A, B and C the indicated coagulation bath is the bore liquid. For D, E and F the indicated coagulation bath is the first external stage of the bath, the second stage was a water bath of 24°C.

No.	*Casting Solution* wt% PVP (MW)	*Coagulation bath* (wt% NMP)	No.	*Casting Solution* wt% PVP (MW)	*Coagulation bath* (wt% NMP)
A	5 (360 000)	40	D	10 (40 000)	20
B	7.5 (360 000)	40	E	10 (160 000)	20
C	10 (360 000)	40	F	10 (360 000)	20

Equilibrium calculations

Phase equilibria were calculated according to the conditions discussed in the theoretical section. The ratio of weight percentages of components 3 and 4 was varied. The resulting phase diagrams are shown in figure 2.

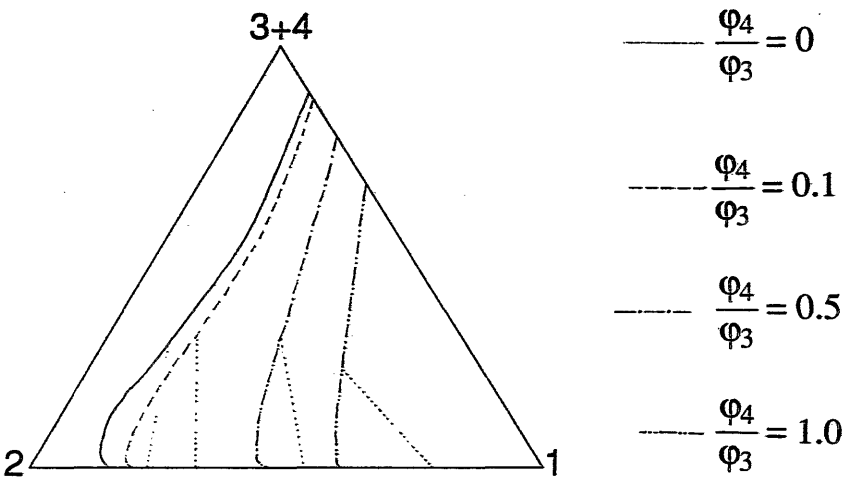

Figure 2; Phase diagrams for the short time scale in systems with a macromolecular additive. Parameters used[5]*:*

$g_{12} = 1.0; g_{23} = 0.5; \chi_{13} = 1.5; g_{14} = 0.4; g_{24} = 0.5; g_{34} = -1.0.$

Molecular weights:

1) 18 g mole^{-1}*; 2) 99 g mole*$^{-1}$*; 3) 18 kg mole*$^{-1}$*; 4) 40 kg mole*$^{-1}$*.*

Parameters used are based on measurements for the system poly(ether sulfone) - 1-methyl-2-pyrrolidone - water, by Tkacik et al.[5], and measurements performed in our own laboratory. These measurements were done with high-pressure osmometry: a PES-NMP solution was brought into contact with NMP via a Cuprophan™ membrane, that swells only slightly in NMP. The polymer was found not to permeate through the membrane measurably over a period of at least one week. By determining the equilibrium osmotic pressure in the solution cell, the interaction parameters could be determined.

It appears from the computations that with increasing content of component 4 (the additive), the binodal shifts to the non-solvent corner.

These phase diagrams are only valid as long as the two polymers cannot move relative to each other, i.e. as long as polymeric additive is absent in the polymer lean phase.

Mass transfer

Initial composition profiles were calculated for a system in which the ratio of the weight fractions of the polymeric components is unity.

It was assumed that the diffusivity of component 4 was equal to the diffusivity of component 3. In our model system consisting of poly(ether sulfone) (3) - poly(vinyl pyrrolidone) (4) - 1-methyl-2-pyrrolidone (2), measurements of diffusion coefficients of both polymeric components (3,4) in the solvent (2) justify this assumption. These measurements were performed in our laboratory with an analytical ultracentrifuge by following a small imposed gradient in the polymer concentration by means of a Schlieren optical system.

A typical composition profile calculated is shown in figure 3. This profile is only valid for the first instances after immersion.

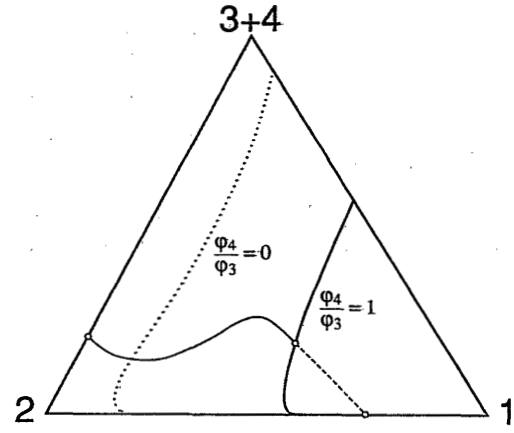

Figure 3; Composition profile for ϕ_4/ϕ_3 = 1.0. Thermodynamic parameters are as in figure 2. Kinetic parameters are valid for the experimental system water - 1-methyl-2-pyrrolidone - poly(ether sulfone) - poly(vinyl pyrrolidone).

The influence of the concentration of solvent in the coagulation bath has been considered, resulting in the curves in figure 4.

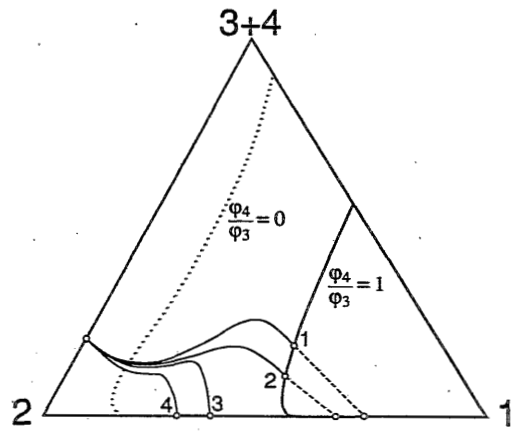

Figure 4; Composition profiles calculated with the same parameters as in figure 3. The concentration of solvent in the coagulation bath is increasing from 0 to 65 vol%.

For higher solvent concentrations in the coagulation bath, there is no composition jump at the interface anymore, because the initial composition profile does not reach a binodal composition anymore. A gradual transition from the casting solution to the coagulation bath is obtained. When a polymeric solution with a composition as discussed is coagulated in a coagulation bath with a high concentration of solvent, the coagulation bath turns slightly turbid, indicating dissolution of some polymer in the coagulation bath. This is in agreement with the calculated results.

Discussion

Experiments showed that only an additive of a certain minimum molecular weight and present at a certain minimum concentration is effective to prevent macrovoid formation. We will now discuss how the calculated results may explain these facts.
Calculations showed that at all concentrations of solvent in the coagulation bath, delay of demixing is obtained with respect to the phase diagram

for the short time scale. After some moments of immersion however, the longer time scale, in which polymer-polymer movement is possible, is gaining importance. When the polymeric additive is able to diffuse into the membrane forming polymer lean phase, the 'real' binodal close to the polymer-solvent axis is gaining importance again. The area of the demixing gap thereby increases dramatically, and the compositions already created in the toplayer appear to be very unstable. Hence, demixing, once started, will be relatively fast in the toplayer.
Complete equilibrium calculations (i.e. without any assumptions concerning concentrations) show that the polymeric additive (4) usually is almost exclusively present in the polymer (3) lean phase. The binodal in this case shifts to lower water concentrations in the polymer (3) rich phase than when no additive (4) would have been present in the system.
Therefore, as an indication for this situation, the binodal valid for a system without any additive present in the system can be used (see figure 4).
The change from the 'virtual' binodal for the short time scale to the 'real' binodal that represents real phase equilibria in the phase diagram implies that for solutions containing a polymeric additive, delay of demixing as described by Reuvers[1] cannot occur at all. Even at high concentrations of solvent in the coagulation bath (where a solution without the additive would exhibit delay of demixing), compositions which are unstable in the long time scale are created in the toplayer during the short time scale. From figure 4, one might even say, that in the toplayer conditions for spinodal demixing are created. We will expand on this topic in part B.
The measurement of light transmission through precipitating membranes indeed indicates that addition of a polymeric additive induces a certain instantaneous demixing process, at conditions that would yield delay of demixing without the additive.
This can be related to the effects the additive has on macrovoid formation, as will be explained in the next paragraph.

Macrovoid formation
Reuvers proposed a mechanism of formation of macrovoids in ternary systems consisting of non-solvent, solvent and membrane forming polymer. This mechanism was presented in the preceding part of this work; it will be summarized in short here.
A casting solution, demixing according to an instantaneous mechanism, develops higher and higher solvent concentrations in the nuclei of the

polymer lean phase present in the proceeding coagulation front. At a certain point, these solvent concentrations become so high locally, that conditions become favorable for delay of demixing (although this is only calculated for a flat geometry, and not for a spherical situation as is present here). Delay of demixing is normally characterized, due to loss of solvent which is larger than the influx of non-solvent, by a shrinkage of the polymer solution. Therefore, an increase in volume of the coagulation bath results. In this case, a nucleus is serving as a tiny coagulation bath. The polymer solution surrounding the nucleus experiences delay of demixing with respect to the nucleus, and the nucleus will grow. As long as the conditions of delayed demixing remain the same, i.e. as long as the solvent concentration in the nucleus remains high enough, the growth of the nucleus continues.

We return to the quaternary system with a polymeric additive. As we have seen, in a system with a polymeric additive, delay of demixing does not take place, as long as the two time scales can be operative. Local conditions for delay of demixing cannot take place. Growth of a nucleus is effectively blocked by the creation of new nuclei. Apparently, the addition of a polymeric additive hinders macrovoid formation.

This effect can only take place when enough additive is present: at lower concentrations the demixing gap does not shift enough to the right in the phase diagram to induce any significant effect during the short time scale.

On the other hand, the diffusion of the two polymers with respect to each other should be slow compared to the diffusion of solvent and non-solvent in the polymer solution. Otherwise, it is not possible to distinguish a short time scale from the longer one. Delay of demixing will then still be possible. To avoid this, a certain minimum molecular weight of both polymers in the system is required. Since in most cases the molecular weight of the membrane forming polymer is fixed, this means that the molecular weight of the additive should have a certain minimum value. This is in agreement with the facts found in the experimental section.

B. Nodular structures in ultrafiltration membranes

Theoretical considerations

Open pore structures in membranes are formed by nucleation and growth of the polymer lean phase in the metastable region between the binodal and the spinodal curve. However, the toplayer of ultrafiltration membranes often does not show an open pore structure nor a completely homogeneous gel layer. It consists of closely packed spheres of polymeric material with a diameter of about 50-200 nm. and is often referred to as a nodular structure[6].
The formation of a nodular structure can not be explained by nucleation of the polymer lean phase. It is also not very likely that nucleation of the polymer concentrated phase occurs because this only happens at initially low polymer concentrations, below the critical point. A possible explanation for the formation of a nodular structure could be that it is a result of spinodal demixing.

Spinodal demixing
In the spinodal region the homogeneous system is unstable. A nucleus of one of the binodal phases is not necessary to initiate phase separation. A theory of spinodal decomposition has been developed by Cahn[7]. Very small concentration fluctuations with a wavelength above a critical value will grow. Due to negative diffusion coefficients 'up-hill' diffusion takes place. This means that the amplitude of the wave grows, whereas the wavelength remains constant. Van Aartsen[8] showed that spinodal demixing can also occur in polymer solutions when quenched to a temperature below the spinodal temperature. Combining Cahn's theory of spinodal demixing and Debije's theory describing random concentration fluctuations in polymer solutions an expression for the fastest growing wavelength (D_m) was found:

$$D_m = \frac{2\pi l}{\sqrt{3\left(1 - \frac{T}{T_s}\right)}} \qquad 10)$$

The wavelength (D_m) is linearly related to the radius of gyration (l) of the polymer and is therefore dependent on molecular weight as well as on the

thermodynamic interaction between polymer and solvent. The wavelength decreases if the quenching temperature (T) is lowered, i.e. if the polymer solution is brought deeper inside the spinodal region. The spinodal temperature is dependent on the polymer concentration and is indicated by T_S. Smolders et al.[9] determined D_m for a 15 weight percent poly-2,6-dimethyl-1,4-phenylene oxide (PPO) solution in caprolactam. The radius of gyration is of the order of 20 nm. At an undercooling of 30°C below the spinodal temperature the calculated wavelength is D_m=260 nm.
According to Smolders et al.[9] the fast spinodal demixing process is followed by a slower phenomenon to reach the final equilibrium phases. At high quenching temperatures this could be measured, using dilatometry and electron microscopy. By dilatometric measurements it was found that a large change in volume occurring upon quenching is followed by a second volume effect on a longer time scale. Electron microscopy showed droplets of the polymer concentrated phase increasing in size with time. The ultimate structure is fairly uniform with a characteristic distance between the polymer rich regions.

Results

Hollow fibers were spun as described in the experimental setup of part A of this paper. The membrane morphology of the toplayer is shown in figure 5.
The surface top view (figure 5A) shows a bi-continuous structure which is typical for spinodal decomposition. Nodule size is estimated at about 50 nm. In the cross section (figure 5B) the structure at the surface is not very well visible. Nodular size increases from 50 nm (at 0.5 μm distance from the surface) to 100 nm (5 μm below the surface). Below the toplayers which are shown, the membranes have an open pore structure (not shown in this picture).
In figure 6 the cross section of a toplayer for moderate coagulation conditions is shown. The coagulation bath contained 60% of the solvent in the non-solvent. Therefore the non-solvent concentration gradient in the toplayer was much smaller. For this membrane nodule size is almost equal over the toplayer thickness. At the surface the nodules are more closely packed.

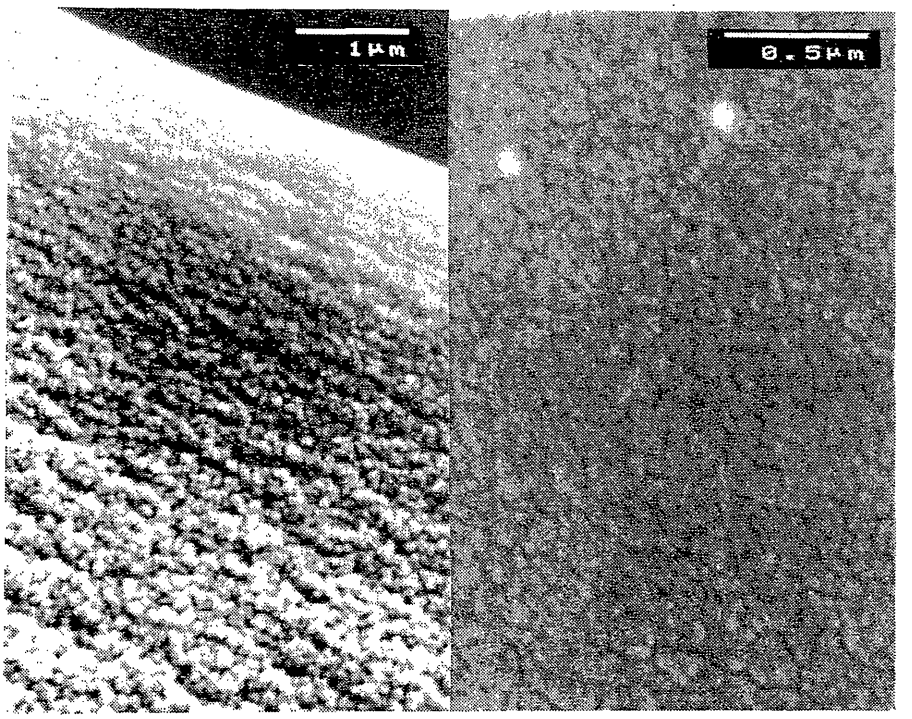

5a 5b

Figure 5; Scanning electron microscopic pictures of hollow fibers. A: surface view, B: cross section at the outside toplayer region. Concentration of poly(ether sulfone) was 17 weight%, concentration of poly(vinyl pyrrolidone) (Mw 360 kg/mole) was 13 weight%. After an airgap of 1.5 cm. the fiber was coagulated in a pure water bath of 26 °C.

Discussion

The nodular structure in ultrafiltration membranes formed by immersion precipitation resembles the structure obtained by quenching a polymer solution. This makes spinodal decomposition a reasonable mechanism for nodule formation. However, spinodal demixing can not be related to the membrane formation model of Reuvers et al.[1] The calculated composition paths can never cross the spinodal curve, because at these compositions the chemical potential gradients and fluxes are all zero. If we assume that for the extremely fast formation of ultrafiltration toplayers

concentration at the spinodal c_x = 20%. The fast mode binary diffusion coefficient for solvent and polymer as given by Tkacik[6] is used as the diffusion coefficient for non-solvent through the polymer network. The relaxation time of the network is t = 1 s. Then the penetration depth can be calculated as x=6μm. This means that a layer of 6μm will be in the spinodal region and can give a nodular structure. This is in agreement with the experimental results.
The wavelength of the fastest growing wave is dependent on the penetration depth into the spinodal region. The composition at the surface is the first to cross the spinodal and therefore will have proceeded further into the spinodal region. Here the wavelength will be smaller. In figure 5 it can be seen that indeed the nodular size is smallest at the surface and becomes larger going deeper into the membrane toplayer.

Quaternary systems
For a quaternary system with two high molecular weight components other conditions may also give rise to spinodal decomposition. In the previous part it has been described that the composition of the polymer solution can enter the spinodal region as long as the relaxation time of the polymer molecules has not elapsed. But the model, proposed in part A, for demixing of quaternary systems can explain the occurrence of spinodal demixing even after the relaxation time has elapsed.
For moderate coagulation conditions, e.g. if the coagulation bath contains a considerable amount of solvent, the diffusion processes are slower. As stated in part A on the short time scale the two polymers can be regarded as one and the relevant binodal is situated on the right hand side of the phase diagram close to the nonsolvent corner. Before this binodal is reached the relaxation time has elapsed and the two polymers can diffuse, but not with respect to each other. Once the two polymers can diffuse with respect to each other, the system gradually starts to react in agreement with the original quaternary binodal and spinodal curve situated more to the left in the phase diagram (see figure 3). From this moment, the compositions in the toplayer lie in the unstable region and spinodal demixing occurs rapidly, finally resulting in a nodular structure.
In figure 6 a nodular structure was formed with a coagulation bath that contained 60% solvent. Due to the smaller concentration difference the coagulation velocity is smaller and normally an open pore structure would be formed. However due to the addition of a second polymer phase separation is faster and a nodular structure is formed.

Conclusions from A and B

Macrovoid formation

It appears that the macromolecular nature of the additive is responsible for the suppression of formation of macrovoids. The reason is that the two polymers present in the same solution have to diffuse with respect to each other in order to phase separate. Since this process, for high enough molecular weight components, is much slower than low-molecular weight diffusion, two time scales are created.
The short time scale is responsible for the creation of a toplayer which has a high non-solvent content without demixing. These compositions are highly unstable in the longer time scale.
Delay of demixing in such a system is not possible anymore. Because the formation of macrovoids is closely connected to the phenomenon of delayed demixing, macrovoid formation is effectively hindered.

Nodular structures

It has been shown that the nodular structure appearing in the toplayer of ultrafiltration membranes is probably a result of spinodal demixing. Although the phase separation process is diffusion controlled there are two ways in which the composition of the polymer solution can cross the spinodal curve.

1 - In the first period of fast immersion processes solvent and non-solvent diffuse trough a "fixed" polymer network. Thermodynamics based on equilibrium states are not valid for these first moments after immersion. Compositions are reached which appear to lie in the spinodal region when polymer molecules become mobile and thermodynamics are valid again.

2 - For systems with a high molecular weight additive, in the first moments after immersion the binodal and spinodal curve are situated close to the non-solvent corner. Upon regaining the normal thermodynamic conditions (for the longer time scale) the compositions are found to lie definitely in the spinodal region of the real phase diagram.

List of Symbols

Units are between brackets.

c_x Concentration at place x (Part B) (kg m^{-3})

c_0 Concentration at the surface (Part B) (kg m^{-3})

c_1 Initial concentration in the film (Part B) (kg m^{-3})

c_i Concentration of component i (Part A) (kg m^{-3})

D_{ij} Binary diffusion coefficient of components i and j (m^2)

D_m Perturbation wavelength (m)

ΔG_m The enthalpy of mixing (J)

g_{ij} Concentration dependent Flory-Huggins interaction parameter between component i and j (-)

L_{ij} Diffusivity between components i and j; to be evaluated with the Stefan-Maxwell approach

l Radius of gyration (m)

m Modified spatial coordinate in the polymer solution;

$$m = \int_{\xi=0}^{\xi=x} \varphi_3 d\xi \quad , (m)$$

n_i Number of moles of component i (moles)

R Gas constant (J $mole^{-1}$ K^{-1})

R_{ij} Stefan-Maxwell friction coefficient between components i and j, found from binary diffusion data[1]

T Temperature (K)

T_s Spinodal temperature (K)

t Time (s)

v_i Specific volume of component i (m^3 kg^{-1})

$\bar{v}_i$ Velocity of component i (m s^{-1})

x Spatial coordinate originating from the interface, going into the polymer solution (m)

y Spatial coordinate originating from the interface, going into the coagulation bath (m)

μ_i Chemical potential of mixing of component i (equal to $\frac{\partial \Delta G_m}{\partial n_i}$) (J $mole^{-1}$)

φ_i Volume fraction of component i (-)

χ_{ij} Concentration independent Flory-Huggins interaction parameter between component i and j (-)

Literature

1. A.J. Reuvers, J.W.A. van den Berg, C.A. Smolders, J. Membrane Sci., **34** (1987) 45
   A.J. Reuvers, C.A. Smolders, J. Membrane Sci., **34** (1987) 67
2. L.Yilmaz, A.J. McHugh, J.Membrane Sci., **28** (1986) 287
3. I. Cabasso, E. Klein, J.K. Smith, J. Appl. Polym. Sci., **21** (1977) 165
   P. Aptel, N. Abidine, F. Ivaldi, J.P. LaFaille, J. Membrane Sci., **22** (1985) 199
   L.Y. Lafrenière, F.D.F. Talbot, T. Matsuura, S. Sourirajan,
   Ind. Eng. Chem. Res., **26** (1987) 2385
   T.A. Tweddle, O. Kutowy, W.L. Thayer, S. Sourirajan,
   Ind. Eng. Chem. Prod. Res. Dev., **22** (1983) 320
4. F. Altena, C.A. Smolders, Macromolecules, **15** (1982) 1491
5. L. Zeman, G. Tkacik, J.Membrane Sci., **36** (1988) 119
   G. Tkacik, L. Zeman, J.Membrane Sci., **31** (1987) 273
6. L. Broens, F.W. Altena, C.A. Smolders, Desalination, **32** (1980) 33
7. J.W. Cahn, J. Chemical Physics, **42** (1965) 93
8. J.J. van Aartsen, European Polymer Journal, **6** (1970) 919
9. C.A. Smolders, J.J. van Aartsen, A. Steenbergen, Kolloid-Z.u.Z.Polymere., **243** (1971) 14
10. K. Kimmerle, Quantitative Betrachtung des Phaseninversionsprozesses bei der Herstellung von Membranen, PhD-thesis, Stuttgart 1988
11. C. Cohen, G.B. Tanny, S. Prager, J.Polymer Sci., **17** (1979) 477
12. J. Crank, The Mathematics of Diffusion., 2nd ed., Oxford, 1975

Second Appendix to this Thesis

A Linearized Cloudpoint (LCP) Curve Correlation for Ternary Systems Consisting of One Polymer, One Solvent and One Nonsolvent

R.M. Boom, Th. van den Boomgaard, J.W.A. van den Berg, C.A. Smolders

Summary

A linear correlation function is found for cloudpoint composition curves of ternary systems consisting of one polymer, one solvent and one nonsolvent. The conditions for validity of this correlation function appear to be that the polymer is strongly incompatible with the nonsolvent, and that only liquid-liquid demixing occurs.

The linearized cloudpoint (lcp) curve is interpreted in terms of the various parameters occurring in the Flory-Huggins theory. The slope of the lcp line appears to be only dependent on the molar volumes of the components. Information about the binary Flory-Huggins interaction parameters and their concentration dependence can be obtained from the intercept of the linearized curve.

Cloudpoints induced by crystallization do not follow the correlation. This gives an opportunity to distinguish between crystallization and liquid-liquid demixing without any additional experiments.

Introduction

Membrane separation as a commercial separation process became practical after the introduction of the phase inversion technique for the preparation of synthetic membranes[1]. Membranes made by phase inversion usually have a very thin, selective top layer and a much thicker porous support.

Phase inversion basically consists of immersing a thin layer of a polymeric solution in a bath which contains a nonsolvent for the polymer. This nonsolvent should be miscible with the solvent present in the polymer solution. The immersion induces an exchange of solvent and nonsolvent between the coagulation bath and the polymer solution[2], by diffusion and convection. Due to these processes, the polymer solution becomes unstable, and phase separation results. In the

Submitted for publication to Polymer

polymer solution, a polymer lean phase forms droplets in an increasingly concentrating polymer rich matrix. The polymer lean droplets grow out to pores; the surrounding matrix eventually forms the solid membrane structure. The concentration profiles created during the diffusion processes may induce a profile in the pore sizes: near the coagulation bath pores are very small. Deeper inside the polymer solution pores are usually larger.

This process is controlled by diffusion kinetics and thermodynamic properties of the system. Knowledge of the thermodynamics of the system gives absolutely essential insight into the membrane structures possibly obtained by a particular system.

The most straightforward method to characterize the thermodynamics of a system is by measuring the cloudpoint curve. The cloudpoint curve is the curve that forms the border between the compositions that are completely stable, and the compositions that are meta- or unstable. In a truly ternary system (in which the polymer is monodisperse), the cloudpoint curve coincides with the binodal: the line that represents compositions that can be at equilibrium with one another.

In a quasi-ternary system (in which the polymer is polydisperse), the polymer becomes fractionated at equilibrium between the two phases[3]. The lower-molecular weight fractions have preference for the polymer lean phase, while the higher-molecular weight fractions are primarily dissolved in the polymer rich phase. This causes the polymer rich phases, in equilibrium with phases leaner in polymer, not to lie exactly on the binodal. The polymer lean phase will also not be located exactly on the binodal.

In a quasi-ternary system the cloudpoint curve represents those compositions which are at the onset of demixing: the demixing has not yet really taken place. The molecular weight distribution of the bulk has therefore not yet changed.

For a thorough theoretical treatment, not only the theory is very complicated, but also the amount of experimental work needed is large. One has to determine all the relevant interaction parameters, eventually also as a function of molecular weight. In practice, the differences between the binodal and the cloud point curves are not large, as long as no compositions near the critical point are considered[3]. This comes from the fact that for a membrane forming system, the polymer and the nonsolvent usually are very incompatible. The polymer lean phase is therefore very low in polymer concentration. The polymer stays completely in the polymer rich phase, and there is practically no change in the molecular weight distribution. For such a system it is possible to treat a quasi-ternary system as a truly ternary system. This simplifies the theory considerably.

For most ternary systems, the interaction parameters between solvent and nonsolvent, and between polymer and solvent can be easily determined from vapor pressure, osmotic pressure[4], or light scattering measurements[5]. The

interaction between polymer and nonsolvent is more difficult. The only experimental point one can obtain is the swelling value of the polymer in the nonsolvent. This is only one point, and it is not possible to find a concentration dependence of this interaction. Usually, one simply assumes an interaction parameter, after which the binodal is calculated[6]. When this calculated binodal is not too far from the experimental cloudpoints and equilibrium data, this value of the interaction parameter is assumed to be approximately correct.
For efficient scanning of the potentialities of membrane systems, it might be useful to have a relation that quickly yields information about the thermodynamics of a membrane forming system. Furthermore, in the fitting procedure mentioned before, one almost forgets the lower concentrations in the phase diagram: the polymer lean phases will be so poor in polymer that in a phase diagram they are effectively situated on the solvent-nonsolvent axis. This makes it impossible to discriminate between weight fractions of e.g. 10^{-3} and 10^{-5}. The full potential of experimental data will therefore not be used to obtain the right polymer-nonsolvent interaction parameter.
The conclusion is that it might be useful to have a representation of cloudpoints that does not have this disadvantage, and which can be useful in the quick interpretation of cloudpoints.

Simple explicit relations for cloudpoint curves in ternary systems.

Craubner[7] derived from perturbation thermodynamics a relation that described the cloudpoint curve for systems dilute in polymer (less than 1 weight percent polymer):

$$\phi_1 = b \ln\phi_3 + a \qquad 1)$$

in which ϕ_1 and ϕ_3 are the weight fractions of nonsolvent (1) and polymer (3), respectively.
This relation indeed holds only for dilute systems. This limits the usefulness of this equation, because for membrane formation also the more concentrated region (up to 40 - 50 weight% polymer) is important.
Another relation was proposed by Li et al.[8]. He observed that for systems with more than 10 weight% polymer, the ratio between the concentrations of solvent and nonsolvent appears to be constant. In formula,

$$\phi_1 = b\,\phi_2 \qquad 2)$$

As can be seen in figure 2, the relation is approximately valid for high concentrations of polymer, but when the critical point is approached (near 9 weight% of polymer), the experimental points deviate sharply form the line.

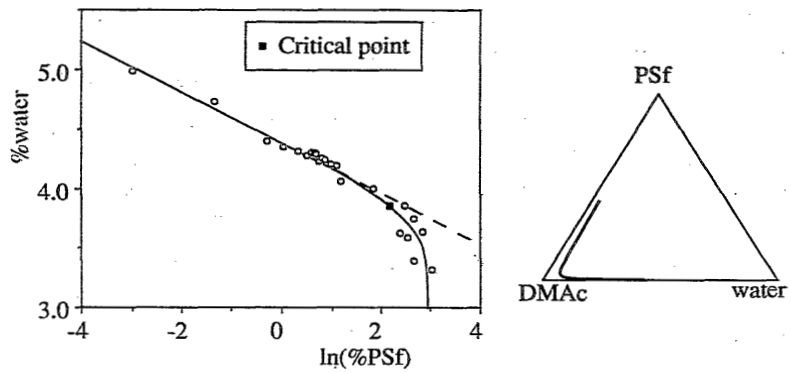

Figure 1: Cloudpoints for the system poly (sulfone) (PSf) - dimethyl acetamide (DMAc) - water, as measured by Li et al.[8], at 20°C, plotted according to the Craubner relation 1).

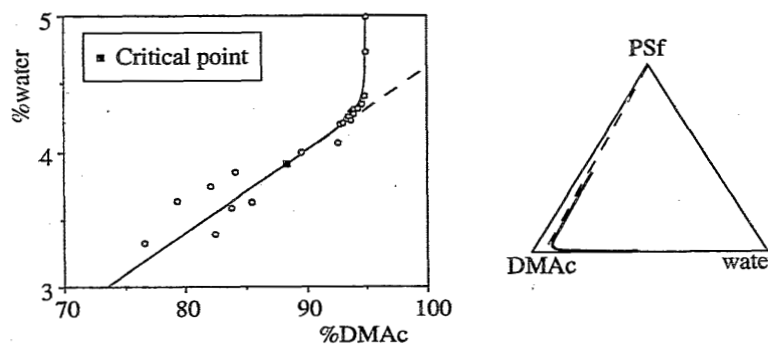

Figure 2: The same cloudpoints as in figure 1, for the system poly (sulfone) (PSf) - dimethyl acetamide (DMAc) - water, as measured by Li et al.[8], at 20°C, plotted according to the Li relation.

An early review of relations meant for all types of ternary systems was made by by Hand[9]. One of the relations describes the 'dineric distributrion', i.e. the distribution of one component, soluble in two phases:

$$\ln \frac{\phi_2'}{\phi_1'} = b \ln \frac{\phi_2''}{\phi_3''} + a \qquad 3)$$

in which ϕ_i signifies the weight fraction of component i. Components 1 and 3 are incompatible; component 2 is miscible with the other two components. The indices ' and " represent the two phases in equilibrium with one another. In fact, this relation can be applied to a demixed, two-phase equilibrium, consisting of a polymer (3), a solvent (2) and a nonsolvent (1). For its verification one needs to measure the equilibrium distribution of component 2 over the two phases, containing mainly component 1, and component 3, respectively.
The linearized cloudpoint (lcp) correlation that is proposed here is closely related to the relation that Hand describes. In our case it correlates the concentrations in any single phase that is on the verge of demixing (the cloudpoints).

$$\ln\frac{\phi_1}{\phi_3} = b\ln\frac{\phi_2}{\phi_3} + a \qquad 4)$$

Here again, the ϕ_i's are the weight fractions; a and b are constants, to be determined experimentally. This relation does not describe a dineric ditribution, but describes the compositions of a single phase at the border between stability and instability, which are easier experimentally determined. For truly ternary systems, these points give the binodal curve; for quasi-ternary membrane forming systems, the binodal curve is approximated. Figure 3 shows the relation for a particular system. In this lcp relation, there are two parameters: the slope (b) and the intercept (a). Figure 4 shows the dependence of the (mathematical) line on these parameters.

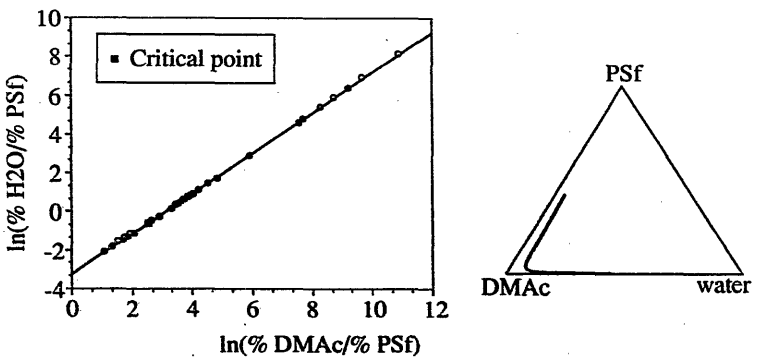

Figure 3: The same cloudpoints as figures 1 and 2, for the system poly (sulfone) (PSf) - dimethylacetamide (DMAc) - water, as measured by Li et al.[8], at 20°C, plotted according to the lcp relation 4).

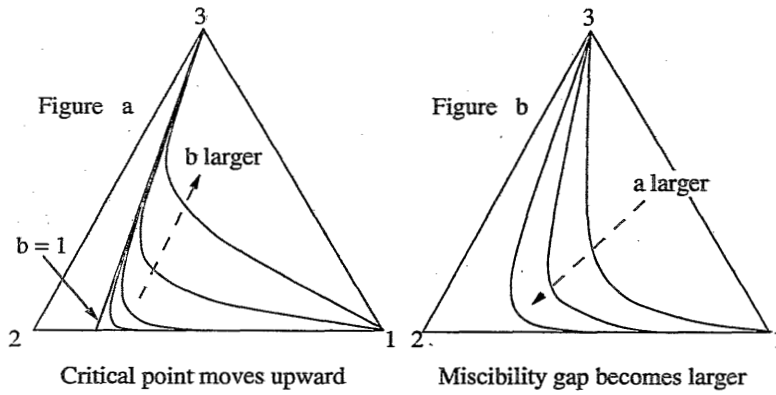

Figure 4: The lcp relation, with varying intercept (a, figure 4a) and varying slope (b, figure 4b)

Verification of the relation.

In figures 5 and 7 a number of systems are represented which are commonly used as membrane forming systems. The cloudpoints represented (from literature and our laboratory) vary over many decades of polymer concentrations, typically from 10^{-3} to 50 weight% of polymer. Since the critical point is usually between 5 and 10 weight% polymer, the relation holds for both sides of the binodal. The relation is following the experimental data over the full concentration range.

In all cases, the slope of the line is somewhat larger than one, while the intercept of the line varies with the system.
It has to be borne in mind that, in the ternary phase diagram, the lcp relation always originates in the point of pure polymer. Since all polymers swell in nonsolvents to a certain extend, the relation is only an approximation. Figure 6 demonstrates this point. The fact that there seems to be no deviation from the line at higher polymer concentrations becomes even more remarkable by this.
During membrane formation, not only liquid-liquid demixing is important. Many polymers tend to crystallize more or less slowly in solution. Although the structure of the membrane formed by phase inversion will usually be controlled by fast liquid-liquid demixing, crystallization can be very important for highly crystalline polymers which rapidly crystallize.

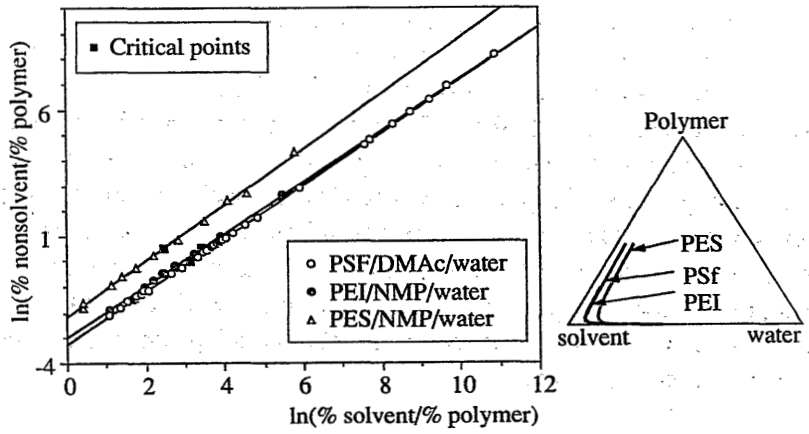

Figure 5: poly (sulfone) (PSf) - dimethyl acetamide (DMAc) - water (from Li[8]), poly (ether sulfone) (PES) - n-methyl pyrrolidone (NMP) - water (from Tkacik et al.[10]), and poly (ether imide (PEI) - n-methyl pyrrolidone (NMP) - water (from Roessink[11]). All cloudpoints were measured at 20°C.

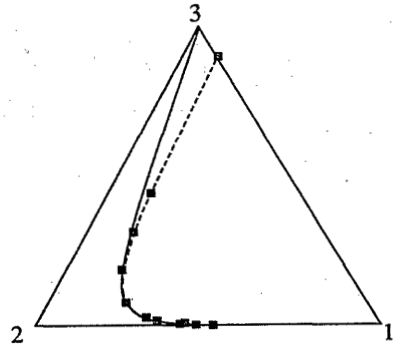

Figure 6: the lcp relation always crosses two corners of the ternary phase diagram. Experimental points usually go to a point of a few percent nonsolvent in the polymer. For matter of clarity, the deviations of the experimental points are exaggerated.

Especially in the more concentrated surface region during phase inversion, crystallization may compete with liquid-liquid phase separation, and therefore determine the separation properties of the ultimate membrane.
During cloudpoint measurement, crystallization is usually very difficult to distinguish from liquid-liquid demixing. In figure 7, cloudpoints are given for

the crystallizable polymer cellulose acetate. To measure the cloudpoints, the polymers solutions were slowly cooled, while the light transmittance through the solution was measured. The temperature at which the transmittance starts to decrease is called the cloudpoint. The occurrence of crystallization was controlled by measuring the cooling rate dependence of the cloudpoint temperatures. At low cooling rate there was a definite cooling rate dependence; at higher cooling rates the rate dependence disappeared. The 'real' liquid-liquid demixing cloudpoint was defined as that cloudpoint where this dependence disappeared. This is based on the observation that for cellulose acetate crystallization is much slower than liquid-liquid demixing. Figure 7 shows that for a crystallizable system, these 'real' liquid-liquid demixing cloudpoints still follow the lcp relation, as observed for completely amorphous systems.

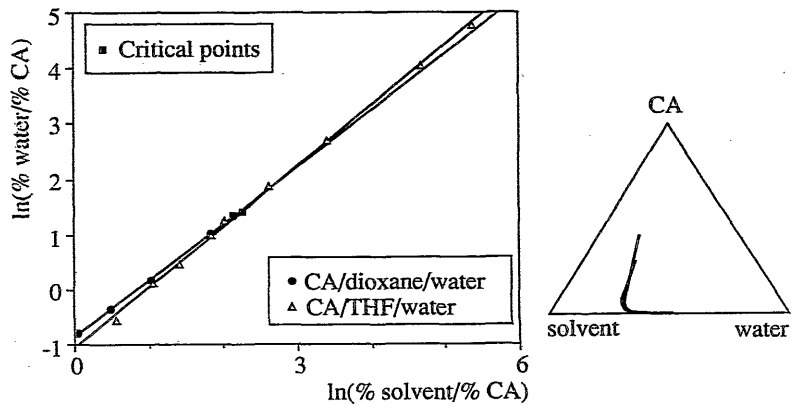

Figure 7: Cloudpoint curves for the system cellulose acetate - tetra hydro furane - water[12], in the ternary phase diagram and in the lcp form. The solvents are respectively tetra hydro furane and acetone.

In figure 8, a system is given in which crystallization is fast and plays a more dominant role. The polymer is poly (dimethyl phenylene oxide), solvent is trichloro ethylene, and the nonsolvent is a mixture of a strong solvent (methanol) and a weak nonsolvent (octanol). The part with lower polymer concentrations (the right hand part in the lcp plot) gives a set of straight lines, all with approximately the same slope, but for each methanol/octanol ratio a different intercept is found. For the system with pure methanol as nonsolvent, i.e. the strongest nonsolvent, the intercept is the smallest. With only octanol as nonsolvent, the largest intercept is obtained (i.e. the smallest liquid-liquid demixing gap).

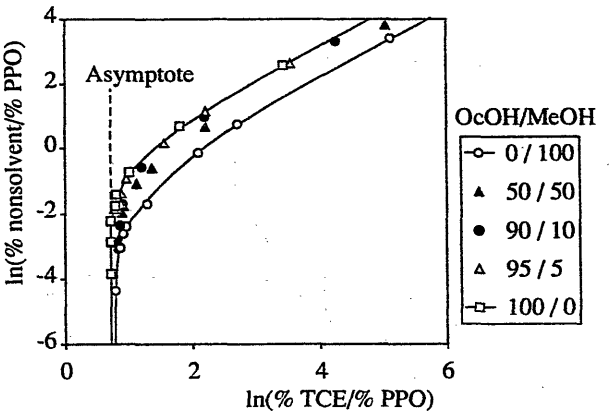

Figure 8: Cloudpoint curves for poly (dimetgyl phenylene oxide) - trichloro ethylene - nonsolvent, in which the nonsolvents are a mixture of methanol and octanol (data from Wijmans[12]). The weight ratio of methanol to octanol was varied.

The part with higher polymer concentrations (the left side of the figure) gives crystallization. For the highest polymer concentrations, which is for low nonsolvent concentrations, the cloudpoint curves converge to the same vertical line. This line extrapolates to the crystallization point of PPO in trichloro ethylene, which is independent of the nonsolvent.
It should be noted that the experimenters[12] observed cooling rate dependence of the cloud points for the higher polymer concentrations, which agrees with the assumption that the 'deviating' cloudpoints are crystallization points. The same followed from differential scanning colorimetry measurements, and pulse induced critical scattering (PICS) measurements by the same authors.
In this way the lcp curve might give a crude but quick way to distinguish between crystallization and liquid-liquid demixing.

For non-polymeric systems, the relation does not seems to hold as nicely as for the systems discussed so far. It appears from figure 9, in which the system water (1) - methanol (2) - diethyl ether (3) is represented, that not a very straight line is obtained. It must be concluded that for non-polymeric systems, the lcp relation is not applicable.

It is interesting to consider a system of two incompatible polymers and a mutual solvent. The nonsolvent here is one of the polymers. Of course, in this case the system is not 'membrane forming' anymore.

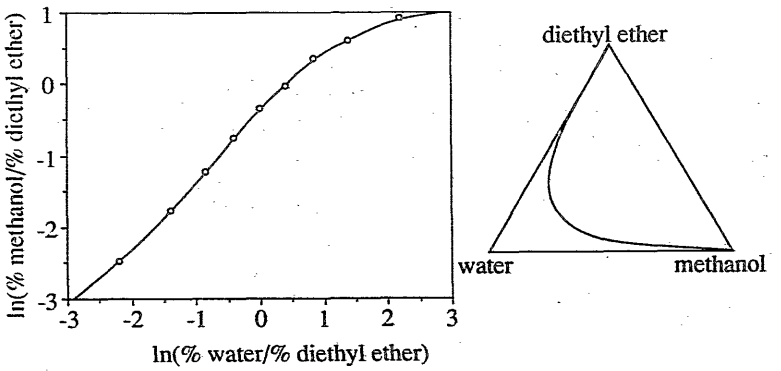

Figure 9: lcc-plot for a low molecular weight system. The two immiscible components are here diethyl ether and water, the "solvent" is methanol. It appears that not a very straight line is obtained. It must be concluded then that the lcc is not applicable to systems without a polymer.

Figure 10 shows the system poly (iso butylene) (1) - toluene (2) - poly (styrene) (3), as measured by v.d. Esker [13]. It appears that the lcp curve is applying reasonably well, when considering the experimental difficulties in obtaining these cloudpoints. The slope here is much larger than one, which agrees with the fact that the critical point is not in the neighbourhood of the toluene/polystyrene axis in the ternary phase diagram.

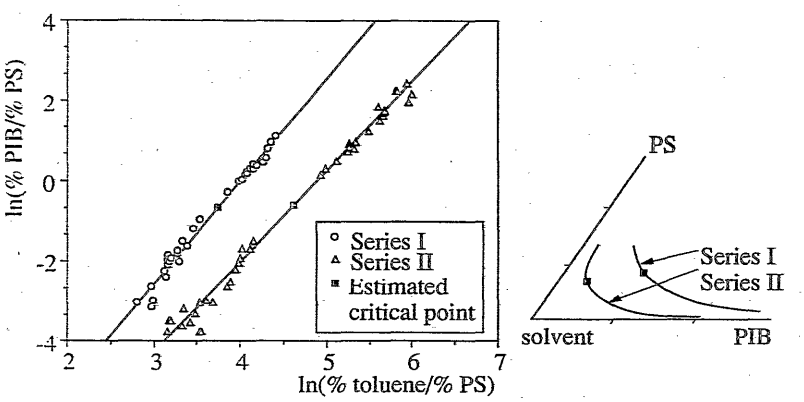

Figure 10: lcp-plot for the system poly (styrene) (3) - toluene (2) - poly (isobutylene) (1), for two systems with different molecular weights: system one: MW_{PS} = 194, MW_{PIB} = 156 kg/mole, and system two: MW_{PS} = 526, MW_{PIB} = 670 kg/mole.

The lcp relation therefore could be useful in gathering information about the interaction between two incompatible polymers. This, however, should be investigated more carefully in future work.

Interpretation of the lcp relation

The lcc relation as was proposed,

$$\ln\frac{\phi_1}{\phi_3} = b \ln\frac{\phi_2}{\phi_3} + a \qquad 4)$$

has two parameters, the slope, b, and the intercept, a. From figure 3, it is clear that the slope could give information about the situation of the critical point in the phase diagram.
For the slope, b, one limiting case is a value of one. This value represents a straight line through the phase diagram. Such a cloudpoint curve would be found for a hypothetical system in which the polymer has infinite molecular weight. In this case, the critical point is situated on the solvent-nonsolvent axis. The other extremum, a rather low molecular weight of the polymer introduces a slope which is larger. A large value of b suggests a critical point near the middle of the binodal curve in the phase diagram.
The intercept a appears to dictate the area covered by the demixing gap (see figure 3), which is mainly governed by enthalpic effects. One would therefore expect that the slope gives only entropic information (the molecular volumes), and that the intercept gives information about enthalpic effects (the g_{ij}'s). The interesting fact about the lcp relation seems to be a decoupling of enthalpic and entropic effects.
To investigate this further, we try to interpret the lcp relation according to the Flory-Huggins theory.
The Flory-Huggins equation gives the free enthalpy of mixing as a function of the concentration of the components. From this equation, the slope and the intercept of the lcp line can be obtained, under the assumption that the line is applicable. This does not follow from the Flory-Huggins interpretation, as should be expected: not for all ternary systems the relation should be valid (see figure 9).
The slope is a function of the molar volumes,

$$b = \frac{v_1 - v_3}{v_2 - v_3} \qquad 5)$$

while the intercept a contains the Flory-Huggins interaction parameters:

$$a = \frac{1}{2}\left\{ \left(g_{12} + g'_{12}\right)\left(-v_2\, b\, \phi_1 + v_1\, \phi_2\right) + g_{13}\left(v_1\, \phi_3 - v_3\,(1\text{-}b)\,\phi_1\right) + \left(g_{12} + g'_{12}\right)\left(-v_2\, b\, \phi_3 + v_3\,(1\text{-}b)\,\phi_2\right) \right\} \qquad 6)$$

In these relations, the following symbols occur:

ϕ_i	volume fraction of component i
v_i	molar volume of component i, in m^3/mole
b	$\frac{v_1 - v_3}{v_2 - v_3}$
g_{ij}	Flory-Huggins interaction parameter between components i and j, usually concentration dependent (no unit)
g_{12}'	derivative of the interaction parameter g_{12}: $u_2(1\text{-}u_2)\frac{\partial g_{12}}{\partial u_2}$
g_{23}'	derivative of the interaction parameter g_{23}: $v_2(1\text{-}v_2)\frac{\partial g_{23}}{\partial v_2}$
u_2	$\phi_2/(\phi_2+\phi_1)$
v_2	$\phi_2/(\phi_2+\phi_3)$

7)

The intercept is a simple relation in the volume fractions and the interaction parameters. Interesting is that the interaction parameters themselves, g_{ij}, and their derivatives, g_{ij}', are taken together as one parameter.
The slope b only contains entropic parameters. Systems with a polymer with a high molecular weight has a slope just larger than one. Systems in which the polymer molecular weight is lower have a larger slope.
The intercept a contains the interaction parameters, together with molar volumes. Apparently, the enthalpic interactions are completely taken into account by the intercept.
Information about the interaction parameters can be obtained directly from the value of the intercept a, via relation 6. The lcp is an explicit relation for a cloudpoint (binodal) curve in a ternary membrane forming system. From the Flory-Huggins theory it is not possible to obtain an explicit relation for the binodal. It appears now that such a relation does exist for certain systems. This relation holds only when the lcp - plot holds, i.e. when the interaction parameter between the polymer and the nonsolvent is high, and when only liquid-liquid demixing occurs.

We can draw the cloudpoint curve as interpreted from the Flory-Huggins theory in the lcp - plot. An example of this is given in figure 11.

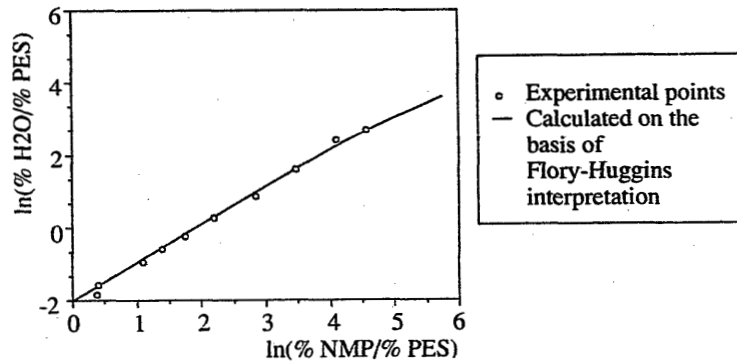

Figure 11: lcc-plot for the system poly (ether sulfone) - n-methyl pyrrolidone - water, and the line as given by the derived slope b and intercept a. The interaction parameters used here are: $g_{12}=0.718+0.669u_2$; $g_{23}=0.290+0.501v_2$ (values taken from Tkacik et al[10]). The polymer-nonsolvent interaction parameter g_{13} is used as a fitting parameter. The optimal value found was 3.6. The variables u_2 and v_2 are defined in the appendix and in the list of symbols.

Results and discussion on slopes and intercepts

1. Amorphous systems with low polymer-nonsolvent interaction

For membrane forming systems, the lcp curve always gives a slope slightly larger than one. It is possible to express the cloudpoint curve as a simple function of the interaction parameters (see figure 11). The slope is independent of the interaction parameters, and is only dependent on the molar volumes. Table 1 gives some of the slopes of the systems previously shown in figure 5.

System	*Experimental slope*	*Theoretical slope*
PSf	1.04	1.002
PEI	1.02	1.003
PES	1.10	1.04

Table 1: the slopes of the lcp -plots shown in figure 1. The slopes agree reasonably well, when the polydispersity of the polymers in practice is considered.

The experimental values agree reasonable well with the values calculated, considering that the polydispersity of the polymer is neglected in our Flory-Huggins interpretation.
In principle, for these types of systems it should be possible to determine a whole cloudpoint curve by simply measuring two points (when the theoretical slope is assumed, even one cloudpoint would suffice). In practice, a few cloudpoints should be enough to check the validity of the relation. From these few measurements, immediate information is then found for the interaction parameters. From figure 11 it appears that the experimental cloudpoints can be approached using independently measured interaction parameters g_{12} and g_{23}. In this figure, the polymer-nonsolvent interaction parameter g_{13} is used as a 'fitting parameter'. Tkacik et al.[10] assumed a value of 1.5 for this parameter, by fitting their binodal on their experimental points. In figure 11, we find a value of 3.6, which is in better agreement with swelling data for the polymer in the nonsolvent. This example shows, that the lcp-plot offers a better basis for such fitting procedures, simply because each experimental cloudpoint obtains the same weight in the fitting procedure.

2. *Systems with crystallizable polymers*

It appears that even for systems with crystallizable polymers, the liquid-liquid demixing points follow the lcp relation. When crystallization occurs predominantly, the cloud points deviate from the lcp line. The deviating points converge to a vertical asymptote (the crystallization point of the polymer in the solvent). This deviation might offer a quick method to see whether a certain system exhibits crystallization phenomena.
The proposed relation is only applicable under certain conditions. These conditions should always be considered before starting any interpretation. It appears that for applicability of the lcp relation, the swelling value of the polymer in the nonsolvent must not be too large. For systems which exhibit crystallization, the crystallization phenomena might influence measurement of that swelling value of the polymer in the nonsolvent that is due solely to liquid-liquid demixing.
The crystallization process is usually several orders of magnitude slower than liquid-liquid demixing. Investigation of the dependence of the cloudpoint curve on the cooling rate of the samples (when thermal demixing is used) is therefore a suitable tool after deviation from the lcp line showed that crystallization might be present.

Conclusions

A linearized cloud point correlation is proposed that gives very good experimental results in membrane forming systems:

$$\ln\frac{\phi_1}{\phi_3} = b \ln\frac{\phi_2}{\phi_3} + a \qquad 4)$$

The plot gives straight experimental lines as long as two conditions are satisfied:

- The polymer and the nonsolvents should have poor interaction (high g_{13} interaction parameter, low swelling value of the polymer in the nonsolvent)
- The polymer should be completely miscible in the solvent in all possible concentrations; the same should apply to the solvent and the nonsolvent .

The lcp relation only describes a cloudpoint curve caused by liquid-liquid demixing. Whenever other demixing (crystallization) effects play a role, a more or less sharp deviation of the lcp line is found.
The simplicity of the relation brings about its usefulness for an quick evaluation of a ternary membrane forming system. Only two parameters have to be determined: the intercept of the line and the slope. The slope is not completely unknown, because for membrane forming systems the slope of the line is always slightly larger than one. It should therefore be enough to determine a few cloudpoints (ideally only one, because the slope could be calculated) for characterization of the complete cloudpoint curve.
The relation has advantages for the estimation of the polymer-nonsolvent interaction parameter from the cloud point curve itself: all experimental cloud points are weighed in the same way, therefore giving a better estimate of this interaction parameter. The relation could also be useful when investigating blends of immiscible polymers with a common solvent. The relation could, after measurement of a few cloudpoints in the dilute region, give fast information for these systems, over a broader concentration range.

Literature

1. S. Loeb, S. Sourirajan, Adv. Chem. Ser. 38 (1962) 117
2. A.J. Reuvers, A.J. Reuvers, J.W.A. van den Berg, C.A. Smolders, J. Membrane Sci., 34 (1987) 45
3. R. Koningsveld, R. Koningsveld, A.J. Staverman, J. Polym. Sci., Part A-2, 6 (1968) 305

4. F. Altena, Phase separation phenomena in ternary cellulose acetate solutions; relation to membrane formation, PhD thesis, University of Twente, The Netherlands, 1984
5. Th.G. Scholte, Eur. Polym. J., 6 (1970) 1063
6. F.W. Altena, C.A. Smolders, Macromolecules, 15 (1982) 1491
7. H.Craubner, Macromolecules, 11(6) (1978) 1161
8. Li Shuguang, J. Chengzang, Z. Yunqi, Desalination, 62 (1987) 79
9. D.B. Hand, Dineric Distribution, J. Phys. Chem., 34 (1930) 1961
10. Tkacik, Zeman, J. Membrane Sci., 36 (1988) 119
11. H.D.W. Roesink, Microfiltration, membrane development and module design, PhD thesis, University of Twente, The Netherlands, 1990
12. J.G. Wijmans, H.J.J. Rutten, C.A. Smolders, J. Polym. Sci. Polym. Phys. Ed. 23 (1985) 1941
13. M.W.J. v.d. Esker, Incompatibility of two polymers in a single solvent, PhD thesis, University of Utrecht, The Netherlands, 1975

Appendix

Derivation of the slope (b) and the intercept (a)

The Flory-Huggins theory gives the free enthalpy of mixing for a ternary system as a function of the concentrations:

$$\frac{\Delta G_m}{RT} = n_1 \ln \phi_1 + n_2 \ln \phi_2 + n_3 \ln \phi_3 + \left(v_1 g_{12} n_1 \phi_2 + v_1 g_{13} n_1 \phi_3 + v_2 g_{23} n_2 \phi_3 \right) \qquad \text{A1)}$$

in which n_i and ϕ_i are respectively the number of moles and the volume fraction of component i. With component number 1 is meant the nonsolvent, number 2 is the solvent and 3 is the polymer. The quantity v_i is the molar volume (in m^3/mole) of component i. The g_{ij}'s are the Flory-Huggins interaction parameters, which are a measure of the enthalpic interaction between components i and j. They are usually not constant, but functions of the concentrations of all the components present. In most cases, it is possible to assume that g_{ij} is only dependent on the concentrations of i and j, and not of the other component present. This means formally:

$$g_{12} = g_{12}(u_2); \quad u_2 = \frac{\phi_2}{\phi_1 + \phi_2}$$
$$g_{23} = g_{23}(v_2); \quad v_2 = \frac{\phi_2}{\phi_2 + \phi_3} \qquad \text{A2)}$$

The interaction parameter g_{13} is assumed to be independent of the concentrations. The chemical potentials of mixing $\Delta\mu_i$ can now be derived by differentiating with respect to the number of moles of each component:

$$\frac{\Delta\mu_1}{v_1 RT} = \frac{\ln\phi_1}{v_1} - \frac{\phi_1}{v_1} - \frac{\phi_2}{v_2} - \frac{\phi_3}{v_3} - \frac{1}{v_1} + \left(g_{12}\phi_2 + g_{13}\phi_3 \right)\left(1 - \phi_1 \right) - g_{23}\phi_2\phi_3 - \phi_2 g_{13}'$$
$$\frac{\Delta\mu_2}{v_2 RT} = \frac{\ln\phi_2}{v_2} - \frac{\phi_1}{v_1} - \frac{\phi_2}{v_2} - \frac{\phi_3}{v_3} - \frac{1}{v_2} + \left(g_{12}\phi_1 + g_{23}\phi_3 \right)\left(1 - \phi_2 \right) - g_{13}\phi_1\phi_3 + \phi_1 g_{13}' + \phi_3 g_{23}' \qquad \text{A3)}$$
$$\frac{\Delta\mu_3}{v_3 RT} = \frac{\ln\phi_3}{v_3} - \frac{\phi_1}{v_1} - \frac{\phi_2}{v_2} - \frac{\phi_3}{v_3} - \frac{1}{v_3} + \left(g_{23}\phi_2 + g_{13}\phi_1 \right)\left(1 - \phi_3 \right) - g_{12}\phi_1\phi_2 - \phi_2 g_{23}'$$

The derivatives of the composition dependent interaction parameters g_{ij}' are defined

as:

$$g_{12}' = u_2 (1 - u_2) \left(\frac{\partial g_{12}}{\partial u_2} \right); \qquad g_{23}' = v_2 (1 - v_2) \left(\frac{\partial g_{23}}{\partial v_2} \right) \tag{A4}$$

Two linear combinations of the chemical potentials are calculated. The following two relations result when the logarithmic terms are isolated at the left sides of the equality signs.

$$\begin{aligned} \frac{\ln\left(\frac{\phi_1}{\phi_2}\right)}{v_1 - v_2} = \left\{ \frac{\Delta\mu_1 - \Delta\mu_2}{(v_1 - v_2) RT} \right\} - \sum_1^3 \frac{\phi_i}{v_i} + \frac{1}{v_1 - v_2} \Big\{ & g_{12} (v_1 \phi_2 (1 - \phi_1) - v_2 \phi_1 (1 - \phi_2)) \\ & - g_{12}' (v_1 \phi_2 - v_2 \phi_1) \\ & + g_{13} (v_1 \phi_3 (1 - \phi_1) + v_3 \phi_1 \phi_3) \\ & + g_{23} (- v_1 \phi_2 \phi_3 - v_2 \phi_3 (1 - \phi_2)) - g_{23}' v_2 \phi_3 \Big\} \\ \frac{\ln\left(\frac{\phi_3}{\phi_2}\right)}{v_3 - v_2} = \left\{ \frac{\Delta\mu_3 - \Delta\mu_2}{(v_3 - v_2) RT} \right\} - \sum_1^3 \frac{\phi_i}{v_i} + \frac{1}{v_3 - v_2} \Big\{ & g_{23} (v_3 \phi_2 (1 - \phi_3) - v_2 \phi_3 (1 - \phi_2)) \\ & - g_{23}' (v_3 \phi_2 - v_2 \phi_3) \\ & + g_{13} (v_1 \phi_3 (1 - \phi_1) + v_2 \phi_1 \phi_3) \\ & + g_{13} (- v_3 \phi_2 \phi_1 - v_2 \phi_1 (1 - \phi_2)) - g_{12}' v_2 \phi_1 \Big\} \end{aligned} \tag{A5}$$

From these expressions, it follows by substracting the equations that

$$\begin{aligned} & \frac{1}{v_1 - v_2} \ln \frac{\phi_1}{\phi_2} - \frac{1}{v_3 - v_2} \ln \frac{\phi_3}{\phi_2} = \left\{ \frac{\Delta\mu_1 - \Delta\mu_2}{(v_1 - v_2) RT} - \frac{\Delta\mu_3 - \Delta\mu_2}{(v_3 - v_2) RT} \right\} + \\ & (g_{12} + g_{12}') (\alpha \phi_1 + \beta_1 \phi_2) + g_{13} (\beta_1 \phi_3 - \beta_3 \phi_1) + (g_{12} + g_{12}') (\alpha \phi_3 + \beta_3 \phi_2) \end{aligned} \tag{A6}$$

in which

$$\begin{aligned} b = \frac{v_3 - v_1}{v_3 - v_2}; \qquad \alpha = \frac{v_2}{v_3 - v_2} \left(\frac{b}{b - 1} \right); \\ \beta_1 = \frac{v_1}{v_1 - v_2}; \qquad \beta_3 = \frac{v_3}{v_3 - v_2} \end{aligned} \tag{A7}$$

For two compositions in equilibrium with each other, the chemical potential of each component in the one phase must be equal to the chemical potential in the other phase.

$$\Delta\mu_i^{\text{one phase}} = \Delta\mu_i^{\text{other phase}} \quad \text{for all i's} \tag{A9}$$

This then also applies to a linear combination of these chemical potentials. When the difference over the two phases is considered, the difference of a linear combination of the chemical potentials over the two phases is zero:

$$\left\{ \frac{\Delta\mu_1 - \Delta\mu_2}{(v_1 - v_2)RT} - \frac{\Delta\mu_3 - \Delta\mu_2}{(v_3 - v_2)RT} \right\}^{\text{one phase}} = \left\{ \frac{\Delta\mu_1 - \Delta\mu_2}{(v_1 - v_2)RT} - \frac{\Delta\mu_3 - \Delta\mu_2}{(v_3 - v_2)RT} \right\}^{\text{other phase}} \qquad \text{A10)}$$

From equation A6, we obtain with this:

$$\Delta\left\{ \frac{1}{v_1 - v_2} \ln\frac{\phi_1}{\phi_2} - \frac{1}{v_3 - v_2} \ln\frac{\phi_3}{\phi_2} \right\} =$$

$$\Delta \left\{ \begin{array}{l} (g_{12} + g_{12}')(\alpha\,\phi_1 + \beta_1\,\phi_2) \\ + g_{13}(\beta_1\,\phi_3 - \beta_3\,\phi_1) \\ + (g_{12} + g_{12}')(\alpha\,\phi_3 + \beta_3\,\phi_2) \end{array} \right\} \qquad \text{A11)}$$

in which the deltas indicate the difference of the quantity between brackets over the two phases in equilibrium. Multiplication with a factor v_1-v_2, and rearrangement of both sides of the equation gives:

$$\Delta\left\{ \ln\frac{\phi_1}{\phi_3} - b \ln\frac{\phi_2}{\phi_3} \right\} =$$

$$= \Delta \left\{ \begin{array}{l} (g_{12} + g_{12}')(-v_2\,b\,\phi_1 + v_1\,\phi_2) \\ + g_{13}(v_1\,\phi_3 - v_3(1 - b)\,\phi_1) \\ + (g_{12} + g_{12}')(-v_2\,b\,\phi_3 + v_3(1 - b)\,\phi_2) \end{array} \right\} \qquad \text{A12)}$$

in which b is:

$$b = \frac{v_1 - v_3}{v_2 - v_3} \qquad \text{A13)}$$

As we can see in practice that the lcc-plot gives a straight line, apparently the difference term at the right side of the equal sign is zero. When this difference would not be zero, we would not obtain a straight lcp line.

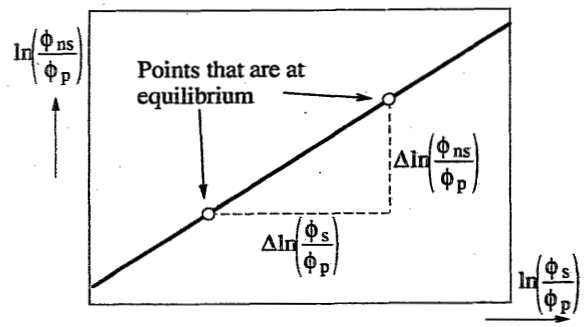

Figure A1: An lcp line on which two points are located which are in equilibrium with one another. The chemical potentialsof all comonents in the two phases must be equal.

The difference over the two phases in equilibrium of the quantity in equation A11,

$$\begin{aligned}&(g_{12}+g_{12}')(-v_2\,b\,\phi_1+v_1\,\phi_2)\\&+g_{13}(v_1\,\phi_3-v_3(1-b)\,\phi_1)\\&+(g_{12}+g_{12}')(-v_2\,b\,\phi_3+v_3(1-b)\,\phi_2)\end{aligned}\qquad A14)$$

must be zero. This indicates that the quantity itself must be constant over the lcp line.
This can be clarified by considering some line, described by

$$y = bx + a \qquad A15)$$

Rewriting this to

$$y - bx = a \qquad A16)$$

gives a formula comparable to A11:

$$\Delta(y - bx) = \Delta a \qquad A17)$$

For each point, it follows now that the parameter a must be constant. Its value can be evaluated by not taking the difference, but the sum over the two phases:

$$\sum^{\text{two phases}} (y - bx) = \sum^{\text{two phases}} a \qquad A18)$$

The value of a is the part of equation A17 right from the equality sign, divided by 2. This is then also applied to quation A11:

$$\sum_{\text{phases}}^{\text{two}} \left\{ \ln\frac{\phi_1}{\phi_3} - b \ln\frac{\phi_2}{\phi_3} \right\} =$$

$$\sum_{\text{phases}}^{\text{two}} \left\{ \begin{array}{l} (g_{12} + g_{12}')(-v_2 b \phi_1 + v_1 \phi_2) \\ + g_{13}(v_1 \phi_3 - v_3(1-b)\phi_1) \\ + (g_{12} + g_{12}')(-v_2 b \phi_3 + v_3(1-b)\phi_2) \end{array} \right\} \qquad \text{A19)}$$

It appears that the intercept a can be written out as:

$$a = \frac{1}{2} \left\{ \begin{array}{l} (g_{12} + g_{12}')(-v_2 b \phi_1 + v_1 \phi_2) \\ + g_{13}(v_1 \phi_3 - v_3(1-b)\phi_1) \\ + (g_{12} + g_{12}')(-v_2 b \phi_3 + v_3(1-b)\phi_2) \end{array} \right\} \qquad \text{A20)}$$

which is an explicit relation for the intercept a in the interaction parameters and the molar volumes.

It should be noted that when for the chemical potentials (equations A3) the enthalpic parts (the terms with the g_{ij}'s) would be replaced by one single constant for each chemical potential, the lcp line would immediately follow from this Flory-Huggins interpretation.

List of symbols

n_i	number of moles of component i (moles); 1 = nonsolvent, 2 = solvent and 3 = polymer
ϕ_i	weight or volume fractions (-)
v_i	molar volumes, in (m^3/mole)
b	slope of the lcc plot, given by $(v_3-v_1)/(v_3-v_2)$ (-)
a	intercept of the lcc plot (-)
g_{ij}	Flory-Huggins interaction parameter between components i and j, usually

	concentration dependent (-)
u_2	$\phi_2/(\phi_2+\phi_1)$
v_2	$\phi_2/(\phi_2+\phi_3)$
$\Delta\mu_i$	chemical potential of mixing for component i (J / mole)
g_{12}'	derivative of the interaction parameter: $u_2(1-u_2)\frac{\partial g_{12}}{\partial u_2}$
g_{23}'	derivative of the interaction parameter: $v_2(1-v_2)\frac{\partial g_{23}}{\partial v_2}$
a	$\frac{v_2}{v_3-v_2}\left(\frac{b}{b-1}\right)$
b_1	$\frac{v_1}{v_1-v_2}$
b_3	$\frac{v_3}{v_3-v_2}$
R	gas constant (J/mole K)
T	temperature (K)
ΔG_m	free enthalpy of mixing (J / mole)

Summary

In this thesis the immersion precipitation process is studied for systems in which two polymers are present.
In its basic form, immersion precipitation is carried out by immersing a thin film of a concentrated polymer solution into a bath of nonsolvent. By exchange of solvent from the polymer solution, and nonsolvent from the coagulation bath, the polymer solution becomes instable. Liquid-liquid phase separation results in a polymer lean phase and a polymer rich phase. The polymer lean phase forms pores inside a matrix created by the polymer rich phase, which forms the membrane.
The objective of this thesis is to investigate the effects of the addition of a *second* polymer into the polymer solution. The use of a second polymer (polymeric additive) that is miscible with the nonsolvent can result in more open porous (co-continuous) structures and a better defined porosity.
In Chapter 2 the thermodynamics of a quaternary system consisting of two (miscible) polymers, a solvent for both polymers and a nonsolvent for one of the polymers are studied on the basis of the Flory-Huggins theory. Important conclusions are that phase separation, induced by the presence of the nonsolvent is (initially) mostly between the polymers: a phase rich in the first polymer, and a phase rich in the other polymer is created. At high contents of the polymeric additive, the *critical line* in the phase diagram shifts to quite high polymer concentrations. The interaction between the two polymers has little influence on the phase behavior as long as they are miscible.
In Chapter 3 the mass transfer that induces the phase separation during the immersion process is studied. A kinetic model for a quaternary system is developed that is generally valid for the first moments. It followed from chapter 2 that phase separation is predominantly taking place between the two polymers. Therefore, the slow polymer-polymer diffusion in a concentrated polymer solution should be taken into account in the model. This leads to a prediction of quite instable compositions in the polymer solution during immersion. It follows that from such a quaternary system, *delay of demixing* (a time interval between immersion and the actual demixing processes) cannot be obtained. Since delay of demixing is related to the formation of macrovoids (large finger-like cavities throughout the membrane cross-section), it follows that addition of a second polymer should suppress macrovoid formation.
In Chapter 4 the quaternary membrane forming system water/n-methyl-pyrrolidone/poly(ether sulfone)/poly(vinyl pyrrolidone) is studied experimentally. The concentrations of PES and PVP in the polymer solution, and the concentration of solvent in the coagulation bath are varied. The membrane structures found indicate that the phase separation (and therefore the

diffusion velocity) between the two polymers plays a key role in the membrane formation process. At high concentrations of PVP and low concentrations of solvent in the coagulation bath, macrovoid formation is suppressed. This is in agreement with the expectations on the basis of the developed model. Reappearance of the macrovoids at higher solvent concentrations in the coagulation bath further confirms the mechanism. Predictions concerning extreme conditions (very high solvent concentrations in the coagulation bath, very thick membranes) appear to be correct.

In Chapter 5, the ideas on membrane formation as presented in chapter 4 are related to a system in which a different kind of polymeric additive is used: poly(styrene). It is found that at fast quenching conditions (low solvent content in the coagulation bath) the two polymers cannot phase separate on any large scale (i.e. > 100 nm). At slower quench conditions (higher solvent content in the bath), large scale polymer-polymer separation did take place (10-100 μm). The slow polymer-polymer diffusion as was assumed earlier is therefore confirmed. The occurrence of macrovoids is in accordance with the formation mechanism. The results indicate that the typical co-continuous membrane structures ultimately obtained with PVP may well be the result of spinodal decomposition.

In Chapter 6, the process of nucleation and successive growth of a polymer lean phase is investigated by means of light scattering measurements during thermal precipitation experiments. An Avrami-type interpretation is used. The Flory-Huggins theory is used to derive a relation for the dependence of the light scattering on supercooling. The results indicate that the number of nuclei is independent of quench time and/or supercooling. The demixing process becomes slower at higher polymer concentrations. The experiments are complicated by differences in refractive indices.

In the First Appendix to this thesis, a first experimental approach on the basis of the mass transfer model presented in chapter 3 is shown. The results are related to the spinning of hollow fiber ultrafiltration membranes. Some of the ideas on macrovoid formation presented in chapter 4 are also shown here. The occurrence of nodular structures in toplayers of membranes is possibly related to the rheological behavior of polymer solutions.

In the Second Appendix of this thesis a linear correlation is shown for isothermal cloudpoints in a polydisperse ternary system (nonsolvent/solvent/polydisperse polymer). The correlation shows a remarkable applicability of the correlation over more than four decades of polymer concentration, consisting of both higher and lower concentrations than the *critical point*. An interpretation of the relation indicates that the slope of the line is only dependent on the molar volumes of the components; the intercept is dependent also on the enthalpic interactions. The relation gives an easy method to distinguish between liquid-liquid phase separation and crystallization of the polymer.

Samenvatting

Membraanvorming door Immersie-Precipitatie:
de Invloed van een Tweede Polymeer

In dit proefschrift wordt het zgn. immersie-precipitatie proces bestudeerd waarbij twee polymeren tegelijkertijd in de polymeeroplossing worden gebruikt.
In essentie bestaat het immersie-precipitatie proces uit het onderdompelen van een dun laagje van een geconcentreerde polymeeroplossing in een bad dat niet-oplosmiddel voor het polymeer bevat. Door uitwisseling van oplosmiddel vanuit de polymeeroplossing en niet-oplosmiddel vanuit het coagulatiebad, wordt de polymeeroplossing instabiel en gaat ontmengen in een polymeerarme fase en een polymeerrijke fase. De polymeerarme fase vormt poriën in een matrix gevormd door de polymeerrijke fase.
In dit proefschrift is de invloed van een tweede polymeer in de polymeeroplossing onderzocht. Als zo'n tweede polymeer oplosbaar is in het niet-oplosmiddel in het coagulatiebad, kunnen membraanstrukturen vervaardigd worden met een zeer open (cocontinue) poriestruktuur.
In hoofdstuk 2 wordt de thermodynamica bestudeerd van een quaternair systeem bestaande uit twee (mengbare) polymeren, een oplosmiddel, en een niet-oplosmiddel voor één van de polymeren, op basis van de Flory-Huggins theorie. Het blijkt dat de vloeistof-vloeistof ontmenging, veroorzaakt door aanwezigheid van een niet-oplosmiddel, voornamelijk plaatsvindt tussen de twee polymeren: een fase rijk aan het ene polymeer, en een fase rijk aan het andere polymeer worden gecreëerd. Bij hoge concentraties van het polymeer dat oplosbaar is in het niet-oplosmiddel verschuift de *kritische lijn* in het fasediagram naar hoge polymeerconcentraties. Het blijkt dat de interactie tussen de twee polymeren weinig invloed heeft op het fasegedrag, zolang de twee polymeren mengbaar zijn.
In hoofdstuk 3 wordt een quaternair model afgeleid voor het massatransport dat leidt tot fasescheiding tijdens immersie-precipitatie, dat algemeen geldig is voor het begin van het immersie proces. In hoofdstuk 2 bleek de optredende fasescheiding voornamelijk tussen de twee polymeren plaats te vinden. Daarom wordt in het model rekening gehouden met de langzame diffusie tussen twee polymeren in een geconcentreerde oplossing. Uit het model volgt dat zeer instabiele samenstellingen in de polymeeroplossing worden gecreëerd. *Uitstel van ontmenging* (het optreden van een tijdsinterval tussen het moment van onderdompelen van de film en het moment dat de fasescheiding begint) blijkt niet mogelijk te zijn in een dergelijk systeem. Aangezien dit proces ten grondslag ligt aan de vorming

van macrovoids (grote, vingervormige holten door bijna de gehele doorsnede van het membraan) zal de vorming van deze holten belemmerd worden door toevoeging van een tweede polymeer.
In hoofdstuk 4 wordt het quaternaire systeem bestaande uit water/n-methyl pyrrolidon/poly(ether sulfon)/poly(vinyl pyrrolidon) experimenteel bestudeerd. De PES en PVP concentraties in de polymere film, en de oplosmiddel (NMP) concentratie in het coagulatiebad zijn gevarieerd. De resulterende membraanstrukturen geven aan dat de fasescheiding (en dus de diffusiesnelheid) tussen de twee polymeren zeer belangrijk is in het proces van membraanvorming. De vorming van macrovoids wordt onderdrukt bij hoge PVP concentraties in de polymeeroplossing en lage oplosmiddelconcentraties in het coagulatiebad. Dit is in overeenstemming met het eerder beschreven model. Ook het opnieuw verschijnen van macrovoids bij hogere oplosmiddelconcentraties in het coagulatiebad bevestigt het eerder omschreven model. Voorspellingen vanuit het model aangaande extreme vormingsomstandigheden (zeer dikke membranen, zeer hoge oplosmiddelconcentraties in het coagulatiebad) blijken correct te zijn.
In hoofdstuk 5 wordt de eerder beschreven modelvorming gerelateerd aan een systeem met een volledig ander polymeer additief: poly(styreen). Dit tweede polymeer is niet oplosbaar in water. Het blijkt dat onder snelle ontmengomstandigheden (lage oplosmiddelconcentraties in het coagulatiebad) de twee polymeren niet op grote schaal (> 100 nm) kunnen ontmengen. Onder langzamere ontmengomstandigheden (meer oplosmiddel in het coagulatiebad) kan deze fasescheiding op grote schaal wèl plaatsvinden (10-100 μm). De langzame polymeer-polymeerdiffusie zoals eerder was aangenomen (in hoofdstuk 3) wordt dus bevestigd. De vorming van macrovoids bevestigt het veronderstelde membraanvormingsmechanisme. De resultaten geven aan dat de typische co-continue struktuur zoals verkregen met PVP het gevolg is van spinodale ontmenging.
In hoofdstuk 6 wordt het proces van kiemvorming en -groei van een polymeerarme fase bestudeerd met behulp van lichtverstrooiingsexperimenten tijdens thermische ontmenging. Een Avrami-benadering is gebruikt, terwijl de Flory-Huggins theorie gebruikt is om een relatie van de afhankelijkheid van de lichtverstrooiing van de onderkoeling af te leiden. Het blijkt dat het aantal kiemen onafhankelijk is van de tijd van ontmenging en de onderkoeling. Verder blijkt dat de ontmenging langzamer gaat bij hogere polymeerconcentratie, hoewel de resultaten worden bemoeilijkt door verschillen in brekingsindex.
In de eerste bijlage van dit proefschrift wordt een eerste experimentele benadering gegeven op basis van het massatransport model in hoofdstuk 3. De resultaten zijn gerelateerd aan het spinnen van holle vezel ultrafiltratie membranen. De vorming van macrovoids wordt bestudeerd, analoog aan

hoofdstuk 4. Nodulaire (bolletjes-) strukturen in de toplagen van de membranen blijken mogelijk gerelateerd te zijn aan het rheologische gedrag van polymeeroplossingen.
In de twee appendix van dit proefschrift wordt een lineaire correlatie voor isotherme troebelingspunten in een polydispers, ternair systeem (niet-oplosmiddel/oplosmiddel/polydispers polymeer) bestudeerd. De correlatie gaat opmerkelijk goed op over meer dan 4 orden van grootte in polymeerconcentratie, die zowel onder als boven het *kritische punt* vallen. Een verdere interpretatie van de correlatie laat zien dat de helling van de lijn slechts afhankelijk is van de molaire volumina; de asafsnede is tevens afhankelijk van de enthalpische interacties. Met behulp van de correlatie kan het verschil tussen vloeistof-vloeistof ontmenging en polymeerkristallisatie eenvoudig worden waargenomen.

Levensloop

Remko Boom werd op 11 mei 1965 geboren te Utrecht. In 1983 behaalde bij zijn VWO-B diploma aan het Kottenpark College te Enschede. In hetzelfde jaar begon hij met de studie Chemische Technologie aan de Universiteit Twente. Hij werd in 1987 door Shell Internationale Petroleum Maatschappij voor drie maanden naar Edmonton, Canada uitgezonden in het kader van de doctoraalstage. In 1988 behaalde hij het doctoraal diploma bij de onderzoekgroep Membraantechnologie met lof, op het ontwikkelen van een tweebads-methode voor het vervaardigen van holle vezel membranen voor gasscheiding.
Van 1 juni 1988 tot 1 juni 1992 was hij werkzaam als onderzoeker in opleiding bij de onderzoekgroep Membraantechnologie, en verrichtte hij het onderzoek zoals beschreven staat in dit proefschrift.

ISBN 90-9005223-2